

**FRACTURE GENERATION AND FLUIDS IN THE SPRABERRY FORMATION,
MIDLAND BASIN, TEXAS**

BY

JENNY L. STERLING

INDEPENDENT STUDY

Presented To the Faculty of

New Mexico Institute Of Mining and Technology

In Partial Fulfillment of the Requirements

For the Degree of

MASTER OF SCIENCE

New Mexico Institute Of Mining and Technology, Socorro, NM

May, 2000

**New Mexico Bureau
of
Geology and Mineral Resources**

ABSTRACT

The Spraberry Formation in the Midland Basin, Texas, is a highly fractured reservoir known for its vast quantities of petroleum as well as its distinct lack of economic oil production. Fractures in the primary oil bearing units of the Spraberry Formation are thought to be the primary means of transmitting fluids. For this reason, understanding the mechanisms and timing of fracture formation is critical to improving petroleum exploration and production. One hypothesis regarding fracture genesis in the Spraberry Formation is that fluid pressures reduced effective stresses during the basin's geologic history, creating conditions for ambient tectonic and lithostatic stresses to induce failure. A comprehensive study of the lithology and history of the Midland Basin was performed to test this hypothesis, illuminating several processes that may have contributed to fracturing.

A number of conventional triaxial shear tests were performed on samples from a horizontal well near the center of the basin to determine if knowledge of rock properties can help explain the observed fracture pattern in the most productive units of the Spraberry Formation. Results of these tests demonstrate that the "1U" and the "5U" sub-units have distinct mechanical properties. In particular, the yield strength of rocks in the 1U is much higher than for those in the 5U. Within either the 1U or the 5U, however, different lithologies behave similarly in triaxial shear tests, indicating little to no mechanical difference between the siltstones and shales.

Permeability measurements were made during selected triaxial shear tests. The results of these measurements corroborate previous findings of extremely low permeability and indicate that permeability decreases with increased load, as expected.

The geologic study of the Midland Basin was used to parameterize a one-dimensional finite difference model of the basin's depositional history. The numerical model simulated sedimentation, erosion, and associated thermal and petroleum generation histories to evaluate the possible timing of high pore pressures. Results of these simulations suggest that potential "windows" of high pore pressure occur between 230-190 Ma and between 140-80 Ma. If sedimentation persisted during the Laramide Orogeny, oil generation would have continued.

Finally, the stress conditions producing failure in the shear tests were used to develop Mohr-Coulomb failure envelopes for the various lithologies and horizons. Knowledge of fracture characteristics, the geologic history, and the failure envelopes were used to identify conditions under which the materials were likely to have failed. Results of this analysis indicate that the fractures may have formed during the periods of elevated fluid pressures suggested by the modeling study. The modeling and the mechanical analysis results provide evidence that although fluids played an important role in creating the observed fractures, regional stress was the primary factor determining fracture development and timing.

ACKNOWLEDGMENTS

I would like to thank Brian McPherson for his efforts as my advisor. David Holcomb has provided invaluable assistance as lab supervisor and committee member through this entire project. His guidance in many aspects of this study has been wholly appreciated. Laurel Goodwin and John Wilson have provided some much-needed direction and I would like to thank them for their insights and efforts in this regard. I am grateful for the

assistance in the form of discussions, documents, and well core provided by David Schechter and the staff of the Petroleum Recovery Research Center. Finally, I would also like to thank Joe Sterling for his participation in this effort, from discussions to moral support, I couldn't have done it without him. This research was funded by the SURP program through Sandia National Laboratories, Geomechanics of Reservoir Management Division and the Department of Energy grant 29P9PU-200.

SYMBOLS USED IN TEXT

A = Arrhenius frequency factor

b = layer thickness

C = effective specific heat

D_0 = no difference

E = Young's modulus

E_a = activation energy

F = the F statistic

g = gravitational constant

h = height of stratigraphic column

K_T = thermal conductivity

k_i = intrinsic permeability

L = sample length

N = total number of samples

N_i = sample size for population i

n = porosity

P = pressure

p = number of populations

q = Darcy flux

R = gas constant

\bar{s} = sedimentation rate

s_i = standard deviation for population i

s_p = standard deviation for all populations

T = temperature

t = time

t = t statistic

\bar{y}_i = mean for population i

\bar{y} = mean for all populations

z = depth

α = acceptable error

ε = strain

μ = viscosity

ν = Poisson's ratio

ρ = density

σ = stress

SUBSCRIPTS USED IN TEXT

0 = original

11 = maximum direction

22 = intermediate direction

33 = minimum direction

b = bulk

e = effective

f = fluid

H = maximum horizontal direction

h = minimum horizontal direction

L = limit

n = normal

s = shear

V = vertical direction

TABLE OF CONTENTS

Abstract

Symbols used in text

Subscripts used in text

List of Tables

List of Figures

List of Appendices

Chapter 1: Fracturing of the Spraberry Formation: Overview and Background Information

1.1 Introduction

1.2 Study Significance

1.3 Geology of Midland Basin: Previous Work and Literature Review

1.3.1 Lithology, Structural Features, and Petroleum Distribution

1.3.2 Tectonic and Depositional Environment History

1.4 Conceptual Model

Chapter 2: Theory and Methods

2.1 Material Properties Testing

2.1.2 Test Methods

2.2 Numerical Modeling

2.2.1 Methods

2.3 Mechanical Analysis

Chapter 3: Results and Discussion

3.1 Geomechanical and Hydrologic Testing Results

3.2 Modeling Results

3.3 Mechanical Analysis Results

Chapter 4: Summary and Conclusions

Bibliography

Appendix A – Laboratory Test Results

Appendix B – Mechanical Analysis Results

Appendix C – Modeling Test Results

LIST OF TABLES

- Table 1: Formation thickness and period of deposition used for model input and values of original surface temperatures used in model
- Table 2: Normalization of n_0 values by formation for model input
- Table 3: Normalization of thermal conductivity values by formation for model input
- Table 4: Results of material properties testing

LIST OF FIGURES

- Figure 1: The Permian Basin and its sub-basins; the Midland Basin, the Delaware Basin, and the Val Verde Basin
- Figure 2: Category nomenclature used in this study for sub-unit, location, horizon and lithofacies types
- Figure 3: The study area and the E.T. O'Daniel No. 28 well
- Figure 4: Fracture distribution and properties in the E.T. O'Daniel No. 28 well
- Figure 5: The three fracture modes
- Figure 6: Sample distribution used in this study
- Figure 7: Photograph of Linear Variable Differential Transformer sample set-up for triaxial shear tests
- Figure 8: Photograph of Strain Gauge sample set-up for triaxial shear tests
- Figure 9: Plot of vertical stress versus time for typical triaxial shear test
- Figure 10: Illustration of Mohr circles and Mohr-Coulomb Failure envelope
- Figure 11: Cross section used for modeling study
- Figure 12: Effects of pore fluid pressure on rock failure
- Figure 13: Plots of σ_{11} vs. E
- Figure 14: Plots of σ_{11} vs. ν
- Figure 15: Plots of σ_L vs σ_{22} by sub-unit for Triaxial Shear tests
- Figure 16: Permeability versus pore pressure increases due to loading during triaxial shear test
- Figure 17: Boxplots of σ_L by sub-unit
- Figure 18: Results of modeling study
- Figure 19: Example of Mohr circles and Mohr Coulomb Failure envelopes developed from triaxial shear data
- Figure 20: Example of effects of stress through geologic time
- Figure 21: Example of added Laramide stress

LIST OF APPENDICES

Appendix A – Laboratory Test Results

Data tables

Moduli versus load curves

Pore pressure with increasing load versus permeability curves

Appendix B – Modeling Test Results

Output figures from Geohist

Appendix C – Mechanical Analysis Results

Mohr Coulomb Failure envelopes

Stress through time with envelopes

Laramide stress with envelopes

1.1 INTRODUCTION

The Spraberry Formation in the Midland Basin, Texas, has long been known as the "largest uneconomic oil field in the world" (Guevara, 1988). Although oil is stored in the matrix, flow through fractures in the Spraberry Formation is thought to be the only effective means of petroleum transport, and thus understanding the mechanisms and timing of fracture formation may lead to more effective oil production.

It is thought that fluid pressures during the basin's geologic history reduced effective stresses, providing conditions for regional stresses to induce failure in the Spraberry Formation. This hypothesis can be tested by analyzing the basin's depositional and stress histories. Equally important is a detailed description of the lithology, fracture patterns, and oil distribution in the Spraberry Formation today.

Knowledge of mechanical and hydrologic properties of the rocks of interest is critical to evaluating the relative roles of regional stresses and local fluids on fracture generation. Results of tests to evaluate these properties in the Spraberry Formation and the geologic history of the basin were used as a basis for mechanical analyses, using the Mohr-Coulomb failure criteria, to find windows of time when fracturing was possible. In addition, the geologic record was used to parameterize a one-dimensional numerical model of the thermal and petroleum generation history of the Spraberry Formation to determine if oil generation may have affected past fluid pressures. The combined results of modeling and the mechanical analysis lead to a strong argument that regional stress was the primary factor determining fracture development and timing. However, fluids did play an important role in creating the observed fractures.

1.2 STUDY SIGNIFICANCE

The Spraberry Formation is one of the largest known oil reservoirs in the world. It had between 8.9 billion barrels (Handford, 1981) and 10.5 billion barrels (Guevara, 1988) of oil originally in place, making it one of the largest known oil reservoirs in the world at the time of its discovery. The materials that make up the Spraberry Formation also possess very low matrix permeability (Guevara, 1988), and it is thought that only 6-15% of the total petroleum is recoverable (Schechter, 1998, verbal communication). As part of an effort to evaluate national petroleum reserves, the US Department of Energy is funding research to determine means of increasing production of the Spraberry Formation; this study is part of this effort.

It has been recognized for many years that the fractures that exist in this region are the primary oil pathways (McDonald and Schechter, 1990; McDonald and Schechter, 1994). An understanding of how these fractures formed can therefore provide information that is ultimately useful for understanding where regions of high or low fracture density might occur. Although extensive research into geology and petroleum recovery has been performed, relatively few studies have examined how the fractures formed, and even fewer have reported mechanical properties, such as the Limit Stress and elastic moduli, of the rocks of the formation. Lorenz (1997) discussed the fracture mode, distribution, orientation, and mineralization of the Spraberry Formation fractures. This study ties in well with that discussion and evaluates the mechanisms that may have produced them.

1.3 GEOLOGIC HISTORY

The Spraberry Formation has been studied extensively since its discovery as an important oil-bearing formation in 1949 (Elkins, 1953). Several aspects of the geologic

history elucidated by previous workers are crucial for the development and testing of a reasonable conceptual model for fracture generation. For example, knowledge of the past depositional and tectonic environments in the Midland Basin is useful for understanding the distribution of various lithologies and structures. This information can be used to narrow the range of possible rock failure mechanisms and may indicate periods of time when conditions were conducive to producing Spraberry Formation fractures.

1.3.1 Lithology, Structural Features, and Petroleum Distribution

The Spraberry Formation lies in the Midland Basin, a sub-basin of the larger Permian Basin of Texas (Figure 1). The Spraberry Trend is the most productive region of the formation and covers an area approximately 128 miles long and 40 to 60 miles wide (Guevara, 1988). The thickness of the formation ranges from 700 feet at the margins to 1400 feet in its depositional center (Stanley, 1951). The Spraberry Formation consists of a series of interbedded siltstones and shales that were deposited during the Leonardian Period, 270 – 275 Ma. (Stanley, 1951; Guevara, 1988; Hill, 1996). These sediments are interpreted as a submarine fan complex (Tyler and Gholsten, 1988; Guevara, 1988). In this type of deposition, deeper areas of the basin slowly and continuously received fine-grained sediments, while short storm events deposited larger grains such as silts from the basin margins through meandering channels cut through the surrounding muds and clays (Handford, 1981; Hill, 1996; Guevara, 1988). As a result, silt layers are continuous only within the channel of deposition, but with a great deal of lateral and vertical heterogeneity. Although the system has been simplified as a “layer cake” conceptual model, the sedimentary facies create discrete compartments and pathways for petroleum movement (Tyler and Gholsten, 1988). The primary "pay" zones, or regions of high oil

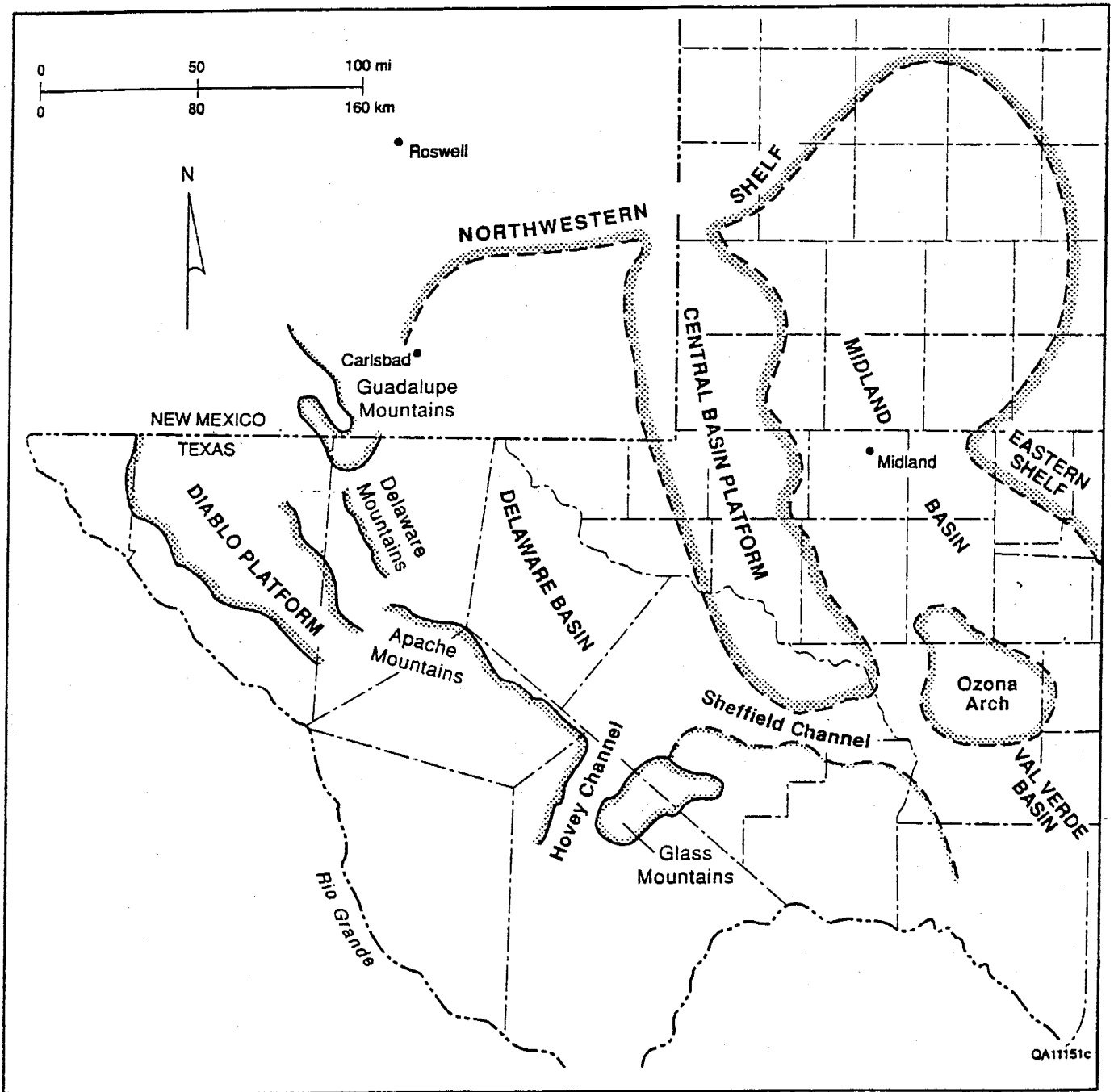


Figure 1: The Permian Basin and its sub-basins; the Midland Basin, the Delaware Basin, and the Val Verde Basin (Guevara, 1988).

production, are the siltstone facies (Reservoirs Inc., 1997). In the recent literature, the Spraberry Formation was divided into sub-units, primarily to distinguish between areas of high and low oil production (Figure 2; Guevara, 1988; Stanley, 1951). In particular, the 1U and 5U siltstones are the most productive reservoir units (Guevara, 1988); petroleum is rare to nonexistent in shale layers (McDonald and Schechter, 1990; McDonald and Schechter, 1994; Schechter, 1998). An analysis of Spraberry Formation core by the Petroleum Recovery Research Center (PRRC), Socorro, NM, revealed distinct lithologic horizons within the horizontal core from the E. T. O'Daniel No. 28 well (Figures 2 and 3; McDonald and Schechter, 1990; McDonald and Schechter, 1994). The horizons consist of 1U and 5U siltstones and the shales lying above and below those layers and possess different porosities, permeabilities, grain size, and oil production capability. This well is thought to have penetrated a thin siltstone layer a few feet above the main 1U reservoir instead of the reservoir itself. The layer that was sampled is thought to be very similar hydrologically to the main reservoir and, in the context of this study, will be referred to as the 1U reservoir. Reservoirs Inc. (1997) identified six lithofacies that also occur in the core from the E. T. O'Daniel No. 28 well (Figure 2). The first lithofacies, Type 1, is comprised of massive claystone or silty claystone that is considered to have no reservoir potential. Lithofacies Type 2 is finely laminated silty shale, and is also thought to have no reservoir potential. The third lithofacies, Type 3, consists of finely laminated siltstone that displays poor to marginal reservoir quality. Lithofacies Type 4 is a bioturbated or disturbed siltstone that is similar in reservoir potential to Type 3. Lithofacies Type 5 consists of dolomite-cemented siltstones or sandstones not identified as having reservoir potential. The final lithofacies, Type 6, is comprised of massive to faintly stratified

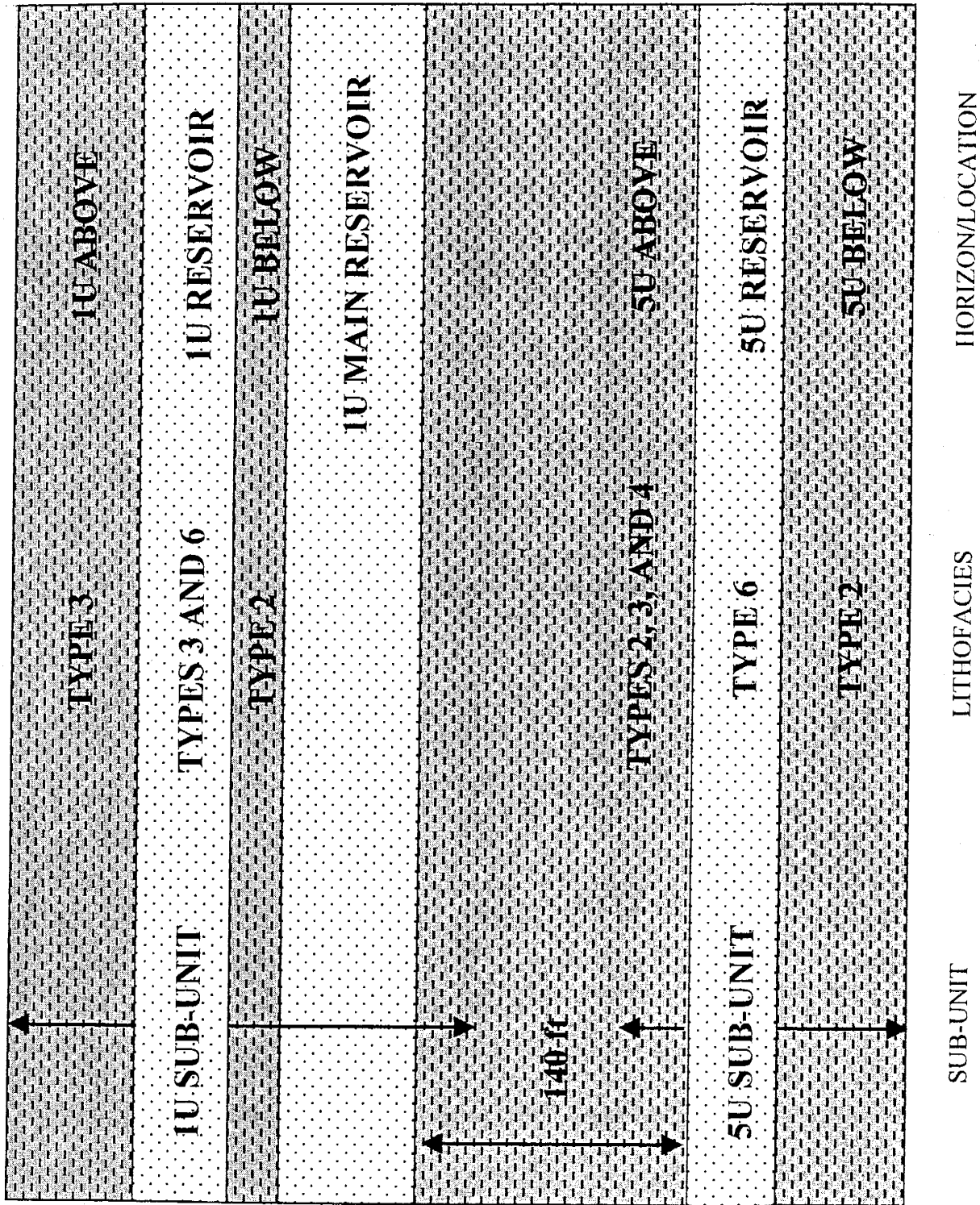


Figure 2: Category nomenclature used in this study for sub-unit, location, horizon and lithofacies types

siltstones that display marginal to good reservoir potential. The horizons identified by McDonald and Schecter (1990, 1994) consist of groups of these lithofacies, with some lithofacies falling into multiple horizons (Figure 2).

Early in the history of Spraberry Formation oil production, it was recognized that the primary pathway for petroleum transport was through fractures (Guevara, 1988; McDonald and Schecter, 1990; McDonald and Schecter, 1994). Fracturing is also known to occur above the Spraberry Formation, but the vertical extent of these fractures is less certain. Stanley (1951) indicates that fractures are limited to 500 feet above the Spraberry Formation and to the base of Leonardian sedimentary rocks. Guevara (1988), on the other hand, relates surface lineaments and fractures to those in the Spraberry Formation, implying a vertical extent of approximately 7000 feet.

An analysis of horizontal core from the E. T. O'Daniel No.28 and No.37 wells (Figure 3) indicated that three sets of fractures are observed in the upper Spraberry Formation (Lorenz, 1997). The three fracture sets are different in orientation, location, spacing, type and mineralization (Figure 4). The first set consists of extension fractures that have a northeast strike (average 43°). These northeast (NE) striking fractures are limited to the 1U siltstone reservoir facies. They also have a low variability in strike, are regularly and closely spaced (average 3.2 ft), and are commonly partially to almost wholly mineralized with barite (Lorenz, 1997). The second set consists of right-lateral shear fractures that strike north-northeast (average 32°). This set is only found in the siltstone layer in the 5U. The spacing of this set is much smaller (average 1.6 ft), and fractures are unmineralized (Lorenz, 1997). The last fracture set strikes east-northeast (average 70°), and also includes extension fractures. This unmineralized set can be

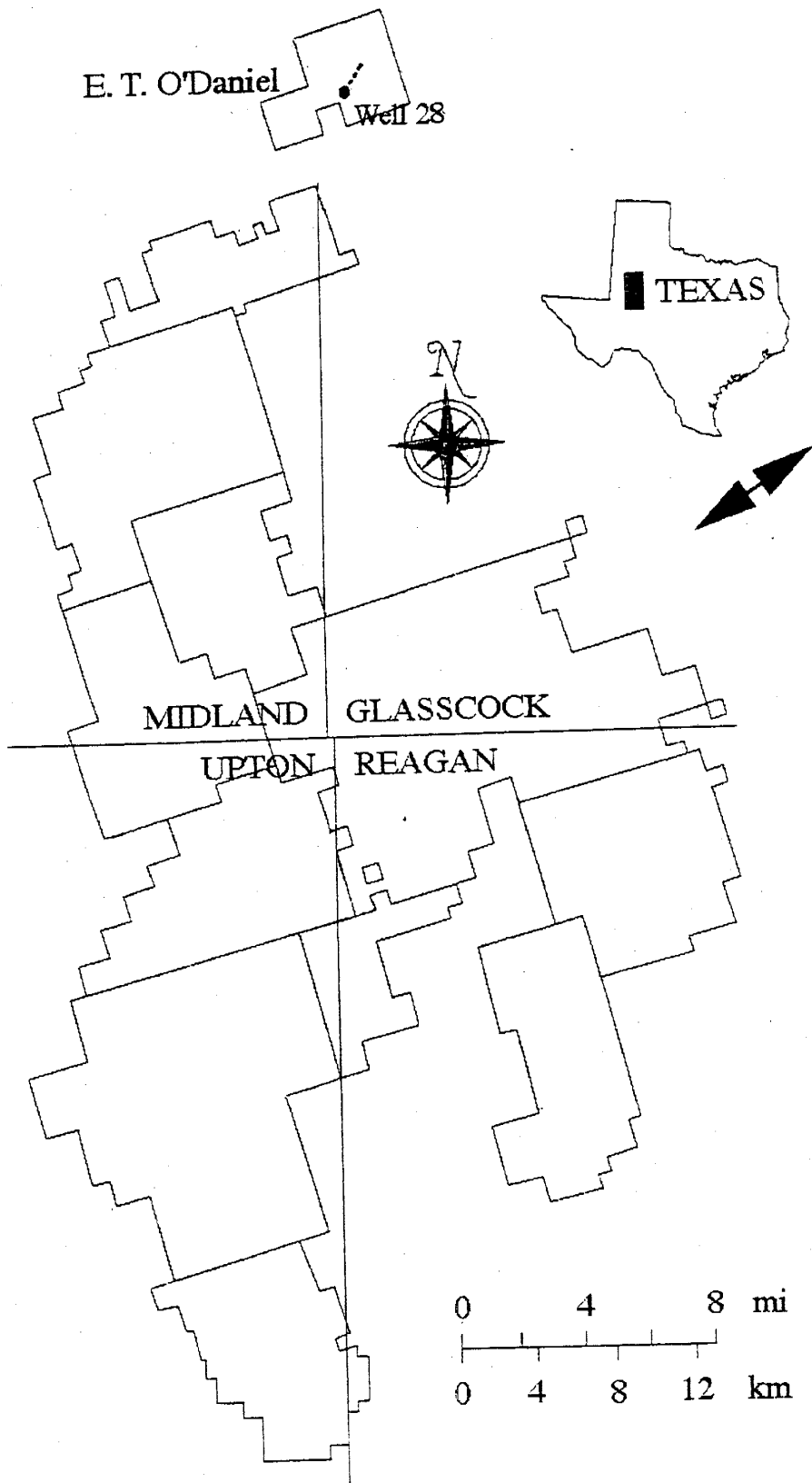


Figure 3: The study area and the E.T. O'Daniel No. 28 well

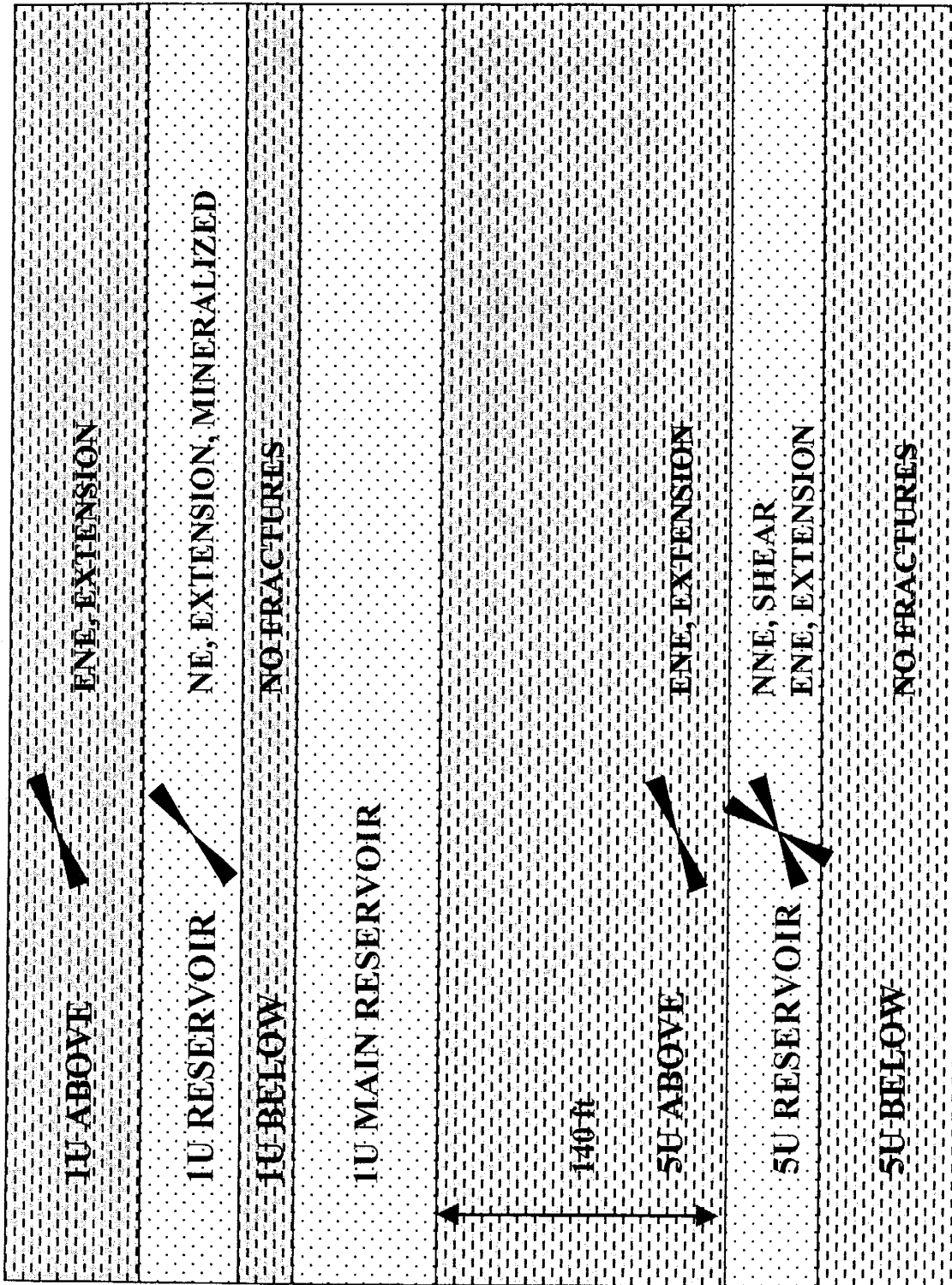


Figure 4: Fracture distribution and properties in the E.T. O'Daniel No. 28 well

found within the 5U-reservoir siltstone unit, as well as within the black shales that overlie both 1U and 5U reservoirs. These fractures have the widest dispersion of strike azimuths (35 degrees), with spacing ranging from fractions of an inch up to 13 ft (average 3.8 ft). There are fractures in all units except the black shales immediately below both the 1U and 5U reservoirs (Lorenz, 1997). These fracture orientations correlate well with the flow anisotropy that has been observed since production of the Spraberry Formation first began in 1949 (D. Schecter, personal communication, 1998).

Fracture generation has been attributed to a range of possible mechanisms. Regional tension, local uplift, and changes in sediment volume due to compaction were all cited by Guevara (1988) and Warn (1959) as possible mechanisms producing the observed fractures. Schmitt (1954) hypothesized that the fractures were due to small stresses applied to the region over a long period of time. Winfree (1995) suggested that forces exerted on the region during the Laramide Orogeny were the primary cause of fracturing.

Although Horak (1985) believed that the oil in the Spraberry Formation formed elsewhere and migrated to its current location, the majority of workers in the area believe that the Spraberry Formation itself is the petroleum source (Stanley, 1951; Houde, 1979; Guevara, 1988; Schmitt, 1954; Tyler and Gholsten, 1988; Schecter, 1998 personal communication). Shales in the Spraberry Formation possess all the characteristics that would indicate that it is a possible petroleum source (Houde, 1979; Schmitt, 1954). For clastic sediments such as those found in the Spraberry Formation to be considered a petroleum source, they must contain greater than 0.5 weight % total organic carbon, or TOC (Tissot and Welte, 1978). Houde (1979) measured TOC values in the Spraberry

Formation that range between 0.68 weight % and 3.57 weight %. Dutton (1980) measured TOC values from 0.888 weight % to 2.772 weight %. Not all sediment with these ranges of TOC will produce petroleum – they must be subject to an appropriate temperature history as well (Tissot et al., 1978). For older basins like the Midland Basin, temperatures must have reached between 60°C and 65°C in order for them to be considered a possible petroleum source (Albrecht, et al., 1976). Houde (1979) used kerogen coloration and analysis of the present geothermal gradient to determine that parts of the Spraberry Formation reached temperatures between 63°C and 77°C, easily surpassing the minimum requirements of a source rock. McDonald and Schecter (1990) found illite and chlorite in the Spraberry Formation shales, suggesting that temperatures higher than 63°C and 77°C were possible.

The Spraberry Formation has notoriously low matrix permeability, ranging from 0 to 1.1 mD (e.g. Houde, 1979; Guevara, 1988). Additionally, the Spraberry Formation is strongly lithologically heterogeneous both laterally and horizontally (Tyler and Gholsten, 1988). Horak's (1985) hypothesis that the oil was generated elsewhere requires oil to have migrated across many stratigraphic and structural boundaries, thousands of feet vertically and approximately 100 miles horizontally. Finally, the characteristics of the oil itself indicate that the Spraberry Formation has a unique source of oil. Many formations within the Midland Basin are oil bearing, but the Spraberry Formation petroleum is chemically distinct from all others (Houde, 1979). The combination of all these characteristics makes it likely that the Spraberry Formation is the source of its own petroleum.

1.3.2 Stress and Depositional Environment History

The structure and stratigraphy of the Midland Basin is directly related to the basin's tectonic and depositional history. Understanding of the structural and depositional history of the basin is therefore an important part of developing a conceptual model of fracture origin. This information was used in conjunction with the fracture descriptions to identify periods of time when fractures may have formed and processes that could have played a role in fracture propagation. Although the geologic history subsequent to Spraberry Formation deposition is of particular interest with respect to fracture generation, preceding stress and temperature conditions may have influenced oil generation and resulting pore pressures in the Spraberry Formation. As a consequence, the prior history could have had profound effects on the stress conditions that ultimately produced the fractures in the Spraberry Formation. The entire depositional and thermal history of the stratigraphic column was simulated in the modeling study in order to include effects exerted by conditions prior to deposition of the Spraberry Formation. The structural and depositional history discussed here was used to identify hydrogeologic and historic information used as input for the model.

Prior to 810 Ma, the region was part of a rift zone (Hill, 1996). The basement of the basin consists of materials that vary in composition from granitic to granitic with metamorphosed sandstone. From 810 - 310 Ma, this region was subject to weak crustal extension which formed the Tobosa Basin, a precursor to the Permian Basin (Hill, 1996). The basin slowly subsided and was covered by a shallow marine sea, producing a thick sequence of carbonates and shales (Hill, 1996). The Ellenburger Formation is the most basal formation, and consists of dolomites deposited between 500-485 Ma (Jones, 1949;

Boggs, 1987; Hill, 1996). Overlying these sediments is the Simpson Group (485-455 Ma; Boggs, 1987), which is composed of limestone that accumulated in the sag of the Tobosa Basin (Jones, 1949; Hill, 1996). The Montoya Group (455-425 Ma; Boggs, 1987), a thick sequence of impermeable, crystalline dolomite and limestone, rests on top of the Simpson Group (Jones, 1949; Hill, 1996). The Fusselman Formation (420 – 417 Ma; Boggs, 1987) lies unconformably over these sediments (Jones, 1949) and consists of dolomites deposited deep in the Tobosa sag (Hill, 1996). Also deposited in the basin deep, is the Silurian Shale (417 – 405 Ma; Boggs, 1987; Hill 1996). Overlying these shales is a deposit of limestone (405-390 Ma, Boggs, 1987; Jones, 1949) which is part of a carbonate sequence deposited along the basin margins (Hill, 1996). A major unconformity overlies these rocks (Jones, 1949) and marks the contact between these sediments and the Woodford Shale (387-380 Ma, Boggs, 1987) that resulted from a transgressing sea (Hill, 1996). The Woodford Shale is also separated from overlying sediments by an unconformity (Jones, 1949). That gap in sediments is followed by the Mississippian Lime (365-340 Ma, Boggs, 1987), a relatively clean crystalline limestone that is easily recognizable in well samples and mechanical logs (Jones, 1949; Hill, 1996). The upper Mississippian sediments are separated by yet another unconformity (Jones, 1949) and are composed of fine-grained silty shales called the Barnett Formation (335-330 Ma, Boggs, 1987; Hill, 1996). These sediments are the result of the Ouchita Orogeny (Gardiner, 1990). Separating the Barnett Formation from the overlying Bend Formation is an additional unconformity (Jones, 1949). The Bend Formation (325-312 Ma, Boggs, 1987) is a series of limestones and shales (Jones, 1949). Algal carbonate reefs produced

the Strawn Formation (312-308 Ma, Boggs, 1987), which lies above the Bend Formation sediments (Jones, 1949; Hill, 1996).

From 310 – 265 Ma, the effects of the collision between Laurasia and Gondwana were felt in the region of interest (Hill, 1996). The Permian Basin was created during this time. Precambrian normal faults were re-activated and the Central Basin Platform uplifted. The platform separated the Permian Basin into smaller sub-basins: the Midland, the Delaware and Val Verde basins (Figure 1, Guevara, 1988). At this time the Permian Basin was still covered by a shallow marine sea, but around 275 Ma the sea began to recede towards the northeast (Hill, 1996). Sediments from this period consist of sands, shales, and carbonates that are separated from earlier deposits by an unconformity (Jones, 1949). The lowermost sediments from this time are the Wolfcampian series (290-275 Ma, Boggs, 1987) which consists of interbedded limestones and shales produced either in the center of the basin or along its margins (Jones, 1949; Hill, 1996). The Dean Formation (275-274 Ma, Boggs, 1987) is a sandstone that overlies this deposit (Jones, 1949). The oil-bearing Dean Formation is Leonardian in age, as is the Spraberry Formation, and is therefore often grouped with the Spraberry Formation (Stanley, et al., 1951). Separating the Dean from the Spraberry Formation is an unnamed shale (274-273 Ma, Boggs, 1987; Jones, 1949). At the time of Spraberry Formation deposition (273-270, Boggs, 1987), the Midland Basin was subsiding more rapidly than the surrounding areas (Hill, 1996), producing thick layers of silt and shale. These deposits are overlain by the Word Formation (270-264.8 Ma, Boggs, 1987) which is another large sequence of shales, sandstones, and limestones (Jones, 1949).

The newly formed Permian Basin then entered a period of relative stability and persisting subsidence (265 - 230 Ma). The sea continued to recede, producing shallow saline sea and terrestrial evaporite deposits (Hill, 1996). The earliest deposit from this time is the San Andres Formation (264.8-261.2 Ma, Boggs, 1987), a cherty sandstone and limestone (Jones, 1949). The San Andres Formation is another important oil-bearing formation, although its main reserves lie in the Central Basin Platform (Hill, 1996). Above the San Andres Formation is the Grayburg Formation (261.2-260 Ma, Boggs, 1987), a massive sandstone and dolomite deposit from a shallow reef environment (Jones, 1949; Hill, 1996). The Queen Formation (260-258.1 Ma, Boggs, 1987) is lithologically similar to the Grayburg Formation, with a much larger proportion of clastic sediments (Hill, 1996). It is overlain by the Seven Rivers Formation (258-257 Ma, Boggs, 1987; Jones, 1949), which is a series of sandstones and evaporite deposits that represent a regression of the sea to the northeast (Hill, 1996). The Yates Formation (257-255.8 Ma, Boggs, 1987) lies above the Seven Rivers Formation and is comprised of sandstone and anhydrite that is both fossiliferous and marked by numerous erosional surfaces (Jones, 1949; Hill, 1996). The Tansill Formation (255.8-255 Ma, Boggs, 1987) is a relatively thin bed of sediments that represent a period of cyclic emergence and submergence (Hill, 1996). The Salado Formation (255-253.3 Ma, Boggs) overlies the Tansill Formation, and consists primarily fine to coarse-grained clear halite (Jones, 1949; Hill, 1996). After Salado time, an extensive advance of the sea occurred and is represented by the overlying Rustler Formation (253-251.6 Ma, Boggs, 1987; Jones, 1949; Hill, 1996). The last of the Permian deposits are lagoonal to continental sediments called the Dewey Lake Red Beds (251.6-250 Ma, Boggs, 1987), which were deposited as the sea regressed for its last time

to the northeast (Jones, 1949; Hill, 1996). An unconformity records the erosion of the uppermost Permian through middle Triassic sediments, including any additional strata deposited between 250-230 Ma. (Jones, 1949; Boggs, 1995; Hill, 1996). This major unconformity was caused by worldwide tectonic changes taking place at that time that involved the final assemblage and breakup of Pangea (Hill, 1996).

The period from 230 to 80 Ma was characterized by tectonic quiescence (Hill, 1996). The Santa Rosa Formation (230-219.5 Ma, Boggs, 1987) is the lowermost deposit from this time and consists of fluvial sands and shales (Jones, 1949; Hill, 1996). It lies under the Chinle Group (219.5-200 Ma, Boggs, 1987), which represents terrestrial, flood plain and alluvial fan deposits of sandstones and shales (Jones, 1949; Hill, 1996).

Another unconformity in the stratigraphic column (Jones, 1949) obliterated sediments deposited between 200 - 140 Ma (Boggs, 1987; Hill, 1996). The youngest formations that remain today are the Paluxy Formation and the Fredericksburg Group that were deposited between 140 - 72 Ma (Boggs, 1987) in fluvial and deltaic environments (Hill, 1996).

This depositional environment was maintained throughout the Laramide Orogeny (80 - 40 Ma, Boggs, 1987; Hill, 1996) which is generally believed to have been produced by the collision of the Farrallon Plate with the North American Craton, and is the only episode of tectonic shortening that post-dated deposition of the Spraberry Formation (Hill, 1996). The Laramide Orogeny has been divided into early (80 - 55 Ma) and late (55 - 40 Ma) phases. The maximum compressive stress (σ_{11}) of the early Laramide (80 - 55 Ma) is inferred to have been oriented northeast (Hill, 1996). During the late Laramide (55 - 40 Ma) the rate of tectonic shortening is thought to have increased significantly and σ_{11} is inferred to have been oriented East-Northeast (Hill, 1996).

The period from 40 to 30 Ma represented a transition from Laramide shortening to Basin and Range extension (30 – 2 Ma, Boggs, 1987; Horak, 1995; Hill, 1996). The Permian Basin has been under continuous extension during Quaternary (2 - 0 Ma) (Hill, 1996). The last unconformity in the stratigraphic section records the erosion of any sediment that may have been deposited since early in the Laramide Orogeny (Jones, 1949; Hill, 1996).

1.4 Conceptual Model of Fracture Origin

As previously mentioned, one set of vertical shear fractures and two sets of vertical extension fractures are observed in the Spraberry Formation (Figure 4). Figure 5 shows the three types of fractures. These fracture sets provide a number of clues about the potential orientations of the stresses that caused them. Shear fractures may appear in sets of two (conjugate sets). The bisector of the acute angle between the fracture sets defines the orientation of the maximum compressive stress (σ_{11}), which is less than 45° from the fracture plane. The line of intersection of the two fracture sets defines the intermediate compressive stress (σ_{22}), and the minimum compressive stress (σ_{33}) is perpendicular to both σ_{11} and σ_{22} (Middleton and Wilcock, 1994). Fracture orientations can be used to estimate the directions of stress that produced them. Rock heterogeneities often produce significant variations from theoretical expectations limiting our confidence in these estimates (Hobbs et al., 1976). Although only one shear fracture set has been observed in the Spraberry Formation, we can still estimate the direction of stress that caused the fractures to form. The geometry of the shear fracture set and sub-horizontal slickenlines observed in the Midland Basin (Lorenz, 1997) suggests that at the time of failure, σ_{11} was horizontal and trended northeast or northwest.

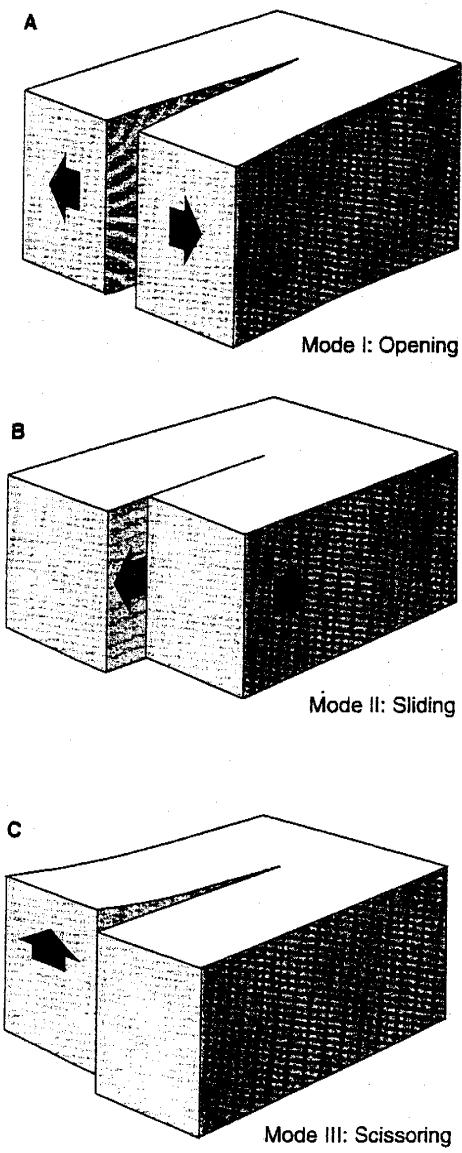


Figure 5: The three modes of fracture generation. Mode I fractures are extension fractures, Mode II and Mode III fractures are shear fractures (Davis and Reynolds, 1996).

As discussed previously, the most likely period of time when the shear fractures could have formed was during the Laramide Orogeny, between 80 - 40 Ma. Two sets of surface lineaments and fractures, striking northeast and northwest, were observed and described by Stanley et al. (1951) and Guevara (1988), and were linked genetically to Spraberry Formation shear fractures by Stanley et al (1951). If this analysis is correct, it would indicate that the Spraberry Formation fractures must have formed since the deposition of surface sediments in the late Cretaceous (97.5-66.4 Ma), and corroborates the assumption of Laramide origin.

Extension fractures form under different stress conditions than those required for shear fractures. Extension fractures parallel the σ_{11} - σ_{22} plane (Hobbs et al, 1976; Davis et al, 1996), leading to the conclusion that σ_{11} was either vertical or horizontal and trended northeast to east-northeast at the time of failure. Since we do not know whether the maximum compressive stress that caused the extension fractures was vertical or horizontal, the task of determining when they formed is more difficult. As previously discussed, the Midland basin was not subject to significant tectonic stresses, but continually subsided from the time of Spraberry Formation deposition until the Laramide Orogeny. The two sources of stress that could have led to extensional fractures during this time are the stresses caused by overlying sediment and horizontal compressive stresses produced by basin subsidence. The extension fractures may have developed during this time.

Sometimes a set of extensional fractures that parallels σ_1 forms synchronously with shear fractures (Hobbs et al., 1976). It is possible that this occurred in the Spraberry Formation. The east-northeast extension fracture set seems the most likely candidate, but

the relationship is not certain. For example, although these fractures form the appropriate theoretical angle with the shear fractures, have similar mineralization, and lie in the same lithologic unit, they are also observed in units not broken by the shear fracture set.

2.1 MATERIAL PROPERTIES TESTING

I performed a series of rock tests to evaluate and interpret the mechanical and hydrologic properties of the various Spraberry Formation shales and siltstones. The purpose of the rock testing in this study was to evaluate if physical properties and material descriptions could be correlated to fracture generation characteristics. Several studies have tried to identify which materials should be targets for oil production efforts. Four methods of categorization were evaluated in this study for their ability to predict fracture occurrence and distribution (Figure 2). As discussed previously, the Spraberry Formation has been divided into sub-units based primarily on the oil production capabilities of different layers within the formation. The two that were the focus of this study are the 1U and the 5U sub-units. An analysis of Spraberry Formation core revealed distinct horizons within the horizontal core from the E. T. O'Daniel No. 28 well (McDonald and Schechter, 1990; McDonald and Schechter, 1994). These horizons have different porosities, permeabilities, grain size, and oil production capability. In the context of this study, they will be referred to as the 1U reservoir, the shales above and below the 1U reservoir, the 5U reservoir and the shales above and below the 5U reservoir. Reservoirs Inc. (1997) identified six lithofacies that occur in the core from the E. T. O'Daniel No. 28 well. The first lithofacies, Type 1, is comprised of massive claystone or silty claystone that is considered to have no reservoir potential. Lithofacies Type 2 is finely laminated silty shale, and is also thought to have no reservoir potential.

The third lithofacies, Type 3, consists of finely laminated siltstone that displays poor to marginal reservoir quality. Lithofacies Type 4 is a bioturbated or disturbed siltstone that is similar in reservoir potential to Type 3. Lithofacies Type 5 consists of dolomite-cemented siltstones or sandstones not identified as having reservoir potential. The final lithofacies, Type 6, is comprised of massive to faintly stratified siltstones that display marginal to good reservoir potential. This study only analyzed core for Types 2, 3, 4, and 6. The horizons identified by McDonald and Schechter (1990, 1994) consist of groups of these lithofacies, with some lithofacies falling into multiple horizons. Lorenz (1997) found that these horizons had distinct fracture patterns and that although the 1U and 5U reservoirs and the shales overlying both reservoirs were fractured, the shales underlying both reservoirs were not. The final description method was a comparison of location relative to the reservoir, regardless of sub-unit. These locations are referred to as the shales above the reservoirs, the reservoirs, and the shales below the reservoirs.

Mechanical and hydrologic tests were performed on samples taken from each horizon and lithofacies to determine the following parameters: limit stress (σ_L), Poisson's ratio (ν), Young's modulus (E), porosity (n), bulk density (ρ_b), and intrinsic permeability (k_i). Tests performed on the selected samples include 73 conventional triaxial shear tests, 10 permeability tests, and 12 porosity and density measurements. Triaxial shear tests simulate conditions in the earth by applying vertical stress (σ_{11}) greater than horizontal stresses (σ_{22} and σ_{33}) to the sample. Core samples were obtained from the PRRC, and all tests were performed in the Geomechanics Laboratory at Sandia National Laboratory in Albuquerque, NM.

2.1.1 TEST METHODS

Samples were chosen to facilitate comparisons between the Spraberry Formation sub-units 1U and 5U, the different horizons within those sub-units, and the lithologic designations made by McDonald and Schecter (1990, 1994). Several triaxial shear tests were performed on samples from each group (Figure 6). For all laboratory tests, cylindrical samples were taken from the E.T. O'Daniel No.28 horizontal core using a diamond core drill. The samples were 1 ± 0.05 inches in diameter and 2 ± 0.05 inches in length. The ends of the samples were ground to be exactly parallel with each other and to remove all asperities greater than 0.0001 inches. The triaxial shear tests were performed using a MTS 220,000 lb. servo-controlled, hydraulic load frame. After the sample was placed in the test cell, the cell was filled with Isopar H and was brought to the desired confining pressure. Isopar H is an oil and was chosen for several reasons, including its price, ability to withstand large pressures, and to prevent equipment corrosion and deterioration. Sample jackets were used to exclude the pressurized fluid from the samples during triaxial shear tests. The samples were then subjected to an increasing axial load until failure occurred. The load was applied using displacement control with a MTS 458 controller and the displacement rate for all tests was $1.0E-5$ in/sec. As the test proceeded, measurements of axial load, confining pressure, and axial and lateral strain were obtained. Sample response to loading was measured in one of two ways: 1) by Linear Variable Differential Transformers (LVDT); or 2) a combination of LVDTs and strain gauges. The first method measured axial and lateral displacement with LVDTs. Plastic shrink tubes were used for sample jackets and were wired to the endcaps of the sample to

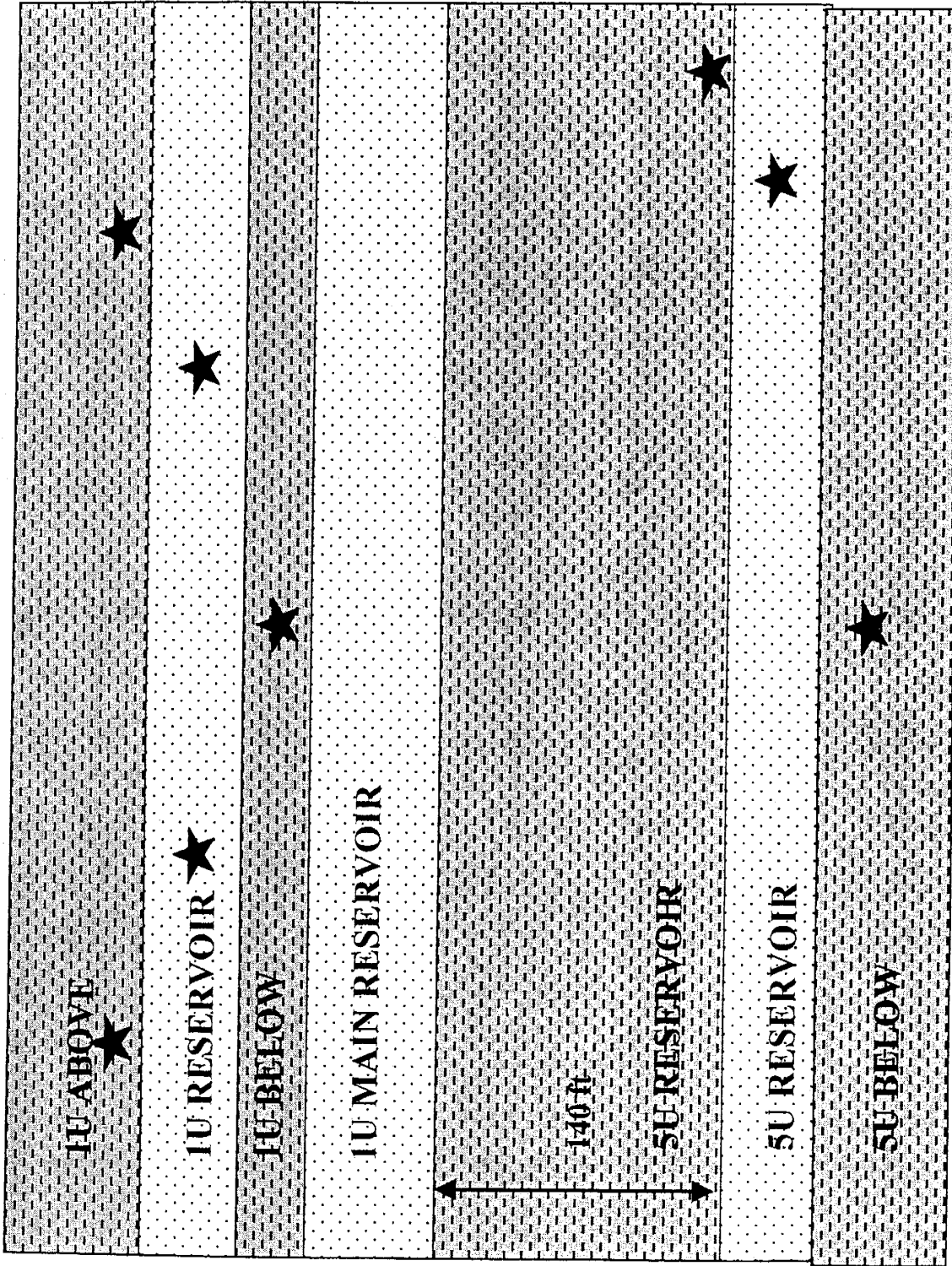


Figure 6: Sample distribution used in this study

prevent leakage, as shown in Figure 7. This method was abandoned after problems with the lateral LVDT were discovered.

The second method was more reliable, albeit more time and effort intensive, and used an axial and lateral Micro-Measurements stacked rosette strain gauge, as well as an axial LVDT (Figure 8). The strain gauges measure strain directly, have a resistance of 350 ohms, and are reliable up to a maximum strain of 1%. The axial LVDT was still included in the sample set-up to maintain the displacement-controlled loading as well as for comparison to the LVDT-only tests. The strain gauge tests used sample jackets made of polyurethane. The sample was encased in liquid polyurethane, and the sample was rotated as the coat dried to ensure an even thickness and minimize flaws in the jacket.

Data obtained by the triaxial shear test was used to calculate the limit stress (σ_L), Young's modulus (E), and Poisson's ratio (ν) for the samples. The limit stress is the stress required to bring the rock to failure and was defined as the maximum stress applied during the test. Young's modulus is a measure of a material's "springiness" and is defined as $E = \sigma_{11}/\epsilon_{11}$ where σ_{11} is axial stress and ϵ_{11} is axial strain (Middleton and Wilcock, 1994). Loads measured during testing were converted to stress by dividing the load by the sample area. Axial strain (parallel to σ_{11}) was either measured directly by strain gauges or was calculated by dividing the displacement obtained from the LVDTs by the sample length. Poisson's ratio is a measure of axial versus transverse sample response and is defined as $\nu = \epsilon_{22}/\epsilon_{11}$ where ϵ_{22} is lateral strain and ϵ_{11} is axial strain (Middleton and Wilcock, 1994). Like axial strain, lateral strain (parallel to $\sigma_{22} = \sigma_{33}$) was either measured directly by strain gauges or was calculated by dividing the displacement determined by LVDTs by the sample diameter. E and ν are elastic moduli; the rock

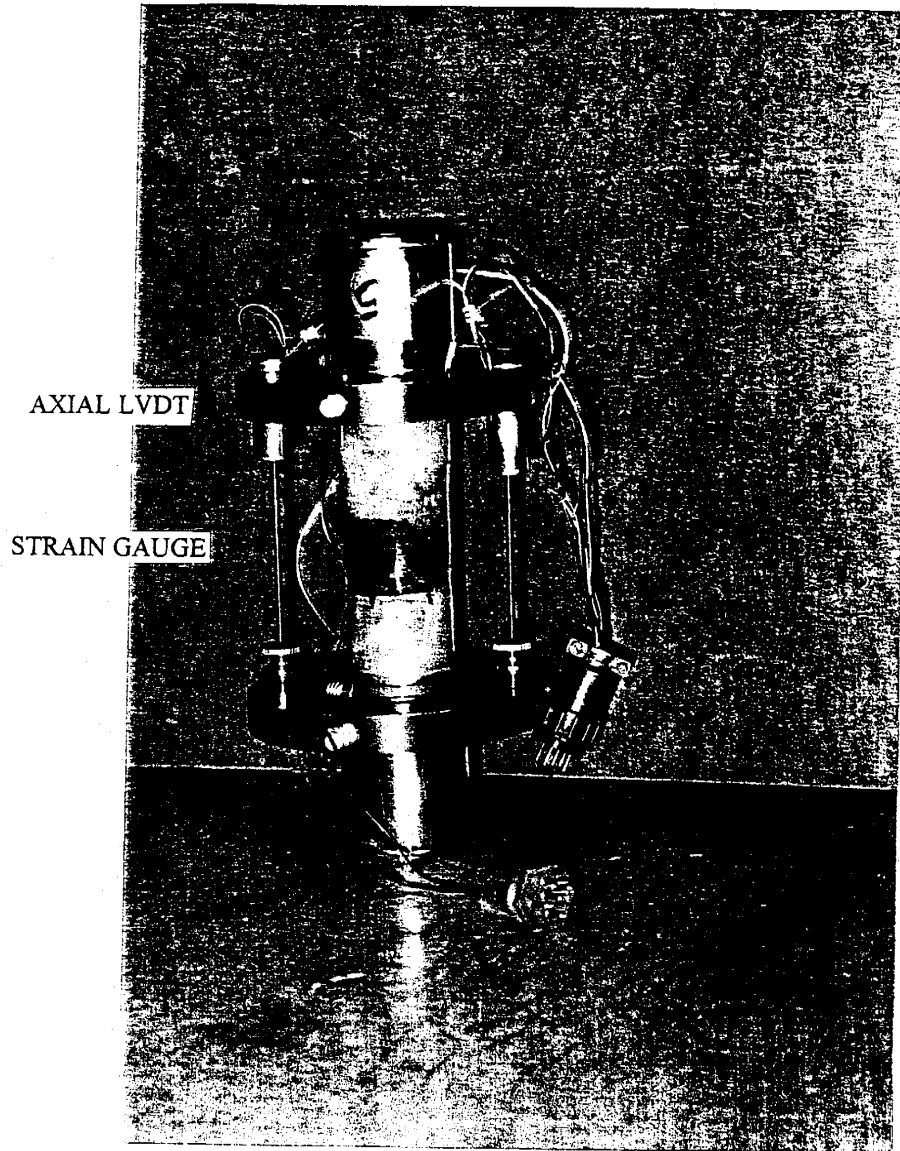


Figure 8: Photograph of Strain Gauge sample set-up for triaxial shear tests.

should behave elastically and return to its pre-stress condition once stress is removed (Middleton and Wilcock, 1994). To obtain measurements that were truly elastic responses to stress, “load-unload” loops were included in each test. A load was applied to the sample, the load application was reversed, and then a load was applied again. A plot of σ_{11} versus time from a typical test illustrates these loops in Figure 9. As the overall vertical load on the sample increased, these loops provided an opportunity to measure elastic responses to the applied stress (cf. Walsh, 1965). Although strain data were collected continuously, the moduli were calculated using only data obtained during the load-unload loop intervals.

An optimal series of tests for a given horizon or lithology included a test performed at each of the following pressures: 0, 0.69, 1.38, 2.07, 3.45, 24.13, and 48.26 MPa. If the number of samples was insufficient to complete this series for a horizon or lithology, one sample was used to obtain information needed to calculate the elastic moduli. Prior to the triaxial shear test, the sample was subjected to the full range of confining pressures. At each pressure, a “load-unload” loop was performed with a minimal amount of vertical load, and strain data were collected. In this way, data collected from one sample were used to calculate E and ν at seven different confining pressures.

At a given stress, the normal (σ_n) and shear stress (σ_s) components on planes of all possible orientations through a single point can be plotted on a diagram that is called a Mohr Circle (O. C. Mohr, 1900). The Mohr circle is defined by the maximum (σ_{11}) and minimum (σ_{33}) normal stresses and is created by plotting σ_{11} and σ_{33} on the σ_n axis and drawing a circle using those two points as the diameter. As shown in Figure 10, a series

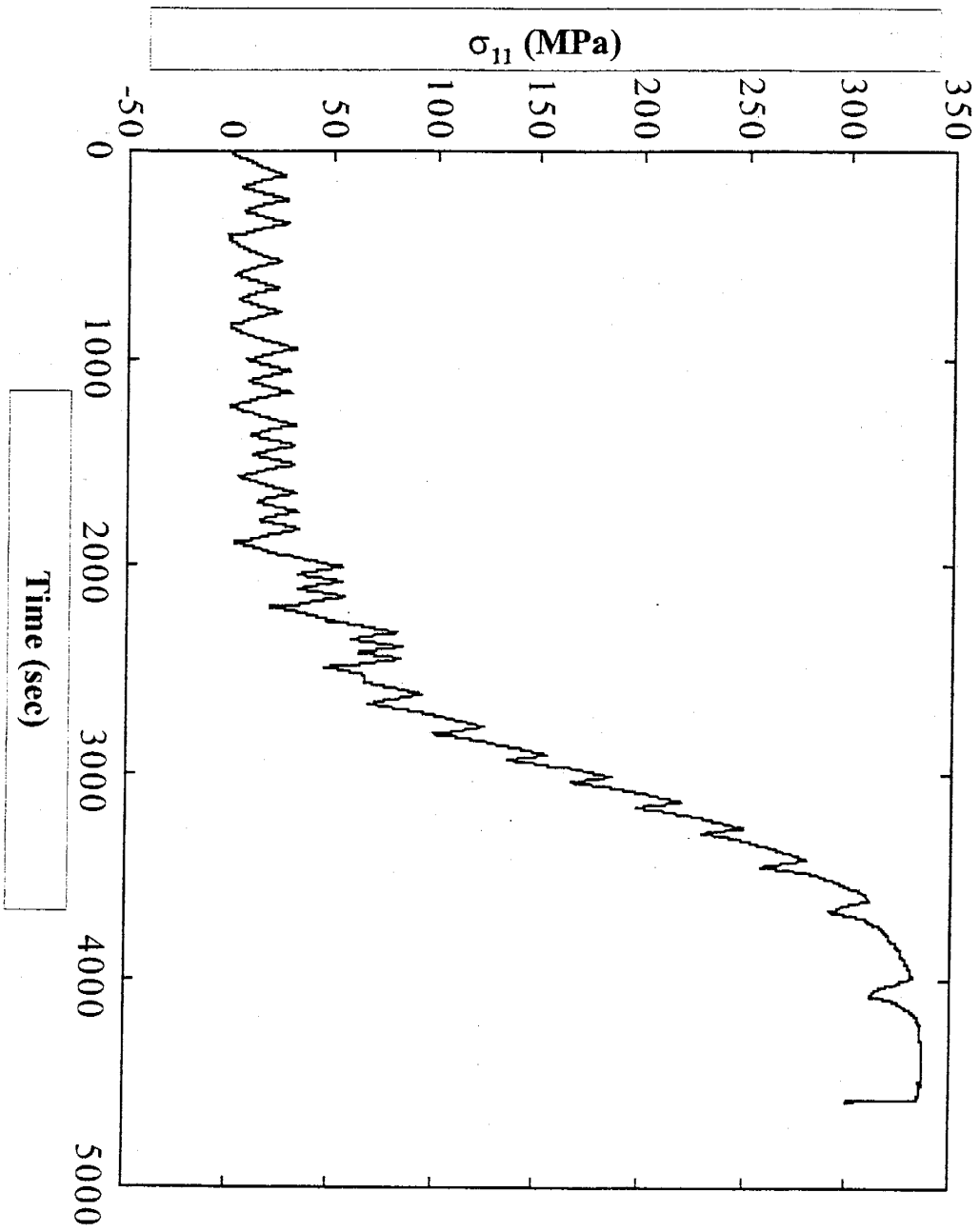


Figure 9: Plot of vertical stress versus time for typical triaxial shear test

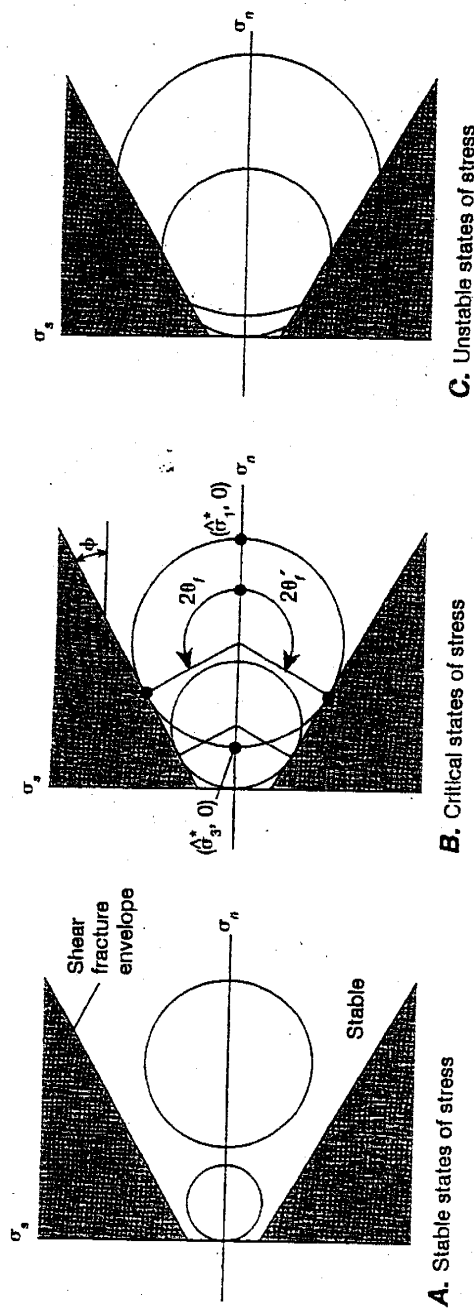


Figure 10: Illustration of Mohr circles and Mohr-Coulomb Failure envelopes (Davis and Reynolds, 1996).

of Mohr circles, each representing the stresses at failure for one sample, may be used to define the Mohr-Coulomb failure envelope, a representation of the mechanical behavior of each material. The failure envelope defines regions of material stability and instability. Stress conditions generating Mohr circles that touch the envelope will induce fracturing (O. C. Mohr, 1900). Triaxial shear test data were used to create Mohr-Coulomb failure envelopes for selected Spraberry Formation horizons and lithologic groups using σ_L , the limit stress, and σ_{22} , the confining pressure. The failure envelope indicates stress conditions conducive to fracturing.

The results of the triaxial shear tests were used to evaluate the relative importance of the sub-units (Guevara, 1988), horizons (McDonald and Schechter, 1990; McDonald and Schechter, 1994), lithofacies (Reservoir Inc., 1997; Lorenz, 1997), and location in determining mechanical properties. Elastic moduli were calculated for both elastic and plastic deformation. It is thought that sediment behavior should be different for these two types of deformation, and the data was analyzed in its entirety as well as for elastic deformation alone. Plots of σ_L versus σ_{22} and several statistical approaches were used as part of this evaluation. Using the statistical program Minitab, boxplots were made for Young's modulus, Poisson's ratio, and the limit stress measurements and grouped by sub-unit, horizon, location and lithofacies. Boxplots are visual representations of several statistical measurements. A box is drawn so that the bottom of the box is at the first quartile (Q1) data value, and the top is at the third quartile (Q3) value. A line is drawn horizontally across the box at the median. Lines extend vertically from the top and bottom of the box to the adjacent values still inside the region defined by the following limits: Lower Limit: $Q1 - 1.5(Q3 - Q1)$, and Upper Limit: $Q3 + 1.5(Q3 - Q1)$. Any

additional data points outside the lower and upper limits are outliers and are plotted with asterisks (*) (Scheaffer and McClave, 1995). One-way analysis of variance (ANOVA) tests were also performed using Minitab. ANOVA calculations test the null hypothesis that the means for all test populations are equal (Scheaffer and McClave, 1995). Data was organized and compared as described for the boxplots, with the test populations being grouped by sub-unit, location, horizon, and lithology. In order to test the null hypothesis, ANOVA calculations use the test statistic:

$$F = \frac{\sum_{i=1}^p N_i (\bar{y}_i - \bar{y})^2}{s_p^2 (p-1)}, \quad (1)$$

where N_i is the sample size for each population, \bar{y}_i is the mean for each population, \bar{y} is the mean for all populations, p is the number of populations, and

$$s_p^2 = \frac{\sum_{i=1}^p (N_i - 1) s_i^2}{N - p}, \quad (2)$$

where N is the total number of samples, and s_i is the standard deviation for each population (Scheaffer and McClave, 1995). ANOVA tests are done with the assumption that each population has a normal probability distribution. If $F > F_{\alpha}(p-1, N-p)$, where F_{α} is F at the acceptable error α , then the null hypothesis should be rejected (Scheaffer and McClave, 1995). F_{α} was determined using the “Tables of percentage points of the inverted Beta (F)-distribution” from Merrington (1943). The p-value represents the probability of making a Type 1 error, or rejecting the null hypothesis when it is true (Scheaffer and McClave, 1995). The smaller the p-value, the smaller the probability that rejection of the null hypothesis would be made in error. The null hypothesis is rejected

when the p-value is less than the cutoff value (Scheaffer and McClave, 1995). The cutoff value often used is α (Scheaffer and McClave, 1995) and in this study was set at 0.05. In addition to the ANOVA tests, 2-sample T tests were performed using Minitab. These tests compute a confidence interval and perform hypothesis testing of the difference between two population means when standard deviations are unknown and samples are drawn independently from each other. Data was organized and compared as described for the boxplots and ANOVA tests, with test populations being grouped by sub-unit, location, horizon, and lithology. The T statistic for comparison of two sample populations is defined by:

$$T = \frac{(\bar{y}_1 - \bar{y}_2) - D_0}{s_p^2 \sqrt{\frac{1}{N_1} + \frac{1}{N_2}}}, \quad (3)$$

where \bar{y}_1 and \bar{y}_2 are the population means for populations 1 and 2, D_0 is the estimated difference or 0, and N_1 and N_2 are the number of samples in population 1 and 2 respectively (Scheaffer and McClave, 1995). If $T > T_\alpha$, where T_α is T at the acceptable error of α , then the null hypothesis was rejected. T_α was determined using the “Table of percentage points of the t-Distribution” from Merrington (1941). This procedure assumes that distributions are normal for both populations (Scheaffer and McClave, 1995). As with the ANOVA tests, p-values were used to help avoid Type I errors. The cutoff value used in this analysis was 0.05.

Permeability testing was attempted for at least one sample from each horizon. Unfortunately, the permeability of silty shale and shale samples was too low to perform tests within a reasonable amount of time. The permeability tests were performed

concurrently with some of the triaxial shear tests, and used the same test configuration with the addition of Isopar H pumped into the bottom of the samples at a rate of 4 ml/hr. The pore pressure at the point of injection was measured using a pressure gauge. [Axial and lateral displacements were always measured with LVDT's because strain gauges have a tendency to separate slightly from the sample when internal fluid pressure is applied, rendering the measurements unreliable.] Using the measured pore pressure and fluid injection rate, it was possible to calculate the permeability of each sample using Darcy's law:

$$k_i = \frac{q\mu L}{\Delta P_f}, \quad (4)$$

where k_i is intrinsic permeability, q is flow volume per unit area, μ is fluid viscosity, L is sample length, and ΔP_f is fluid pressure change across the length of the sample (Domenico and Schwartz, 1990).

Porosity and bulk density measurements were performed on at least one sample from each horizon and lithology. Porosity measurements were made using a Coberly-Stevens porosimeter and helium (Brown, 1981). Bulk density calculations were made by dividing the weight of the sample by the volume of the sample. The volume was calculated by placing the sample into a known volume of water and determining the amount of water displaced by the sample. This process was performed quickly so as to minimize the amount of water entering the pores of the sample.

2.2 MODELING METHODS

The depositional and thermal histories of the Midland Basin, specifically the area of the E. T. O'Daniel No. 28 well, was simulated using a 1-dimensional numerical model.

Heat conduction in a 1-dimensional fixed reference frame is governed by the diffusion equation:

$$\frac{\partial^2(K_T T)}{\partial z^2} + A = \rho_b C \left(\frac{\partial T}{\partial t} + \frac{\partial T}{\partial z} \bar{s} \right), \quad (5)$$

where T is temperature, K_T is thermal conductivity, ρ_b is bulk density, C is effective specific heat, \bar{s} is sedimentation or erosion rate, A is radioactive heat generation per unit volume, z is depth, and t is time (Furlong and Edman, 1984). This equation is solved for $T(z,t)$ using a finite-difference solution scheme, implementing the Crank-Nicholson approach (Hornbeck, 1975). The solution accounts for the effects on subsurface temperature of changing porosity, erosion, and surface temperature. The thermal history model and formulation is an adaptation of an algorithm discussed by Furlong and Edman (1984).

Boundary conditions include a specified heat flux at the base of the model and a specified temperature at the surface of the model (Table 1). The finite difference model is node-centered, with a constant node spacing of 50 m. The numerical solution was tested for simple conditions against an analytical solution for erosion and deposition (Kappelmeyer and Haenel, 1974).

Additionally, the hydrocarbon generation history was estimated within the model, to evaluate the timing of potential elevated fluid pressures by hydrocarbon generation and the possible hydrofracturing associated with the overpressuring. Oil and gas generation rates were calculated using a first order kinetics approach, by integrating

Table 1: Formation thickness and period of deposition used for model input and values of T_0 used in model

LAYER NUMBER	FORMATION NAME	THICKNESS (m)	TIME START	TIME END	LOW T_0 (°c)	AVERAGE T_0 (°c)	HIGH T_0 (°c)
1	FREDERICKSBURG/PALUXY UNCONFORMITY	48	140	72	20	21.5	23
2	CHINLE	192	200	140	20	21.5	23
3	SANTA ROSA UNCONFORMITY	120	219.5	200	16	17.5	19
4	DEWEY LAKE UNCONFORMITY	120	230	219.5	16	17.5	19
5	RUSTLER	60	250	230	18	19.5	21
6	SALADO	192	251.6	250	20	21.5	23
7	TANSILL	72	253.3	253.3	18	19	20
8	YATES	120	255	255	18	19	20
9	SEVEN RIVERS	108	255.8	255.8	18	19	20
10	QUEEN	192	257	257	18	19	20
11	GRAYBURG	120	258.1	258.1	18	19	20
12	SAN ANDRES	360	260	260	18	19	20
13	WORD	528	261.2	261.2	10	12.5	15
14	SPRABERRY	288	264.8	264.8	18	19	20
15	UNNAMED SHALE	144	270	270	18	19	20
16	DEAN	48	273	273	15	16.5	18
17	WOLFCAMP UNCONFORMITY	432	274	274	15	16.5	18
18	STRAWN	48	275	275	18	19	20
19	BEND UNCONFORMITY	192	290	290	18	19	20
20	BARNETT/MISSISSIPPIAN LIME/WOODFORD UNCONFORMITY	72	308	308	15.0	16.5	17.6
21	DEVONIAN	72	312	312	18	19	20
22	SILURIAN SHALE/FUSSELMAN UNCONFORMITY	48	325	325	18	19	20
23	MONTROYA/SIMPSON	48	330	330	8.0	9.0	10.0
24	ELLENBURGER	216	387	387	14	15.75	17.5
			425	420	16.5	17.75	19
			455	485	18	19	20

$$\frac{dy}{dt} = -\frac{dx}{dt} = -k(T)x \quad , \quad (6)$$

where component x is being converted to component y (e.g. kerogen to oil and oil to gas), t is time and T is temperature (Sweeney, 1990). The Arrhenius equation has been used since the late 1800's to describe $k(T)$:

$$k = A \exp\left(-\frac{E}{RT}\right) \quad (7)$$

where A is a frequency factor in s^{-1} , the Arrhenius constant; E is the activation energy in J/mol; and R is the gas constant, equal to 8.31 J/mol $^{\circ}$ K (Sweeney, 1990). During the model simulation of the basin's history, the integration is performed to calculate rates of conversion from kerogen to oil and rates at which oil cracks to gas. Temperatures calculated within the model for this process, but output from oil and gas generation calculations are not used in the temperature calculations.

The constants A and E are independent kinetic parameters which need to be identified individually. Different depositional environments produce three types of kerogens with very different values of A and E (Tissot and Welte, 1984; Sweeney, 1990). Type I kerogens are lacustrine in origin, Type II are derived from marine sediments, and Type III are produced from terrestrial deposits (Tissot and Welte, 1984; Sweeney, 1990). As discussed earlier, petroleum in the Spraberry Formation is thought to be derived from organic carbon deposited concurrently with the Spraberry Formation. The Spraberry Formation originated in a marine environment, which would indicate that the kerogens are Type II. Based on this evaluation, values of A and E applicable to Type II kerogens were assigned in the model, including $A = 4.69E+13 s^{-1}$, and $E = 2.09E+5 J/mol$ for conversion of kerogen to oil (Tissot and Welte, 1984). For cracking of oil to gas, $A =$

$1.00\text{E}+13 \text{ s}^{-1}$, and $E = 2.3\text{E}+5 \text{ J/mol}$ were used as input parameters (Tissot and Welte, 1984). Once the kinetic parameters have been identified and equation (7) substituted into (6), equation (6) is integrated over the geologic history.

The geologic history must be assumed a priori. Specific information necessary for the model is listed in Tables 1 through 3. The Humble No. 1 Buchanan well was used to estimate the formation thicknesses (listed in Table 1) and is shown in Figure 11. This Well is located a few miles from the E. T. O'Daniel No. 28 well, whose core was used for the laboratory testing. Timing of deposition for the different stratigraphic layers were estimated from the geologic history discussed previously (Table 1). Environment of deposition and possible surface temperatures were inferred from the geologic history.

Ranges of temperatures produced by different marine environments were estimated from temperature versus depth profiles from the website of San Francisco State University (Grove, 2000, world-wide-web publication). The midpoint of the range appropriate for a particular environment was used for the original surface temperature (T_o) in this study. The model's sensitivity to variations in this parameter was tested using the extremes of the range identified by Grove (2000, world-wide-web publication). Values used in this study are shown in Table 1.

Fluid and temperature flow parameters such as original porosity (n_o) and thermal conductivity (K_T) are also required in the input file. The model assumes that as a result of compaction, n_o was significantly larger than porosity (n) is today. Hubbert and Ruby (1960) showed that for lithostatic pressures, n can be represented by the equation:

$$n = n_o \exp^{(-zC)} \quad (8)$$

Table 2: Normalization of n_0 values by formation for model input

LAYER NUMBER	FORMATION NAME	LITHOLOGIC MATERIAL	THICKNESS (m)	LOW n_0		MEAN n_0		HIGH n_0	
				ORIG n_0	ARITHMETIC AVERAGE n_0	ORIG n_0	ARITHMETIC AVERAGE n_0	ORIG n_0	ARITHMETIC AVERAGE n_0
1	FREDERICKSBURG/PALUXY	LIMESTONE	23.99	0.00	0.13	0.25	0.32	0.50	0.52
2	CHINLE	SANDSTONE	23.99	0.26		0.40		0.53	
		SHALE	132.01	0.34	0.33	0.47	0.47	0.60	0.60
		SANDSTONE	12.01	0.26		0.40		0.53	
		SHALE	47.98	0.34		0.47		0.60	
3	SANTA ROSA	SANDSTONE	60.02	0.26	0.27	0.40	0.40	0.53	0.54
		SHALE	12.01	0.34		0.47		0.60	
		SANDSTONE	47.98	0.26		0.40		0.53	
4	DEWEY LAKE	SANDSTONE	120.00	0.26	0.26	0.40	0.40	0.53	0.53
5	RUSTLER	SANDSTONE	36.00	0.01	0.11	0.03	0.17	0.05	0.24
		SALT & ANHYDRITE	23.99	0.26		0.40		0.53	
6	SALADO	SALT	191.99	0.01	0.01	0.01	0.01	0.01	0.01
7	TANSILL	ANHYDRITE	47.98	0.01	0.09	0.03	0.15	0.05	0.21
		SANDSTONE	23.99	0.26		0.40		0.53	
8	YATES	ANHYDRITE	96.01	0.01	0.06	0.03	0.10	0.05	0.15
		SANDSTONE	23.99	0.26		0.40		0.53	
9	SEVEN RIVERS	ANHYDRITE	47.98	0.01	0.09	0.03	0.15	0.05	0.20
		SALT	23.99	0.01		0.01		0.01	
		SANDSTONE	36.00	0.26		0.40		0.53	
10	QUEEN	ANHYDRITE	47.98	0.01	0.05	0.03	0.09	0.05	0.13
		SANDSTONE	23.99	0.26		0.40		0.53	
		ANHYDRITE	36.00	0.01		0.03		0.05	
		SALT	47.98	0.01		0.01		0.01	
		ANHYDRITE	23.99	0.01		0.03		0.05	
		SANDSTONE	12.01	0.26		0.40		0.53	
11	GRAYBURG	DOLOMITE	120.00	0.00	0.00	0.10	0.10	0.20	0.20
12	SAN ANDRES	LIMESTONE	96.01	0.00	0.07	0.25	0.29	0.50	0.51
13	WORD	SANDSTONE	23.99	0.26		0.40		0.53	
		LIMESTONE	120.00	0.00		0.25		0.50	
		SANDSTONE	23.99	0.26		0.40		0.53	
		LIMESTONE	47.98	0.00		0.25		0.50	
		SANDSTONE	47.98	0.26		0.40		0.53	
		LIMESTONE	23.99	0.00	0.27	0.25	0.42	0.50	0.56
		SANDSTONE	240.00	0.00		0.40		0.53	
		LIMESTONE	23.99	0.00		0.25		0.50	
		SHALE	240.00	0.34		0.47		0.60	
14	SPRABERRY	SANDSTONE	96.01	0.26	0.30	0.40	0.43	0.53	0.56
		SHALE	36.00	0.34		0.47		0.60	
		SANDSTONE	12.01	0.26		0.40		0.53	

Table 2: Normalization of n_0 values by formation for model input

LAYER NUMBER	FORMATION NAME	LITHOLOGIC MATERIAL	THICKNESS (m)	LOW n_0		MEAN n_0		HIGH n_0	
				ORIG n_0	ARITHMETIC AVERAGE n_0	ORIG n_0	ARITHMETIC AVERAGE n_0	ORIG n_0	ARITHMETIC AVERAGE n_0
15	UNNAMED SHALE	SHALE	47.98	0.34	0.47	0.60			
16	DEAN	SANDSTONE	23.99	0.26	0.40	0.53			
17	WOLFCAMP	SHALE	47.98	0.34	0.47	0.60			
		SANDSTONE	23.99	0.26	0.40	0.53			
		SHALE	143.99	0.34	0.47	0.60	0.34	0.47	0.60
		SANDSTONE	47.98	0.26	0.40	0.53	0.26	0.40	0.53
		LIMESTONE	96.01	0.00	0.25	0.50	0.21	0.38	0.56
		SHALE	47.98	0.34	0.47	0.60			
		LIMESTONE	71.99	0.00	0.25	0.50			
		SHALE	216.01	0.34	0.47	0.60			
18	STRAWN	LIMESTONE	47.98	0.00	0.25	0.50	0.00	0.25	0.50
19	BEND	LIMESTONE	47.98	0.00	0.25	0.50	0.26	0.42	0.58
		SHALE	143.99	0.34	0.47	0.60			
20	BARNETT/MISSISSIPPIAN LIMEWOODFORD	SHALE	23.99	0.34	0.47	0.60	0.23	0.40	0.57
		LIMESTONE	23.99	0.00	0.25	0.50			
		SHALE	23.99	0.34	0.47	0.60			
21	DEVONIAN	LIMESTONE	143.99	0.00	0.25	0.50	0.00	0.25	0.50
22	SILURIAN SHALE/FUSSELMAN	LIMESTONE & SHALE	47.98	0.00	0.25	0.50	0.00	0.20	0.40
		DOLOMITE	23.99	0.00	0.10	0.20	0.00	0.25	0.50
23	MONTOYA/SIMPSON	LIMESTONE	23.99	0.00	0.25	0.50	0.00	0.25	0.50
		LIMESTONE	23.99	0.00	0.25	0.50	0.00	0.25	0.50
24	ELLENBURGER	DOLOMITE	216.01	0.00	0.10	0.20	0.00	0.10	0.20

Table 3: Normalization of effective thermal conductivity values by formation for model input

LAYER NUMBER	FORMATION NAME	LITHOLOGIC MATERIAL	THICKNESS (m)	HIGH k_T			MEAN k_T			LOW k_T		
				THERM k_T	GEOMETRIC MEAN k_T	THERM k_T	THERM k_T	GEOMETRIC MEAN k_T	THERM k_T	GEOMETRIC MEAN k_T	THERM k_T	GEOMETRIC MEAN k_T
1	FREDERICKSBURG/PALUXY	LIMESTONE	23.99	3.25	4.03	2.02	2.44	1.25	1.48			
		SANDSTONE	23.99	5.00	2.96		1.75					
		SHALE	132.01	3.50	3.94	2.29	2.49	1.50	1.58			
2	CHINLE	SANDSTONE	12.01	5.00		2.96		1.75				
		SHALE	47.98	3.50		2.29		1.50				
		SANDSTONE	60.02	5.00	4.44	2.96	2.72	1.75	1.66			
3	SANTA ROSA	SHALE	12.01	3.50		2.29		1.50				
		SANDSTONE	47.98	5.00		2.96		1.75				
		SANDSTONE	120.00	5.00	5.00	2.96	2.96	1.75	1.75			
4	DEWEY LAKE	SANDSTONE	120.00	5.00	5.00	2.96	2.96	1.75	1.75			
		SANDSTONE	36.00	6.60	5.74	5.30	3.96	4.25	2.73			
		SALT & ANHYDRITE	23.99	5.00		2.96		1.75				
5	RUSTLER	SANDSTONE	191.99	6.60	6.60	5.30	5.30	4.25	4.25			
		SHALE	47.98	6.60	5.74	5.30	3.96	4.25	2.73			
		SANDSTONE	23.99	5.00		2.96		1.75				
6	SALADO	SANDSTONE	96.01	6.60	5.74	5.30	3.96	4.25	2.73			
		SHALE	23.99	5.00		2.96		1.75				
		SANDSTONE	23.99	5.00	6.02	5.30	4.36	4.25	3.16			
7	TANSILL	SHALE	47.98	6.60	6.02	5.30	4.36	4.25	3.16			
		SANDSTONE	36.00	5.00		2.96		1.75				
		SHALE	47.98	6.60	6.02	5.30	4.36	4.25	3.16			
8	YATES	SANDSTONE	23.99	5.00		2.96		1.75				
		SHALE	36.00	6.60		2.96		1.75				
		SANDSTONE	23.99	5.00	6.02	5.30	4.36	4.25	3.16			
9	SEVEN RIVERS	SANDSTONE	47.98	6.60	6.02	5.30	4.36	4.25	3.16			
		SHALE	23.99	5.00		2.96		1.75				
		SANDSTONE	36.00	6.60	6.02	5.30	4.36	4.25	3.16			
10	QUEEN	SANDSTONE	47.98	6.60	6.02	5.30	4.36	4.25	3.16			
		SHALE	23.99	5.00		2.96		1.75				
		SANDSTONE	36.00	6.60	6.02	5.30	4.36	4.25	3.16			
11	GRAYBURG	SANDSTONE	47.98	6.60	6.02	5.30	4.36	4.25	3.16			
		SHALE	23.99	5.00		2.96		1.75				
		SANDSTONE	36.00	6.60	6.02	5.30	4.36	4.25	3.16			
12	SAN ANDRES	SANDSTONE	47.98	6.60	6.02	5.30	4.36	4.25	3.16			
		SHALE	23.99	5.00		2.96		1.75				
		SANDSTONE	36.00	6.60	6.02	5.30	4.36	4.25	3.16			
13	WORD	SANDSTONE	47.98	6.60	6.02	5.30	4.36	4.25	3.16			
		SHALE	23.99	5.00		2.96		1.75				
		SANDSTONE	36.00	6.60	6.02	5.30	4.36	4.25	3.16			
14	SPRABERRY	SANDSTONE	47.98	6.60	6.02	5.30	4.36	4.25	3.16			
		SHALE	23.99	5.00		2.96		1.75				
		SANDSTONE	36.00	6.60	6.02	5.30	4.36	4.25	3.16			

Table 3: Normalization of effective thermal conductivity values by formation for model input

LAYER NUMBER	FORMATION NAME	LITHOLOGIC MATERIAL	THICKNESS (m)	HIGH k_T			MEAN k_T			LOW k_T		
				THERM k_T	GEOMETRIC MEAN k_T	THERM k_T	GEOMETRIC MEAN k_T	THERM k_T	GEOMETRIC MEAN k_T	THERM k_T	GEOMETRIC MEAN k_T	
15	UNNAMED SHALE	SANDSTONE	12.01	5.00		2.96		1.75				
16	DEAN	SHALE	47.98	3.50		2.29		1.50				
17	WOLFCAMP	SANDSTONE	23.99	5.00		2.96		1.75				
		SHALE	47.98	3.50		2.29		1.50				
		SANDSTONE	23.99	5.00		2.96		1.75				
		SHALE	143.99	3.50	3.50	2.29	2.29	1.50	1.50			
		SANDSTONE	47.98	5.00	5.00	2.96	2.96	1.75	1.75			
		LIMESTONE	96.01	3.25	3.37	2.02	2.02	1.25	1.25			
		SHALE	47.98	3.50		2.29		1.50				
		LIMESTONE	71.99	3.25		2.02		1.25				
		SHALE	216.01	3.50		2.29		1.50				
18	STRAWN	LIMESTONE	47.98	3.25	3.25	2.02	2.02	1.25	1.25			
19	BEND	LIMESTONE	47.98	3.25	3.37	2.02	2.02	1.25	1.25			
		SHALE	143.99	3.50		2.29		1.50				
20	BARNETT/MISSISSIPPIAN LIME/WOODFORD	SHALE	23.99	3.50	3.41	2.29	2.29	1.50	1.50			
		LIMESTONE	23.99	3.25		2.02		1.25				
		SHALE	23.99	3.50		2.29		1.50				
21	DEVONIAN	LIMESTONE	143.99	3.25	3.25	2.02	2.02	1.25	1.25			
22	SILURIAN SHALE/FUSSELMAN	LIMESTONE & SHALE	47.98	3.25	4.32	2.02	2.02	1.25	1.25			
		DOLOMITE	23.99	5.75		3.60		2.25				
23	MONTOYASIMPSON	LIMESTONE	23.99	3.25	3.25	2.02	2.02	1.25	1.25			
		LIMESTONE	23.99	3.25		2.02		1.25				
24	ELLENBURGER	DOLOMITE	216.01	5.75	5.75	3.60	3.60	2.25	2.25			

where z is burial depth and C is a constant equal to the depth at which porosity is reduced to $\frac{n_0}{\exp}$. Sclater and Christie (1980) made comparisons between porosity and depth and identified a range of C from 0.27 to 0.71, depending on lithology. This study area is dominated by rocks with the lower range of C values. Therefore the following equation was used in the model:

$$n = n_0 \exp^{(-z/3)} \quad (9)$$

Estimates of n_0 assigned in the model are listed in Table 2. Domenico and Schwartz (1990) identified ranges of n values for unconsolidated sediments. It is assumed that sand is a precursor to sandstone, and therefore the porosity for sand is an appropriate representation of n_0 for sandstone. Similarly, clay porosity represents n_0 for shale, and so on. As shown in Figure 11 (Jones, 1949), a particular formation may consist of layers of different lithologies and widely varying porosity. Mean n_0 values were calculated for each formation by applying

$$n_{o,mean} = \frac{(n_{oi}b_i + n_{oj}b_j)}{(b_i + b_j)}, \quad (10)$$

where i and j indicate distinct rock types within one formation and b is equal to layer thickness. The surface porosity values applied in this study (Table 2) are mean n_0 values from average n values for the lithologic descriptions identified from the cross section (Figure 12) reported by Domenico and Schwartz (1990). A sensitivity study was performed using normalized n_0 for the endpoints of the ranges identified.

Finally, thermal conductivity is also needed to solve the diffusion equation (Equation 5). Tissot et al. (1978) identified ranges of thermal conductivity, K_T , for

different rock types. The geometric mean k_T of a formation was determined using the equation:

$$K_{T,mean} = (K_{T1}K_{T2}...K_{Tn})^{1/n}, \quad (11)$$

where n is the number of rock types in the formation. Domenico and Schwartz (1990) and Fetter (1994) both indicate that a geometric mean is more appropriate than either arithmetic or harmonic means for identifying a representative conductivity value. The midpoints of ranges identified by Tissot et al. (1978) were used to determine the mean K_T . A sensitivity analysis was performed using the mean K_T obtained from the maximum and minimum values. Table 3 lists the K_T values used in this study.

2.3 MECHANICAL ANALYSIS

A geomechanical analysis was performed to provide information about the stress and pore fluid pressure conditions that produced the Spraberry Formation fractures. To facilitate analysis, the Spraberry Formation was initially assumed to be under uniaxial strain (ε). In this study, uniaxial strain is used to refer to the condition where horizontal deformation is equal in both directions ($\varepsilon_H = \varepsilon_h$) and not equal to vertical deformation (ε_V). This scenario is similar to a laboratory test in which a sample is compressed vertically but confined laterally by a steel jacket. Uniaxial strain is the simplest and most common assumption used for stress-strain calculations (Erdlac, 1990).

A description of the resulting stresses and strains may be determined from the stress-strain equations:

$$E\varepsilon_H = \sigma_H - \nu(\sigma_V + \sigma_h) \quad (12)$$

$$E\varepsilon_V = \sigma_V - \nu(\sigma_H + \sigma_h) \quad (13)$$

$$E\varepsilon_h = \sigma_h - \nu(\sigma_V + \sigma_H) \quad , \quad (14)$$

where E is Young's modulus, ν is Poisson's ratio, and V , H and h denote vertical, maximum horizontal, and minimum horizontal directions, respectively (Price, 1959; Twiss and Moores, 1992). These equations are based on the following assumptions; 1) linear elastic deformation, 2) strain is infinitesimal, and 3) isotropic elastic moduli. Price (1959) combines the assumption of uniaxial strain with the stress-strain equations to produce the following pre-tectonic conditions:

$$\sigma_V = \rho_b gh \quad (15)$$

$$\sigma_H = \sigma_h = \left(\frac{\nu}{1-\nu} \right) \rho_b gh \quad (16)$$

$$\varepsilon_V = \left[\frac{\rho_b gh}{E} \left(1 - \frac{2\nu^2}{1-\nu} \right) \right], \quad (17)$$

where ρ_b is the bulk density of the sediment, g is gravity, and h is the depth. In other words, equations (15) through (17) describe the stress-strain conditions resulting from a vertical load, in the absence of tectonic forcing. When an additional tectonic stress is imposed in the horizontal direction, the principle of superposition provides total σ_H :

$$\sigma_H = \left(\frac{\nu}{1-\nu} \right) \rho_b gh + \Delta\sigma_H, \quad (18)$$

where $\Delta\sigma_H$ is the additional stress from tectonic forcing. If we now depart from the uniaxial strain condition and assume plane strain with no changes in vertical stress ($\Delta\sigma_V = 0$) and no additional strain in the h direction ($\Delta\varepsilon_h = 0$), then stress and strain can be described by:

$$\sigma_V = \rho_b gh \quad (19)$$

$$\sigma_h = \left(\frac{\nu}{1-\nu} \right) \rho_b gh + \nu\Delta\sigma_H \quad (20)$$

$$\Delta\varepsilon_H = \frac{(1-\nu^2)}{E} \Delta\sigma_H \quad (21)$$

$$\Delta\varepsilon_V = \frac{(\nu+\nu^2)}{E} \Delta\sigma_H \quad (22)$$

where the additional stress from horizontal tectonic compression or extension is related to the imposed strain $\Delta\varepsilon_H$ by:

$$\Delta\sigma_H = \frac{E\Delta\varepsilon_H}{(1-\nu)} \quad (23)$$

If increments of $\Delta\varepsilon_H$ are specified, these equations can be used to calculate σ_H and σ_h for increasing amounts of strain by substituting equation (23) into equations (18) and (20). In this analysis, it is assumed that subsidence and the resulting extension is not having an effect on the stress conditions. In order to produce changes in σ_H that were relatively small but still clearly evident, increments for $\Delta\varepsilon_H$ of 0.00005 were used in this study to determine the effects of the stress produced by the Laramide Orogeny.

It is impossible to determine how much the Spraberry Formation was strained before fracturing occurred, but a range of reasonable strains can be suggested. Each rock is likely to behave differently under similar stress conditions due to different E , ν , and σ_L . The Mohr Coulomb failure envelopes derived from the triaxial shear tests were used to determine the limit of what the rocks can tolerate without failing. The amount of stress that produces failure, or limit stress, measured in triaxial shear can be used to determine an upper boundary of stress that a given material may withstand. We assume that the Spraberry Formation rock layers failed at the limit stress and that the limit stress is independent of time. Lorenz (1997) observed that both the shales above the reservoir units and the reservoirs were fractured, but shales underlying the siltstone reservoirs were

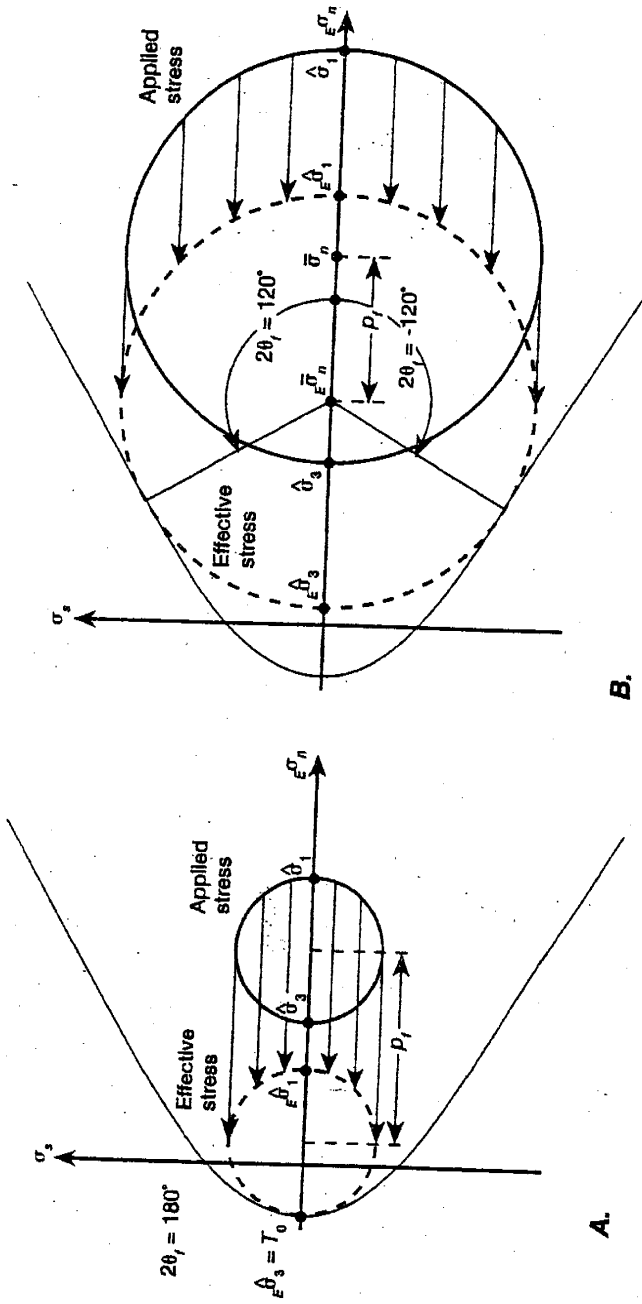


Figure 11: Effects of pore fluid pressure on effective stress and rock failure (Davis and Reynolds, 1996).

to plastic deformation. Tables presenting this information are included in Appendix A. Although the majority of values of E calculated from the test data fall in the middle to low end of the spectrum identified for these rock types, there are a significant number that are well above the range reported by Middleton and Wilcock (1994). Values of E up to $1.41E+05$ MPa were found, which is typical of crystalline rocks such as dunite (Middleton and Wilcock, 1994). Beyond a certain limit, some materials respond to increasing stress with decreasing increments of strain and are said to exhibit strain hardening (Middleton and Wilcock, 1994). Larger E values with increasing axial or lateral stress are expected for rocks where strain hardening occurs and were observed in this study (Figure 13).

The range of Poisson's Ratio (ν) measured during these tests was 0.002 to 0.471 (Table 4, and Appendix A), with the vast majority below 0.2. Middleton and Wilcock (1994) stated that the ν of shales should fall between 0.1-0.2, and sandstone values range from 0.2-0.3, while the range for dolomites has not been identified. Values determined in this study are relatively low, with the majority falling within the range associated with shales. When samples were subjected to greater vertical load, ν also increased (Figure 14). During the triaxial shear tests, a constant rate of vertical displacement was applied, leading to constant increments of vertical strain (ϵ_{11}). As a sample neared failure, increments of lateral strain increased dramatically, ultimately creating fractures. This behavior produced the relationship of increased ν with increasing vertical stress (σ_{11}) shown in Figure 14. Limit strengths (σ_L) from 58.7 to 549.6 MPa were observed in this study, with values depending not only on the rock being tested but also σ_{22} (Figure 15).

Figure 13: Plots of E vs σ_{11} by location for Triaxial Shear tests

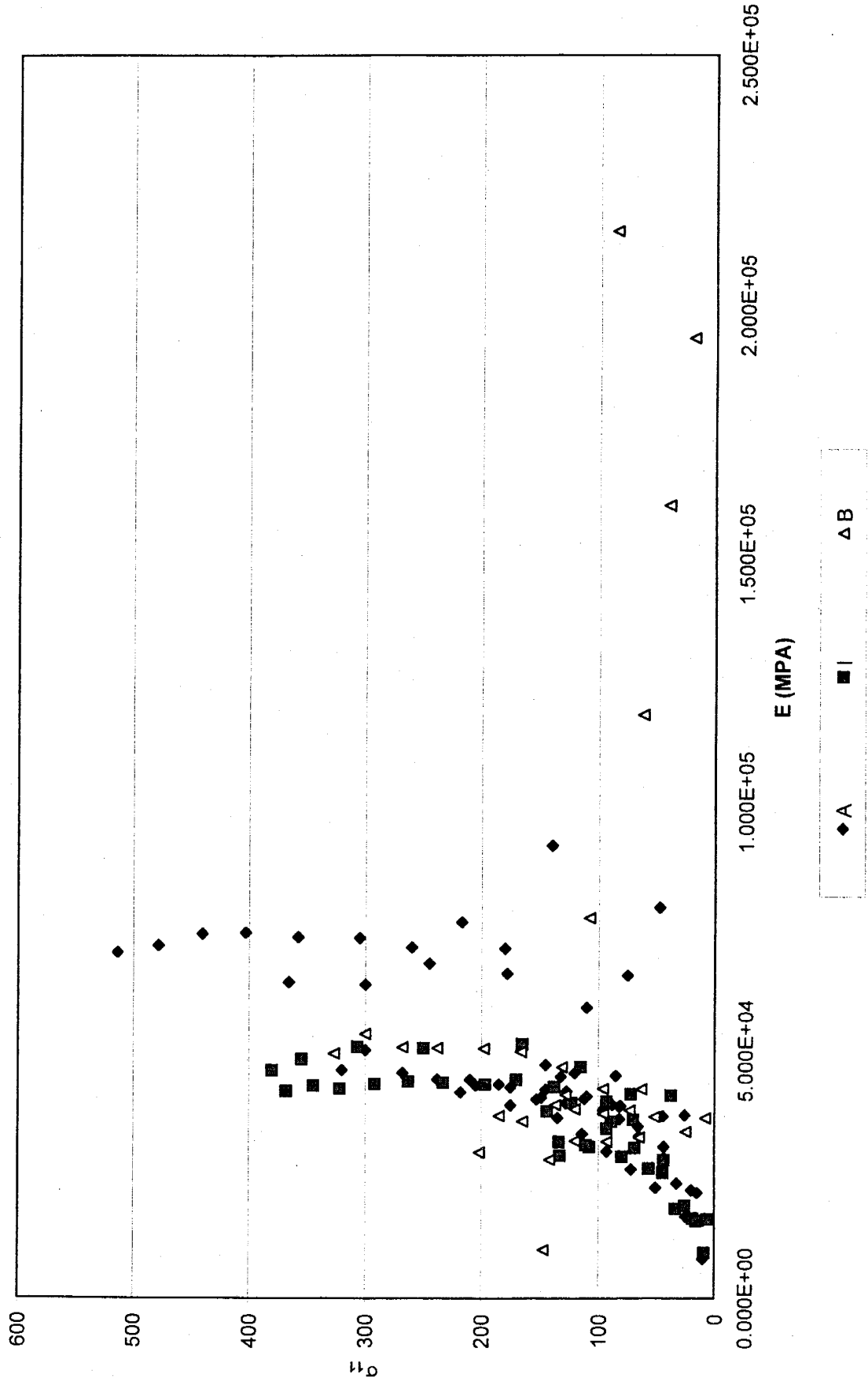


Figure 14: Plots of σ_{11} vs v by location for Triaxial Shear tests

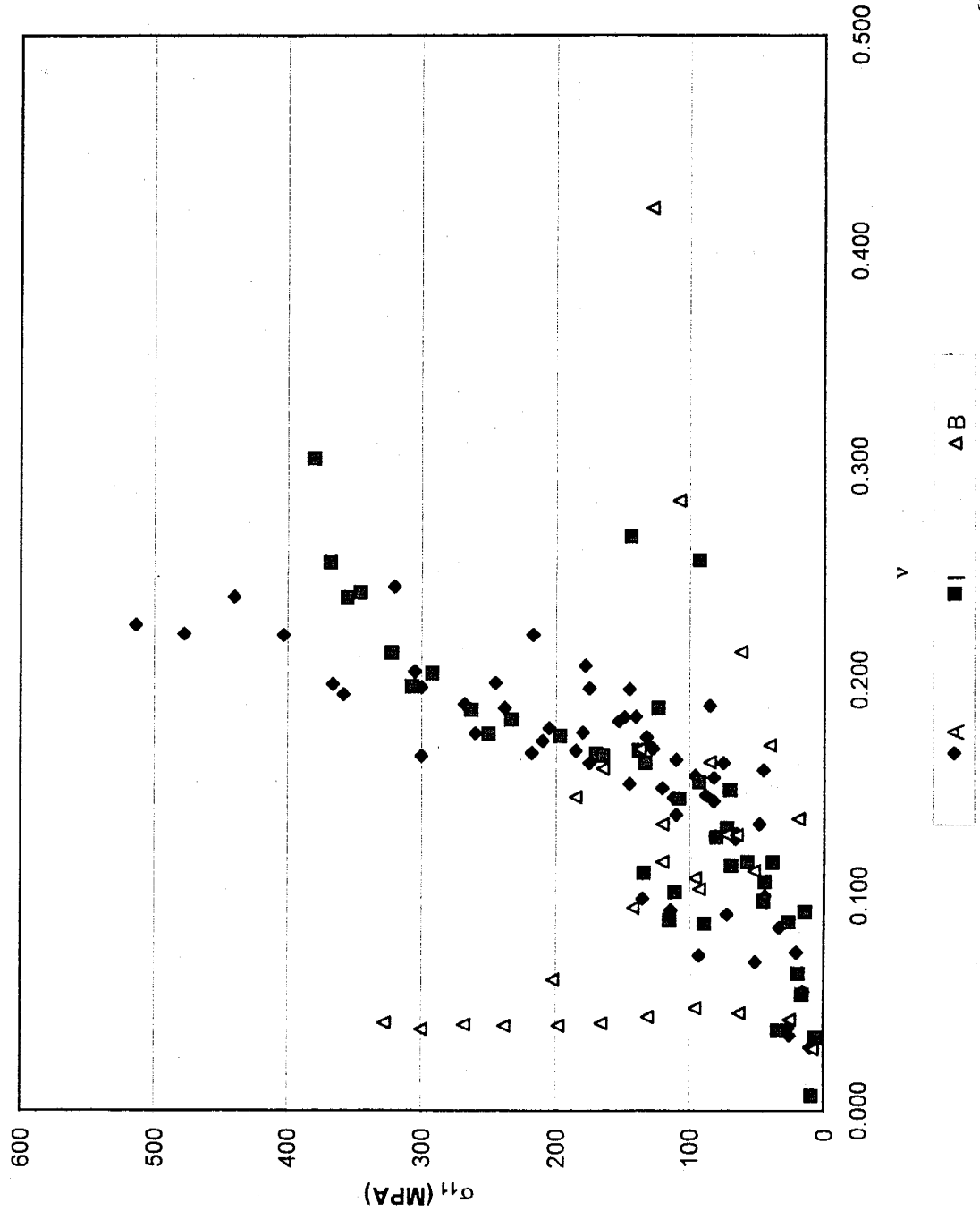
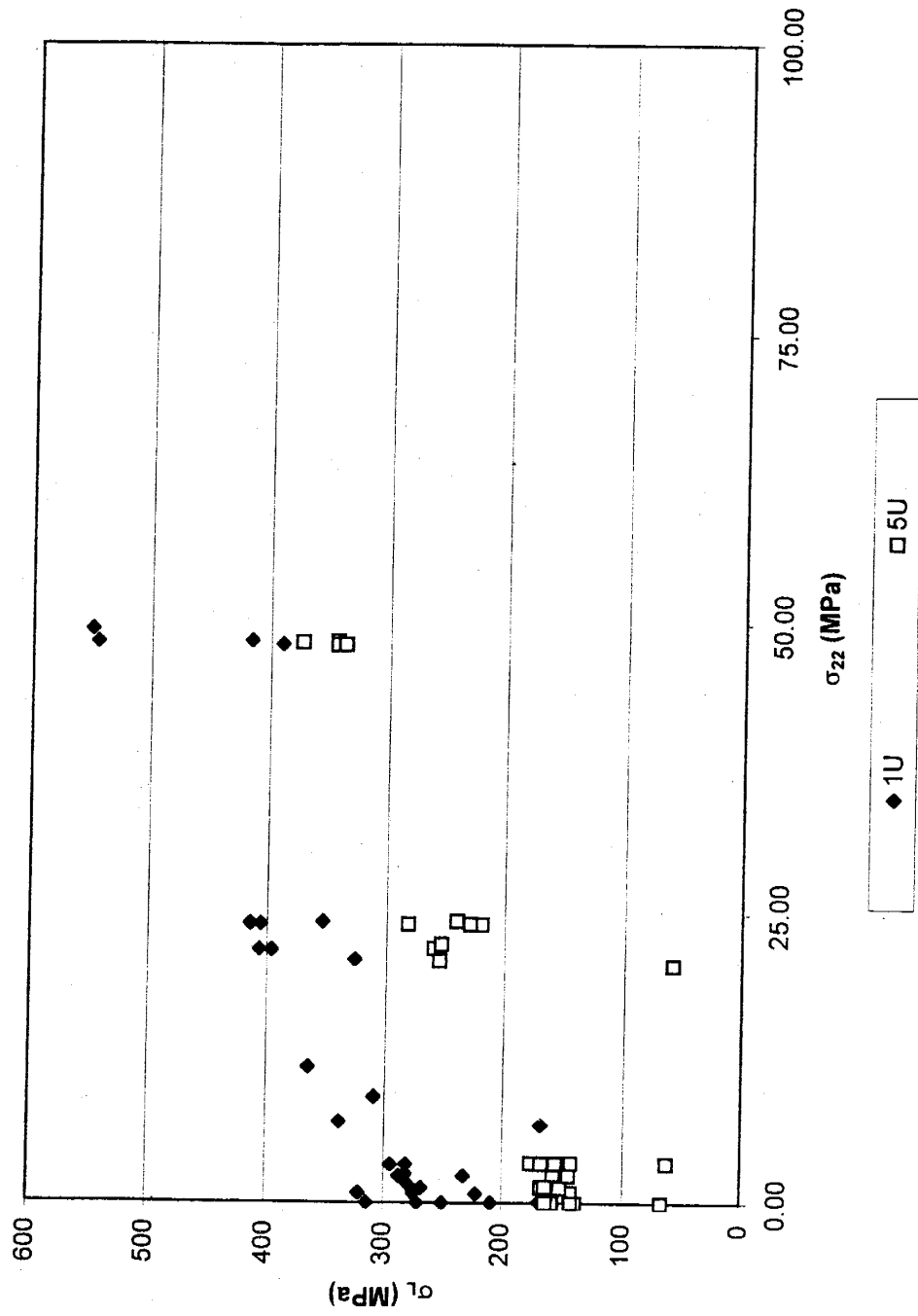


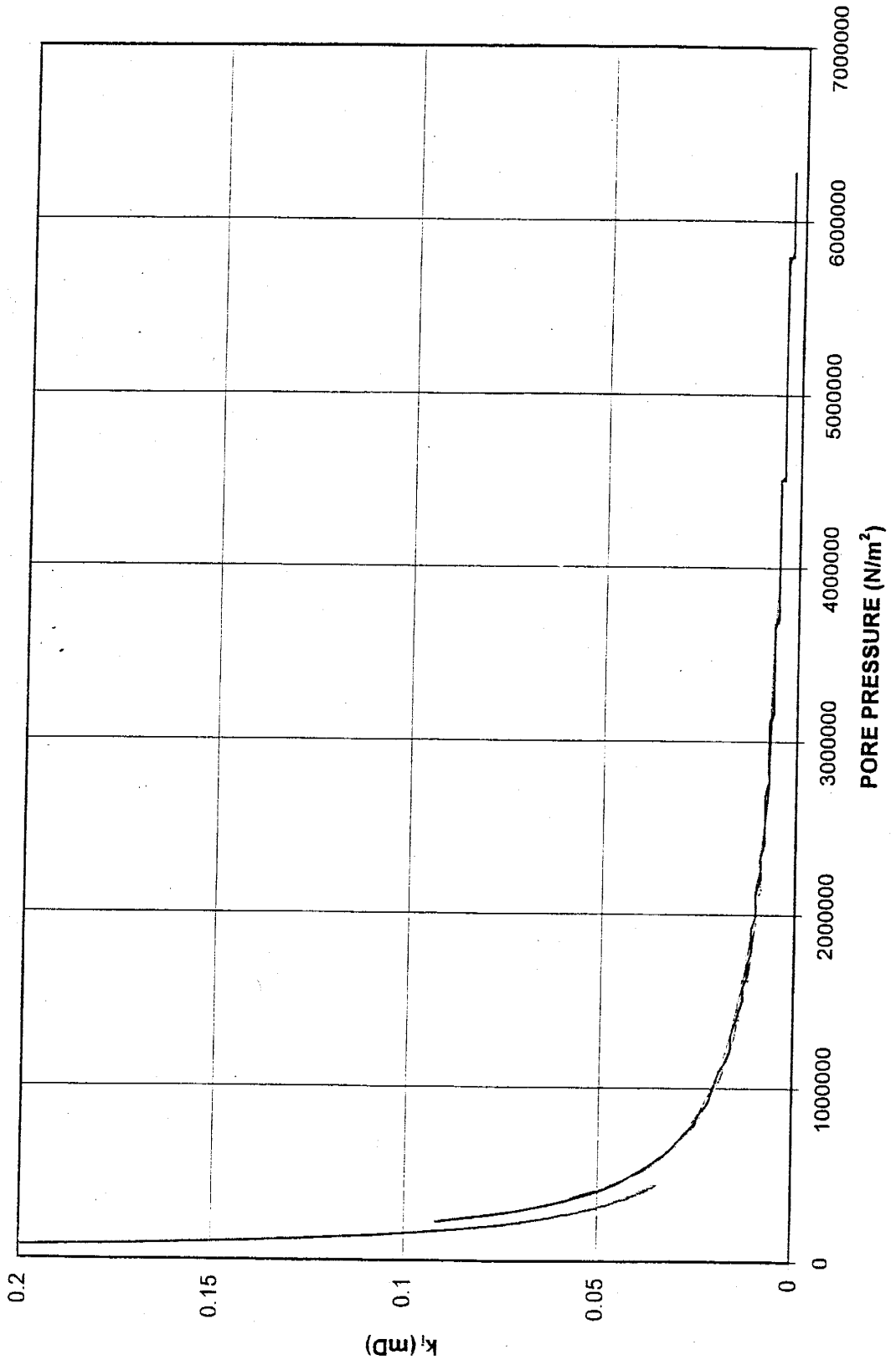
Figure 15: Plots of σ_L vs σ_{22} by sub-unit for Triaxial Shear tests



In general, the σ_L of rocks increases linearly with increase in σ_{22} , as observed in this study (Figure 16).

Intrinsic permeability (k_i), porosity (n), and bulk density (ρ_b) of Spraberry Formation rocks have been measured by a number of researchers. It has been observed that matrix k_i are exceptionally low, which is one of the primary reasons it is so difficult to produce from the Spraberry Formation (Elkins, 1953; Guevara, 1988; McDonald and Schechter, 1990; McDonald and Schechter, 1994). Reported values range from 0.0001-5.0 mD for all Spraberry Formation materials (McDonald and Schechter, 1990; McDonald and Schechter, 1994; Reservoir Inc., 1997). In this study, k_i values were measured only for samples from the reservoir zones, and of these samples the majority were of lithology Type 6 (Figure 2, Table 4). Values for k_i correspond well with the values found in previous research (McDonald and Schechter, 1990; McDonald and Schechter, 1994; Reservoir Inc., 1997). Unlike previous workers, I evaluated k_i during triaxial shear tests. As Figure 16 illustrates, k_i values dropped exponentially with increasing pore pressure, which correlates with increasing σ_{11} . This is most likely in response to the elimination of pore space as the rock was compressed. During these tests, vertical load was applied for a period of time, then stopped in order to allow the sample to equilibrate, and then increases in load were resumed again. As the permeability test continued, it often became difficult to maintain a pore pressure and allow the sample to equilibrate to the new σ_{11} . In several instances, it appeared as if the sample had failed and the test was terminated, only to find that the sample remained intact. I believe that this behavior was due to the development of microfractures in the sample. These microfractures are commonly known as Griffith cracks (Griffith, 1920).

Figure 16: Permeability versus pore pressure increases due to loading during triaxial shear tests



Porosity values determined in other studies for Spraberry Formation rocks have been used to distinguish between pay and non-pay zones (McDonald and Schechter, 1990; McDonald and Schechter, 1994; Reservoir Inc., 1997). Pay zones were found to possess porosity (n) greater than 7%, but averaged 10%, while non-pay zones often had n less than 7%. Porosity measurements made in this study ranged between 6 and 11% (Table 4). Density measurements had a range of values between 2.64 and 2.76 (Table 4).

As mentioned in the discussion about geology and structures of the Spraberry Formation, Lorenz (1997) reported three fracture sets in the formation. These sets are distinct fracture types with distinct distributions and orientations. North-east striking extension fractures (NE) are found only in the 1U reservoir, north-northeast striking extension fractures (NNE) are found only in the 5U pay zone, and east-northeast striking extension and shear fractures (ENE) is found in both the 5U reservoir and shales overlying both pay zones. A remaining issue is how layers that are directly adjacent to each other were able to develop such distinct fracture orientations. In order to answer this question it was first necessary to determine whether sub-unit, location, horizon, lithology, or some combination of the above is the best indicator of mechanical properties and subsequent failure of the Spraberry Formation. It was possible to use the parameters discussed above to make this determination.

Analysis of the data obtained during triaxial shear tests was used to evaluate the relative importance of each category (sub-unit, location, horizon, and lithology) for identifying mechanical properties during elastic and plastic deformation. As mentioned previously, this analysis was performed using analysis of variance (ANOVA) tests, two-sample t tests, boxplots, and plots of σ_L versus σ_{22} . Distinctions between the 1U and 5U

sub-units proved to be quite significant. The null hypothesis for ANOVA tests is that all test populations have the same mean. ANOVA tests comparing means for Young's modulus (E) and Poisson's ratio (ν) determined that the null hypothesis should be rejected, 1U and 5U have statistically different E and ν . The two-sample t test is similar to ANOVA tests. The t test null hypothesis is a bit more explicit than that of the ANOVA tests, the hypothesis is that the means of the two test populations being compared in the test are equal. T test results also indicated that the 1U and 5U have statistically unequal E and ν . These results were the same for elastic and plastic deformation. Results for these tests can be found in Appendix A. Comparisons of limit stress (σ_L) for the two sub-units using boxplots (Figure 17) and a plot of σ_L versus confining pressure (σ_{22}) (Figure 15) indicate that the 1U is much stronger than the 5U. This information is quite as expected. Lorenz (1997) reported variations between the sub-unit fracture patterns. The results just reported are validation that the sub-units should have unique mechanical properties, and therefore should have distinct fracture patterns. In addition, it has been noted that the 1U is a more productive reservoir than the 5U (McDonald and Schecter, 1990; McDonald and Schecter, 1994). This characteristic may also be an artifact of the disparity between the mechanical properties of the two sub-units. The distinct fracture patterns produced by these mechanical differences may ultimately be the cause of production dissimilarities.

As noted earlier, Lorenz (1997) found that the shales underneath the reservoirs are undisturbed, but the reservoirs and shales above them are fractured. By assessing the mechanical properties of a material's location relative to the reservoir, I hoped to identify similarities between the sands and upper shales as well as dissimilarities between shales above and those below pay zones. Based on the geologic setting that produced the

Boxplots of Limit Stress by Sub-unit

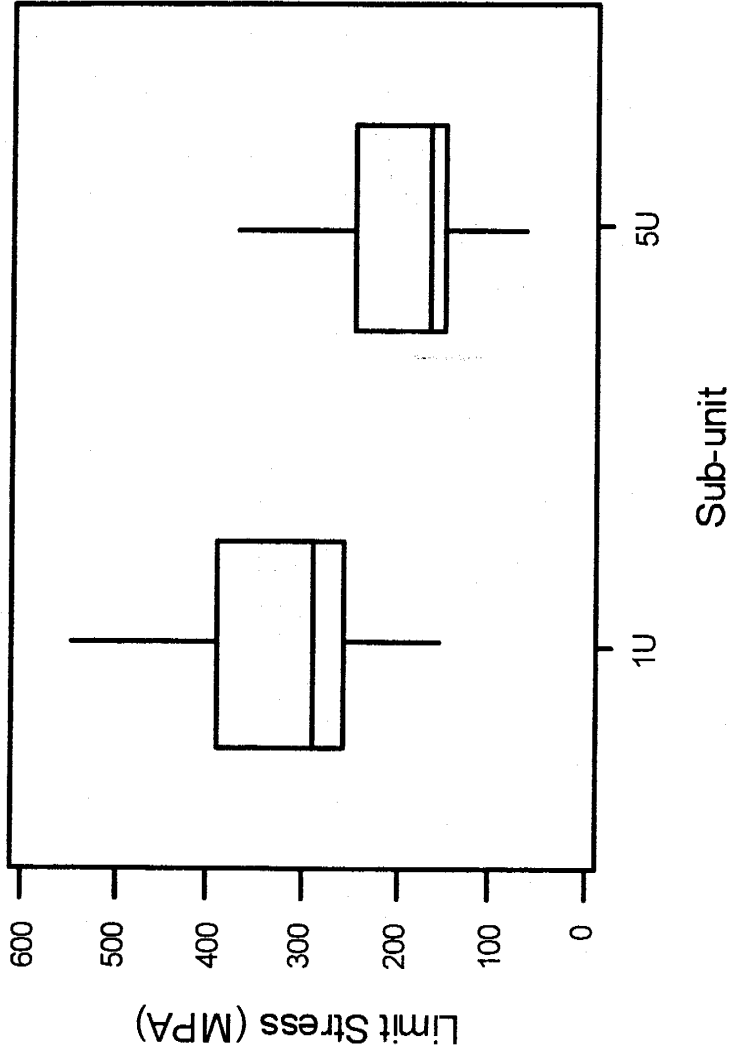


Figure 17: Boxplots of σ_L by sub-unit

Spraberry Formation, it seems likely that the lower contacts of the sand layers would be abrupt as storms washed large amounts of sediment quickly into the basin. In contrast, I expect that there would be a more gradual lithologic transition above the pay zones, as sands and silts continued to filter down with the sediments normally adding to the sedimentary column. These proposed differences between upper and lower contacts might have lead to additional post-depositional similarities in cementation. Fluids flowing through the sandy zones may have penetrated further into upper shales than those beneath because of the reduced contrast in permeability, leading to fewer contrasts in cement composition. Results of ANOVA and t tests indicate that there is no statistical difference between the locations (reservoirs, and shales above and below) for ν in elastic or plastic deformation. These tests did indicate, however, that location is a good indicator for E. Although the results for elastic deformation conflict somewhat with those for plastic deformation, elastic moduli were considered to be better descriptors of elastic behavior and were therefore given greater weight when discrepancies occurred. Results of these tests can be found in Appendix A. Boxplots were not able to illustrate any information to contradict the ANOVA and t test findings, but were able to show that the shales below the reservoirs have a much more compact distribution for σ_L than the other two locations (Appendix A). This indicates a similarity between materials that we know to be fractured that is not shared with the unfractured shales underlying the pay zones. Although this information is useful, it is not clear from the other findings why this behavior occurs. The split in results, with location being a good indicator for E and σ_L , but not for ν , indicates that location is only moderately useful for prediction of mechanical properties.

The usefulness of horizon as an indicator for mechanical properties is less clear than for sub-unit and location. ANOVA tests indicate that there is strong evidence that not all horizon means are equal (Appendix A). T test comparisons were made between the horizons within the 1U, between the horizons within the 5U, as well as between similarly located horizons within the 1U and 5U (i.e. shales above the 1U reservoir versus shales above the 5U reservoir). These tests show that there is no statistical difference in the elastic moduli between the 5U horizons above and below the reservoir, between the 5U reservoir and shales below, between the 1U and 5U reservoirs, or between the shales in the 1U sub-unit (Appendix A). A statistical difference in E and ν is indicated between the shales overlying both reservoirs as well as between the 1U reservoir and shales above it (Appendix A). For all other comparisons, the results depend on the parameter in question. Shales below both pay zones have significantly different E , but ν shows no differentiation (Appendix A). The same relationship was found when comparing the 1U reservoir to the shales below it (Appendix A). Comparison of the 5U reservoir to the shales above it determined the opposite relationship, E is not significantly different, but ν is (Appendix A). As with t test outcomes for location, there was some conflict between results for elastic versus plastic deformation. Because Young's modulus and Poisson's ratio are measures of elastic behavior, results for elastic deformation were considered to be the most accurate. Many of these findings conflict with our understanding of the fracture patterns that exist. Similarities are indicated between horizons that are fractured and unfractured. Dissimilarities and lack of substantive evidence were found in horizons that observed fracture patterns suggest should share mechanical properties.

Boxplots were used to verify the findings of the t tests. In many cases, the boxplots of elastic moduli corroborated the results. Boxplots of σ_L , however, often conflicted with t test results for the elastic moduli; indicating that two groups were statistically different when t tests for moduli had suggested the opposite. Although boxplot differences are a weaker tool than the t test, σ_L is a stronger indicator than elastic moduli of how rocks will ultimately fail. Evaluation of boxplots indicated that the σ_L for shales above the 1U reservoir was similar to the 1U reservoir (Appendix A). The same relationship was found for the 5U, although the σ_L values for 1U rocks were much greater than those for the 5U (Appendix A). All other boxplot comparisons illustrated dissimilarity between horizons. These findings are a better fit with known fracture distribution in the Spraberry Formation than t test results for the elastic moduli. Despite this strong σ_L correlation to known fracture patterns, horizon must be considered a poor predictor of mechanical properties. The t test results offer no explanation for the σ_L relationship and are moduli dependent.

Lithology, as a predictive tool for mechanical properties, makes the most intuitive sense; it seems that a rock's propensity to break should have something to do with its makeup, and that lithologic descriptions should encompass that quality. ANOVA tests indicated that not all lithofacies' means could be considered equal (Appendix A). T tests show that Type 4 (bioturbated or disturbed siltstone, Figure 2) has statistically different elastic moduli from all other lithologic types tested (Appendix A). This relationship was true for both elastic and plastic deformation. Furthermore, t tests provide evidence that Type 3 (finely laminated siltstone, Figure 2) is not distinct from Type 6 (massive to faintly stratified siltstone, Figure 2)(Appendix A). This is interesting, as both lithology

Type 3 and Type 6 have been identified as reservoir material (Figure 2). Whether or not Type 2 (finely laminated silty shale, Figure 2) can be lumped with Types 3 and 6 remains unclear from the t test results. Lithology Type 2 has a Young's modulus that is statistically different than that for Types 3 and 6, but ν does not show the same relationship. Boxplots show that Type 2 has a different distribution of moduli values and σ_L than for Type 3 (Appendix A). The plots do not illustrate the same when comparisons of Type 2 and 6 moduli are made. When boxplots of σ_L are reviewed, Type 6 is shown to have a distinctly larger median and range than Type 2 (Appendix A). This relationship was also evaluated using a plot of σ_L versus σ_{22} (Appendix A). This analysis, in conjunction with the above discussion, indicates that Type 2 is more likely than not to be mechanically different from Types 3 and 6. As a result of this analysis, lithology seems to be a reasonable indicator of mechanical properties.

Boxplots of porosity (n) and bulk density (ρ_b) would suggest that those parameters might be responsible for some of the findings discussed in this section (Appendix A). As only a few measurements of n and ρ_b were performed, the horizon category did not contain enough measurements to perform ANOVA and t tests. Both tests demonstrate that there is no significant difference in n between any other group (Appendix A). ANOVA tests for density produced results that indicate that only the 1U and 5U sub-units do not have statistically different ρ_b (Appendix A). The limited t tests that could be performed showed that ρ_b for the reservoir is not significantly different from the shales lying below the reservoirs (Appendix A). Results of this evaluation are inconclusive due to their limited scope, but contradict the results illustrated in the boxplots. Although further analysis may indeed show that mechanical properties are due

to differences in porosity and density, other factors might prove more useful. Cementation and grain lithology may possibly be more indicative of mechanical properties and ultimately be shown to be the source of the mechanical relationships discussed above.

The conclusion that can be drawn from all of these comparisons is that sub-unit, location, horizon, and lithology are all factors contributing to the mechanical behavior of the Spraberry Formation rocks. There are good reasons for all of them to be useful as predictive tools for identifying mechanical properties. The strongest relationship seems to be that between the sub-units. All tests indicated that the 1U is significantly different from the 5U. Other categories also provided useful information, but relationships were parameter dependent or test results sometimes conflicted with each other.

These parameters can also be used to answer the question: did material properties play an important role in developing the complicated pattern of fractures observed in the Spraberry Formation? Limit stress variations offer the simplest explanation for the observed fracture patterns. Figures 15 and 17 clearly illustrate that the 1U rocks are stronger than their 5U counterparts; significantly lower stresses would provide conditions conducive to producing failure in the 5U, while leaving the 1U intact. Based on this assessment alone, it would be expected that the two zones exhibit different fracture patterns. An additional conclusion that might be drawn from this observation is that the 5U sub-unit failed first. Cather (1997) indicated that the NNE fractures found in the 5U are likely to have formed prior to the NE set found in the 1U based on fracture mineralization. If the shear fractures formed during the Laramide Orogeny, as

hypothesized earlier, this analysis would suggest that NE fractures also formed during the Laramide Orogeny or at some time since.

Cather (1997) postulated that the ENE fracture set found in 5U siltstones and shales above both pay zones formed prior to the NNE set. Once again, Figures 15 and 17 indicate that 5U rocks would fail under conditions that might not produce fractures in the 1U sub-unit. There is little in the previous analysis, however, that explains how the shales overlying the 1U reservoir would fail under stresses that would not produce fractures in the 1U reservoir itself. Limit stresses for reservoir rocks were shown to be statistically similar to the shales that overly them. The analysis of E and ν by horizon showed that the 1U reservoir has elastic moduli that are distinct from the shales above that zone. Both E and ν are higher for the shales than for the siltstones in those horizons, indicating more brittle behavior is likely in the shales. This conclusion is not backed up by the σ_L boxplot results of this study, which show no major differences between the two horizons.

Although the elastic moduli may provide the reason for this pattern, it is not clearly evident from the results of this study. In order to adequately answer this question, further study is warranted.

3.2 MODELING RESULTS

The modeling exercise performed in this study was designed to answer three questions. First, given the geologic and thermal history of the basin, is it possible that the Spraberry Formation is its own source of petroleum? If the Spraberry Formation was generating oil and gas, could this process have had an effect on stresses that produced the formation's fractures? The last question to be answered relates to the reliability of our

estimations. How sensitive is the model to parameter input, and how do changes in these parameters alter the results?

Modeling results indicate that pressures and temperatures were conducive to oil and gas generation in the Spraberry Formation. Houde (1979) made calculations based on current geothermal gradients and determined that parts of the Spraberry Formation reached temperatures between 63° C and 77° C. The results from this study suggest that temperatures reached a maximum of 103° C between 80-70 Ma (Figure 18E). Although these temperatures are higher than Houde (1979) indicated, they are not inconsistent with his findings that temperatures were high enough in the Spraberry Formation's history to have generated petroleum. Temperatures and pressures were enough for solid kerogens to begin converting to oil about 250 Ma, with significant amounts of oil (10%) developing by 210-200 Ma (Figure 18D). Oil generation rates were most rapid between 230-190 Ma. The peak rate was of 1.58 %/Ma during this time. After a period of decreasing oil generation rates, the period between 140-110 Ma evidenced renewed oil conversion (Figure 18C). The second episode only realized small increases in oil generation rates, and reached a maximum rate of 0.29 %/Ma and was terminated when sedimentation ceased. Although the model indicates that conditions are still conducive to oil generation today, rates have slowed significantly and any additional oil conversion is taking place very slowly (Figure 18C).

Model results indicate that ultimately about 76% of the kerogen present was converted to petroleum. Oil began cracking to gas about 245 Ma, about the time that petroleum first began to form. The rates of gas generation peaked at 0.4 %/Ma between 210-200 Ma. As with petroleum generation, the model suggests that oil is still cracking to

Figure 18: Results of modeling study

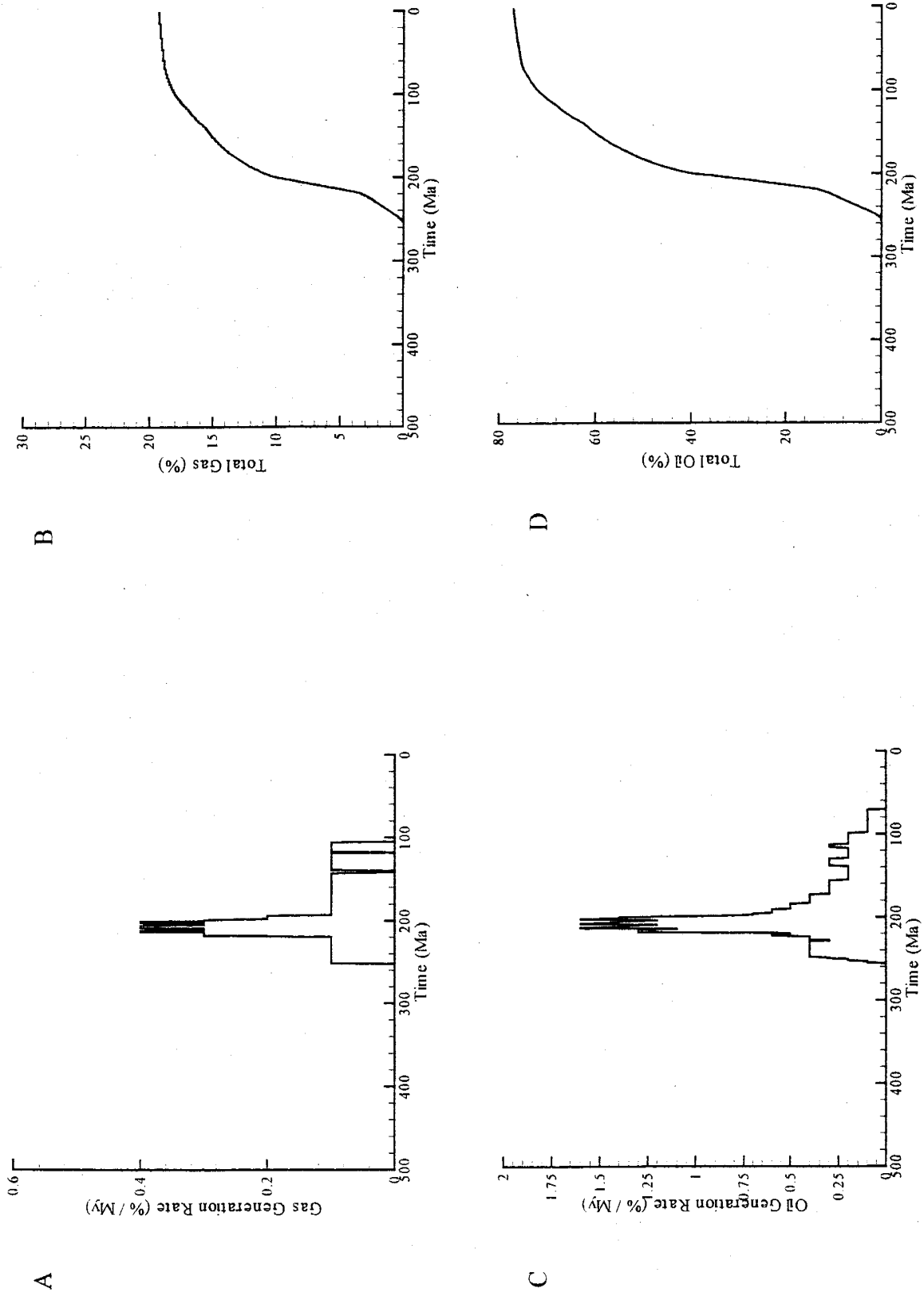
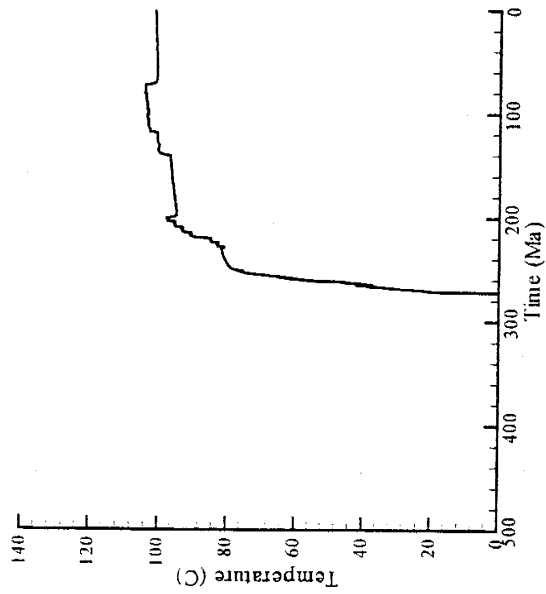
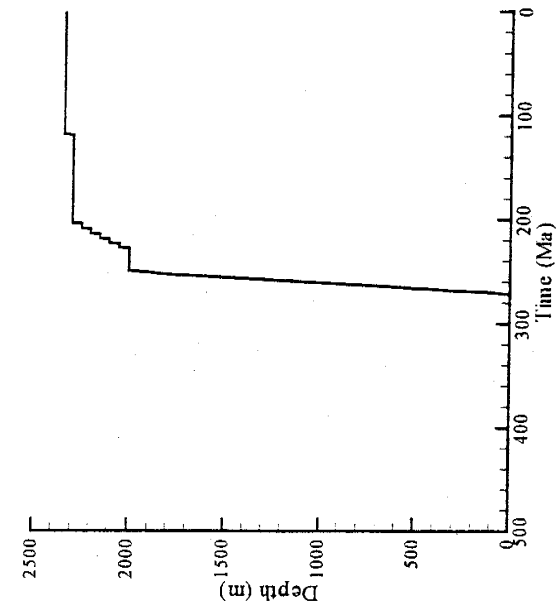


Figure 18: Results of modeling study



gas, but that the rate at which this is occurring has slowed considerably (Figures 18A and B). It is likely that the model was at least reasonably simulating changes in porosity with burial, as final simulated depth of the Spraberry Formation (2350 m) corresponds well with an observed burial depth of approximately 2300 m.

Spraberry Formation petroleum generation may well have had an effect on fluid pressures in the formation. The conversion of kerogen to petroleum results in a volume increase, if the sediments do not permit the new fluid volume to dissipate, elevated pore pressures may be produced. The periods of rapid oil generation are also periods when the formation may not have been able to adjust to volume increases. Modeling results indicate one period of accelerated conversion of kerogen to oil occurred (Figure 18C). This episode took place between 230-190 Ma, when the Santa Rosa Formation and the Chinle Formation were being deposited. A second period of minor increases in oil generation rates is suggested by the modeling results between 140-110 Ma, as the Paluxy Formation was deposited. This period of renewed oil conversion is modeled as ending at the beginning of the Laramide Orogeny, an unconformity that is interpreted to represent the cessation of sedimentation. If, in contrast, sediment deposition did take place during the Laramide and the resulting sediments have since been eroded, petroleum generation could have continued and produced elevated fluid pressures. As discussed previously, pore pressures can act to reduce effective stresses and encourage fracture formation in stress conditions that might not otherwise produce fracturing. In summary, the model results indicate that pore pressures may have been high during two periods, and both should be the focus of increased scrutiny for possible timing of fracturing. The later

phase could have had the effect of decreasing effective Laramide stresses, further encouraging fracture formation.

The sensitivity analysis performed in this study indicates that variations in parameter input do not change the conclusion that the Spraberry Formation could be its own petroleum source. The timing of oil generation and peak pressures, however, may be somewhat altered depending on the choice of parameter values. The results from a simulation performed using high values of thermal conductivity indicate that oil is still generated within the Spraberry Formation, but that onset is delayed and total oil production is drastically reduced due to the dissipation of temperatures through the medium (Appendix B). The results of this simulation produced essentially the same results as Houde (1979), with peak temperatures of 76° C (Appendix B). Although this would indicate that high K_T values are more accurate, the low total petroleum generation conflicts with the knowledge that the Spraberry Formation is one of the largest oil reservoirs in the world. In the results of a simulation performed using low K_T values, the first oil and gas generation rate peak are still evident. The second period, of renewed oil generation, is missing in this simulation (Appendix B). After 200 Ma, oil is rapidly converted to gas in the scenario using low K_T values (Appendix B). This is likely due to the higher temperatures produced in this model. Two model simulation results suggest that low K_T values are not ideal. Decreases in total oil generated after 200 Ma conflict with the evidence of vast quantities of petroleum still in place. Another indicator that low K_T values are not appropriate, is the finding of peak temperatures of approximately 144° C, which are much greater than those found by Houde (1979).

Results from the simulations using a range of original porosity (n_0) values indicate that the model is insensitive to variations of this parameter (Appendix B). Oil and gas are generated at about the same rates and times regardless of n_0 , and temperature and depth histories are virtually unchanged (Appendix B). Model results are affected only slightly more by variations in values of T_0 than they were by changes in n_0 . Although the oil generation history is very similar, oil conversion from kerogen terminates a few million years earlier in high T_0 value simulations than in those with low T_0 values (Appendix B). All other model results are essentially the same regardless of T_0 value, indicating relative insensitivity to this parameter.

As a measure of the degree of certainty that the Spraberry Formation is its own source of petroleum, a simulation was performed using Arrhenius constants and activation energies appropriate for terrigenous sediments, as opposed to those typical for the marine sediments of the Spraberry Formation. Terrigenous kerogen have reactions initiated at different temperatures and with different reaction rates than for kerogens found in marine sediments. Results of these simulations indicate that these changes have a profound effect on the timing and rate of oil generation (Appendix B). Petroleum does not begin to form until approximately 230 Ma in the simulation using terrigenous kinetic parameters, when most other simulations indicated significant oil generation would occur 40 Ma earlier (Appendix B). Model results also indicate that two major peaks in petroleum conversion rates would occur, although the maximum generation rates are much smaller in this simulation than in other scenarios (Appendix B). The first peak occurs at 200 Ma and is coincident with peaks found in other simulations. The maximum kerogen conversion rate at this time is 0.32%/Ma (Appendix B). At 110 Ma, a second

peak of almost equal magnitude was modeled (Appendix B). The combined result of delayed conversion and lower rates results in the cumulative oil percent being significantly smaller than that found in other simulations, at 48% (Appendix B). Delayed oil generation and the second production peak indicated by this simulation may both have had significant impacts on the timing of rock failure. The second peak coincides with the Laramide Orogeny and increased pore pressures made possible by rapid oil conversion could have reduced effective stresses exerted on the region by the orogeny. There is strong evidence that the Spraberry Formation did form in a marine environment, and it is therefore likely that kerogen would be similar to other marine kerogens. What the simulation using terrigenous kinetic parameters does show, is that variations in the kerogen for marine sediments are likely to have significant impacts on the timing and magnitude of oil generation. Future investigations would be advised to more closely constrain values for kinetic parameters for these sediments due to the significance of their impacts.

The conclusion that can be drawn from the sensitivity analyses and the modeling study as a whole, is that there is a reasonable amount of confidence that the Spraberry Formation is its own source for petroleum. Although it is likely that significant amounts of oil was generated and that this may have resulted in elevated fluid pressures at some time during the history of the Spraberry Formation, it is not clear from the model results how important this process was in the production of fractures. The geologic and tectonic history indicate that at least some of the Spraberry Formation fractures are likely to have formed during the Laramide Orogeny. Model simulations indicate that elevated fluid pressures are possible during that time. The depositional history is uncertain at that time

due to an unconformity (Figure 11), and the impact of additional sedimentation on oil generation and subsequent increases in fluid pressures is unknown. Variations in kinetic parameters may also have significant impacts on the timing and magnitude of oil generation. Additional material characterization that constrains these values may produce modeling results that are more reliable.

The modeling methodology used in this study is relatively crude, and could be improved in future studies. The node-centered approach only provides a rough approximation of stratigraphy and does not simulate sedimentation or erosion well. The use of constant node spacing can not adequately reproduce compaction and the resulting changes in layer thickness. A more robust model would be one that is block-centered and has variable node spacing. Such a model could provide a more refined grid that more effectively approximates the effects of compaction on layer thickness. Thermal and hydraulic conductivity can both be altered due to sediment compaction. The effects of these modifications can be very important for temperature flow and the resulting temperature gradients, and should be simulated. Future research that implements these changes could provide more persuasive results than those produced in this study.

3.2 MECHANICAL ANALYSIS RESULTS

This analysis evaluated the conceptual model for fracture generation discussed earlier using the parameters gathered during laboratory testing, knowledge of the stress history, and information about the fractures and conditions that must have produced them. Using the methods described earlier, stress conditions through geologic time was simulated for the different locations, horizons, and lithofacies. The Mohr Coulomb failure envelope was defined for each of these groups and evaluated against the stresses

produced by sediment loading through time (Figure 19). This analysis produced similar results for all materials and indicated that lithostatic stresses, absent abnormal fluid pressures, were insufficient to produce failure in any of the Spraberry Formation rocks (Figure 20). When additional horizontal stresses were applied using constant increments of strain ($\Delta\varepsilon$) to simulate the effects of the Laramide orogeny, shear failure could be produced in all materials (Figure 21). Knowing that the shales beneath the pay zones were unfractured, the least amount of $\Delta\varepsilon$ needed to produce shear failure in those rocks was used as the upper limit that could have been produced by the Laramide compression (Figure 21). As shales beneath both the 1U and 5U sands are the weakest materials evaluated in this study, the added Laramide strain (0.00045) alone did not produce failure in any other rocks (Appendix C). If the tensile strength of the rocks is between 0 and 15 MPa, as is common for most rocks, then the P_f large enough to shift the Mohr circles into a region where extensional failure would occur can be determined. The modeling results indicated that there were two periods of rapid oil generation that are periods of time when elevated P_f were fairly likely. The first period falls between 230-190 Ma, and the second between 140-110 Ma. As discussed previously, the second period of rapid oil generation may well have continued during the Laramide orogeny if additional sedimentation, that is no longer evident due to the presence of an unconformity, was taking place. During the first period of rapid oil generation, the horizontal stresses ($\sigma_{H=h}$) were determined to be between 17 and 19 MPa, indicating that P_f must have been at least 17–34 MPa to shift the Mohr circles into a region of the plot where extension fractures would develop. The same fluid pressures were needed to produce extensional failure even if the second period continued into the time of Laramide Orogeny. Based on the lithostatic pressures alone,

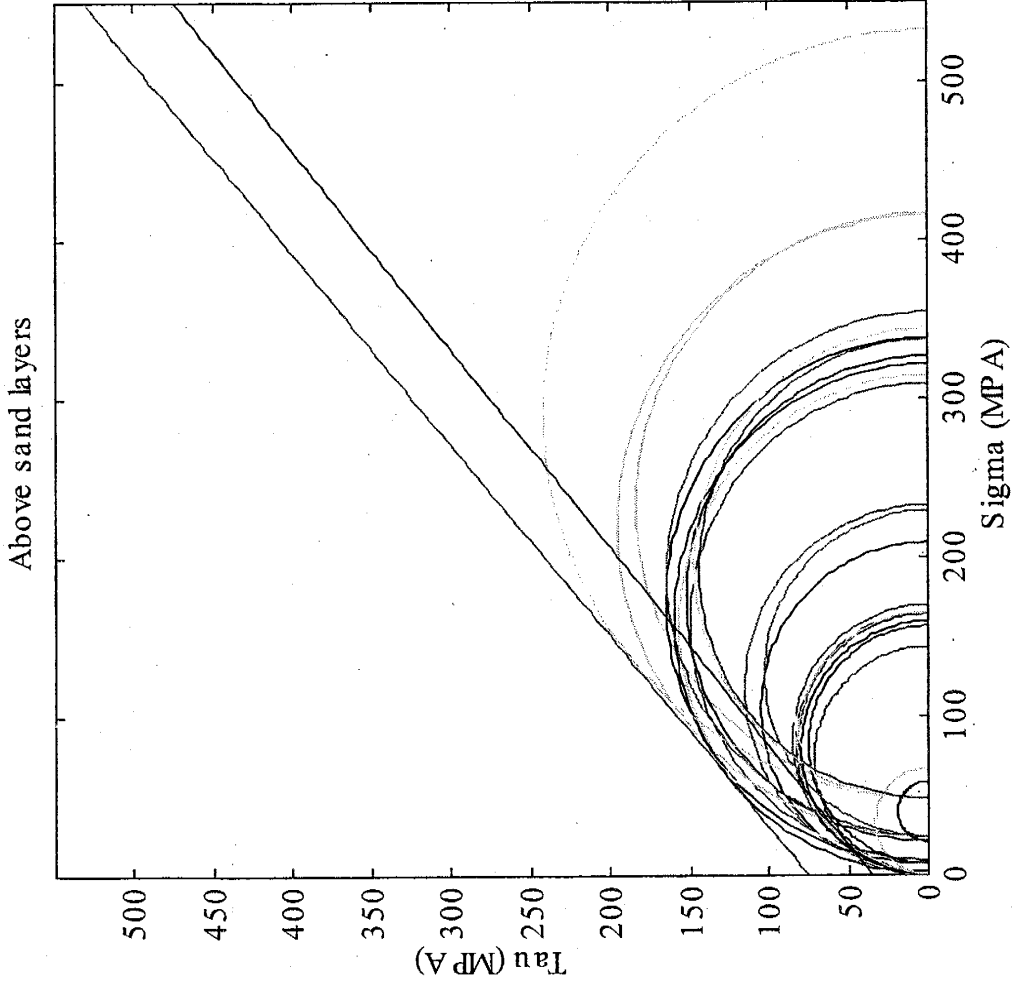


Figure 19: Example of Mohr circles and Mohr Coulomb Failure envelopes developed from triaxial shear data. Multiple failure envelopes are drawn when data do not provide strong evidence for only one failure envelope.

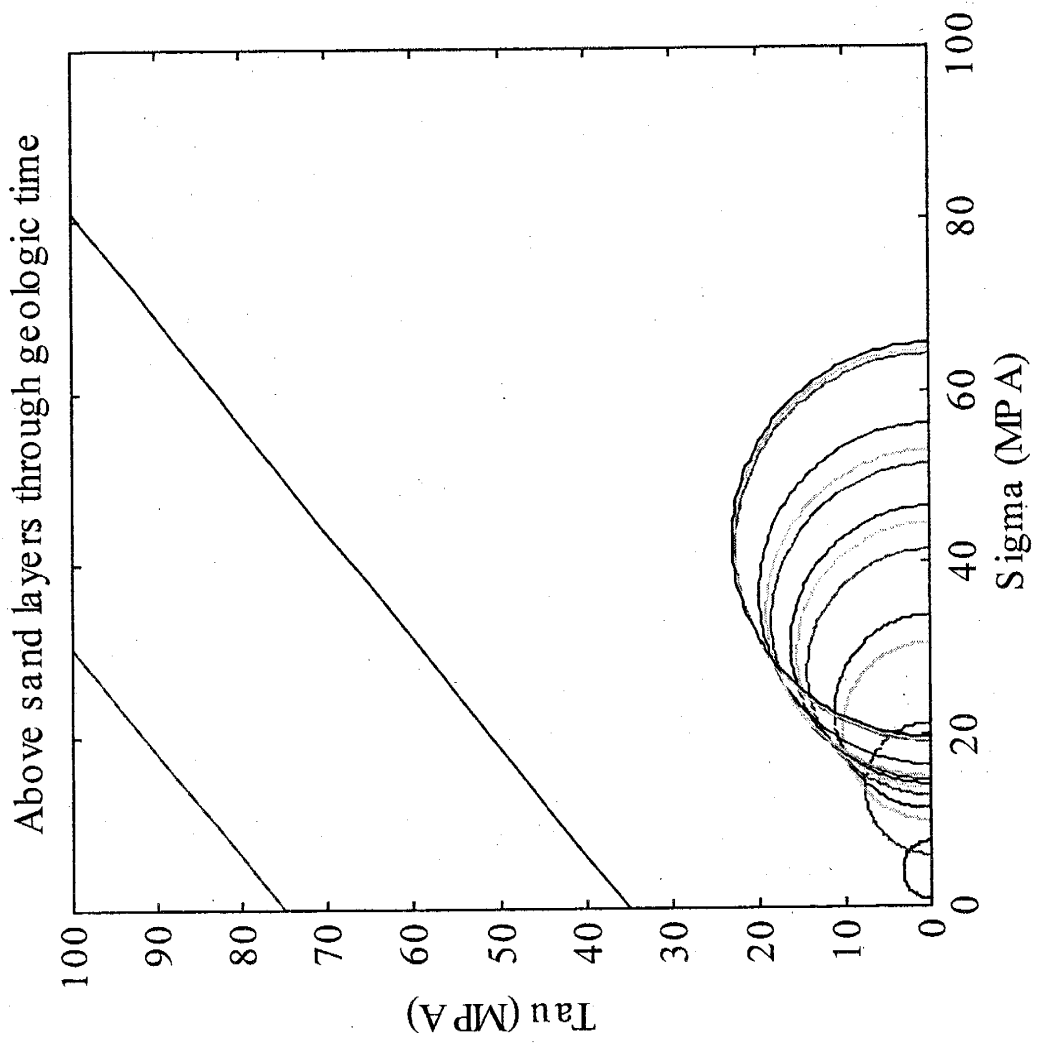


Figure 20: Example of effects of stress through geologic time. Multiple failure envelopes are drawn when data do not provide strong evidence for only one failure envelope.

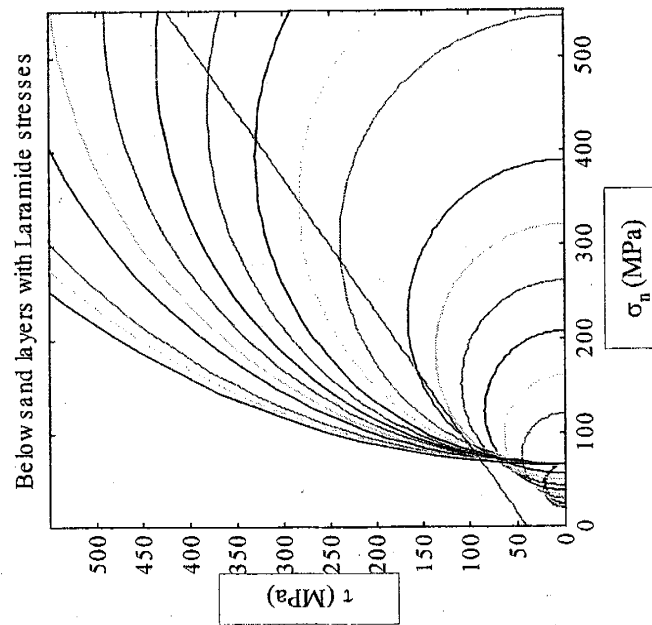
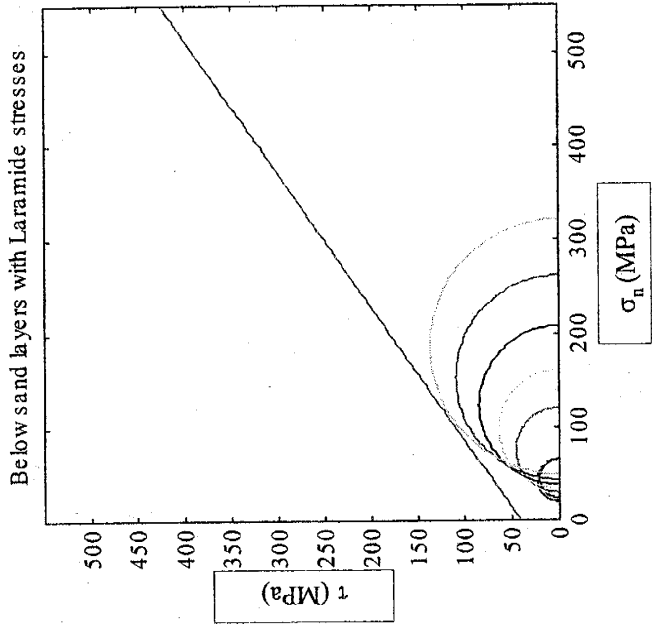



Figure 21: Example of added Laramide stress and imposed limit of $\Delta\epsilon = 0.000045$.

Lorenz (1997), there must have been a pressure differential between layers. If all P_f was uniformly increased, then all horizons would be cut by extensional fractures, which is contrary to what has been observed (Lorenz, 1997). This leads to the conclusion that P_f should have been higher in the reservoirs and shales above them than in the shales below. Exact timing of fluid pressure increases may have played a deciding role in the fracturing process and may be a reason for the observed differences in fracture patterns. This finding indicates that the driving mechanism that produced the Spraberry Formation fractures must have been pore fluid pressure (P_f). 

4. SUMMARY AND CONCLUSIONS

The Spraberry Formation is one of the largest oil reservoirs in the world, and has therefore been the focus of attention for many years. Although the formation is characterized by very low matrix permeability, the ability to produce from the Spraberry Formation is enhanced by three sets of fractures (McDonald and Schecter, 1990, 1994; Lorenz, 1997). Understanding how these fractures formed may lead to a better understanding of their location and distribution. Several approaches were taken in this study to help shed light on the fracture pattern observed in the formation. Laboratory tests were performed to evaluate the mechanical and material properties of the Spraberry Formation. From this study, it was determined that several methods of characterization are useful for predicting Spraberry Formation material properties and failure. The formation has been divided into separate sub-units based on ability to produce oil. This study found evidence that these sub-units are strongly correlated to mechanical parameters such as Young's modulus, Poisson's ratio, and limit stress. Position relative to the reservoir rocks and lithologic descriptions are also correlated with mechanical

corroborated by the mechanical analysis performed in this study. Extensional fractures could not have formed in the shales overlying either reservoir during the Laramide Orogeny under the stress conditions necessary to produce the NNE shear fractures in the 5U reservoir. Lithostatic pressure was also not enough to induce failure in any rocks prior to the Laramide Orogeny. Modeling, however, suggests that two earlier periods of elevated P_f resulting from oil generation were likely. During those times, P_f could have, and is likely to, have produced the ENE extension fractures. Fluid pressure differences between the shale horizons is the most plausible reason that shales above the reservoirs failed while those below remain intact. The conclusion of all analysis performed in this study is that the only time when the NNE shear fractures could have formed in the 5U reservoir was during the Laramide Orogeny. The NE extension fractures identified in the 1U reservoir may also have formed during the Laramide Orogeny. Although the 1U reservoir rocks are stronger than those in the 5U reservoir suggesting later development of the NE fracture set as determined by Cather (1997), it is also possible that fluid pressure influences may have produced failure earlier than would otherwise be expected. These conclusions could be further substantiated with the assistance of a refined mechanical analysis with closer approximations of fluid pressure determined from a more detailed modeling study. The direct effects of temperature on rock failure could be incorporated into future studies by integrating them into the stress-strain equations. These last suggestions would be an effective means of improving the link between the modeling study and the mechanical analysis.

REFERENCES

- Albrecht, P., Vanderbroucke, M., Mandengue, M., 1976, Geochemical studies on the organic matter from the Douala Basin (Cameroon). I-Evaluation of the extractable organic matter and the formation of petroleum; *Geochemica et. Cosmochemica, Acta*, v. 40, pp. 791-799.
- Bartley, J. H., 1952, Geology of the Spraberry Trend; *The Oil and Gas Journal*, April 1952, pp. 157-159.
- Boggs, S. Jr., 1995, *Principles of sedimentology and stratigraphy*, second edition; Prentice Hall, Englewood Cliffs, New Jersey.
- Brown, E. T., 1981, Rock characterization testing and monitoring, ISRM suggested methods; editor, E. T. Brown, Pergamon Press, p. 211
- Cather, M., 1997, Spraberry fracture diagenesis, the microscopic view of fractures; *The 3rd Naturally Fractured Reservoir Symposium proceedings*.
- Davis, G. H., Reynolds, S. J., 1996, *Structural geology of rocks and regions*, second Edition; John Wiley and Sons, New York.
- Domenico, P. A., Schwartz, F. W., 1990, *Physical and chemical hydrogeology*; John Wiley and Sons, New York.
- Dutton, S. P., 1980, Petroleum source rock potential and thermal maturity, Palo Duro Basin, Texas; *The University of Texas at Austin, Bureau of Economic Geology Circular 80-10*, 48 p.
- Elkins, L. F., 1953, Reservoir performance and well spacing, Spraberry Trend Area Field of West Texas; *Petroleum Transactions, AIME 198*, pp. 177-196.
- Elkins, L. F., Skov, A. M., 1963, Determination of fracture orientation from pressure Interference; *Petroleum Transactions, AIME 219*, pp. 301-304.
- Erdlac, R. J., Jr., 1990, A Laramide-age push-up block: the structures and formation of the Terilingua-solitario structural block, Big Bend region, Texas; *GSA Bulletin*, v 102, 198, pp. 1065-1079.
- Fetter, C. W., 1994, *Applied Hydrogeology*; Prentice Hall, Englewood Cliffs, New Jersey, Third Edition.
- Furlong, K. P., Edman, J. D., 1984, Graphic approach to determination of

- hydrocarbon maturation in overthrust terrains; AAPG Bulletin, v. 68, p. 1818-1824.
- Grove, K., 2000, <http://twister.sfsu.edu/courses/geol1103/labs/currents/structure.html>; world-wide-web publication.
- Griffith, A. A., 1920, The phenomena of rupture and flow in solids; Philosophical Transactions Royal Society, series A, v. 221, p. 163-198.
- Guevara, E. H., 1988, Geological characterization of Permian submarine fan reservoirs of The Driver waterflood unit, Spraberry Trend, Midland Basin, Texas; Report of Investigations No. 172, Bureau of Economic Geology, Austin, TX.
- Handford, C. R., 1981, Sedimentology and genetic stratigraphy of Dean and Spraberry Formations (Permian), Midland Basin, West Texas; American Association of Petroleum Geologists.
- Hill, C. A., 1996, Geology of the Delaware Basin Guadalupe, Apache and Glass Mountains, New Mexico and West Texas; Permian Basin Section – SEPM, publication 96 – 39.
- Horak, R. L., 1985, Tectonic and hydrocarbon maturation history in the Permian Basin; Oil and Gas Journal, pp. 124 - 128.
- Hornbeck, R. W., 1975, Numerical methods, Quantum Publishers, New York, 310 p.
- Houde, R. F., 1979, Sedimentology, diagenesis, and source bed geochemistry of the Spraberry sandstone, subsurface Midland Basin, West Texas, Thesis.
- Hubbert, M. K., Ruby, W. W., 1960, Role of fluid pressure in mechanics overthrust faulting, II, overthrust belt in geosynclinal area of western Wyoming in light of fluid-pressure hypothesis; GSA Bulletin, 60, pp. 167-205.
- Jones, T. S., 1949, East-West cross-section through the Permian Basin of West Texas; West Texas Geological Society, Midland, Texas.
- Kappelmeyer, O., Haenel, R., 1974, Geothermics with special reference to application: Geoexploration Monograph 4, 238 p.
- Lorenz, J. C., 1997, Description of fractures in horizontal cores of the 1U and 5U units of the Spraberry Reservoir, E. T. O'Daniel #28 well; The 3rd Fractured Reservoir Symposium proceedings.
- McDonald, P., Schechter, D. S., 1990, Advanced reservoir characterization and evaluation

of CO₂ gravity drainage in the naturally fractured Spraberry Trend area, 1st annual technical report; Petroleum Recovery Research Center Report 96-42, New Mexico Petroleum Recovery Research Center, Socorro, NM.

McDonald, P., Schechter, D. S., 1994, Advanced reservoir characterization and evaluation of CO₂ gravity drainage in the naturally fractured Spraberry Trend Reservoir; Parker and Parsley Development Co., US DOE proposal.

Merrington, M., 1941, Tables of percentage points of the t - distribution; *Biometrika*, 32, p. 300.

Merrington, M., Thompson, C. M., 1943, Tables of percentage points of the inverted Beta (F) - distribution; *Biometrika*, 33, pp. 73-88.

Middleton, G. V., Wilcock, P. R., 1994, *Mechanics in the earth and environmental sciences*; Cambridge University Press, Cambridge, Great Britain.

Mohr, O. C., 1900, Welche umstände begingen die elastizitätsgrenze und den bruch eines materials; *Zeitschrift der Vereines Deutscher Ingenieure*, v. 44, p. 1524-1530 and 1572-1577.

Price, N. J., 1959, Mechanics of jointing in rocks; *Geological Magazine*, v. 96, p. 149-167.

Reservoirs, Inc, 1997, Volume 2, Geological and petrophysical analysis of the upper Spraberry Formation in Midland County, Texas, E. T. O'Daniel No. 28 horizontal cores; prepared for Parker and Parsley Development Company, Midland, Texas.

Scheaffer, R. L., McClave, J. T., 1995, *Probability and Statistics for engineers*; Duxbury Press, An Imprint of Wadsworth Publishing Company, Belmont, CA.

Schmitt, G. T., 1954, Genesis and depositional history of Spraberry Formation, Midland Basin, Texas, *AAPG Bulletin*, 38, No. 9, 1957-1978.

Sclater, J. C., Christie, P. A. F., 1980, Continental stretching: an explanation of the post-mid cretaceous subsidence of the central North Sea Basin; *Journal of Geophysical Research*, v. 85, No. B7, pp. 3711-3739.

Stanley, T. B., Levinson, S. A., Masson, P. H., Pratt, W. L., Osanik, A., 1951, Geological investigation of the 'Spraberry', Midland Basin, West Texas, Report by Humble Oil and Refining Company.

Suppe, J., 1985, *Principles of structural geology*, Prentice-Hall Inc., Englewood Cliffs, NJ.

- Sweeney, J. J., 1990, BASINMAT, FORTRAN program calculates oil and gas generation using a distribution of discrete Activation Energies; *Geobyte*, 37 v. 5, pp. 37-43.
- Tissot, B. P., Welte, D. H., 1978, *Petroleum formation and occurrence*, Springer-Verlag, Germany, 358 p.
- Tissot, B. P., Welte, D. H., 1984, *Petroleum formation and occurrence*, Springer-Verlag, New York, 669 p.
- Twiss, R. J., Moores, E. M., 1992, *Structural geology*; W. H. Freeman and Company, New York.
- Tyler, N., Gholston, J. C., 1988, Heterogeneous deep-sea fan reservoirs, Shackelford and Preston waterflood units, Spraberry Trend, West Texas, Report of Investigation No. 171, Bureau of Economic Geology, The University of Texas at Austin.
- Walsh, J. B., 1965, The effects of cracks on the uniaxial elastic compression of rocks, *Journal of Geophysical Res.*, vol. 70, pp. 399-411.
- Warn, G. F., Sidwell, R., 1953, Petrology of the Spraberry sands of West Texas, *Journal of Sedimentology and Petrology*, 23, No. 2, pp. 67-74.
- Whigham, C., 1988, Overview of DOE Class III field demonstration: CO₂ pilot in the naturally fractured Spraberry Trend area; The 4th Naturally Fractured Reservoir Symposium proceedings.
- Winfrey, K. E., 1995, Did Laramide compressional stresses fracture the Spraberry sandstones in the Midland Basin?; *West Texas Geological society*, November 1995, vol. 35, no. 3.

APPENDIX A

Elastic moduli during elastic deformation for tests using strain gauges

SAMPLE NUMBER	SAMPLE SUBUNIT	SAMPLE LOCATION	SAMPLE HORIZON	SAMPLE LITHOLOGY	σ_{22} (MPa)	ν	E (MPa)
4	1U	BELOW	1U-BELOW	2	0.00	0.066	3.32E+04
4	1U	BELOW	1U-BELOW	2	0.00	0.075	3.57E+04
4	1U	BELOW	1U-BELOW	2	0.68	0.097	3.40E+04
4	1U	BELOW	1U-BELOW	2	0.68	0.128	3.86E+04
4	1U	BELOW	1U-BELOW	2	1.41	0.067	3.30E+04
4	1U	BELOW	1U-BELOW	2	1.41	0.071	3.50E+04
4	1U	BELOW	1U-BELOW	2	2.05	0.091	3.55E+04
4	1U	BELOW	1U-BELOW	2	2.05	0.092	3.60E+04
4	1U	BELOW	1U-BELOW	2	3.43	0.074	3.47E+04
4	1U	BELOW	1U-BELOW	2	3.43	0.102	3.65E+04
4	1U	BELOW	1U-BELOW	2	24.14	0.147	3.89E+04
4	1U	BELOW	1U-BELOW	2	24.14	0.121	3.93E+04
4	1U	BELOW	1U-BELOW	2	48.26	0.148	4.19E+04
4	1U	BELOW	1U-BELOW	2	48.26	0.179	4.43E+04
10	1U	ABOVE	1U-ABOVE	3	0.00	0.105	2.23E+04
10	1U	ABOVE	1U-ABOVE	3	0.00	0.112	2.52E+04
10	1U	ABOVE	1U-ABOVE	3	0.70	0.093	2.29E+04
10	1U	ABOVE	1U-ABOVE	3	0.70	0.116	2.66E+04
10	1U	ABOVE	1U-ABOVE	3	1.40	0.086	2.23E+04
10	1U	ABOVE	1U-ABOVE	3	1.40	0.089	2.56E+04
10	1U	ABOVE	1U-ABOVE	3	2.09	0.089	1.91E+04
10	1U	ABOVE	1U-ABOVE	3	2.09	0.078	2.67E+04
10	1U	ABOVE	1U-ABOVE	3	3.51	0.077	1.93E+04
10	1U	ABOVE	1U-ABOVE	3	3.51	0.120	2.40E+04
10	1U	ABOVE	1U-ABOVE	3	24.14	0.134	3.25E+04
10	1U	ABOVE	1U-ABOVE	3	24.14	0.140	3.70E+04
10	1U	ABOVE	1U-ABOVE	3	48.24	0.172	4.28E+04
10	1U	ABOVE	1U-ABOVE	3	48.24	0.173	4.28E+04
10	1U	ABOVE	1U-ABOVE	3	48.24	0.200	4.51E+04
18	1U	ABOVE	1U-ABOVE	3	0.00	0.084	4.87E+04
18	1U	ABOVE	1U-ABOVE	3	0.00	0.094	4.94E+04
18	1U	ABOVE	1U-ABOVE	3	0.00	0.103	5.59E+04
18	1U	ABOVE	1U-ABOVE	3	0.70	0.088	5.22E+04
18	1U	ABOVE	1U-ABOVE	3	0.70	0.172	8.09E+04
18	1U	ABOVE	1U-ABOVE	3	1.38	0.101	4.57E+04
18	1U	ABOVE	1U-ABOVE	3	1.38	0.122	7.08E+04
18	1U	ABOVE	1U-ABOVE	3	1.38	0.219	1.00E+05
18	1U	ABOVE	1U-ABOVE	3	2.05	0.125	5.31E+04
18	1U	ABOVE	1U-ABOVE	3	2.05	0.127	5.39E+04
18	1U	ABOVE	1U-ABOVE	3	2.05	0.133	6.76E+04
18	1U	ABOVE	1U-ABOVE	3	3.45	0.117	5.16E+04
18	1U	ABOVE	1U-ABOVE	3	3.45	0.119	5.45E+04
18	1U	ABOVE	1U-ABOVE	3	3.45	0.135	8.23E+04
18	1U	ABOVE	1U-ABOVE	3	24.10	0.139	5.97E+04
18	1U	ABOVE	1U-ABOVE	3	24.10	0.162	7.00E+04
18	1U	ABOVE	1U-ABOVE	3	24.10	0.150	1.09E+05
18	1U	ABOVE	1U-ABOVE	3	48.28	0.160	6.55E+04
18	1U	ABOVE	1U-ABOVE	3	48.28	0.142	7.43E+04
18	1U	ABOVE	1U-ABOVE	3	48.28	0.045	1.41E+05
22	1U	ABOVE	1U-ABOVE	3	0.00	0.098	3.72E+04
22	1U	ABOVE	1U-ABOVE	3	0.00	0.085	4.02E+04
22	1U	ABOVE	1U-ABOVE	3	0.00	0.184	5.02E+04
22	1U	ABOVE	1U-ABOVE	3	0.70	0.079	3.89E+04
22	1U	ABOVE	1U-ABOVE	3	0.70	0.111	4.22E+04
22	1U	ABOVE	1U-ABOVE	3	0.70	0.165	4.67E+04
22	1U	ABOVE	1U-ABOVE	3	1.39	0.069	3.87E+04
22	1U	ABOVE	1U-ABOVE	3	1.39	0.123	4.22E+04
22	1U	ABOVE	1U-ABOVE	3	1.39	0.124	4.57E+04
22	1U	ABOVE	1U-ABOVE	3	2.05	0.139	4.32E+04
22	1U	ABOVE	1U-ABOVE	3	2.05	0.134	4.48E+04
22	1U	ABOVE	1U-ABOVE	3	2.05	0.130	4.55E+04
22	1U	ABOVE	1U-ABOVE	3	3.46	0.122	4.29E+04
22	1U	ABOVE	1U-ABOVE	3	3.46	0.122	4.46E+04
22	1U	ABOVE	1U-ABOVE	3	3.46	0.121	4.51E+04
22	1U	ABOVE	1U-ABOVE	3	24.12	0.121	5.37E+04
22	1U	ABOVE	1U-ABOVE	3	24.12	0.155	5.43E+04
22	1U	ABOVE	1U-ABOVE	3	24.12	0.215	6.17E+04
22	1U	ABOVE	1U-ABOVE	3	48.23	0.188	6.34E+04
22	1U	ABOVE	1U-ABOVE	3	48.23	0.201	6.38E+04
22	1U	ABOVE	1U-ABOVE	3	48.23	0.209	6.50E+04
37	5U	BELOW	5U-BELOW	2	0.00	0.037	1.19E+04
37	5U	BELOW	5U-BELOW	2	0.00	0.075	1.91E+04
37	5U	BELOW	5U-BELOW	2	0.68	0.056	1.42E+04
37	5U	BELOW	5U-BELOW	2	0.68	0.092	2.23E+04
37	5U	BELOW	5U-BELOW	2	0.68	0.033	1.03E+04
37	5U	BELOW	5U-BELOW	2	0.68	0.098	2.45E+04
37	5U	BELOW	5U-BELOW	2	1.39	0.035	1.09E+04
37	5U	BELOW	5U-BELOW	2	1.39	0.046	1.22E+04
37	5U	BELOW	5U-BELOW	2	1.39	0.049	1.57E+04
37	5U	BELOW	5U-BELOW	2	2.08	0.041	1.13E+04
37	5U	BELOW	5U-BELOW	2	2.08	0.043	1.91E+04
37	5U	BELOW	5U-BELOW	2	3.45	0.066	1.43E+04
37	5U	BELOW	5U-BELOW	2	3.45	0.095	2.11E+04
37	5U	BELOW	5U-BELOW	2	24.12	0.128	2.79E+04

Elastic moduli during elastic deformation for tests using strain gauges

SAMPLE NUMBER	SAMPLE SUBUNIT	SAMPLE LOCATION	SAMPLE HORIZON	SAMPLE LITHOLOGY	σ_{22} (MPa)	ν	E (MPa)
37	5U	BELOW	5U-BELOW	2	24.12	0.145	3.02E+04
37	5U	BELOW	5U-BELOW	2	48.28	0.145	3.14E+04
37	5U	BELOW	5U-BELOW	2	48.28	0.145	3.83E+04
47	5U	ABOVE	5U-ABOVE	4	0.00	0.022	1.18E+04
47	5U	ABOVE	5U-ABOVE	4	0.00	0.018	1.20E+04
47	5U	ABOVE	5U-ABOVE	4	0.00	0.023	2.05E+04
47	5U	ABOVE	5U-ABOVE	4	0.70	0.027	7.25E+03
47	5U	ABOVE	5U-ABOVE	4	0.70	0.030	1.10E+04
47	5U	ABOVE	5U-ABOVE	4	0.70	0.022	1.91E+04
47	5U	ABOVE	5U-ABOVE	4	1.40	0.025	1.09E+04
47	5U	ABOVE	5U-ABOVE	4	1.40	0.035	2.11E+04
47	5U	ABOVE	5U-ABOVE	4	2.10	0.029	1.13E+04
47	5U	ABOVE	5U-ABOVE	4	2.10	0.032	1.33E+04
47	5U	ABOVE	5U-ABOVE	4	2.10	0.048	2.30E+04
47	5U	ABOVE	5U-ABOVE	4	3.47	0.033	9.81E+03
47	5U	ABOVE	5U-ABOVE	4	3.47	0.038	1.24E+04
47	5U	ABOVE	5U-ABOVE	4	3.47	0.042	1.96E+04
47	5U	ABOVE	5U-ABOVE	4	6.92	0.096	2.63E+04
47	5U	ABOVE	5U-ABOVE	4	24.12	0.068	1.92E+04
47	5U	ABOVE	5U-ABOVE	4	24.12	0.072	2.02E+04
47	5U	ABOVE	5U-ABOVE	4	48.23	0.083	2.34E+04
50	5U	ABOVE	5U-ABOVE	4	0.00	0.052	2.28E+03
50	5U	ABOVE	5U-ABOVE	4	0.00	0.058	1.59E+04
50	5U	ABOVE	5U-ABOVE	4	0.74	0.049	1.30E+04
50	5U	ABOVE	5U-ABOVE	4	0.74	0.062	1.76E+04
50	5U	ABOVE	5U-ABOVE	4	1.35	0.048	1.39E+04
50	5U	ABOVE	5U-ABOVE	4	1.35	0.074	1.96E+04
50	5U	ABOVE	5U-ABOVE	4	2.11	0.085	2.16E+04
50	5U	ABOVE	5U-ABOVE	4	2.11	0.078	2.22E+04
50	5U	ABOVE	5U-ABOVE	4	3.44	0.061	1.62E+04
50	5U	ABOVE	5U-ABOVE	4	3.44	0.072	1.88E+04
50	5U	ABOVE	5U-ABOVE	4	24.12	0.092	2.33E+04
50	5U	ABOVE	5U-ABOVE	4	24.12	0.110	2.89E+04
50	5U	ABOVE	5U-ABOVE	4	48.30	0.132	3.49E+04
50	5U	ABOVE	5U-ABOVE	4	48.30	0.153	3.56E+04
51	5U	ABOVE	5U-ABOVE	4	0.00	0.042	1.34E+04
51	5U	ABOVE	5U-ABOVE	4	0.00	0.037	1.40E+04
51	5U	ABOVE	5U-ABOVE	4	0.00	0.062	1.63E+04
51	5U	ABOVE	5U-ABOVE	4	0.72	0.045	1.44E+04
51	5U	ABOVE	5U-ABOVE	4	0.72	0.046	1.63E+04
51	5U	ABOVE	5U-ABOVE	4	1.40	0.045	1.49E+04
51	5U	ABOVE	5U-ABOVE	4	1.40	0.055	1.60E+04
51	5U	ABOVE	5U-ABOVE	4	1.40	0.044	1.63E+04
51	5U	ABOVE	5U-ABOVE	4	2.07	0.051	1.52E+04
51	5U	ABOVE	5U-ABOVE	4	2.07	0.057	1.74E+04
51	5U	ABOVE	5U-ABOVE	4	3.45	0.055	1.53E+04
51	5U	ABOVE	5U-ABOVE	4	3.45	0.060	1.76E+04
51	5U	ABOVE	5U-ABOVE	4	24.19	0.088	2.25E+04
51	5U	ABOVE	5U-ABOVE	4	24.19	0.085	2.30E+04
51	5U	ABOVE	5U-ABOVE	4	24.19	0.067	2.67E+04
51	5U	ABOVE	5U-ABOVE	4	48.24	0.123	3.22E+04
51	5U	ABOVE	5U-ABOVE	4	48.24	0.111	3.29E+04
51	5U	ABOVE	5U-ABOVE	4	48.24	0.133	3.95E+04
62	5U	RESERVOIR	5U-RESERVOIR	6	0.00	0.101	1.77E+04
62	5U	RESERVOIR	5U-RESERVOIR	6	0.00	0.112	1.91E+04
62	5U	RESERVOIR	5U-RESERVOIR	6	0.76	0.092	1.74E+04
62	5U	RESERVOIR	5U-RESERVOIR	6	0.76	0.123	2.32E+04
62	5U	RESERVOIR	5U-RESERVOIR	6	1.39	0.090	1.41E+04
62	5U	RESERVOIR	5U-RESERVOIR	6	1.39	0.109	1.45E+04
62	5U	RESERVOIR	5U-RESERVOIR	6	2.06	0.101	1.47E+04
62	5U	RESERVOIR	5U-RESERVOIR	6	2.06	0.097	1.92E+04
62	5U	RESERVOIR	5U-RESERVOIR	6	3.47	0.064	1.03E+04
62	5U	RESERVOIR	5U-RESERVOIR	6	3.47	0.064	1.63E+04
62	5U	RESERVOIR	5U-RESERVOIR	6	24.16	0.104	2.34E+04
62	5U	RESERVOIR	5U-RESERVOIR	6	24.16	0.089	3.06E+04
62	5U	RESERVOIR	5U-RESERVOIR	6	48.38	0.133	3.36E+04
62	5U	RESERVOIR	5U-RESERVOIR	6	48.38	0.148	3.67E+04
79	1U	RESERVOIR	1U-RESERVOIR	6	0.00	0.098	2.15E+04
79	1U	RESERVOIR	1U-RESERVOIR	6	0.00	0.113	2.51E+04
79	1U	RESERVOIR	1U-RESERVOIR	6	0.00	0.100	2.91E+04
79	1U	RESERVOIR	1U-RESERVOIR	6	0.00	0.117	2.99E+04
79	1U	RESERVOIR	1U-RESERVOIR	6	0.68	0.107	2.22E+04
79	1U	RESERVOIR	1U-RESERVOIR	6	0.68	0.080	2.27E+04
79	1U	RESERVOIR	1U-RESERVOIR	6	1.38	0.091	2.25E+04
79	1U	RESERVOIR	1U-RESERVOIR	6	1.38	0.103	2.52E+04
79	1U	RESERVOIR	1U-RESERVOIR	6	2.11	0.109	2.28E+04
79	1U	RESERVOIR	1U-RESERVOIR	6	2.11	0.119	2.67E+04
79	1U	RESERVOIR	1U-RESERVOIR	6	3.43	0.094	2.33E+04
79	1U	RESERVOIR	1U-RESERVOIR	6	3.43	0.123	2.46E+04
79	1U	RESERVOIR	1U-RESERVOIR	6	3.43	0.117	2.67E+04
79	1U	RESERVOIR	1U-RESERVOIR	6	24.14	0.135	3.63E+04
79	1U	RESERVOIR	1U-RESERVOIR	6	24.14	0.116	3.80E+04
79	1U	RESERVOIR	1U-RESERVOIR	6	24.14	0.139	4.20E+04
79	1U	RESERVOIR	1U-RESERVOIR	6	48.26	0.134	3.91E+04

Elastic moduli during elastic deformation for tests using strain gauges

SAMPLE NUMBER	SAMPLE SUBUNIT	SAMPLE LOCATION	SAMPLE HORIZON	SAMPLE LITHOLOGY	σ_{22} (MPa)	ν	E (MPa)
79	1U	RESERVOIR	1U-RESERVOIR	6	48.26	0.141	4.22E+04
79	1U	RESERVOIR	1U-RESERVOIR	6	48.26	0.150	4.32E+04
82	1U	RESERVOIR	1U-RESERVOIR	3	0.00	0.086	1.44E+04
82	1U	RESERVOIR	1U-RESERVOIR	3	0.00	0.097	1.85E+04
82	1U	RESERVOIR	1U-RESERVOIR	3	0.68	0.088	1.50E+04
82	1U	RESERVOIR	1U-RESERVOIR	3	0.68	0.108	1.81E+04
82	1U	RESERVOIR	1U-RESERVOIR	3	1.38	0.094	1.45E+04
82	1U	RESERVOIR	1U-RESERVOIR	3	1.38	0.104	1.70E+04
82	1U	RESERVOIR	1U-RESERVOIR	3	2.07	0.085	1.67E+04
82	1U	RESERVOIR	1U-RESERVOIR	3	2.07	0.088	1.70E+04
82	1U	RESERVOIR	1U-RESERVOIR	3	3.43	0.084	1.50E+04
82	1U	RESERVOIR	1U-RESERVOIR	3	3.43	0.108	1.69E+04
82	1U	RESERVOIR	1U-RESERVOIR	3	24.14	0.104	2.49E+04
82	1U	RESERVOIR	1U-RESERVOIR	3	24.14	0.101	2.63E+04
82	1U	RESERVOIR	1U-RESERVOIR	3	48.28	0.112	3.31E+04
82	1U	RESERVOIR	1U-RESERVOIR	3	48.28	0.141	3.36E+04
94	5U	ABOVE	5U-ABOVE	3	0.86	0.092	2.25E+04
94	5U	ABOVE	5U-ABOVE	3	0.86	0.070	2.60E+04
94	5U	ABOVE	5U-ABOVE	3	0.86	0.069	2.74E+04
94	5U	ABOVE	5U-ABOVE	3	1.41	0.104	1.94E+04
94	5U	ABOVE	5U-ABOVE	3	2.09	0.101	2.03E+04
94	5U	ABOVE	5U-ABOVE	3	2.09	0.077	2.46E+04
94	5U	ABOVE	5U-ABOVE	3	2.09	0.070	2.72E+04
94	5U	ABOVE	5U-ABOVE	3	2.13	0.095	1.91E+04
94	5U	ABOVE	5U-ABOVE	3	3.44	0.104	1.98E+04
94	5U	ABOVE	5U-ABOVE	3	3.44	0.076	2.46E+04
94	5U	ABOVE	5U-ABOVE	3	3.44	0.075	2.47E+04
94	5U	ABOVE	5U-ABOVE	3	20.74	0.083	2.49E+04
94	5U	ABOVE	5U-ABOVE	3	20.74	0.065	2.75E+04
94	5U	ABOVE	5U-ABOVE	3	20.74	0.054	3.43E+04
94	5U	ABOVE	5U-ABOVE	3	48.27	0.056	3.49E+04
94	5U	ABOVE	5U-ABOVE	3	48.27	0.057	3.63E+04
94	5U	ABOVE	5U-ABOVE	3	48.27	0.407	3.98E+04
97	5U	ABOVE	5U-ABOVE	3	0.70	0.048	1.631E+04
97	5U	ABOVE	5U-ABOVE	3	0.70	0.048	1.633E+04
97	5U	ABOVE	5U-ABOVE	3	0.70	0.049	1.719E+04
97	5U	ABOVE	5U-ABOVE	3	1.39	0.057	1.861E+04
97	5U	ABOVE	5U-ABOVE	3	1.39	0.057	1.875E+04
97	5U	ABOVE	5U-ABOVE	3	1.39	0.059	1.902E+04
97	5U	ABOVE	5U-ABOVE	3	2.07	0.050	1.597E+04
97	5U	ABOVE	5U-ABOVE	3	2.07	0.052	1.613E+04
97	5U	ABOVE	5U-ABOVE	3	2.07	0.054	1.683E+04
97	5U	ABOVE	5U-ABOVE	3	3.48	0.061	1.809E+04
97	5U	ABOVE	5U-ABOVE	3	3.48	0.061	1.837E+04
97	5U	ABOVE	5U-ABOVE	3	3.48	0.064	2.007E+04
103	5U	ABOVE	5U-ABOVE	2	0.00	0.065	1.788E+04
103	5U	ABOVE	5U-ABOVE	2	0.00	0.065	1.805E+04
103	5U	ABOVE	5U-ABOVE	2	0.00	0.067	1.860E+04
103	5U	ABOVE	5U-ABOVE	2	0.68	0.054	1.513E+04
103	5U	ABOVE	5U-ABOVE	2	0.68	0.059	1.663E+04
103	5U	ABOVE	5U-ABOVE	2	0.68	0.062	1.731E+04
103	5U	ABOVE	5U-ABOVE	2	1.37	0.071	1.998E+04
103	5U	ABOVE	5U-ABOVE	2	1.37	0.074	2.096E+04
103	5U	ABOVE	5U-ABOVE	2	1.37	0.135	2.842E+04
103	5U	ABOVE	5U-ABOVE	2	2.06	0.075	2.169E+04
103	5U	ABOVE	5U-ABOVE	2	2.06	0.075	2.183E+04
103	5U	ABOVE	5U-ABOVE	2	2.06	0.079	2.264E+04
103	5U	ABOVE	5U-ABOVE	2	3.46	0.083	2.401E+04
103	5U	ABOVE	5U-ABOVE	2	3.46	0.075	2.426E+04
103	5U	ABOVE	5U-ABOVE	2	3.46	0.080	2.507E+04
103	5U	ABOVE	5U-ABOVE	2	20.71	0.104	3.305E+04
103	5U	ABOVE	5U-ABOVE	2	20.71	0.080	3.344E+04
103	5U	ABOVE	5U-ABOVE	2	20.71	0.102	3.397E+04
103	5U	ABOVE	5U-ABOVE	2	48.26	0.126	4.226E+04
103	5U	ABOVE	5U-ABOVE	2	48.26	0.105	4.244E+04
103	5U	ABOVE	5U-ABOVE	2	48.26	0.120	4.320E+04
105	5U	ABOVE	5U-ABOVE	2	0.00	0.063	1.540E+04
105	5U	ABOVE	5U-ABOVE	2	0.00	0.068	1.614E+04
105	5U	ABOVE	5U-ABOVE	2	0.00	0.069	1.755E+04
105	5U	ABOVE	5U-ABOVE	2	0.70	0.068	1.681E+04
105	5U	ABOVE	5U-ABOVE	2	0.70	0.069	1.686E+04
105	5U	ABOVE	5U-ABOVE	2	0.70	0.072	1.863E+04
105	5U	ABOVE	5U-ABOVE	2	1.39	0.070	1.743E+04
105	5U	ABOVE	5U-ABOVE	2	1.39	0.069	1.760E+04
105	5U	ABOVE	5U-ABOVE	2	1.39	0.074	1.901E+04
105	5U	ABOVE	5U-ABOVE	2	2.05	0.074	1.953E+04
105	5U	ABOVE	5U-ABOVE	2	2.05	0.075	1.959E+04
105	5U	ABOVE	5U-ABOVE	2	2.05	0.074	1.983E+04
105	5U	ABOVE	5U-ABOVE	2	3.46	0.074	2.026E+04
105	5U	ABOVE	5U-ABOVE	2	3.46	0.078	2.114E+04
105	5U	ABOVE	5U-ABOVE	2	3.46	0.079	2.161E+04
105	5U	ABOVE	5U-ABOVE	2	20.68	0.104	2.983E+04
105	5U	ABOVE	5U-ABOVE	2	20.68	0.104	3.007E+04
105	5U	ABOVE	5U-ABOVE	2	20.68	0.104	3.017E+04

Elastic moduli during elastic deformation for tests using strain gauges

SAMPLE NUMBER	SAMPLE SUBUNIT	SAMPLE LOCATION	SAMPLE HORIZON	SAMPLE LITHOLOGY	σ_{22} (MPa)	ν	E (MPa)
105	5U	ABOVE	5U-ABOVE	2	48.29	0.132	3.847E+04
105	5U	ABOVE	5U-ABOVE	2	48.29	0.127	3.880E+04
105	5U	ABOVE	5U-ABOVE	2	48.29	0.123	4.038E+04
107	1U	RESERVOIR	1U-RESERVOIR	3	0.00	0.042	1.691E+04
107	1U	RESERVOIR	1U-RESERVOIR	3	0.70	0.048	1.400E+04
107	1U	RESERVOIR	1U-RESERVOIR	3	0.70	0.052	1.411E+04
107	1U	RESERVOIR	1U-RESERVOIR	3	0.70	0.053	1.543E+04
107	1U	RESERVOIR	1U-RESERVOIR	3	1.41	0.057	1.543E+04
107	1U	RESERVOIR	1U-RESERVOIR	3	1.41	0.060	1.576E+04
107	1U	RESERVOIR	1U-RESERVOIR	3	1.41	0.063	1.622E+04
107	1U	RESERVOIR	1U-RESERVOIR	3	2.06	0.057	1.549E+04
107	1U	RESERVOIR	1U-RESERVOIR	3	2.06	0.058	1.596E+04
107	1U	RESERVOIR	1U-RESERVOIR	3	2.06	0.060	1.648E+04
107	1U	RESERVOIR	1U-RESERVOIR	3	2.73	0.060	1.612E+04
107	1U	RESERVOIR	1U-RESERVOIR	3	2.73	0.058	1.634E+04
107	1U	RESERVOIR	1U-RESERVOIR	3	2.73	0.059	1.636E+04
107	1U	RESERVOIR	1U-RESERVOIR	3	3.41	0.066	1.764E+04
107	1U	RESERVOIR	1U-RESERVOIR	3	3.41	0.067	1.790E+04
107	1U	RESERVOIR	1U-RESERVOIR	3	3.41	0.066	1.806E+04
107	1U	RESERVOIR	1U-RESERVOIR	3	20.67	0.098	2.877E+04
107	1U	RESERVOIR	1U-RESERVOIR	3	20.67	0.098	2.981E+04
107	1U	RESERVOIR	1U-RESERVOIR	3	20.67	0.100	3.038E+04
107	1U	RESERVOIR	1U-RESERVOIR	3	48.21	0.116	3.994E+04
107	1U	RESERVOIR	1U-RESERVOIR	3	48.21	0.129	4.087E+04
107	1U	RESERVOIR	1U-RESERVOIR	3	48.21	0.141	4.298E+04
108	1U	RESERVOIR	1U-RESERVOIR	3	0.00	0.077	1.747E+04
108	1U	RESERVOIR	1U-RESERVOIR	3	0.00	0.080	1.814E+04
108	1U	RESERVOIR	1U-RESERVOIR	3	0.00	0.084	1.985E+04
108	1U	RESERVOIR	1U-RESERVOIR	3	0.72	0.074	1.775E+04
108	1U	RESERVOIR	1U-RESERVOIR	3	0.72	0.074	1.804E+04
108	1U	RESERVOIR	1U-RESERVOIR	3	0.72	0.077	1.828E+04
108	1U	RESERVOIR	1U-RESERVOIR	3	1.39	0.073	1.701E+04
108	1U	RESERVOIR	1U-RESERVOIR	3	1.39	0.074	1.743E+04
108	1U	RESERVOIR	1U-RESERVOIR	3	1.39	0.081	1.863E+04
108	1U	RESERVOIR	1U-RESERVOIR	3	2.08	0.085	2.047E+04
108	1U	RESERVOIR	1U-RESERVOIR	3	2.08	0.084	2.057E+04
108	1U	RESERVOIR	1U-RESERVOIR	3	2.08	0.091	2.121E+04
108	1U	RESERVOIR	1U-RESERVOIR	3	3.48	0.078	1.767E+04
108	1U	RESERVOIR	1U-RESERVOIR	3	3.48	0.078	1.868E+04
108	1U	RESERVOIR	1U-RESERVOIR	3	3.48	0.082	1.881E+04
108	1U	RESERVOIR	1U-RESERVOIR	3	20.68	0.117	2.819E+04
108	1U	RESERVOIR	1U-RESERVOIR	3	20.68	0.114	2.833E+04
108	1U	RESERVOIR	1U-RESERVOIR	3	20.68	0.118	2.856E+04
108	1U	RESERVOIR	1U-RESERVOIR	3	48.29	0.150	3.657E+04
108	1U	RESERVOIR	1U-RESERVOIR	3	48.29	0.150	3.673E+04
108	1U	RESERVOIR	1U-RESERVOIR	3	48.29	0.145	3.879E+04
109	1U	BELOW	1U-BELOW	2	0.00	0.078	6.621E+04
10	1U	ABOVE	1U-ABOVE	3	0.07	0.146	3.20E+04
103	5U	ABOVE	5U-ABOVE	2	48.20	0.128	3.89E+04
105	5U	ABOVE	5U-ABOVE	2	1.39	0.073	2.20E+04
107	1U	RESERVOIR	1U-RESERVOIR	3	0.00	0.034	1.61E+04
108	1U	RESERVOIR	1U-RESERVOIR	3	48.18	0.153	3.98E+04
11	1U	ABOVE	1U-ABOVE	3	48.50	0.147	3.18E+04
12	1U	ABOVE	1U-ABOVE	3	21.09	0.154	2.89E+04
13	1U	ABOVE	1U-ABOVE	3	0.77	0.019	2.12E+04
14	1U	ABOVE	1U-ABOVE	3	2.34	0.015	2.44E+04
15	1U	ABOVE	1U-ABOVE	3	0.00	0.011	4.83E+04
16	1U	ABOVE	1U-ABOVE	3	7.02	0.019	4.30E+04
17	1U	ABOVE	1U-ABOVE	3	9.22	0.104	4.42E+04
18	1U	ABOVE	1U-ABOVE	3	24.10	0.369	3.85E+04
19	1U	ABOVE	1U-ABOVE	3	0.85	0.033	3.47E+04
20	1U	ABOVE	1U-ABOVE	3	11.76	0.013	4.34E+04
21	1U	ABOVE	1U-ABOVE	3	24.29	0.021	4.10E+04
22	1U	ABOVE	1U-ABOVE	3	48.22	0.400	3.83E+04
23	5U	BELOW	5U-BELOW	2	0.00	0.002	1.28E+04
25	5U	BELOW	5U-BELOW	2	2.11	0.115	1.13E+04
26	5U	ABOVE	5U-ABOVE	2	0.00	0.112	2.08E+04
27	5U	ABOVE	5U-ABOVE	2	0.86	0.189	4.09E+04
29	5U	ABOVE	5U-ABOVE	4	0.00	0.104	2.24E+04
30	5U	ABOVE	5U-ABOVE	4	0.90	0.124	1.68E+04
31	5U	ABOVE	5U-ABOVE	4	0.01	0.253	2.02E+04
32	5U	BELOW	5U-BELOW	2	1.36	0.114	3.45E+04
33	5U	BELOW	5U-BELOW	2	3.47	0.117	4.16E+04
34	5U	BELOW	5U-BELOW	2	48.47	0.145	2.82E+04
35	5U	BELOW	5U-BELOW	2	24.40	0.108	3.92E+04
36	5U	BELOW	5U-BELOW	2	0.00	0.020	2.63E+04
37	5U	BELOW	5U-BELOW	2	24.10	0.128	3.23E+04
4	1U	BELOW	1U-BELOW	2	3.45	0.076	2.53E+04
40	5U	RESERVOIR	5U-RESERVOIR	6	0.00	0.054	4.51E+04
41	5U	RESERVOIR	5U-RESERVOIR	6	1.31	0.157	3.33E+04
42	5U	RESERVOIR	5U-RESERVOIR	6	3.40	0.229	3.28E+04
43	5U	RESERVOIR	5U-RESERVOIR	6	48.38	0.166	2.95E+04
46	5U	RESERVOIR	5U-RESERVOIR	6	2.46	0.223	2.55E+04
47	5U	ABOVE	5U-ABOVE	4	6.92	0.029	7.90E+03

Elastic moduli during elastic deformation for tests using strain gauges

SAMPLE NUMBER	SAMPLE SUBUNIT	SAMPLE LOCATION	SAMPLE HORIZON	SAMPLE LITHOLOGY	σ_{22} (MPa)	ν	E (MPa)
50	5U	ABOVE	5U-ABOVE	4	24.14	0.038	3.70E+04
51	5U	ABOVE	5U-ABOVE	4	24.15	0.155	3.88E+04
55	5U	RESERVOIR	5U-RESERVOIR	6	24.14	0.032	2.17E+04
56	5U	RESERVOIR	5U-RESERVOIR	6	21.03	0.025	2.92E+04
57	5U	RESERVOIR	5U-RESERVOIR	6	3.48	0.025	2.03E+04
58	5U	RESERVOIR	5U-RESERVOIR	6	3.45	0.309	1.93E+04
59	5U	RESERVOIR	5U-RESERVOIR	6	2.37	0.049	1.98E+04
60	5U	RESERVOIR	5U-RESERVOIR	6	22.07	0.003	3.05E+04
61	5U	RESERVOIR	5U-RESERVOIR	6	22.42	0.471	2.10E+04
62	5U	RESERVOIR	5U-RESERVOIR	6	3.42	0.008	9.22E+03
64	1U	RESERVOIR	1U-RESERVOIR	6	0.00	0.088	4.21E+04
65	1U	RESERVOIR	1U-RESERVOIR	6	1.51	0.193	4.18E+04
66	1U	RESERVOIR	1U-RESERVOIR	6	3.32	0.010	3.49E+04
67	1U	RESERVOIR	1U-RESERVOIR	6	49.50	0.144	4.78E+04
68	1U	RESERVOIR	1U-RESERVOIR	6	0.80	0.010	4.00E+04
69	1U	RESERVOIR	1U-RESERVOIR	6	2.03	0.009	4.34E+04
70	1U	RESERVOIR	1U-RESERVOIR	6	24.17	0.186	3.59E+04
71	1U	RESERVOIR	1U-RESERVOIR	6	2.49	0.052	3.23E+04
72	1U	RESERVOIR	1U-RESERVOIR	6	21.95	0.035	4.05E+04
73	1U	RESERVOIR	1U-RESERVOIR	6	0.00	0.033	3.72E+04
74	1U	RESERVOIR	1U-RESERVOIR	6	1.28	0.008	3.52E+04
75	1U	RESERVOIR	1U-RESERVOIR	6	3.32	0.174	3.81E+04
76	1U	RESERVOIR	1U-RESERVOIR	6	48.39	0.123	5.00E+04
77	1U	RESERVOIR	1U-RESERVOIR	6	0.83	0.012	3.81E+04
78	1U	RESERVOIR	1U-RESERVOIR	6	2.31	0.213	4.40E+04
79	1U	RESERVOIR	1U-RESERVOIR	6	24.12	0.332	3.38E+04
8	1U	ABOVE	1U-ABOVE	3	0.00	0.030	3.87E+04
80	1U	RESERVOIR	1U-RESERVOIR	6	21.93	0.035	4.67E+04
82	1U	RESERVOIR	1U-RESERVOIR	3	3.45	0.108	2.08E+04
94	5U	ABOVE	5U-ABOVE	3	48.16	0.045	4.23E+04
97	5U	ABOVE	5U-ABOVE	3	20.63		

Notes:

- 1) See Figure 2 for position of sub-unit, horizon, location, and lithology
- 2) Lithology Type 2 is finely laminated, silty shale; Type 3 is finely laminated siltstone, Type 4 is bioturbated or disturbed siltstone, and Type 6 is massive to faintly stratified siltstone

Elastic moduli for elastic and plastic deformation for tests using strain gauges

SAMPLE NUMBER	SAMPLE SUBUNIT	SAMPLE LOCATION	SAMPLE HORIZON	SAMPLE LITHOLOGY	σ_{22} (MPa)	σ_{11} (MPa)	ν	E (MPa)
4	1U	BELOW	1U-BELOW	2	0.00	15.00	0.066	3.32E+04
4	1U	BELOW	1U-BELOW	2	0.00	15.00	0.075	3.57E+04
4	1U	BELOW	1U-BELOW	2	0.68	15.00	0.097	3.40E+04
4	1U	BELOW	1U-BELOW	2	0.68	15.00	0.128	3.86E+04
4	1U	BELOW	1U-BELOW	2	1.41	15.00	0.067	3.30E+04
4	1U	BELOW	1U-BELOW	2	1.41	15.00	0.071	3.50E+04
4	1U	BELOW	1U-BELOW	2	2.05	15.00	0.091	3.55E+04
4	1U	BELOW	1U-BELOW	2	2.05	15.00	0.092	3.60E+04
4	1U	BELOW	1U-BELOW	2	3.43	15.00	0.074	3.47E+04
4	1U	BELOW	1U-BELOW	2	3.43	15.00	0.102	3.65E+04
4	1U	BELOW	1U-BELOW	2	24.14	40.00	0.121	3.93E+04
4	1U	BELOW	1U-BELOW	2	24.14	40.00	0.147	3.89E+04
4	1U	BELOW	1U-BELOW	2	48.26	75.00	0.148	4.19E+04
4	1U	BELOW	1U-BELOW	2	48.26	75.00	0.179	4.43E+04
4	1U	BELOW	1U-BELOW	2	3.45	8	0.029	3.649E+04
4	1U	BELOW	1U-BELOW	2	3.45	25	0.042	3.371E+04
4	1U	BELOW	1U-BELOW	2	3.45	52	0.111	3.675E+04
4	1U	BELOW	1U-BELOW	2	3.45	73	0.128	3.801E+04
4	1U	BELOW	1U-BELOW	2	3.45	96	0.108	3.736E+04
4	1U	BELOW	1U-BELOW	2	3.45	120	0.133	3.820E+04
4	1U	BELOW	1U-BELOW	2	3.45	137	0.168	3.907E+04
10	1U	ABOVE	1U-ABOVE	3	0.00	12.00	0.112	2.52E+04
10	1U	ABOVE	1U-ABOVE	3	0.00	12.00	0.105	2.23E+04
10	1U	ABOVE	1U-ABOVE	3	0.70	12.00	0.116	2.66E+04
10	1U	ABOVE	1U-ABOVE	3	0.70	12.00	0.093	2.29E+04
10	1U	ABOVE	1U-ABOVE	3	1.40	12.00	0.086	2.23E+04
10	1U	ABOVE	1U-ABOVE	3	1.40	12.00	0.089	2.56E+04
10	1U	ABOVE	1U-ABOVE	3	2.09	12.00	0.089	1.91E+04
10	1U	ABOVE	1U-ABOVE	3	2.09	12.00	0.078	2.67E+04
10	1U	ABOVE	1U-ABOVE	3	3.51	12.00	0.077	1.93E+04
10	1U	ABOVE	1U-ABOVE	3	3.51	12.00	0.120	2.40E+04
10	1U	ABOVE	1U-ABOVE	3	24.14	42.00	0.134	3.25E+04
10	1U	ABOVE	1U-ABOVE	3	24.14	42.00	0.140	3.70E+04
10	1U	ABOVE	1U-ABOVE	3	48.24	75.00	0.173	4.28E+04
10	1U	ABOVE	1U-ABOVE	3	48.24	75.00	0.200	4.51E+04
10	1U	ABOVE	1U-ABOVE	3	48.24	75.00	0.172	4.28E+04
10	1U	ABOVE	1U-ABOVE	3	0.07	15	0.055	2.143E+04
10	1U	ABOVE	1U-ABOVE	3	0.07	45	0.158	3.686E+04
10	1U	ABOVE	1U-ABOVE	3	0.07	85	0.188	4.500E+04
10	1U	ABOVE	1U-ABOVE	3	0.07	120	0.150	4.553E+04
10	1U	ABOVE	1U-ABOVE	3	0.07	145	0.195	4.716E+04
18	1U	ABOVE	1U-ABOVE	3	0.00	13.00	0.084	4.87E+04
18	1U	ABOVE	1U-ABOVE	3	0.00	13.00	0.094	4.94E+04
18	1U	ABOVE	1U-ABOVE	3	0.00	13.00	0.103	5.59E+04
18	1U	ABOVE	1U-ABOVE	3	0.70	13.00	0.088	5.22E+04
18	1U	ABOVE	1U-ABOVE	3	0.70	13.00	0.172	8.09E+04
18	1U	ABOVE	1U-ABOVE	3	1.38	13.00	0.122	7.08E+04
18	1U	ABOVE	1U-ABOVE	3	1.38	13.00	0.101	4.57E+04
18	1U	ABOVE	1U-ABOVE	3	1.38	13.00	0.219	1.00E+05
18	1U	ABOVE	1U-ABOVE	3	2.05	13.00	0.125	5.31E+04
18	1U	ABOVE	1U-ABOVE	3	2.05	13.00	0.127	5.39E+04
18	1U	ABOVE	1U-ABOVE	3	2.05	13.00	0.133	6.76E+04
18	1U	ABOVE	1U-ABOVE	3	3.45	13.00	0.119	5.45E+04
18	1U	ABOVE	1U-ABOVE	3	3.45	13.00	0.117	5.16E+04
18	1U	ABOVE	1U-ABOVE	3	3.45	13.00	0.135	8.23E+04
18	1U	ABOVE	1U-ABOVE	3	24.10	43.00	0.162	7.00E+04
18	1U	ABOVE	1U-ABOVE	3	24.10	43.00	0.139	5.97E+04
18	1U	ABOVE	1U-ABOVE	3	24.10	43.00	0.150	1.09E+05
18	1U	ABOVE	1U-ABOVE	3	48.28	65.00	0.142	7.43E+04
18	1U	ABOVE	1U-ABOVE	3	48.28	65.00	0.160	6.55E+04
18	1U	ABOVE	1U-ABOVE	3	48.28	65.00	0.045	1.41E+05
18	1U	ABOVE	1U-ABOVE	3	24.10	48	0.133	7.880E+04
18	1U	ABOVE	1U-ABOVE	3	24.10	75	0.161	6.505E+04
18	1U	ABOVE	1U-ABOVE	3	24.10	110	0.137	5.858E+04
18	1U	ABOVE	1U-ABOVE	3	24.10	140	0.183	9.123E+04
18	1U	ABOVE	1U-ABOVE	3	24.10	178	0.206	6.543E+04
18	1U	ABOVE	1U-ABOVE	3	24.10	245	0.199	6.743E+04
18	1U	ABOVE	1U-ABOVE	3	24.10	300	0.196	6.314E+04
18	1U	ABOVE	1U-ABOVE	3	24.10	366	0.198	6.361E+04
22	1U	ABOVE	1U-ABOVE	3	0.00	13.00	0.085	4.02E+04
22	1U	ABOVE	1U-ABOVE	3	0.00	13.00	0.098	3.72E+04
22	1U	ABOVE	1U-ABOVE	3	0.00	13.00	0.184	5.02E+04
22	1U	ABOVE	1U-ABOVE	3	0.70	13.00	0.079	3.89E+04
22	1U	ABOVE	1U-ABOVE	3	0.70	13.00	0.111	4.22E+04
22	1U	ABOVE	1U-ABOVE	3	0.70	13.00	0.165	4.67E+04
22	1U	ABOVE	1U-ABOVE	3	1.39	13.00	0.123	4.22E+04
22	1U	ABOVE	1U-ABOVE	3	1.39	13.00	0.069	3.87E+04
22	1U	ABOVE	1U-ABOVE	3	1.39	13.00	0.124	4.57E+04
22	1U	ABOVE	1U-ABOVE	3	2.05	13.00	0.139	4.32E+04
22	1U	ABOVE	1U-ABOVE	3	2.05	13.00	0.134	4.48E+04
22	1U	ABOVE	1U-ABOVE	3	2.05	13.00	0.130	4.55E+04
22	1U	ABOVE	1U-ABOVE	3	3.46	13.00	0.121	4.51E+04

Elastic moduli for elastic and plastic deformation for tests using strain gauges

SAMPLE NUMBER	SAMPLE SUBUNIT	SAMPLE LOCATION	SAMPLE HORIZON	SAMPLE LITHOLOGY	σ_{22} (MPa)	σ_{11} (MPa)	ν	E (MPa)
22	1U	ABOVE	1U-ABOVE	3	3.46	13.00	0.122	4.29E+04
22	1U	ABOVE	1U-ABOVE	3	3.46	13.00	0.122	4.46E+04
22	1U	ABOVE	1U-ABOVE	3	24.12	35.00	0.121	5.37E+04
22	1U	ABOVE	1U-ABOVE	3	24.12	35.00	0.155	5.43E+04
22	1U	ABOVE	1U-ABOVE	3	24.12	35.00	0.215	6.17E+04
22	1U	ABOVE	1U-ABOVE	3	48.23	65.00	0.209	6.50E+04
22	1U	ABOVE	1U-ABOVE	3	48.23	65.00	0.188	6.34E+04
22	1U	ABOVE	1U-ABOVE	3	48.23	65.00	0.201	6.38E+04
22	1U	ABOVE	1U-ABOVE	3	48.22	180	0.175	7.053E+04
22	1U	ABOVE	1U-ABOVE	3	48.22	217	0.221	7.579E+04
22	1U	ABOVE	1U-ABOVE	3	48.22	260	0.175	7.071E+04
22	1U	ABOVE	1U-ABOVE	3	48.22	305	0.204	7.262E+04
22	1U	ABOVE	1U-ABOVE	3	48.22	358	0.193	7.274E+04
22	1U	ABOVE	1U-ABOVE	3	48.22	403	0.221	7.363E+04
22	1U	ABOVE	1U-ABOVE	3	48.22	440	0.239	7.339E+04
22	1U	ABOVE	1U-ABOVE	3	48.22	478	0.221	7.106E+04
22	1U	ABOVE	1U-ABOVE	3	48.22	514	0.226	6.971E+04
37	5U	BELOW	5U-BELOW	2	0.00	12.00	0.037	1.19E+04
37	5U	BELOW	5U-BELOW	2	0.00	12.00	0.075	1.91E+04
37	5U	BELOW	5U-BELOW	2	0.68	12.00	0.056	1.42E+04
37	5U	BELOW	5U-BELOW	2	0.68	12.00	0.092	2.23E+04
37	5U	BELOW	5U-BELOW	2	0.68	12.00	0.033	1.03E+04
37	5U	BELOW	5U-BELOW	2	0.68	12.00	0.098	2.45E+04
37	5U	BELOW	5U-BELOW	2	1.39	12.00	0.046	1.22E+04
37	5U	BELOW	5U-BELOW	2	1.39	12.00	0.035	1.09E+04
37	5U	BELOW	5U-BELOW	2	1.39	12.00	0.049	1.57E+04
37	5U	BELOW	5U-BELOW	2	2.08	12.00	0.041	1.13E+04
37	5U	BELOW	5U-BELOW	2	2.08	12.00	0.043	1.91E+04
37	5U	BELOW	5U-BELOW	2	3.45	12.00	0.066	1.43E+04
37	5U	BELOW	5U-BELOW	2	3.45	12.00	0.095	2.11E+04
37	5U	BELOW	5U-BELOW	2	24.12	45.00	0.128	2.79E+04
37	5U	BELOW	5U-BELOW	2	24.12	45.00	0.145	3.02E+04
37	5U	BELOW	5U-BELOW	2	48.28	68.00	0.145	3.14E+04
37	5U	BELOW	5U-BELOW	2	48.28	68.00	0.145	3.83E+04
37	5U	BELOW	5U-BELOW	2	24.10	65	0.128	3.254E+04
37	5U	BELOW	5U-BELOW	2	24.10	93	0.103	3.176E+04
37	5U	BELOW	5U-BELOW	2	24.10	120	0.116	3.186E+04
37	5U	BELOW	5U-BELOW	2	24.10	142	0.094	2.805E+04
37	5U	BELOW	5U-BELOW	2	24.10	165	0.159	3.576E+04
37	5U	BELOW	5U-BELOW	2	24.10	185	0.146	3.686E+04
37	5U	BELOW	5U-BELOW	2	24.10	202	0.061	2.950E+04
47	5U	ABOVE	5U-ABOVE	4	0.00	15.00	0.022	1.18E+04
47	5U	ABOVE	5U-ABOVE	4	0.00	15.00	0.018	1.20E+04
47	5U	ABOVE	5U-ABOVE	4	0.00	15.00	0.023	2.05E+04
47	5U	ABOVE	5U-ABOVE	4	0.70	15.00	0.030	1.10E+04
47	5U	ABOVE	5U-ABOVE	4	0.70	15.00	0.027	7.25E+03
47	5U	ABOVE	5U-ABOVE	4	0.70	15.00	0.022	1.91E+04
47	5U	ABOVE	5U-ABOVE	4	1.40	15.00	0.025	1.09E+04
47	5U	ABOVE	5U-ABOVE	4	1.40	15.00	0.035	2.11E+04
47	5U	ABOVE	5U-ABOVE	4	2.10	15.00	0.032	1.33E+04
47	5U	ABOVE	5U-ABOVE	4	2.10	15.00	0.029	1.13E+04
47	5U	ABOVE	5U-ABOVE	4	2.10	15.00	0.048	2.30E+04
47	5U	ABOVE	5U-ABOVE	4	3.47	15.00	0.038	1.24E+04
47	5U	ABOVE	5U-ABOVE	4	3.47	15.00	0.033	9.81E+03
47	5U	ABOVE	5U-ABOVE	4	3.47	15.00	0.042	1.96E+04
47	5U	ABOVE	5U-ABOVE	4	24.12	39.00	0.068	1.92E+04
47	5U	ABOVE	5U-ABOVE	4	24.12	39.00	0.072	2.02E+04
47	5U	ABOVE	5U-ABOVE	4	48.23	65.00	0.083	2.34E+04
47	5U	ABOVE	5U-ABOVE	4	6.92	65.00	0.096	2.63E+04
47	5U	ABOVE	5U-ABOVE	4	6.92	10	0.029	7.896E+03
47	5U	ABOVE	5U-ABOVE	4	6.92	25	0.035	1.657E+04
47	5U	ABOVE	5U-ABOVE	4	6.92	51	0.069	2.244E+04
47	5U	ABOVE	5U-ABOVE	4	6.92	72	0.091	2.615E+04
47	5U	ABOVE	5U-ABOVE	4	6.92	93	0.072	2.981E+04
47	5U	ABOVE	5U-ABOVE	4	6.92	114	0.093	3.328E+04
47	5U	ABOVE	5U-ABOVE	4	6.92	135	0.098	3.646E+04
50	5U	ABOVE	5U-ABOVE	4	0.00	15.00	0.058	1.59E+04
50	5U	ABOVE	5U-ABOVE	4	0.00	15.00	0.052	2.28E+03
50	5U	ABOVE	5U-ABOVE	4	0.74	15.00	0.049	1.30E+04
50	5U	ABOVE	5U-ABOVE	4	0.74	15.00	0.062	1.76E+04
50	5U	ABOVE	5U-ABOVE	4	1.35	15.00	0.048	1.39E+04
50	5U	ABOVE	5U-ABOVE	4	1.35	15.00	0.074	1.96E+04
50	5U	ABOVE	5U-ABOVE	4	2.11	25.00	0.085	2.16E+04
50	5U	ABOVE	5U-ABOVE	4	2.11	25.00	0.078	2.22E+04
50	5U	ABOVE	5U-ABOVE	4	3.44	25.00	0.061	1.62E+04
50	5U	ABOVE	5U-ABOVE	4	3.44	25.00	0.072	1.88E+04
50	5U	ABOVE	5U-ABOVE	4	24.12	38.00	0.092	2.33E+04
50	5U	ABOVE	5U-ABOVE	4	24.12	38.00	0.110	2.89E+04
50	5U	ABOVE	5U-ABOVE	4	48.30	72.00	0.132	3.49E+04
50	5U	ABOVE	5U-ABOVE	4	48.30	72.00	0.153	3.56E+04
50	5U	ABOVE	5U-ABOVE	4	24.14	26	0.038	3.703E+04
50	5U	ABOVE	5U-ABOVE	4	24.14	44	0.100	2.848E+04

Elastic moduli for elastic and plastic deformation for tests using strain gauges

SAMPLE NUMBER	SAMPLE SUBUNIT	SAMPLE LOCATION	SAMPLE HORIZON	SAMPLE LITHOLOGY	σ_{22} (MPa)	σ_{11} (MPa)	ν	E (MPa)
50	5U	ABOVE	5U-ABOVE	4	24.14	65	0.129	3.280E+04
50	5U	ABOVE	5U-ABOVE	4	24.14	96	0.155	3.810E+04
50	5U	ABOVE	5U-ABOVE	4	24.14	128	0.168	3.942E+04
50	5U	ABOVE	5U-ABOVE	4	24.14	153	0.181	4.013E+04
50	5U	ABOVE	5U-ABOVE	4	24.14	175	0.196	3.898E+04
51	5U	ABOVE	5U-ABOVE	4	0.00	13.00	0.042	1.34E+04
51	5U	ABOVE	5U-ABOVE	4	0.00	13.00	0.037	1.40E+04
51	5U	ABOVE	5U-ABOVE	4	0.00	13.00	0.062	1.63E+04
51	5U	ABOVE	5U-ABOVE	4	0.72	13.00	0.045	1.44E+04
51	5U	ABOVE	5U-ABOVE	4	0.72	13.00	0.046	1.63E+04
51	5U	ABOVE	5U-ABOVE	4	1.40	13.00	0.044	1.63E+04
51	5U	ABOVE	5U-ABOVE	4	1.40	13.00	0.045	1.49E+04
51	5U	ABOVE	5U-ABOVE	4	1.40	13.00	0.055	1.60E+04
51	5U	ABOVE	5U-ABOVE	4	2.07	13.00	0.051	1.52E+04
51	5U	ABOVE	5U-ABOVE	4	2.07	13.00	0.057	1.74E+04
51	5U	ABOVE	5U-ABOVE	4	3.45	13.00	0.055	1.53E+04
51	5U	ABOVE	5U-ABOVE	4	3.45	13.00	0.060	1.76E+04
51	5U	ABOVE	5U-ABOVE	4	24.19	34.00	0.085	2.30E+04
51	5U	ABOVE	5U-ABOVE	4	24.19	34.00	0.088	2.25E+04
51	5U	ABOVE	5U-ABOVE	4	24.19	34.00	0.067	2.67E+04
51	5U	ABOVE	5U-ABOVE	4	48.24	64.00	0.111	3.29E+04
51	5U	ABOVE	5U-ABOVE	4	48.24	64.00	0.123	3.22E+04
51	5U	ABOVE	5U-ABOVE	4	48.24	64.00	0.133	3.95E+04
51	5U	ABOVE	5U-ABOVE	4	24.15	33	0.085	2.333E+04
51	5U	ABOVE	5U-ABOVE	4	24.15	82	0.155	3.876E+04
51	5U	ABOVE	5U-ABOVE	4	24.15	82	0.144	3.626E+04
51	5U	ABOVE	5U-ABOVE	4	24.15	127	0.168	4.183E+04
51	5U	ABOVE	5U-ABOVE	4	24.15	149	0.182	4.058E+04
51	5U	ABOVE	5U-ABOVE	4	24.15	185	0.167	4.320E+04
51	5U	ABOVE	5U-ABOVE	4	24.15	205	0.177	4.303E+04
51	5U	ABOVE	5U-ABOVE	4	24.15	218	0.166	4.159E+04
62	5U	RESERVOIR	5U-RESERVOIR	6	0.00	20.00	0.101	1.77E+04
62	5U	RESERVOIR	5U-RESERVOIR	6	0.00	20.00	0.112	1.91E+04
62	5U	RESERVOIR	5U-RESERVOIR	6	0.76	20.00	0.092	1.74E+04
62	5U	RESERVOIR	5U-RESERVOIR	6	0.76	20.00	0.123	2.32E+04
62	5U	RESERVOIR	5U-RESERVOIR	6	1.39	20.00	0.090	1.41E+04
62	5U	RESERVOIR	5U-RESERVOIR	6	1.39	20.00	0.109	1.45E+04
62	5U	RESERVOIR	5U-RESERVOIR	6	2.06	20.00	0.101	1.47E+04
62	5U	RESERVOIR	5U-RESERVOIR	6	2.06	20.00	0.097	1.92E+04
62	5U	RESERVOIR	5U-RESERVOIR	6	3.47	13.00	0.064	1.03E+04
62	5U	RESERVOIR	5U-RESERVOIR	6	3.47	13.00	0.064	1.63E+04
62	5U	RESERVOIR	5U-RESERVOIR	6	24.16	36.00	0.104	2.34E+04
62	5U	RESERVOIR	5U-RESERVOIR	6	24.16	36.00	0.089	3.06E+04
62	5U	RESERVOIR	5U-RESERVOIR	6	48.38	68.00	0.133	3.36E+04
62	5U	RESERVOIR	5U-RESERVOIR	6	48.38	68.00	0.148	3.67E+04
62	5U	RESERVOIR	5U-RESERVOIR	6	3.42	9	0.007	9.220E+03
62	5U	RESERVOIR	5U-RESERVOIR	6	3.42	19	0.064	1.629E+04
62	5U	RESERVOIR	5U-RESERVOIR	6	3.42	34	0.037	1.820E+04
62	5U	RESERVOIR	5U-RESERVOIR	6	3.42	57	0.116	2.633E+04
62	5U	RESERVOIR	5U-RESERVOIR	6	3.42	80	0.127	2.877E+04
62	5U	RESERVOIR	5U-RESERVOIR	6	3.42	108	0.145	3.073E+04
62	5U	RESERVOIR	5U-RESERVOIR	6	3.42	133	0.162	2.895E+04
79	1U	RESERVOIR	1U-RESERVOIR	6	0.00	12.00	0.113	2.51E+04
79	1U	RESERVOIR	1U-RESERVOIR	6	0.00	12.00	0.098	2.15E+04
79	1U	RESERVOIR	1U-RESERVOIR	6	0.00	12.00	0.100	2.91E+04
79	1U	RESERVOIR	1U-RESERVOIR	6	0.00	12.00	0.117	2.99E+04
79	1U	RESERVOIR	1U-RESERVOIR	6	0.68	12.00	0.107	2.22E+04
79	1U	RESERVOIR	1U-RESERVOIR	6	0.68	12.00	0.080	2.27E+04
79	1U	RESERVOIR	1U-RESERVOIR	6	1.38	12.00	0.091	2.25E+04
79	1U	RESERVOIR	1U-RESERVOIR	6	1.38	12.00	0.103	2.52E+04
79	1U	RESERVOIR	1U-RESERVOIR	6	2.11	15.00	0.109	2.28E+04
79	1U	RESERVOIR	1U-RESERVOIR	6	2.11	15.00	0.119	2.67E+04
79	1U	RESERVOIR	1U-RESERVOIR	6	3.43	15.00	0.094	2.33E+04
79	1U	RESERVOIR	1U-RESERVOIR	6	3.43	15.00	0.123	2.46E+04
79	1U	RESERVOIR	1U-RESERVOIR	6	3.43	15.00	0.117	2.67E+04
79	1U	RESERVOIR	1U-RESERVOIR	6	24.14	38.00	0.116	3.80E+04
79	1U	RESERVOIR	1U-RESERVOIR	6	24.14	38.00	0.135	3.63E+04
79	1U	RESERVOIR	1U-RESERVOIR	6	24.14	38.00	0.139	4.20E+04
79	1U	RESERVOIR	1U-RESERVOIR	6	48.26	75.00	0.141	4.22E+04
79	1U	RESERVOIR	1U-RESERVOIR	6	48.26	75.00	0.134	3.91E+04
79	1U	RESERVOIR	1U-RESERVOIR	6	48.26	75.00	0.150	4.32E+04
79	1U	RESERVOIR	1U-RESERVOIR	6	24.12	38	0.115	4.108E+04
79	1U	RESERVOIR	1U-RESERVOIR	6	24.12	72	0.131	4.135E+04
79	1U	RESERVOIR	1U-RESERVOIR	6	24.12	115	0.088	4.681E+04
79	1U	RESERVOIR	1U-RESERVOIR	6	24.12	165	0.165	5.125E+04
79	1U	RESERVOIR	1U-RESERVOIR	6	24.12	250	0.175	5.048E+04
79	1U	RESERVOIR	1U-RESERVOIR	6	24.12	307	0.197	5.073E+04
79	1U	RESERVOIR	1U-RESERVOIR	6	24.12	355	0.239	4.824E+04
79	1U	RESERVOIR	1U-RESERVOIR	6	24.12	380	0.303	4.602E+04
82	1U	RESERVOIR	1U-RESERVOIR	3	0.00	13.00	0.086	1.44E+04
82	1U	RESERVOIR	1U-RESERVOIR	3	0.00	13.00	0.097	1.85E+04
82	1U	RESERVOIR	1U-RESERVOIR	3	0.68	13.00	0.088	1.50E+04

Elastic moduli for elastic and plastic deformation for tests using strain gauges

SAMPLE NUMBER	SAMPLE SUBUNIT	SAMPLE LOCATION	SAMPLE HORIZON	SAMPLE LITHOLOGY	σ_{22} (MPa)	σ_{11} (MPa)	ν	E (MPa)
82	1U	RESERVOIR	1U-RESERVOIR	3	0.68	13.00	0.108	1.81E+04
82	1U	RESERVOIR	1U-RESERVOIR	3	1.38	13.00	0.094	1.45E+04
82	1U	RESERVOIR	1U-RESERVOIR	3	1.38	13.00	0.104	1.70E+04
82	1U	RESERVOIR	1U-RESERVOIR	3	2.07	13.00	0.085	1.67E+04
82	1U	RESERVOIR	1U-RESERVOIR	3	2.07	13.00	0.088	1.70E+04
82	1U	RESERVOIR	1U-RESERVOIR	3	3.43	13.00	0.084	1.50E+04
82	1U	RESERVOIR	1U-RESERVOIR	3	3.43	13.00	0.108	1.69E+04
82	1U	RESERVOIR	1U-RESERVOIR	3	24.14	34.00	0.104	2.49E+04
82	1U	RESERVOIR	1U-RESERVOIR	3	24.14	34.00	0.101	2.63E+04
82	1U	RESERVOIR	1U-RESERVOIR	3	48.28	58.00	0.112	3.31E+04
82	1U	RESERVOIR	1U-RESERVOIR	3	48.28	58.00	0.141	3.36E+04
82	1U	RESERVOIR	1U-RESERVOIR	3	3.45	14	0.092	1.584E+04
82	1U	RESERVOIR	1U-RESERVOIR	3	3.45	26	0.088	1.890E+04
82	1U	RESERVOIR	1U-RESERVOIR	3	3.45	45	0.097	2.553E+04
82	1U	RESERVOIR	1U-RESERVOIR	3	3.45	69	0.114	3.050E+04
82	1U	RESERVOIR	1U-RESERVOIR	3	3.45	89	0.087	3.581E+04
82	1U	RESERVOIR	1U-RESERVOIR	3	3.45	111	0.102	3.107E+04
82	1U	RESERVOIR	1U-RESERVOIR	3	3.45	134	0.111	3.167E+04
94	5U	ABOVE	5U-ABOVE	3	1.41	12.00	0.104	1.94E+04
94	5U	ABOVE	5U-ABOVE	3	2.13	12.00	0.095	1.91E+04
94	5U	ABOVE	5U-ABOVE	3	0.86	24.00	0.070	2.60E+04
94	5U	ABOVE	5U-ABOVE	3	0.86	24.00	0.069	2.74E+04
94	5U	ABOVE	5U-ABOVE	3	0.85	24.00	0.092	2.25E+04
94	5U	ABOVE	5U-ABOVE	3	2.09	29.00	0.070	2.72E+04
94	5U	ABOVE	5U-ABOVE	3	2.09	29.00	0.077	2.46E+04
94	5U	ABOVE	5U-ABOVE	3	2.09	29.00	0.101	2.03E+04
94	5U	ABOVE	5U-ABOVE	3	3.44	29.00	0.075	2.47E+04
94	5U	ABOVE	5U-ABOVE	3	3.44	29.00	0.076	2.46E+04
94	5U	ABOVE	5U-ABOVE	3	3.44	29.00	0.104	1.98E+04
94	5U	ABOVE	5U-ABOVE	3	20.74	39.00	0.054	3.43E+04
94	5U	ABOVE	5U-ABOVE	3	20.74	39.00	0.066	2.75E+04
94	5U	ABOVE	5U-ABOVE	3	20.74	39.00	0.083	2.49E+04
94	5U	ABOVE	5U-ABOVE	3	48.27	67.00	0.056	3.49E+04
94	5U	ABOVE	5U-ABOVE	3	48.27	67.00	0.407	3.98E+04
94	5U	ABOVE	5U-ABOVE	3	48.27	67.00	0.057	3.63E+04
94	5U	ABOVE	5U-ABOVE	3	48.16	63	0.045	4.231E+04
94	5U	ABOVE	5U-ABOVE	3	48.16	96	0.048	4.233E+04
94	5U	ABOVE	5U-ABOVE	3	48.16	131	0.044	4.666E+04
94	5U	ABOVE	5U-ABOVE	3	48.16	166	0.041	4.974E+04
94	5U	ABOVE	5U-ABOVE	3	48.16	198	0.040	5.037E+04
94	5U	ABOVE	5U-ABOVE	3	48.16	238	0.040	5.044E+04
94	5U	ABOVE	5U-ABOVE	3	48.16	268	0.040	5.062E+04
94	5U	ABOVE	5U-ABOVE	3	48.16	300	0.038	5.325E+04
94	5U	ABOVE	5U-ABOVE	3	48.16	327	0.041	4.940E+04
97	5U	ABOVE	5U-ABOVE	3	0.70	13.00	0.048	1.631E+04
97	5U	ABOVE	5U-ABOVE	3	0.70	13.00	0.048	1.633E+04
97	5U	ABOVE	5U-ABOVE	3	0.70	13.00	0.049	1.719E+04
97	5U	ABOVE	5U-ABOVE	3	1.39	18.00	0.057	1.861E+04
97	5U	ABOVE	5U-ABOVE	3	1.39	18.00	0.057	1.875E+04
97	5U	ABOVE	5U-ABOVE	3	1.39	18.00	0.059	1.902E+04
97	5U	ABOVE	5U-ABOVE	3	2.07	16.00	0.052	1.613E+04
97	5U	ABOVE	5U-ABOVE	3	2.07	16.00	0.050	1.597E+04
97	5U	ABOVE	5U-ABOVE	3	2.07	16.00	0.054	1.683E+04
97	5U	ABOVE	5U-ABOVE	3	3.48	21.00	0.061	1.837E+04
97	5U	ABOVE	5U-ABOVE	3	3.48	21.00	0.061	1.809E+04
97	5U	ABOVE	5U-ABOVE	3	3.48	21.00	0.064	2.007E+04
103	5U	ABOVE	5U-ABOVE	2	0.00	17.00	0.065	1.788E+04
103	5U	ABOVE	5U-ABOVE	2	0.00	17.00	0.065	1.805E+04
103	5U	ABOVE	5U-ABOVE	2	0.00	17.00	0.067	1.860E+04
103	5U	ABOVE	5U-ABOVE	2	0.68	14.00	0.054	1.513E+04
103	5U	ABOVE	5U-ABOVE	2	0.68	14.00	0.059	1.663E+04
103	5U	ABOVE	5U-ABOVE	2	0.68	14.00	0.062	1.731E+04
103	5U	ABOVE	5U-ABOVE	2	1.37	20.00	0.071	1.998E+04
103	5U	ABOVE	5U-ABOVE	2	1.37	20.00	0.135	2.842E+04
103	5U	ABOVE	5U-ABOVE	2	1.37	20.00	0.074	2.096E+04
103	5U	ABOVE	5U-ABOVE	2	2.06	22.00	0.075	2.183E+04
103	5U	ABOVE	5U-ABOVE	2	2.06	22.00	0.079	2.264E+04
103	5U	ABOVE	5U-ABOVE	2	2.06	22.00	0.075	2.169E+04
103	5U	ABOVE	5U-ABOVE	2	3.46	24.00	0.075	2.426E+04
103	5U	ABOVE	5U-ABOVE	2	3.46	24.00	0.080	2.507E+04
103	5U	ABOVE	5U-ABOVE	2	3.46	24.00	0.083	2.401E+04
103	5U	ABOVE	5U-ABOVE	2	20.71	45.00	0.080	3.344E+04
103	5U	ABOVE	5U-ABOVE	2	20.71	45.00	0.102	3.397E+04
103	5U	ABOVE	5U-ABOVE	2	20.71	45.00	0.104	3.305E+04
103	5U	ABOVE	5U-ABOVE	2	48.26	70.00	0.105	4.244E+04
103	5U	ABOVE	5U-ABOVE	2	48.26	70.00	0.120	4.320E+04
103	5U	ABOVE	5U-ABOVE	2	48.26	70.00	0.126	4.226E+04
103	5U	ABOVE	5U-ABOVE	2	48.26	81	0.128	3.892E+04
103	5U	ABOVE	5U-ABOVE	2	48.26	112	0.145	4.030E+04
103	5U	ABOVE	5U-ABOVE	2	48.26	145	0.152	4.221E+04
103	5U	ABOVE	5U-ABOVE	2	48.26	175	0.161	4.260E+04
103	5U	ABOVE	5U-ABOVE	2	48.26	210	0.171	4.414E+04

Elastic moduli for elastic and plastic deformation for tests using strain gauges

SAMPLE NUMBER	SAMPLE SUBUNIT	SAMPLE LOCATION	SAMPLE HORIZON	SAMPLE LITHOLOGY	σ_z (MPa)	σ_{11} (MPa)	ν	E (MPa)
103	5U	ABOVE	5U-ABOVE	2	48.26	238	0.187	4.418E+04
103	5U	ABOVE	5U-ABOVE	2	48.26	268	0.189	4.550E+04
103	5U	ABOVE	5U-ABOVE	2	48.26	300	0.165	5.007E+04
103	5U	ABOVE	5U-ABOVE	2	48.26	320	0.243	4.608E+04
105	5U	ABOVE	5U-ABOVE	2	0.00	15.00	0.068	1.614E+04
105	5U	ABOVE	5U-ABOVE	2	0.00	15.00	0.063	1.540E+04
105	5U	ABOVE	5U-ABOVE	2	0.00	15.00	0.069	1.755E+04
105	5U	ABOVE	5U-ABOVE	2	0.70	16.00	0.069	1.686E+04
105	5U	ABOVE	5U-ABOVE	2	0.70	16.00	0.068	1.681E+04
105	5U	ABOVE	5U-ABOVE	2	0.70	16.00	0.072	1.863E+04
105	5U	ABOVE	5U-ABOVE	2	1.39	17.00	0.069	1.760E+04
105	5U	ABOVE	5U-ABOVE	2	1.39	17.00	0.070	1.743E+04
105	5U	ABOVE	5U-ABOVE	2	1.39	17.00	0.074	1.901E+04
105	5U	ABOVE	5U-ABOVE	2	2.05	19.00	0.074	1.953E+04
105	5U	ABOVE	5U-ABOVE	2	2.05	19.00	0.074	1.983E+04
105	5U	ABOVE	5U-ABOVE	2	2.05	19.00	0.075	1.959E+04
105	5U	ABOVE	5U-ABOVE	2	3.46	23.00	0.078	2.114E+04
105	5U	ABOVE	5U-ABOVE	2	3.46	23.00	0.074	2.026E+04
105	5U	ABOVE	5U-ABOVE	2	3.46	23.00	0.079	2.161E+04
105	5U	ABOVE	5U-ABOVE	2	20.68	45.00	0.104	2.983E+04
105	5U	ABOVE	5U-ABOVE	2	20.68	45.00	0.104	3.007E+04
105	5U	ABOVE	5U-ABOVE	2	20.68	45.00	0.104	3.017E+04
105	5U	ABOVE	5U-ABOVE	2	48.29	72.00	0.123	4.038E+04
105	5U	ABOVE	5U-ABOVE	2	48.29	72.00	0.132	3.847E+04
105	5U	ABOVE	5U-ABOVE	2	48.29	72.00	0.127	3.880E+04
105	5U	ABOVE	5U-ABOVE	2	4.42	20	0.073	2.196E+04
105	5U	ABOVE	5U-ABOVE	2	4.42	44	0.106	3.073E+04
105	5U	ABOVE	5U-ABOVE	2	4.42	66	0.126	3.479E+04
105	5U	ABOVE	5U-ABOVE	2	4.42	88	0.146	3.913E+04
105	5U	ABOVE	5U-ABOVE	2	4.42	110	0.163	4.081E+04
105	5U	ABOVE	5U-ABOVE	2	4.42	132	0.173	4.478E+04
107	1U	RESERVOIR	1U-RESERVOIR	3	0.00	6.00	0.042	1.691E+04
107	1U	RESERVOIR	1U-RESERVOIR	3	0.70	13.00	0.053	1.543E+04
107	1U	RESERVOIR	1U-RESERVOIR	3	0.70	13.00	0.048	1.400E+04
107	1U	RESERVOIR	1U-RESERVOIR	3	0.70	13.00	0.052	1.411E+04
107	1U	RESERVOIR	1U-RESERVOIR	3	1.41	16.00	0.060	1.576E+04
107	1U	RESERVOIR	1U-RESERVOIR	3	1.41	16.00	0.057	1.543E+04
107	1U	RESERVOIR	1U-RESERVOIR	3	1.41	16.00	0.063	1.622E+04
107	1U	RESERVOIR	1U-RESERVOIR	3	2.06	18.00	0.058	1.596E+04
107	1U	RESERVOIR	1U-RESERVOIR	3	2.06	18.00	0.060	1.648E+04
107	1U	RESERVOIR	1U-RESERVOIR	3	2.06	18.00	0.057	1.549E+04
107	1U	RESERVOIR	1U-RESERVOIR	3	2.73	19.00	0.059	1.636E+04
107	1U	RESERVOIR	1U-RESERVOIR	3	2.73	19.00	0.058	1.634E+04
107	1U	RESERVOIR	1U-RESERVOIR	3	2.73	19.00	0.060	1.612E+04
107	1U	RESERVOIR	1U-RESERVOIR	3	3.41	20.00	0.066	1.806E+04
107	1U	RESERVOIR	1U-RESERVOIR	3	3.41	20.00	0.066	1.764E+04
107	1U	RESERVOIR	1U-RESERVOIR	3	3.41	20.00	0.067	1.790E+04
107	1U	RESERVOIR	1U-RESERVOIR	3	20.67	40.00	0.098	2.877E+04
107	1U	RESERVOIR	1U-RESERVOIR	3	20.67	40.00	0.098	2.981E+04
107	1U	RESERVOIR	1U-RESERVOIR	3	20.67	40.00	0.100	3.035E+04
107	1U	RESERVOIR	1U-RESERVOIR	3	48.21	70.00	0.129	4.087E+04
107	1U	RESERVOIR	1U-RESERVOIR	3	48.21	70.00	0.116	3.994E+04
107	1U	RESERVOIR	1U-RESERVOIR	3	48.21	70.00	0.141	4.298E+04
107	1U	RESERVOIR	1U-RESERVOIR	3	0.00	6	0.034	1.607E+04
107	1U	RESERVOIR	1U-RESERVOIR	3	0.00	16	0.054	1.564E+04
107	1U	RESERVOIR	1U-RESERVOIR	3	0.00	44	0.106	2.804E+04
107	1U	RESERVOIR	1U-RESERVOIR	3	0.00	70	0.149	3.616E+04
107	1U	RESERVOIR	1U-RESERVOIR	3	0.00	93	0.256	3.438E+04
107	1U	RESERVOIR	1U-RESERVOIR	3	0.00	123	0.187	3.956E+04
107	1U	RESERVOIR	1U-RESERVOIR	3	0.00	144	0.267	3.779E+04
108	1U	RESERVOIR	1U-RESERVOIR	3	0.00	15.00	0.077	1.747E+04
108	1U	RESERVOIR	1U-RESERVOIR	3	0.00	15.00	0.080	1.814E+04
108	1U	RESERVOIR	1U-RESERVOIR	3	0.00	15.00	0.084	1.985E+04
108	1U	RESERVOIR	1U-RESERVOIR	3	0.72	15.00	0.074	1.804E+04
108	1U	RESERVOIR	1U-RESERVOIR	3	0.72	15.00	0.077	1.828E+04
108	1U	RESERVOIR	1U-RESERVOIR	3	0.72	15.00	0.074	1.775E+04
108	1U	RESERVOIR	1U-RESERVOIR	3	1.39	15.00	0.073	1.701E+04
108	1U	RESERVOIR	1U-RESERVOIR	3	1.39	15.00	0.074	1.743E+04
108	1U	RESERVOIR	1U-RESERVOIR	3	1.39	15.00	0.081	1.863E+04
108	1U	RESERVOIR	1U-RESERVOIR	3	2.08	20.00	0.084	2.057E+04
108	1U	RESERVOIR	1U-RESERVOIR	3	2.08	20.00	0.085	2.047E+04
108	1U	RESERVOIR	1U-RESERVOIR	3	2.08	20.00	0.091	2.121E+04
108	1U	RESERVOIR	1U-RESERVOIR	3	3.48	20.00	0.078	1.868E+04
108	1U	RESERVOIR	1U-RESERVOIR	3	3.48	20.00	0.078	1.767E+04
108	1U	RESERVOIR	1U-RESERVOIR	3	3.48	20.00	0.082	1.881E+04
108	1U	RESERVOIR	1U-RESERVOIR	3	20.68	43.00	0.117	2.819E+04
108	1U	RESERVOIR	1U-RESERVOIR	3	20.68	43.00	0.114	2.833E+04
108	1U	RESERVOIR	1U-RESERVOIR	3	20.68	43.00	0.118	2.856E+04
108	1U	RESERVOIR	1U-RESERVOIR	3	48.29	80.00	0.150	3.657E+04
108	1U	RESERVOIR	1U-RESERVOIR	3	48.29	80.00	0.145	3.879E+04
108	1U	RESERVOIR	1U-RESERVOIR	3	48.29	80.00	0.150	3.673E+04
108	1U	RESERVOIR	1U-RESERVOIR	3	48.29	93	0.153	3.982E+04

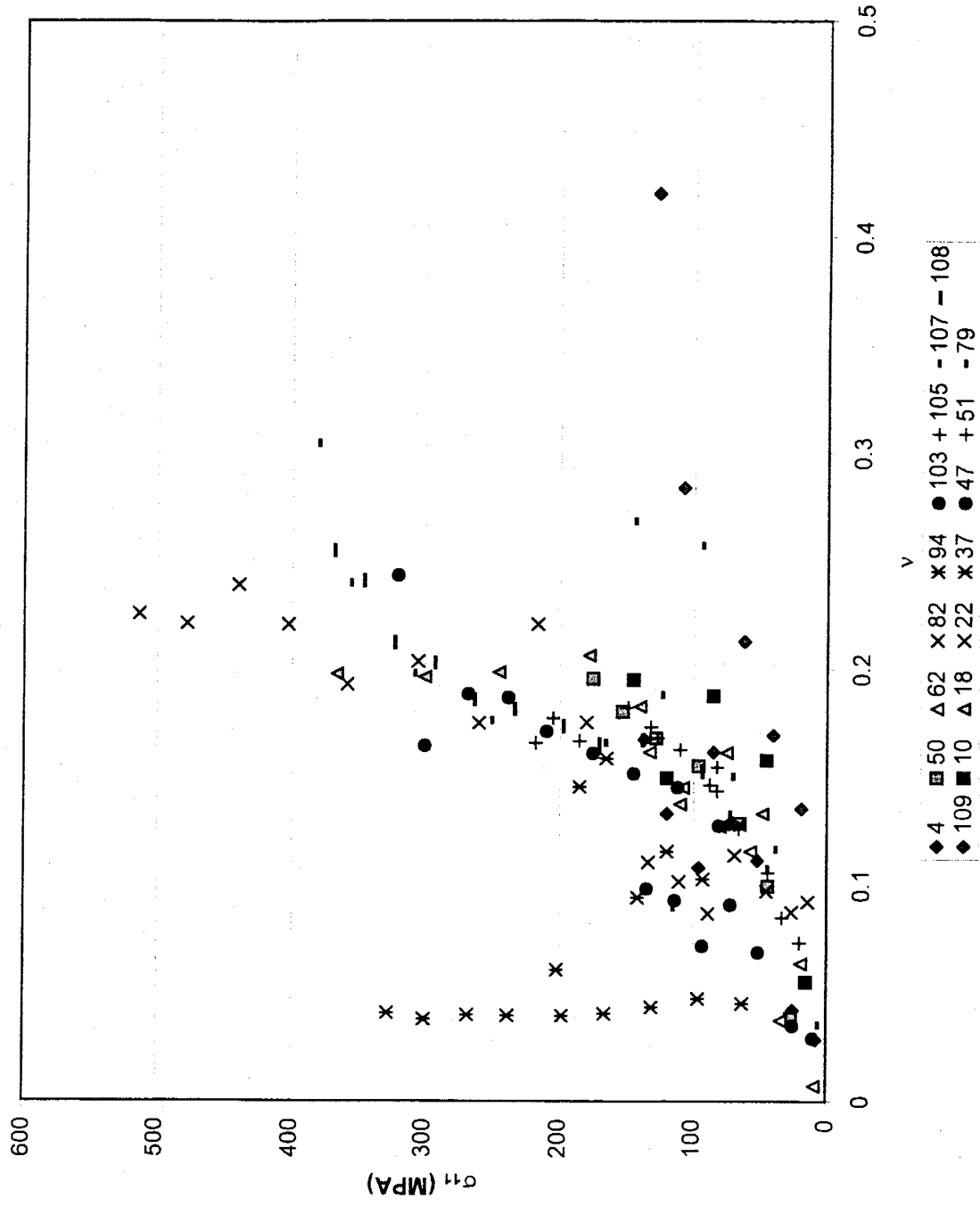
Elastic moduli for elastic and plastic deformation for tests using strain gauges

SAMPLE NUMBER	SAMPLE SUBUNIT	SAMPLE LOCATION	SAMPLE HORIZON	SAMPLE LITHOLOGY	σ_{22} (MPa)	σ_{11} (MPa)	ν	E (MPa)
108	1U	RESERVOIR	1U-RESERVOIR	3	48.29	138	0.167	4.275E+04
108	1U	RESERVOIR	1U-RESERVOIR	3	48.29	170	0.166	4.420E+04
108	1U	RESERVOIR	1U-RESERVOIR	3	48.29	197	0.174	4.319E+04
108	1U	RESERVOIR	1U-RESERVOIR	3	48.29	233	0.182	4.356E+04
108	1U	RESERVOIR	1U-RESERVOIR	3	48.29	263	0.186	4.377E+04
108	1U	RESERVOIR	1U-RESERVOIR	3	48.29	292	0.203	4.330E+04
108	1U	RESERVOIR	1U-RESERVOIR	3	48.29	322	0.212	4.235E+04
108	1U	RESERVOIR	1U-RESERVOIR	3	48.29	345	0.241	4.298E+04
108	1U	RESERVOIR	1U-RESERVOIR	3	48.29	368	0.255	4.186E+04

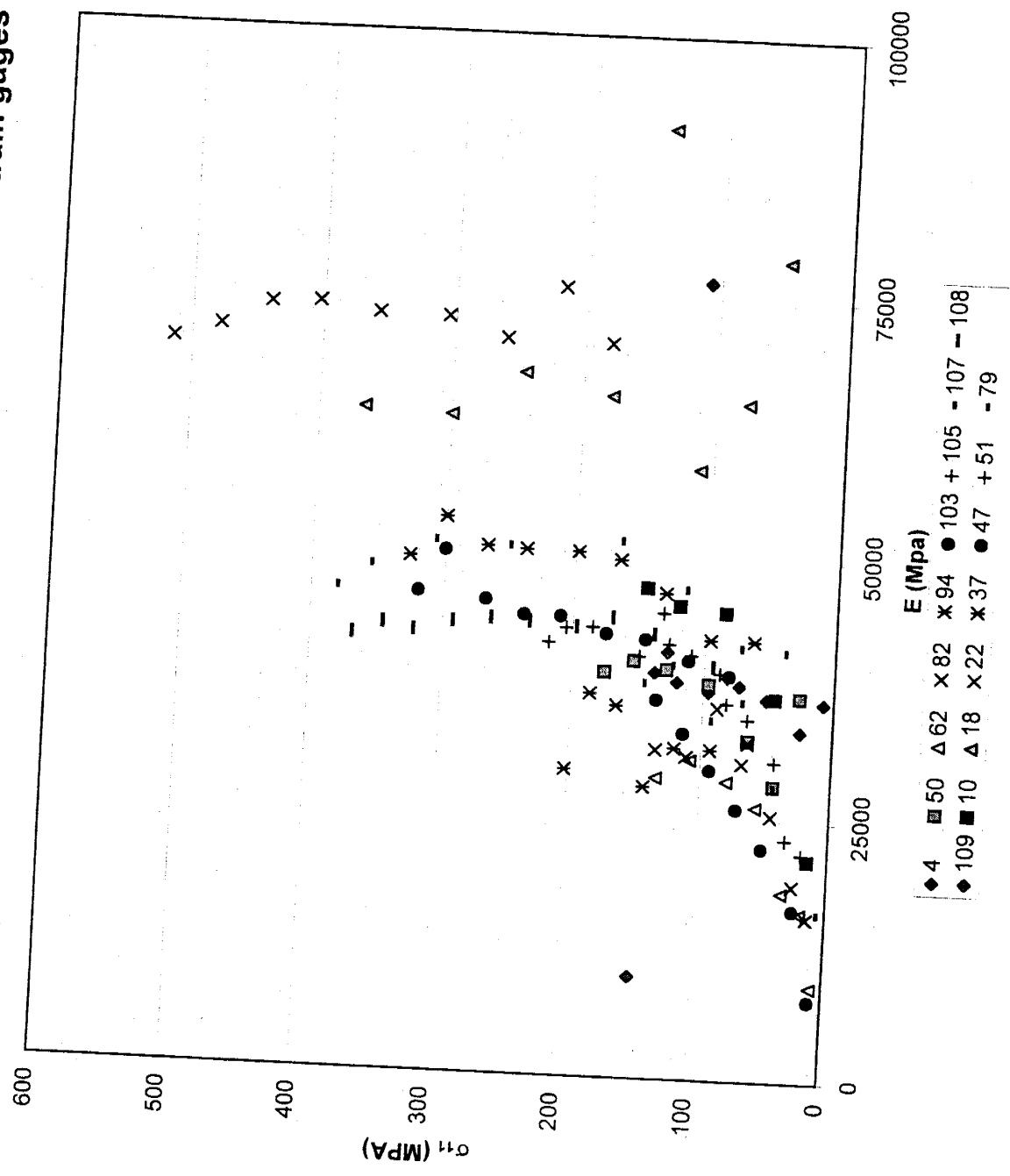
Notes:

- 1) See Figure 2 for position of sub-unit, horizon, location, and lithology
- 2) Lithology Type 2 is finely laminated, silty shale; Type 3 is finely laminated siltstone, Type 4 is bioturbated or disturbed siltstone, and Type 6 is massive to faintly stratified siltstone

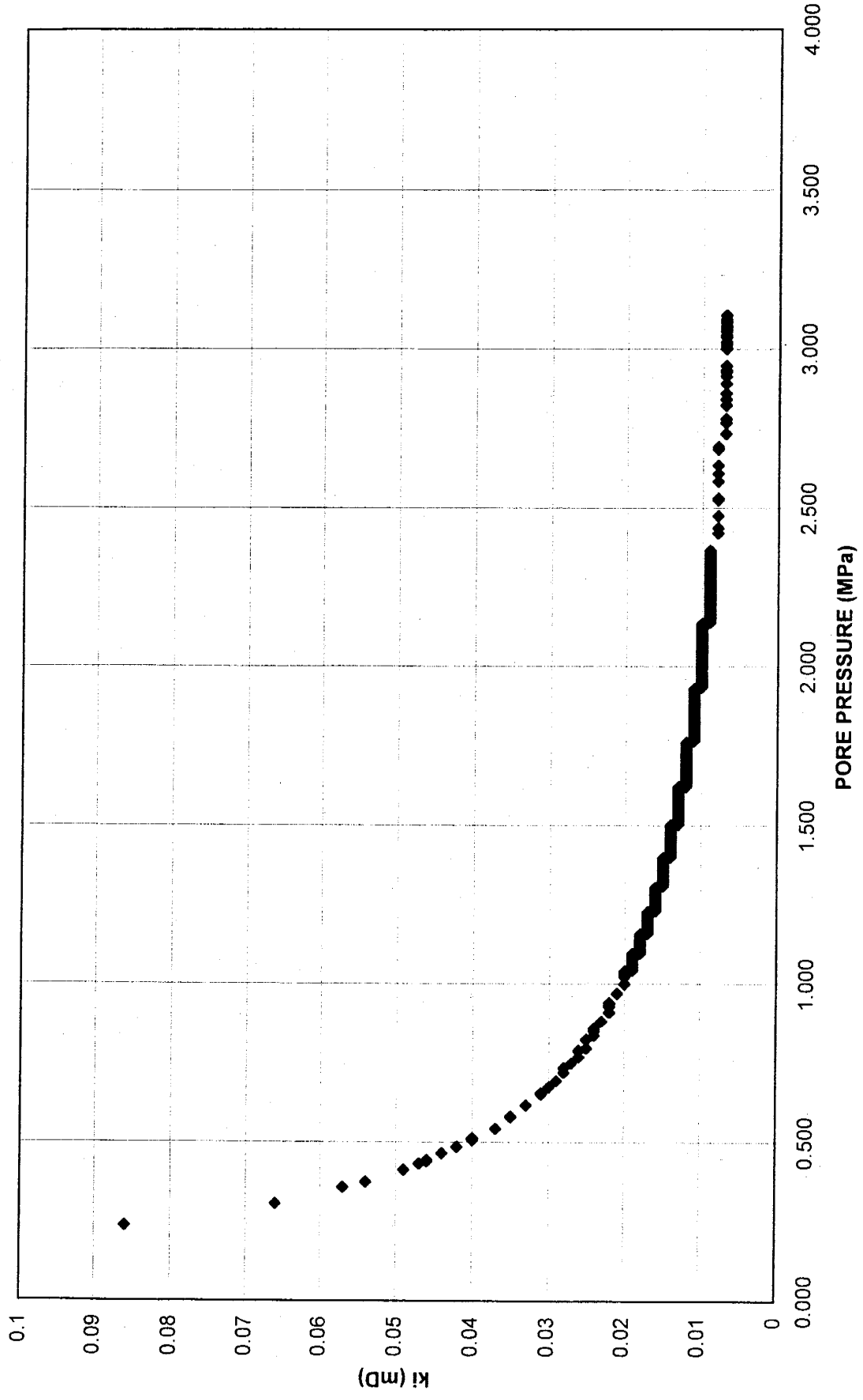
Plots of ν vs σ_{11} by sample for Triaxial Shear tests with strain gages



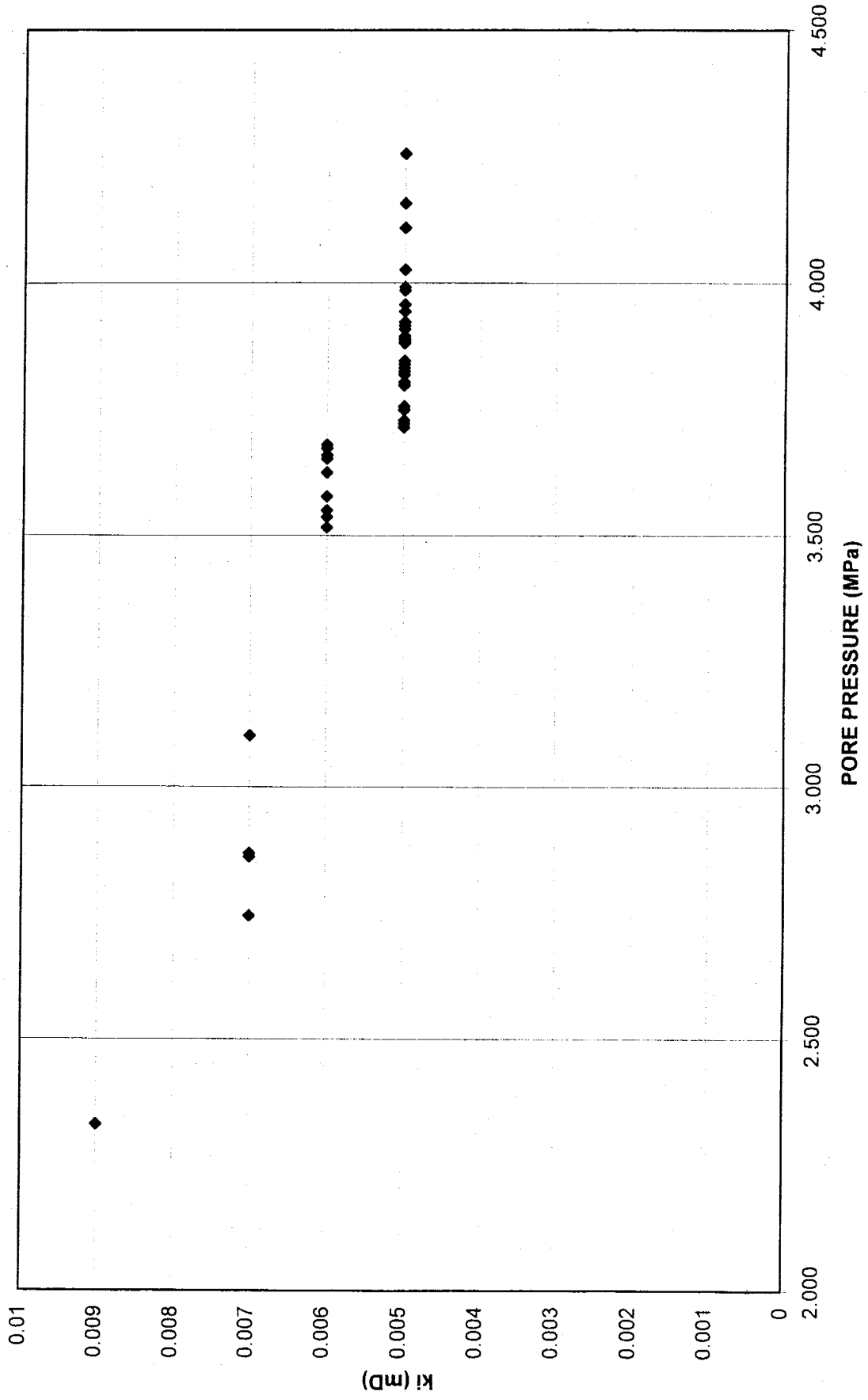
Plots of E vs σ_{11} by sample for Triaxial Shear tests with strain gages



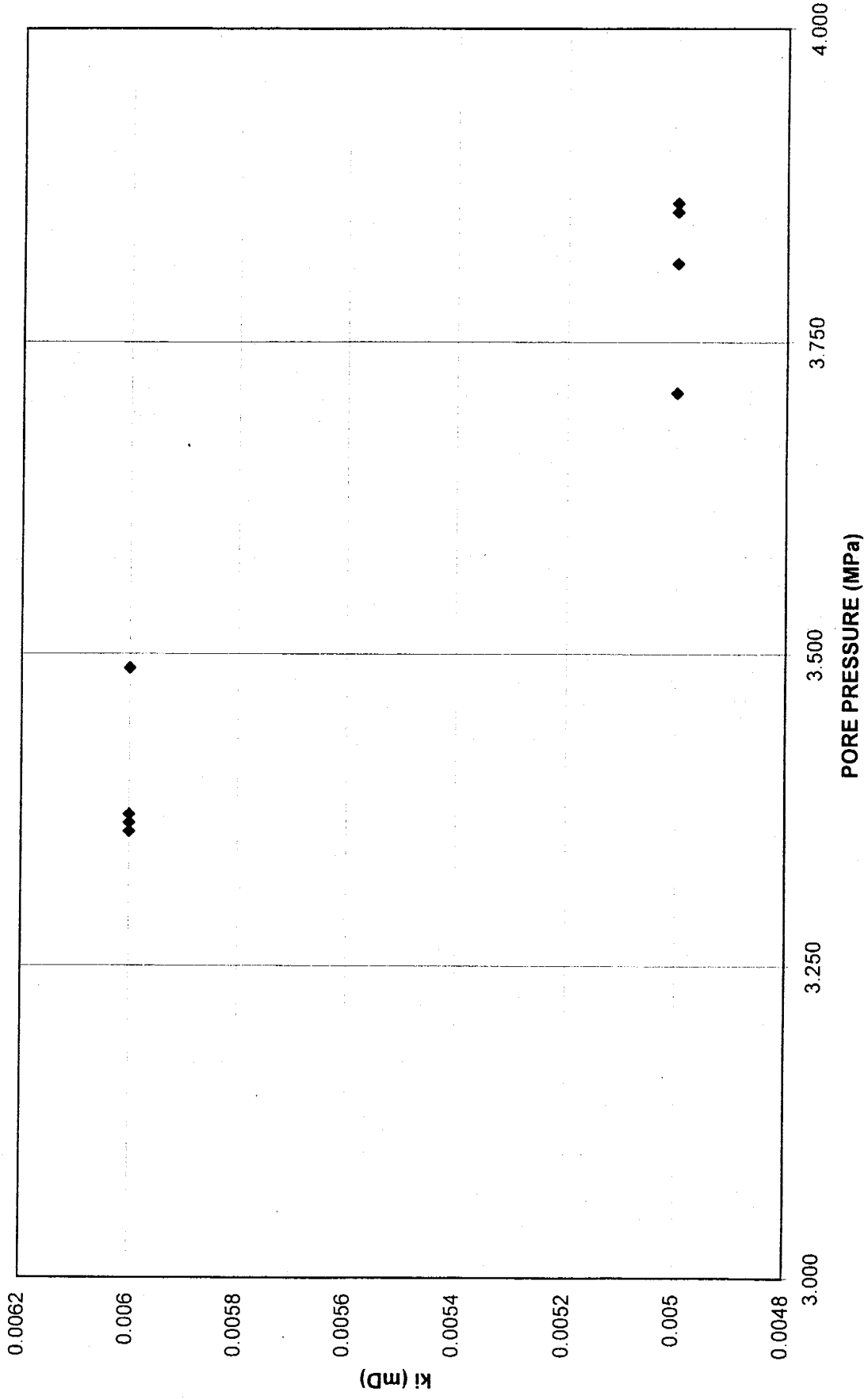
Permeability versus increased pore pressure resulting from increases in vertical load - Sample 37



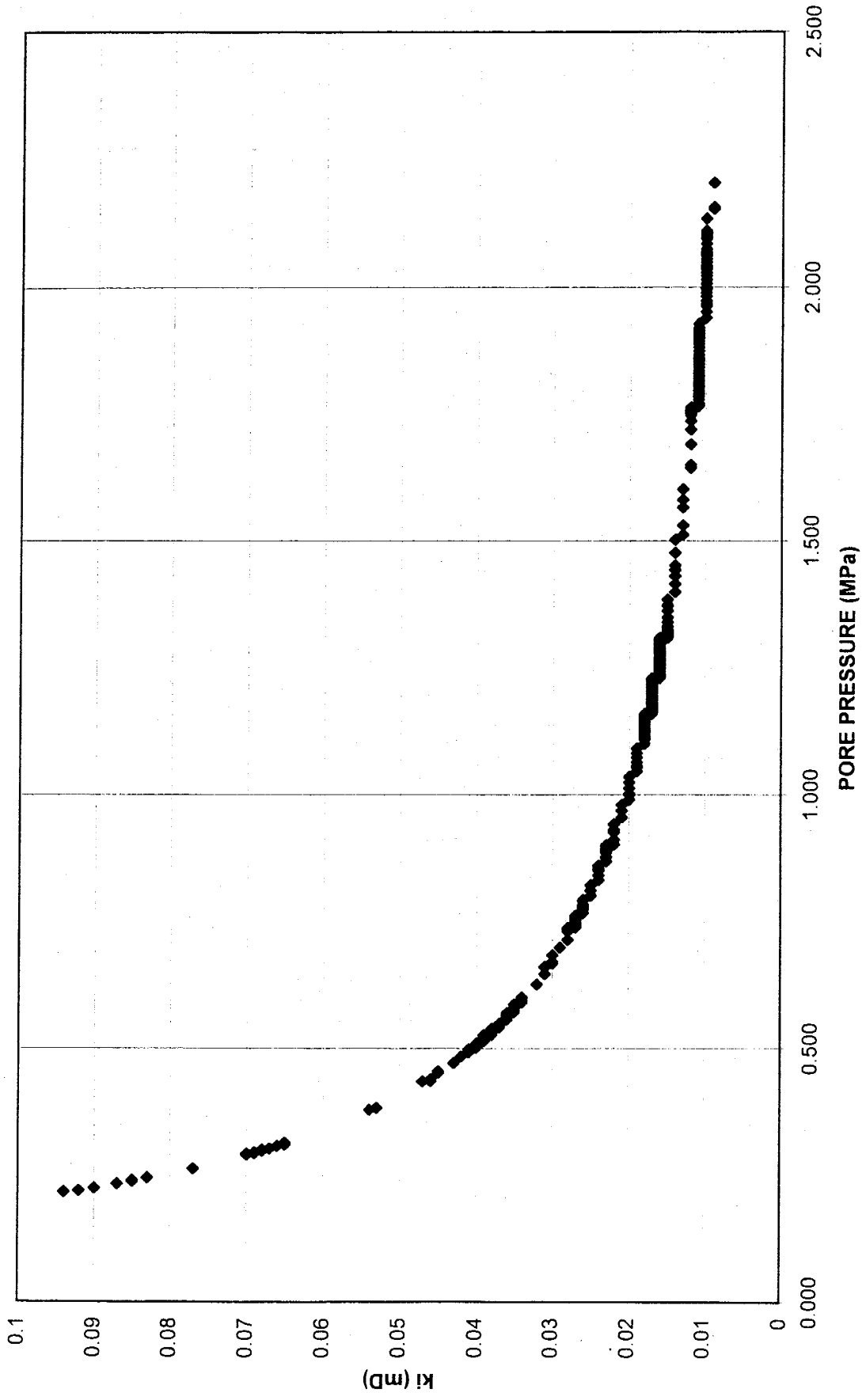
Permeability versus increased pore pressure resulting from increases in vertical load - Sample 56



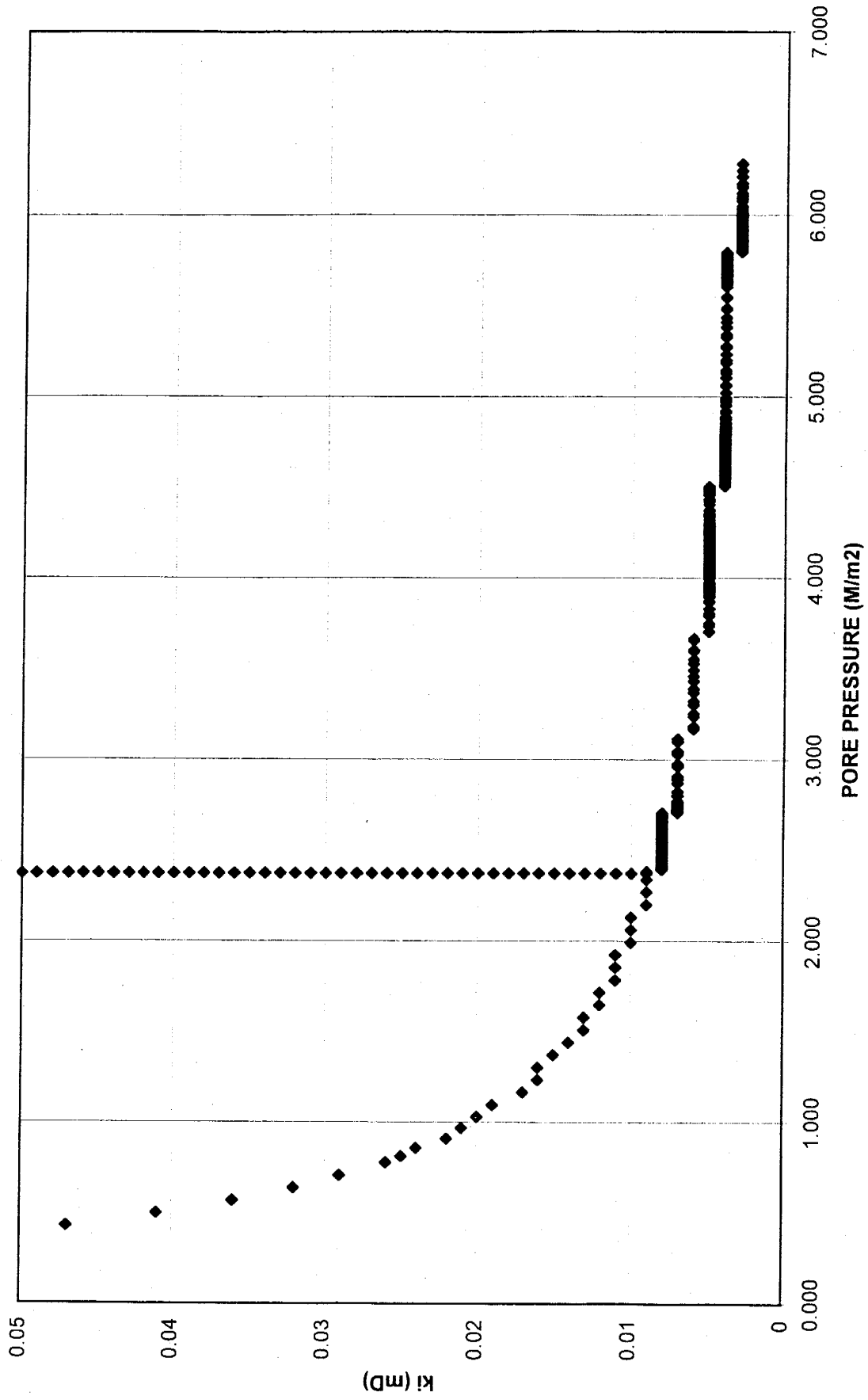
Permeability versus increased pore pressure resulting from increases in vertical load - Sample 57



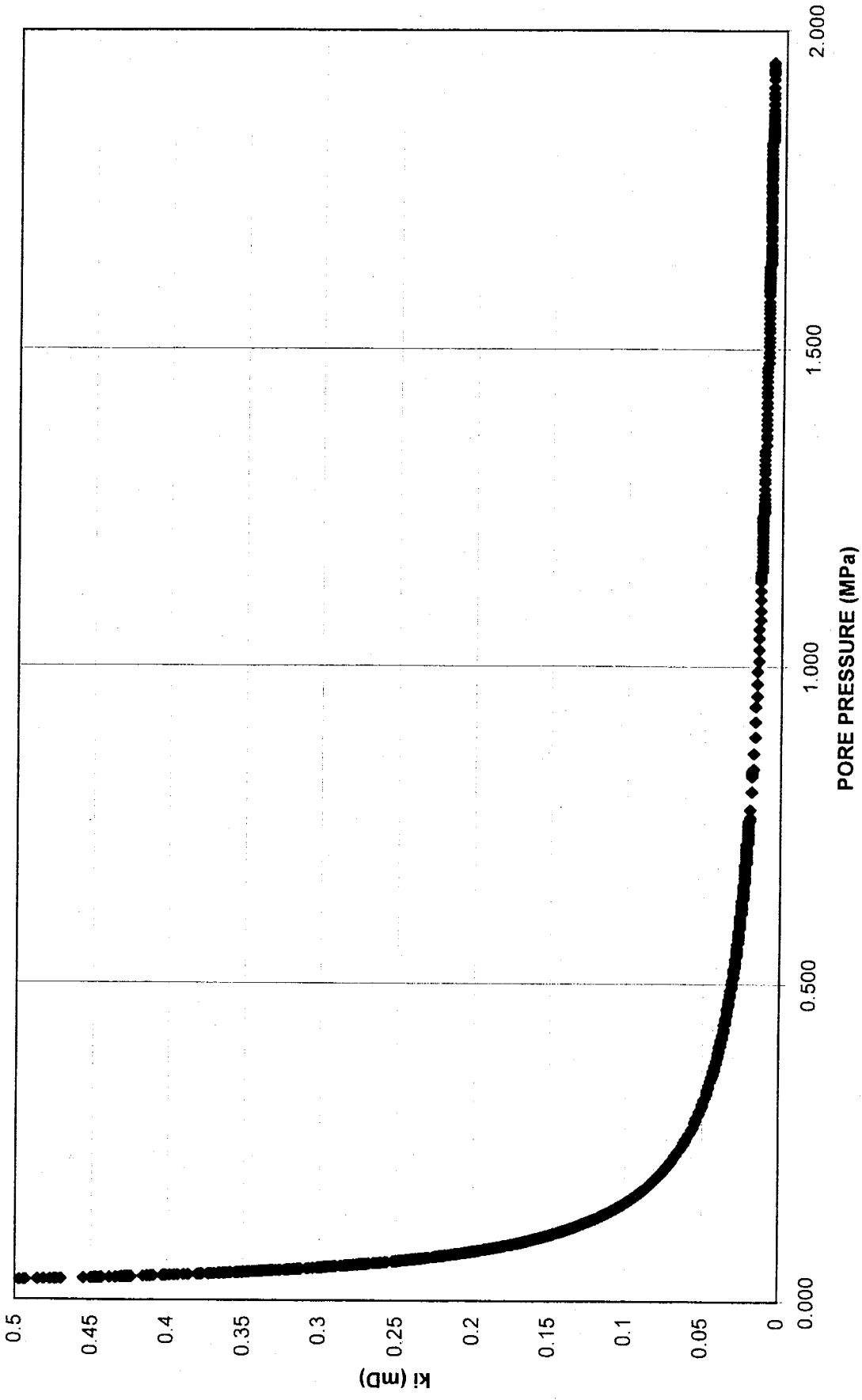
Permeability versus increased pore pressure resulting from increases in vertical load - Sample 58



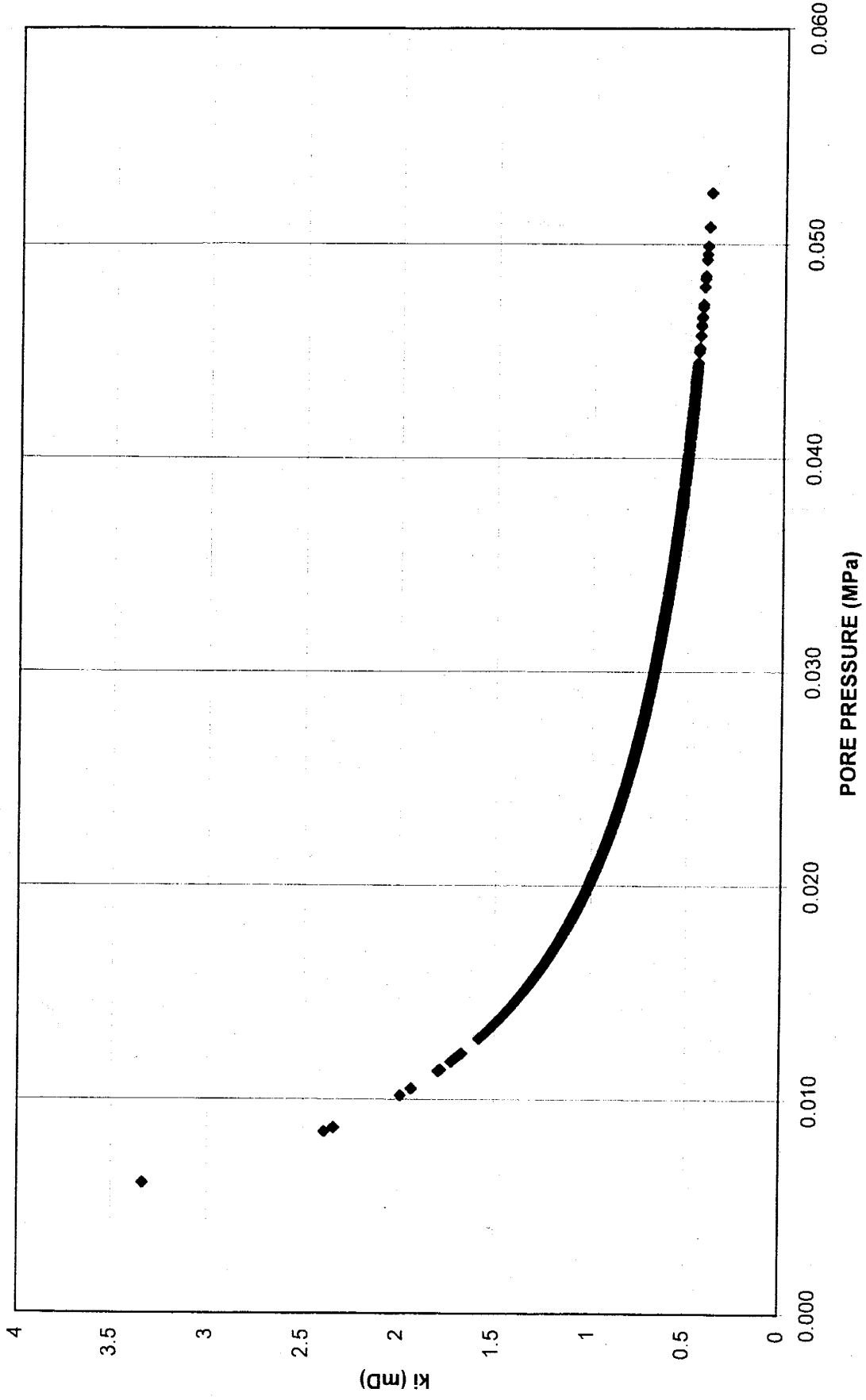
Permeability versus increased pore pressure resulting from increases in vertical load - Sample 60



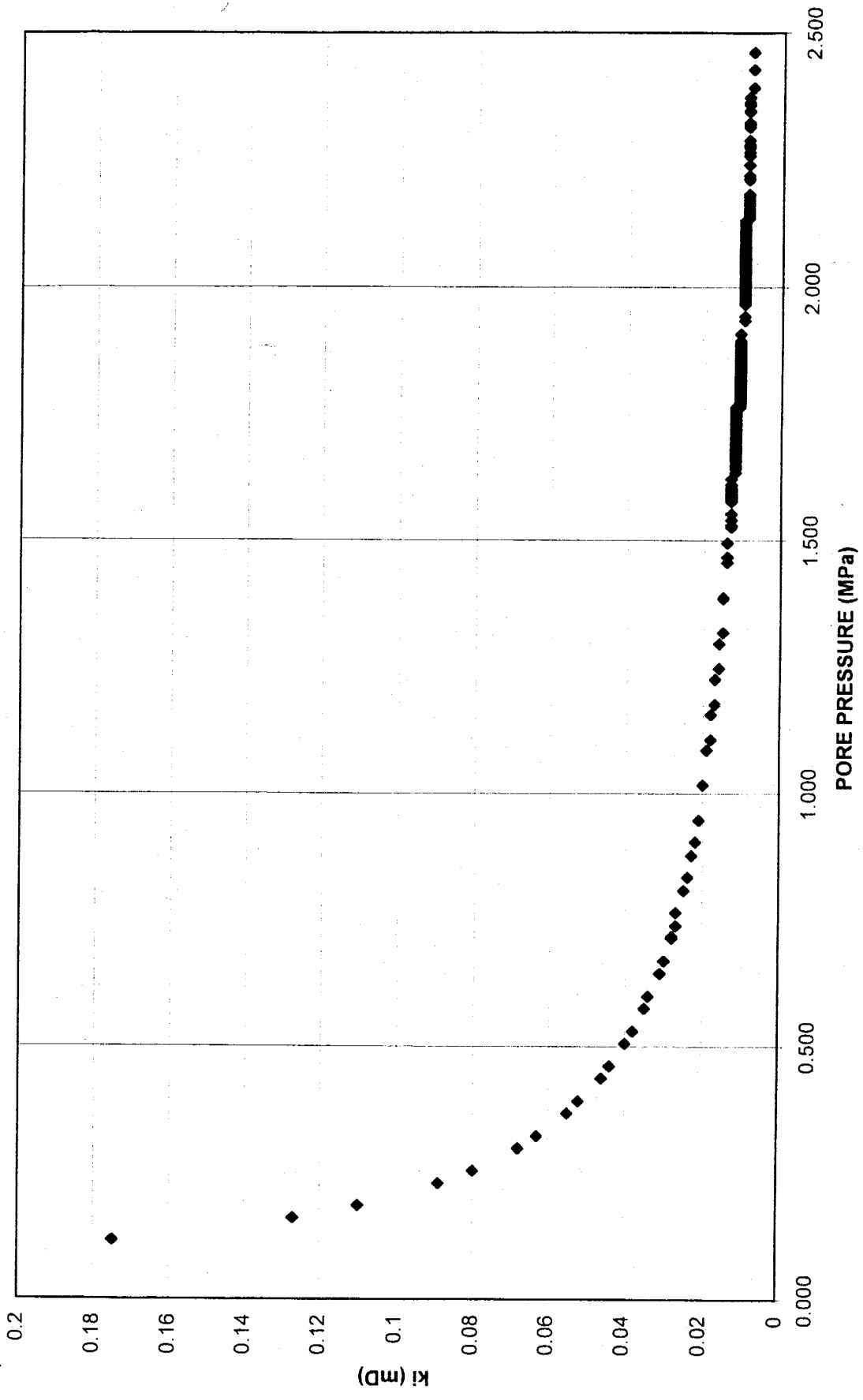
Permeability versus increased pore pressure resulting from increases in vertical load - Sample 61



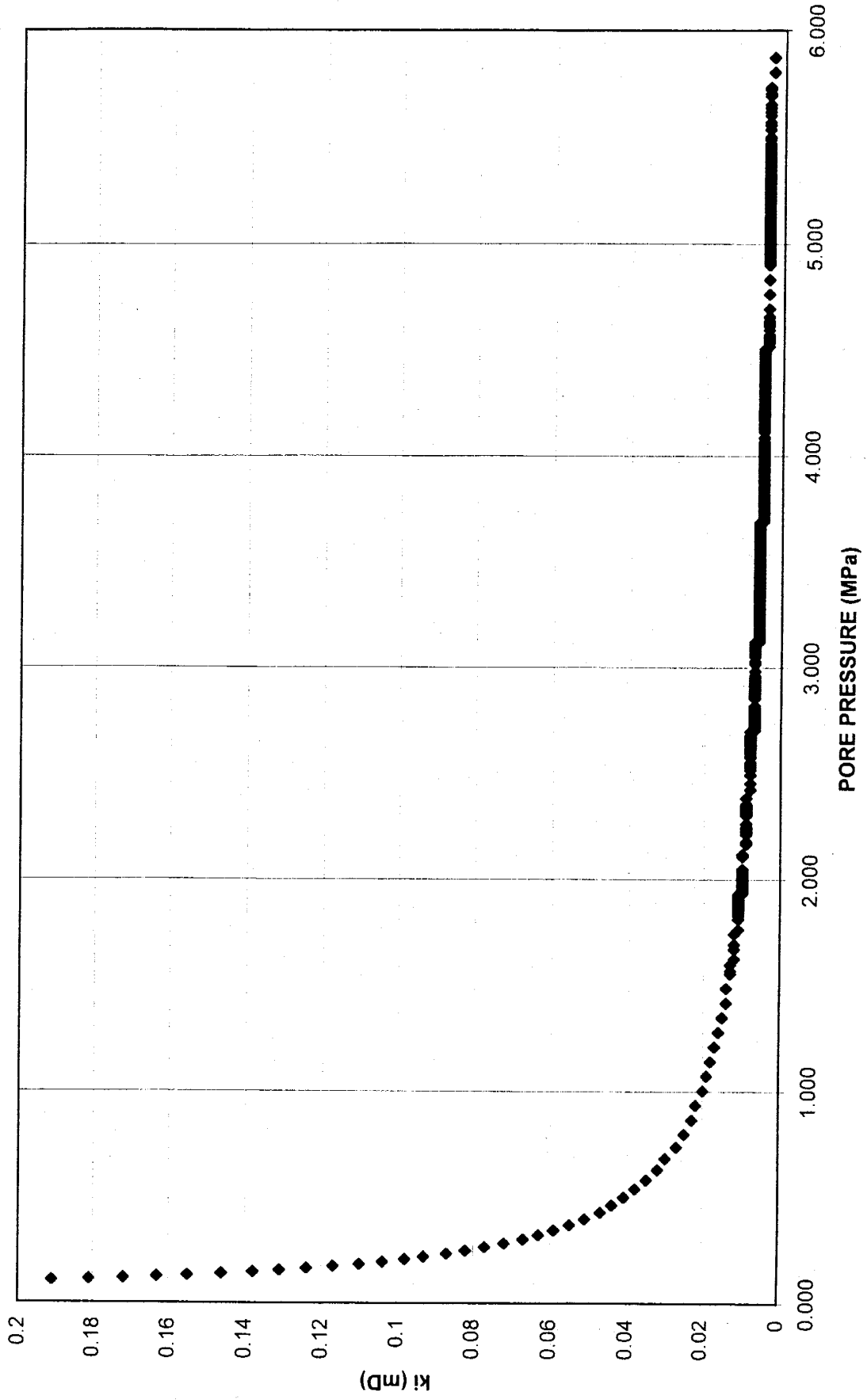
Permeability versus increased pore pressure resulting from increases in vertical load - Sample 62



Permeability versus increased pore pressure resulting from increases in vertical load - Sample 71



Permeability versus increased pore pressure resulting from increases in vertical load - Sample 72



Permeability versus increased pore pressure resulting from increases in vertical load - Sample 80

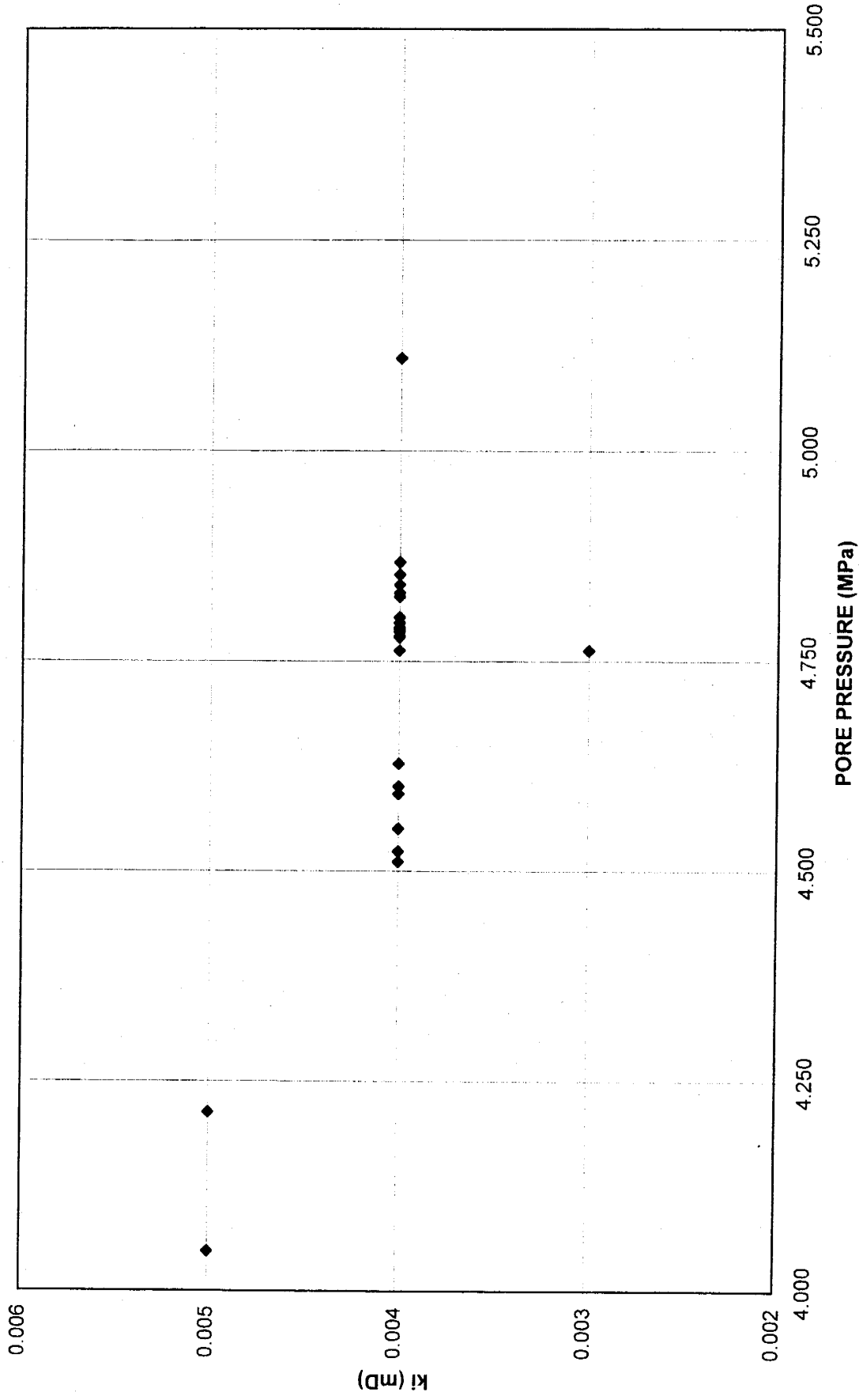


Table 5: Statistical summary of materials property testing

ELASTIC DEFORMATION

CATEGORY	STANDARD		MEDIAN	MEAN ν	STANDARD		MEDIAN ν
	MEAN E (MPa)	DEVIATION E (MPa)			DEVIATION ν	DEVIATION ν	
1U	62195	73927	34950	0.1075	0.0538	0.1015	
5U	22433	8696	20135	0.0838	0.0576	0.0720	
ABOVE	31076	18651	24500	0.0934	0.0581	0.0785	
RESERVOIR	25844	10007	22700	0.1001	0.0627	0.0940	
BELOW	112797	111107	31400	0.0987	0.0388	0.0920	
1U ABOVE	47696	21148	44400	0.1242	0.0672	0.1220	
1U RESERVOIR	26570	10287	28050	0.0951	0.0472	0.0910	
1U BELOW	38007	8628	35850	0.1007	0.0342	0.0915	
5U ABOVE	22263	8505	19905	0.0770	0.0449	0.0695	
5U RESERVOIR	23260	8621	21000	0.1177	0.0996	0.1010	
5U BELOW	22436	10013	21100	0.0831	0.0448	0.0920	
TYPE 2	77357	96036	24260	0.0942	0.0348	0.0780	
TYPE 3	26086	12642	27800	0.0935	0.0483	0.0915	
TYPE 4	19338	8082	17600	0.0675	0.0427	0.0560	
TYPE 6	29729	10161	29500	0.1114	0.0818	0.1040	

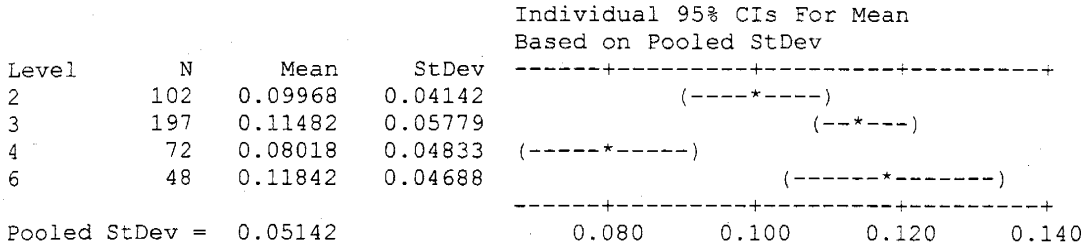
ELASTIC AND PLASTIC DEFORMATION

CATEGORY	STANDARD		MEDIAN	MEAN ν	STANDARD		MEDIAN ν
	MEAN E (MPa)	DEVIATION E (MPa)			DEVIATION ν	DEVIATION ν	
1U	31997	17237	36860	0.1056	0.0529	0.1160	
5U	25555	10908	22470	0.0875	0.0483	0.0745	
ABOVE	35255	20066	30730	0.1044	0.0561	0.0890	
RESERVOIR	26683	10850	23400	0.1113	0.0500	0.1010	
BELOW	29709	9770	33200	0.0958	0.0412	0.0850	
1U ABOVE	54230	21540	51900	0.1442	0.0466	0.1360	
1U RESERVOIR	27713	11086	25150	0.1137	0.0519	0.1015	
1U BELOW	36950	2827	36500	0.1037	0.0396	0.1020	
5U ABOVE	26393	11332	22500	0.0857	0.0503	0.0720	
5U RESERVOIR	21388	7799	19100	0.0993	0.0373	0.1010	
5U BELOW	23373	9269	28400	0.0890	0.0422	0.0930	
TYPE 2	29108	10284	30465	0.0997	0.0414	0.0920	
TYPE 3	37481	21009	34880	0.1148	0.0578	0.1010	
TYPE 4	23270	10517	20800	0.1184	0.0483	0.0675	
TYPE 6	28924	11514	26515	0.1184	0.0469	0.1140	

One-way ANOVA for moduli during elastic and plastic deformation in tests using strain gauges

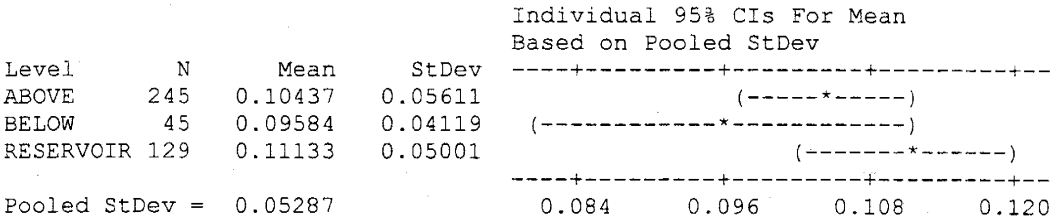
One-way ANOVA: Poisson's ratio versus lithology

Source	DF	SS	MS	F	P
Treatment	3	0.07474	0.02491	9.42	0.000
Error	415	1.09707	0.00264		
Total	418	1.17181			



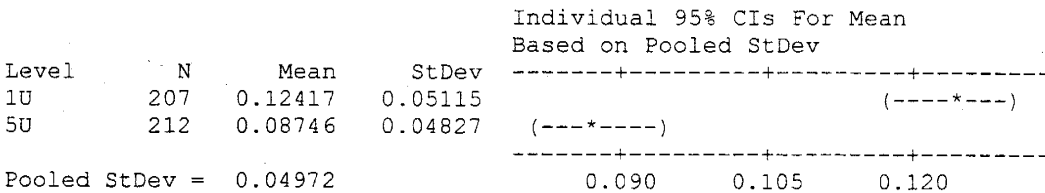
One-way ANOVA: Poisson's ratio versus location

Source	DF	SS	MS	F	P
Treatment	2	0.00888	0.00444	1.59	0.205
Error	416	1.16293	0.00280		
Total	418	1.17181			



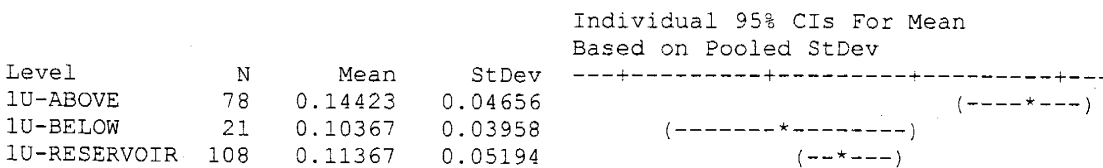
One-way ANOVA: Poisson's ratio versus sub-unit

Source	DF	SS	MS	F	P
Treatment	1	0.14116	0.14116	57.11	0.000
Error	417	1.03066	0.00247		
Total	418	1.17181			



One-way ANOVA: n versus SAMPLE HORIZON

Source	DF	SS	MS	F	P
Treatment	5	0.19677	0.03935	16.67	0.000
Error	413	0.97504	0.00236		
Total	418	1.17181			



5U-ABOVE	167	0.08575	0.05027	(--*--)
5U-BELOW	24	0.08900	0.04217	(-----*-----)
5U-RESERVOIR	21	0.09929	0.03729	(-----*-----)

Pooled StDev = 0.04859 0.075 0.100 0.125 0.150

One-way ANOVA: E (MPa) versus horizon

Source	DF	SS	MS	F	P
Treatment	5	5.043E+10	1.009E+10	56.70	0.000
Error	413	7.347E+10	177886019		
Total	418	1.239E+11			

Individual 95% CIs For Mean
Based on Pooled StDev

Level	N	Mean	StDev
1U-ABOVE	78	54227	21521
1U-BELOW	21	36961	2834
1U-RESERVOIR	108	27712	11087
5U-ABOVE	167	26396	11327
5U-BELOW	24	23376	9263
5U-RESERVOIR	21	21395	7801

Pooled StDev = 13337 24000 36000 48000

One-way ANOVA: E (MPa) versus lithology

Source	DF	SS	MS	F	P
Treatment	3	1.270E+10	4.234E+09	15.80	0.000
Error	415	1.112E+11	267940136		
Total	418	1.239E+11			

Individual 95% CIs For Mean
Based on Pooled StDev

Level	N	Mean	StDev
2	102	29111	10284
3	197	37481	21000
4	72	23277	10510
6	48	28924	11515

Pooled StDev = 16369 24000 30000 36000

One-way ANOVA: E (MPa) versus location

Source	DF	SS	MS	F	P
Treatment	2	6.479E+09	3.239E+09	11.48	0.000
Error	416	1.174E+11	282252840		
Total	418	1.239E+11			

Individual 95% CIs For Mean
Based on Pooled StDev

Level	N	Mean	StDev
ABOVE	245	35257	20056
BELOW	45	29716	9772
RESERVOIR	129	26684	10851

Pooled StDev = 16800 24000 28000 32000 36000

One-way ANOVA: E (MPa) versus sub-unit

Source	DF	SS	MS	F	P
Treatment	1	1.793E+10	1.793E+10	70.54	0.000
Error	417	1.060E+11	254123297		
Total	418	1.239E+11			

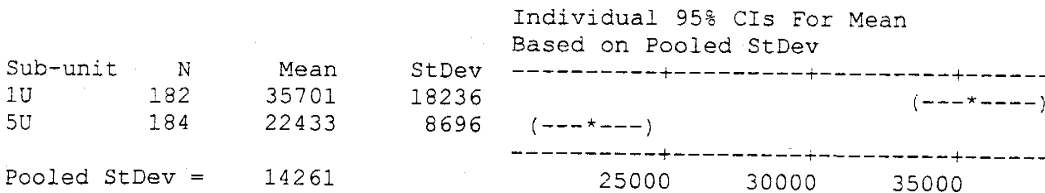
Individual 95% CIs For Mean
Based on Pooled StDev

Level	N	Mean	StDev	-----+-----+-----+-----+-----			
1U	207	38642	19815				(---*---)
5U	212	25559	10903	(---*---)			
Pooled StDev = 15941				25000	30000	35000	40000

One-way ANOVA for moduli during elastic deformation in tests using strain gauges

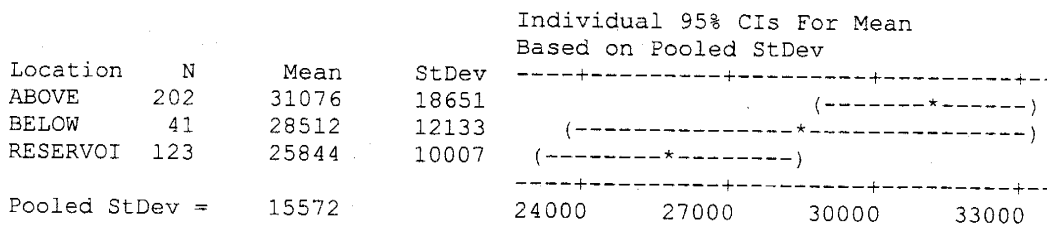
One-way ANOVA: E (MPa) versus sub-unit

Source	DF	SS	MS	F	P
Treatment	1	1.611E+10	1.611E+10	79.20	0.000
Error	364	7.403E+10	203369616		
Total	365	9.013E+10			



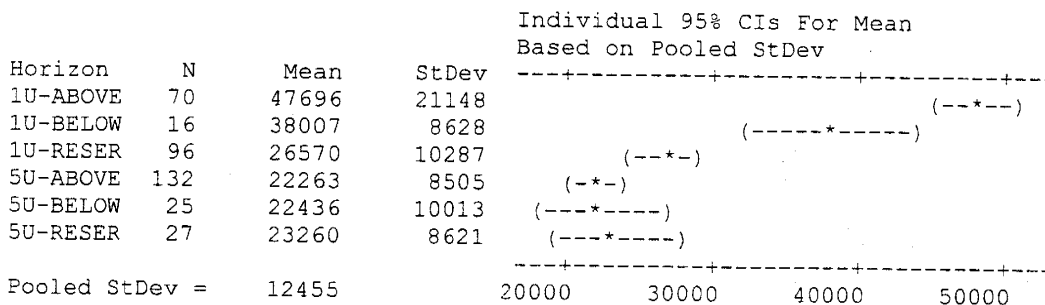
One-way ANOVA: E (MPa) versus location

Source	DF	SS	MS	F	P
Treatment	2	2.106E+09	1.053E+09	4.34	0.014
Error	363	8.803E+10	242500391		
Total	365	9.013E+10			



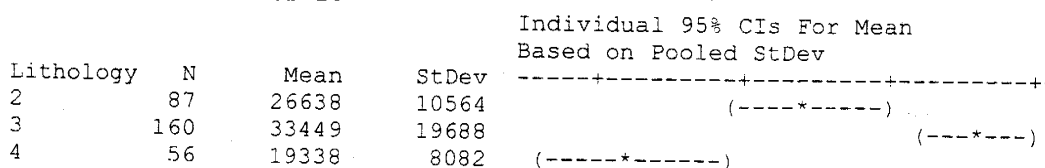
One-way ANOVA: E (MPa) versus horizon

Source	DF	SS	MS	F	P
Treatment	5	3.429E+10	6.858E+09	44.21	0.000
Error	360	5.584E+10	155123395		
Total	365	9.013E+10			



One-way ANOVA: E (MPa) versus lithology

Source	DF	SS	MS	F	P
Treatment	3	8.913E+09	2.971E+09	13.24	0.000
Error	362	8.122E+10	224366785		
Total	365	9.013E+10			



Estimate for difference: -8373
 95% CI for difference: (-12715, -4030)
 T-Test of difference = 0 (vs not =): T-Value = -3.79 P-Value = 0.000 DF = 297
 Both use Pooled StDev = 18090

Two-sample T-Tests and Confidence Intervals for Young's Modulus during elastic and plastic deformation in tests using strain gauges

Two-Sample T-Test and Confidence Interval: Lithology 2, 4

	N	Mean	StDev	SE Mean
2	102	29108	10284	1018
4	72	23270	10517	1239

Estimate for difference: 5838
 95% CI for difference: (2684, 8992)
 T-Test of difference = 0 (vs not =): T-Value = 3.65 P-Value = 0.000 DF = 172
 Both use Pooled StDev = 10381

Two-Sample T-Test and Confidence Interval: Lithology 2, 6

	N	Mean	StDev	SE Mean
2	102	29108	10284	1018
6	48	28924	11514	1662

Estimate for difference: 184
 95% CI for difference: (-3514, 3881)
 T-Test of difference = 0 (vs not =): T-Value = 0.10 P-Value = 0.922 DF = 148
 Both use Pooled StDev = 10690

Two-Sample T-Test and Confidence Interval: Lithology 3, 6

	N	Mean	StDev	SE Mean
3	197	37481	21009	1497
6	48	28924	11514	1662

Estimate for difference: 8557
 95% CI for difference: (2362, 14751)
 T-Test of difference = 0 (vs not =): T-Value = 2.72 P-Value = 0.007 DF = 243
 Both use Pooled StDev = 19536

Two-Sample T-Test and Confidence Interval: Lithology 4, 6

	N	Mean	StDev	SE Mean
4	72	23270	10517	1239
6	48	28924	11514	1662

Estimate for difference: -5654
 95% CI for difference: (-9686, -1623)
 T-Test of difference = 0 (vs not =): T-Value = -2.78 P-Value = 0.006 DF = 118
 Both use Pooled StDev = 10925

Two-sample T-Tests and Confidence Intervals for Young's Modulus during elastic and plastic deformation in tests using strain gauges

Two-Sample T-Test and Confidence Interval: Lithology 4, 3

	N	Mean	StDev	SE Mean
4	72	23270	10517	1239
3	197	37481	21009	1497

Estimate for difference: -14211
 95% CI for difference: (-19308, -9113)
 T-Test of difference = 0 (vs not =): T-Value = -5.49 P-Value = 0.000 DF = 267
 Both use Pooled StDev = 18800

Two-Sample T-Test and Confidence Interval: 5U Reservoir, 5U Below

	N	Mean	StDev	SE Mean
5r	21	21388	7799	1702
5b	24	23373	9269	1892

Estimate for difference: -1985
 95% CI for difference: (-7177, 3207)
 T-Test of difference = 0 (vs not =): T-Value = -0.77 P-Value = 0.445 DF = 43
 Both use Pooled StDev = 8616

Two-Sample T-Test and Confidence Interval: 5U Reservoir, 5U Above

	N	Mean	StDev	SE Mean
5r	21	21388	7799	1702
5a	167	26393	11332	877

Estimate for difference: -5004
 95% CI for difference: (-10032, 23)
 T-Test of difference = 0 (vs not =): T-Value = -1.96 P-Value = 0.051 DF = 186
 Both use Pooled StDev = 11006

Two-Sample T-Test and Confidence Interval: 5U Reservoir, 1U Reservoir

	N	Mean	StDev	SE Mean
5r	21	21388	7799	1702
1r	108	27713	11086	1067

Estimate for difference: -6325
 95% CI for difference: (-11344, -1305)
 T-Test of difference = 0 (vs not =): T-Value = -2.49 P-Value = 0.014 DF = 127
 Both use Pooled StDev = 10636

Two-Sample T-Test and CI: 5U Below, 5U Above

	N	Mean	StDev	SE Mean
5b	24	23373	9269	1892
5a	167	26393	11332	877

Estimate for difference: -3020
 95% CI for difference: (-7800, 1761)
 T-Test of difference = 0 (vs not =): T-Value = -1.25 P-Value = 0.214 DF = 189
 Both use Pooled StDev = 11101

Two-sample T-Tests and Confidence Intervals for Young's Modulus during elastic and plastic deformation in tests using strain gauges

Two-Sample T-Test and Confidence Interval: 5U Below, 1U Below

	N	Mean	StDev	SE Mean
5b	24	23373	9269	1892
1b	21	36950	2827	617

Difference = μ 5b - μ 1b
 Estimate for difference: -13577
 95% CI for difference: (-17824, -9330)
 T-Test of difference = 0 (vs not =): T-Value = -6.45 P-Value = 0.000 DF = 43
 Both use Pooled StDev = 7048

Two-Sample T-Test and Confidence Interval: 5U Above, 1U Above

	N	Mean	StDev	SE Mean
5a	167	26393	11332	877
1a	78	54230	21540	2439

Estimate for difference: -27838
 95% CI for difference: (-31977, -23699)
 T-Test of difference = 0 (vs not =): T-Value = -13.25 P-Value = 0.000 DF = 243
 Both use Pooled StDev = 15321

Two-Sample T-Test and Confidence Interval: 1U Below, 1U Above

	N	Mean	StDev	SE Mean
1b	21	36950	2827	617
1a				

Estimate for difference: -17280
 95% CI for difference: (-26665, -7895)
 T-Test of difference = 0 (vs not =): T-Value = -3.65 P-Value = 0.000 DF = 97
 Both use Pooled StDev = 19234

Two-Sample T-Test and Confidence Interval: 1U Reservoir, 1U Above

	N	Mean	StDev	SE Mean
1r	108	27713	11086	1067
1a	78	54230	21540	2439

Estimate for difference: -26517
 95% CI for difference: (-31296, -21739)
 T-Test of difference = 0 (vs not =): T-Value = -10.95 P-Value = 0.000 DF = 184
 Both use Pooled StDev = 16298

Two-sample T-Tests and Confidence Intervals for Young's Modulus during elastic and plastic deformation in tests using strain gauges

Two-Sample T-Test and Confidence Interval: 1U Reservoir, 1U Below

	N	Mean	StDev	SE Mean
1r	108	27713	11086	1067
1b	21	36950	2827	617

Estimate for difference: -9237
 95% CI for difference: (-14069, -4406)
 T-Test of difference = 0 (vs not =): T-Value = -3.78 P-Value = 0.000 DF = 127
 Both use Pooled StDev = 10237

Two-Sample T-Test and Confidence Interval: 1U Reservoir, 1U Below

	N	Mean	StDev	SE Mean
1r	108	0.1137	0.0519	0.0050
1b	21	0.1037	0.0396	0.0086

Estimate for difference: 0.0100
 95% CI for difference: (-0.0137, 0.0337)
 T-Test of difference = 0 (vs not =): T-Value = 0.84 P-Value = 0.405 DF = 127
 Both use Pooled StDev = 0.0502

Two-Sample T-Test and Confidence Interval: 1U Reservoir, 1U Above

	N	Mean	StDev	SE Mean
1r	108	0.1137	0.0519	0.0050
1a	78	0.1442	0.0466	0.0053

Estimate for difference: -0.03056
 95% CI for difference: (-0.04515, -0.01598)
 T-Test of difference = 0 (vs not =): T-Value = -4.13 P-Value = 0.000 DF = 184
 Both use Pooled StDev = 0.0498

Two-Sample T-Test and Confidence Interval: 1U Below, 1U Above

	N	Mean	StDev	SE Mean
1b	21	0.1037	0.0396	0.0086
1a	78	0.1442	0.0466	0.0053

Estimate for difference: -0.0406
 95% CI for difference: (-0.0626, -0.0185)
 T-Test of difference = 0 (vs not =): T-Value = -3.65 P-Value = 0.000 DF = 97
 Both use Pooled StDev = 0.0452

Two-sample T-Tests and Confidence Intervals for Young's Modulus during elastic and plastic deformation in tests using strain gauges

Two-Sample T-Test and Confidence Interval: 5U Above, 1U Above

	N	Mean	StDev	SE Mean
5a	167	0.0857	0.0503	0.0039
1a	78	0.1442	0.0466	0.0053

Estimate for difference: -0.05848
 95% CI for difference: (-0.07175, -0.04521)
 T-Test of difference = 0 (vs not =): T-Value = -8.68 P-Value = 0.000 DF = 243
 Both use Pooled StDev = 0.0491

Two-Sample T-Test and Confidence Interval: 5U Above, 5U Below

	N	Mean	StDev	SE Mean
5a	167	0.0857	0.0503	0.0039
5b	24	0.0890	0.0422	0.0086

Estimate for difference: -0.0033
 95% CI for difference: (-0.0245, 0.0180)
 T-Test of difference = 0 (vs not =): T-Value = -0.30 P-Value = 0.763 DF = 189
 Both use Pooled StDev = 0.0494

Two-Sample T-Test and Confidence Interval: 5U Above, 5U Reservoir

	N	Mean	StDev	SE Mean
5a	167	0.0857	0.0503	0.0039
5r	21	0.0993	0.0373	0.0081

Estimate for difference: -0.0135
 95% CI for difference: (-0.0359, 0.0089)
 T-Test of difference = 0 (vs not =): T-Value = -1.19 P-Value = 0.235 DF = 186
 Both use Pooled StDev = 0.0490

Two-Sample T-Test and Confidence Interval: 1U Reservoir, 5U Reservoir

	N	Mean	StDev	SE Mean
1r	108	0.1137	0.0519	0.0050
5r	21	0.0993	0.0373	0.0081

Estimate for difference: 0.0144
 95% CI for difference: (-0.0092, 0.0379)
 T-Test of difference = 0 (vs not =): T-Value = 1.21 P-Value = 0.229 DF = 127
 Both use Pooled StDev = 0.0499

Two-Sample T-Test and Confidence Interval: 1U Below, 5U Below

	N	Mean	StDev	SE Mean
1b	21	0.1037	0.0396	0.0086
5b	24	0.0890	0.0422	0.0086

Estimate for difference: 0.0147
 95% CI for difference: (-0.0100, 0.0394)
 T-Test of difference = 0 (vs not =): T-Value = 1.20 P-Value = 0.238 DF = 43
 Both use Pooled StDev = 0.0410

Two-sample T-Tests and Confidence Intervals for Young's Modulus during elastic and plastic deformation in tests using strain gauges

Two-Sample T-Test and Confidence Interval: 1U Above, 5U Above

	N	Mean	StDev	SE Mean
1a	78	0.1442	0.0466	0.0053
5a	167	0.0857	0.0503	0.0039

Estimate for difference: 0.05848
 95% CI for difference: (0.04521, 0.07175)
 T-Test of difference = 0 (vs not =): T-Value = 8.68 P-Value = 0.000 DF = 243
 Both use Pooled StDev = 0.0491

Two-Sample T-Test and Confidence Interval: Lithology 6, 4

	N	Mean	StDev	SE Mean
6	48	0.1184	0.0469	0.0068
4	72	0.0802	0.0483	0.0057

Estimate for difference: 0.03824
 95% CI for difference: (0.02061, 0.05586)
 T-Test of difference = 0 (vs not =): T-Value = 4.30 P-Value = 0.000 DF = 118
 Both use Pooled StDev = 0.0478

Two-Sample T-Test and Confidence Interval: Lithology 6, 3

	N	Mean	StDev	SE Mean
6	48	0.1184	0.0469	0.0068
3	197	0.1148	0.0578	0.0041

Estimate for difference: 0.00359
 95% CI for difference: (-0.01411, 0.02130)
 T-Test of difference = 0 (vs not =): T-Value = 0.40 P-Value = 0.690 DF = 243
 Both use Pooled StDev = 0.0558

Two-Sample T-Test and Confidence Interval: Lithology 6, 2

	N	Mean	StDev	SE Mean
6	48	0.1184	0.0469	0.0068
2	102	0.0997	0.0414	0.0041

Estimate for difference: 0.01874
 95% CI for difference: (0.00379, 0.03369)
 T-Test of difference = 0 (vs not =): T-Value = 2.48 P-Value = 0.014 DF = 148
 Both use Pooled StDev = 0.0432

Two-sample T-Tests and Confidence Intervals for Young's Modulus during elastic and plastic deformation in tests using strain gauges

Two-Sample T-Test and Confidence Interval: Lithology 4, 2

	N	Mean	StDev	SE Mean
4	72	0.0802	0.0483	0.0057
2	102	0.0997	0.0414	0.0041

Estimate for difference: -0.01950
 95% CI for difference: (-0.03299, -0.00600)
 T-Test of difference = 0 (vs not =): T-Value = -2.85 P-Value = 0.005 DF = 172
 Both use Pooled StDev = 0.0444

Two-Sample T-Test and Confidence Interval: Lithology 3, 2

	N	Mean	StDev	SE Mean
3	197	0.1148	0.0578	0.0041
2	102	0.0997	0.0414	0.0041

Estimate for difference: 0.01515
 95% CI for difference: (0.00247, 0.02782)
 T-Test of difference = 0 (vs not =): T-Value = 2.35 P-Value = 0.019 DF = 297
 Both use Pooled StDev = 0.0528

Two-Sample T-Test and Confidence Interval: Lithology 3, 4

	N	Mean	StDev	SE Mean
3	197	0.1148	0.0578	0.0041
4	72	0.0802	0.0483	0.0057

Estimate for difference: 0.03464
 95% CI for difference: (0.01961, 0.04967)
 T-Test of difference = 0 (vs not =): T-Value = 4.54 P-Value = 0.000 DF = 267
 Both use Pooled StDev = 0.0554

Two-Sample T-Test and Confidence Interval: Reservoir, Below

	N	Mean	StDev	SE Mean
r	129	0.1113	0.0500	0.0044
b	45	0.0958	0.0412	0.0061

Estimate for difference: 0.01548
 95% CI for difference: (-0.00089, 0.03185)
 T-Test of difference = 0 (vs not =): T-Value = 1.87 P-Value = 0.064 DF = 172
 Both use Pooled StDev = 0.0479

Two-Sample T-Test and Confidence Interval: Reservoir, Above

	N	Mean	StDev	SE Mean
r	129	0.1113	0.0500	0.0044
a	245	0.1044	0.0561	0.0036

Estimate for difference: 0.00696
 95% CI for difference: (-0.00461, 0.01853)
 T-Test of difference = 0 (vs not =): T-Value = 1.18 P-Value = 0.238 DF = 372
 Both use Pooled StDev = 0.0541

Two-sample T-Tests and Confidence Intervals for Young's Modulus during elastic and plastic deformation in tests using strain gauges

Two-Sample T-Test and Confidence Interval: Below, Above

	N	Mean	StDev	SE Mean
b	45	0.0958	0.0412	0.0061
a	245	0.1044	0.0561	0.0036

Estimate for difference: -0.00852

95% CI for difference: (-0.02579, 0.00875)

T-Test of difference = 0 (vs not =): T-Value = -0.97 P-Value = 0.332 DF = 288

Both use Pooled StDev = 0.0541

Two-Sample T-Test and Confidence Interval: 5U, 1U

	N	Mean	StDev	SE Mean
5u	212	0.0875	0.0483	0.0033
1u	419	0.1056	0.0529	0.0026

Estimate for difference: -0.01814

95% CI for difference: (-0.02665, -0.00963)

T-Test of difference = 0 (vs not =): T-Value = -4.18 P-Value = 0.000 DF = 629

Both use Pooled StDev = 0.0514

Two-Sample T-Test and Confidence Interval: Below, Reservoir

	N	Mean	StDev	SE Mean
B	68	112797	111107	13474
R	123	25844	10007	902

Estimate for difference: 86954

95% CI for difference: (67089, 106818)

T-Test of difference = 0 (vs not =): T-Value = 8.63 P-Value = 0.000 DF = 189

Both use Pooled StDev = 66639

Two-Sample T-Test and Confidence Interval: Below, Above

	N	Mean	StDev	SE Mean
B	68	112797	111107	13474
A	202	31076	18651	1312

Estimate for difference: 81721

95% CI for difference: (65751, 97691)

T-Test of difference = 0 (vs not =): T-Value = 10.08 P-Value = 0.000 DF = 268

Both use Pooled StDev = 57854

Two-Sample T-Test and Confidence Interval: Reservoir, Above

	N	Mean	StDev	SE Mean
R	123	25844	10007	902
A	202	31076	18651	1312

Estimate for difference: -5233

95% CI for difference: (-8821, -1645)

T-Test of difference = 0 (vs not =): T-Value = -2.87 P-Value = 0.004 DF = 323

Both use Pooled StDev = 15947

Two-Sample T-Test and Confidence Interval: 1U, 5U

	N	Mean	StDev	SE Mean
1U	209	62195	73927	5114
5U	184	22433	8696	641

Estimate for difference: 39762

95% CI for difference: (28981, 50544)

T-Test of difference = 0 (vs not =): T-Value = 7.25 P-Value = 0.000 DF = 391

Both use Pooled StDev = 54247

Two-Sample T-Test and Confidence Interval: Lithology 2, 3

	N	Mean	StDev	SE Mean
2	114	77357	96036	8995
3	103	26086	12642	1246

Estimate for difference: 51272

95% CI for difference: (32471, 70073)

T-Test of difference = 0 (vs not =): T-Value = 5.38 P-Value = 0.000 DF = 215

Both use Pooled StDev = 70166

Two-sample T-Tests and Confidence Intervals for Young' Modulus for elastic deformation for tests using strain gauges

Two-Sample T-Test and CI: 2, 4

	N	Mean	StDev	SE Mean
2	114	77357	96036	8995
4	56	19338	8082	1080

Estimate for difference: 58019

95% CI for difference: (32602, 83437)

T-Test of difference = 0 (vs not =): T-Value = 4.51 P-Value = 0.000 DF = 168

Both use Pooled StDev = 78898

Two-Sample T-Test and Confidence Interval: Lithology 2, 6

	N	Mean	StDev	SE Mean
2	114	77357	96036	8995
6	63	29729	10161	1280

Estimate for difference: 47628

95% CI for difference: (23645, 71612)

T-Test of difference = 0 (vs not =): T-Value = 3.92 P-Value = 0.000 DF = 175

Both use Pooled StDev = 77408

Two-Sample T-Test and Confidence Interval: Lithology 4, 6

	N	Mean	StDev	SE Mean
4	56	19338	8082	1080
6	63	29729	10161	1280

Estimate for difference: -10391

95% CI for difference: (-13752, -7029)

T-Test of difference = 0 (vs not =): T-Value = -6.12 P-Value = 0.000 DF = 117

Both use Pooled StDev = 9242

Two-Sample T-Test and Confidence Interval: Lithology 3, 6

	N	Mean	StDev	SE Mean
3	103	26086	12642	1246
6	63	29729	10161	1280

Estimate for difference: -3643

95% CI for difference: (-7359, 73)

T-Test of difference = 0 (vs not =): T-Value = -1.94 P-Value = 0.055 DF = 164

Both use Pooled StDev = 11766

Two-Sample T-Test and Confidence Interval: Lithology 3, 4

	N	Mean	StDev	SE Mean
3	103	26086	12642	1246
4	56	19338	8082	1080

Estimate for difference: 6747

95% CI for difference: (3056, 10439)

T-Test of difference = 0 (vs not =): T-Value = 3.61 P-Value = 0.000 DF = 157

Both use Pooled StDev = 11257

Two-sample T-Tests and Confidence Intervals for Young' Modulus for elastic deformation for tests using strain gauges

Two-Sample T-Test and Confidence Interval: 5U-Reservoir, 5U-Below

	N	Mean	StDev	SE Mean
5U-R	27	23260	8621	1659
5U-B	25	22436	10013	2003

Estimate for difference: 824
95% CI for difference: (-4369, 6017)
T-Test of difference = 0 (vs not =): T-Value = 0.32 P-Value = 0.751 DF = 50
Both use Pooled StDev = 9315

Two-Sample T-Test and Confidence Interval: 5U-Reservoir, 5U-Above

	N	Mean	StDev	SE Mean
5U-R	27	23260	8621	1659
5U-A	132	22263	8505	740

Estimate for difference: 997
95% CI for difference: (-2560, 4553)
T-Test of difference = 0 (vs not =): T-Value = 0.55 P-Value = 0.581 DF = 157
Both use Pooled StDev = 8525

Two-Sample T-Test and Confidence Interval: 5U-Below, 5U-Above

	N	Mean	StDev	SE Mean
5U-B	25	22436	10013	2003
5U-A	132	22263	8505	740

Estimate for difference: 173
95% CI for difference: (-3600, 3945)
T-Test of difference = 0 (vs not =): T-Value = 0.09 P-Value = 0.928 DF = 155
Both use Pooled StDev = 8756

Two-Sample T-Test and Confidence Interval: 1U-Above, 5U-Above

	N	Mean	StDev	SE Mean
1U-A	70	47696	21148	2528
5U-A	132	22263	8505	740

Estimate for difference: 25433
95% CI for difference: (21292, 29573)
T-Test of difference = 0 (vs not =): T-Value = 12.11 P-Value = 0.000 DF = 200
Both use Pooled StDev = 14201

Two-Sample T-Test and Confidence Interval: 1U-Below, 5U-Below

	N	Mean	StDev	SE Mean
1U-B	16	38007	8628	2157
5U-B	25	22436	10013	2003

Estimate for difference: 15571
95% CI for difference: (9416, 21725)
T-Test of difference = 0 (vs not =): T-Value = 5.12 P-Value = 0.000 DF = 39
Both use Pooled StDev = 9504

Two-sample T-Tests and Confidence Intervals for Young' Modulus for elastic deformation for tests using strain gauges

Two-Sample T-Test and Confidence Interval: 1U-Reservoir, 5U-Reservoir

	N	Mean	StDev	SE Mean
1U-R	96	26570	10287	1050
5U-R	27	23260	8621	1659

Estimate for difference: 3310
 95% CI for difference: (-982, 7603)
 T-Test of difference = 0 (vs not =): T-Value = 1.53 P-Value = 0.129 DF = 121
 Both use Pooled StDev = 9953

Two-Sample T-Test and Confidence Interval: 1U-Reservoir, 1U-Below

	N	Mean	StDev	SE Mean
1U-R	96	26570	10287	1050
1U-B	16	38007	8628	2157

Estimate for difference: -11437
 95% CI for difference: (-16829, -6044)
 T-Test of difference = 0 (vs not =): T-Value = -4.20 P-Value = 0.000 DF = 110
 Both use Pooled StDev = 10077

Two-Sample T-Test and Confidence Interval: 1U-Reservoir, 1U-Above

	N	Mean	StDev	SE Mean
1U-R	96	26570	10287	1050
1U-A	70	47696	21148	2528

Difference = μ 1U-R - μ 1U-A
 Estimate for difference: -21126
 95% CI for difference: (-26027, -16224)
 T-Test of difference = 0 (vs not =): T-Value = -8.51 P-Value = 0.000 DF = 164
 Both use Pooled StDev = 15794

Two-Sample T-Test and Confidence Interval: 1U-Below, 1U-Above

	N	Mean	StDev	SE Mean
1U-B	16	38007	8628	2157
1U-A	70	47696	21148	2528

Estimate for difference: -9689
 95% CI for difference: (-20440, 1062)
 T-Test of difference = 0 (vs not =): T-Value = -1.79 P-Value = 0.077 DF = 84
 Both use Pooled StDev = 19511

Two-Sample T-Test and Confidence Interval: 1U-Below, 1U-Above

	N	Mean	StDev	SE Mean
1U-B	16	0.1007	0.0342	0.0086
1U-A	70	0.1242	0.0672	0.0080

Estimate for difference: -0.0235
 95% CI for difference: (-0.0580, 0.0110)
 T-Test of difference = 0 (vs not =): T-Value = -1.35 P-Value = 0.180 DF = 84
 Both use Pooled StDev = 0.0626

Two-sample T-Tests and Confidence Intervals for Young' Modulus for elastic deformation for tests using strain gauges

Two-Sample T-Test and Confidence Interval: 1U-Below, 1U-Reservoir

	N	Mean	StDev	SE Mean
1U-B	16	0.1007	0.0342	0.0086
1U-R	96	0.0951	0.0472	0.0048

Estimate for difference: 0.0056
 95% CI for difference: (-0.0188, 0.0301)
 T-Test of difference = 0 (vs not =): T-Value = 0.46 P-Value = 0.649 DF = 110
 Both use Pooled StDev = 0.0456

Two-Sample T-Test and Confidence Interval: 1U-Above, 1U-Reservoir

	N	Mean	StDev	SE Mean
1U-A	70	0.1242	0.0672	0.0080
1U-R	96	0.0951	0.0472	0.0048

Estimate for difference: 0.02912
 95% CI for difference: (0.01158, 0.04665)
 T-Test of difference = 0 (vs not =): T-Value = 3.28 P-Value = 0.001 DF = 164
 Both use Pooled StDev = 0.0565

Two-Sample T-Test and Confidence Interval: 1U-Above, 5U-Above

	N	Mean	StDev	SE Mean
1U-A	70	0.1242	0.0672	0.0080
5U-A	132	0.0770	0.0449	0.0039

Estimate for difference: 0.04722
 95% CI for difference: (0.03158, 0.06287)
 T-Test of difference = 0 (vs not =): T-Value = 5.95 P-Value = 0.000 DF = 200
 Both use Pooled StDev = 0.0537

Two-Sample T-Test and Confidence Interval: 1U- Reservoir, 5U-Reservoir

	N	Mean	StDev	SE Mean
1U-R	96	0.0951	0.0472	0.0048
5U-R	27	0.1177	0.0996	0.019

Estimate for difference: -0.0226
 95% CI for difference: (-0.0494, 0.0043)
 T-Test of difference = 0 (vs not =): T-Value = -1.66 P-Value = 0.099 DF = 121
 Both use Pooled StDev = 0.0623

Two-Sample T-Test and Confidence Interval: 1U-Below, 5U-Below

	N	Mean	StDev	SE Mean
1U-B	16	0.1007	0.0342	0.0086
5U-B	25	0.0831	0.0448	0.0090

Estimate for difference: 0.0176
 95% CI for difference: (-0.0089, 0.0442)
 T-Test of difference = 0 (vs not =): T-Value = 1.34 P-Value = 0.187 DF = 39
 Both use Pooled StDev = 0.0410

Two-sample T-Tests and Confidence Intervals for Young' Modulus for elastic deformation for tests using strain gauges

Two-Sample T-Test and Confidence Interval: 5U-Above, 5U-Below

	N	Mean	StDev	SE Mean
5U-A	132	0.0770	0.0449	0.0039
5U-B	25	0.0831	0.0448	0.0090

Estimate for difference: -0.00610
 95% CI for difference: (-0.02543, 0.01323)
 T-Test of difference = 0 (vs not =): T-Value = -0.62 P-Value = 0.534 DF = 155
 Both use Pooled StDev = 0.0449

Two-Sample T-Test and Confidence Interval: 5U-Reservoir, 5U-Below

	N	Mean	StDev	SE Mean
5U-R	27	0.1177	0.0996	0.019
5U-B	25	0.0831	0.0448	0.0090

Estimate for difference: 0.0346
 95% CI for difference: (-0.0090, 0.0782)
 T-Test of difference = 0 (vs not =): T-Value = 1.59 P-Value = 0.117 DF = 50
 Both use Pooled StDev = 0.0782

Two-Sample T-Test and Confidence Interval: 5U-Reservoir, 5U-Above

	N	Mean	StDev	SE Mean
5U-R	27	0.1177	0.0996	0.019
5U-A	132	0.0770	0.0449	0.0039

Estimate for difference: 0.0407
 95% CI for difference: (0.0166, 0.0647)
 T-Test of difference = 0 (vs not =): T-Value = 3.34 P-Value = 0.001 DF = 157
 Both use Pooled StDev = 0.0576

Two-Sample T-Test and Confidence Interval: Lithology 6, 4

	N	Mean	StDev	SE Mean
6	63	0.1114	0.0818	0.010
4	56	0.0675	0.0427	0.0057

Estimate for difference: 0.0440
 95% CI for difference: (0.0198, 0.0681)
 T-Test of difference = 0 (vs not =): T-Value = 3.61 P-Value = 0.000 DF = 117
 Both use Pooled StDev = 0.0664

Two-Sample T-Test and Confidence Interval: Lithology 6, 3

	N	Mean	StDev	SE Mean
6	63	0.1114	0.0818	0.010
3	103	0.0935	0.0483	0.0048

Estimate for difference: 0.0179
 95% CI for difference: (-0.0020, 0.0379)
 T-Test of difference = 0 (vs not =): T-Value = 1.78 P-Value = 0.077 DF = 164
 Both use Pooled StDev = 0.0631

Two-sample T-Tests and Confidence Intervals for Young' Modulus for elastic deformation for tests using strain gauges

Two-Sample T-Test and Confidence Interval: Lithology 6, 2

	N	Mean	StDev	SE Mean
6	63	0.1114	0.0818	0.010
2	114	0.0942	0.0348	0.0033

Estimate for difference: 0.01724
 95% CI for difference: (-0.00016, 0.03465)
 T-Test of difference = 0 (vs not =): T-Value = 1.95 P-Value = 0.052 DF = 175
 Both use Pooled StDev = 0.0562

Two-Sample T-Test and Confidence Interval: Lithology 3, 2

	N	Mean	StDev	SE Mean
3	103	0.0935	0.0483	0.0048
2	114	0.0942	0.0348	0.0033

Estimate for difference: -0.00070
 95% CI for difference: (-0.01189, 0.01050)
 T-Test of difference = 0 (vs not =): T-Value = -0.12 P-Value = 0.902 DF = 215
 Both use Pooled StDev = 0.0418

Two-Sample T-Test and Confidence Interval: Lithology 4, 2

	N	Mean	StDev	SE Mean
4	56	0.0675	0.0427	0.0057
2	114	0.0942	0.0348	0.0033

Estimate for difference: -0.02674
 95% CI for difference: (-0.03885, -0.01463)
 T-Test of difference = 0 (vs not =): T-Value = -4.36 P-Value = 0.000 DF = 168
 Both use Pooled StDev = 0.0376

Two-Sample T-Test and Confidence Interval: Lithology 4, 3

	N	Mean	StDev	SE Mean
4	56	0.0675	0.0427	0.0057
3	103	0.0935	0.0483	0.0048

Estimate for difference: -0.02604
 95% CI for difference: (-0.04127, -0.01082)
 T-Test of difference = 0 (vs not =): T-Value = -3.38 P-Value = 0.001 DF = 157
 Both use Pooled StDev = 0.0464

Two-Sample T-Test and CI: 5U, 1U

	N	Mean	StDev	SE Mean
5U	184	0.0838	0.0576	0.0042
1U	209	0.1075	0.0538	0.0037

Estimate for difference: -0.02365
 95% CI for difference: (-0.03470, -0.01261)
 T-Test of difference = 0 (vs not =): T-Value = -4.21 P-Value = 0.000 DF = 391
 Both use Pooled StDev = 0.0556

Two-sample T-Tests and Confidence Intervals for Poisson's Ratio for elastic deformation for tests using strain gauges

Two-Sample T-Test and Confidence Interval: Reservoir, Below

	N	Mean	StDev	SE Mean
R	123	0.1001	0.0627	0.0057
B	68	0.0987	0.0388	0.0047

Estimate for difference: 0.00139

95% CI for difference: (-0.01513, 0.01791)

T-Test of difference = 0 (vs not =): T-Value = 0.17 P-Value = 0.868 DF = 189

Both use Pooled StDev = 0.0554

Two-Sample T-Test and Confidence Interval: Reservoir, Above

	N	Mean	StDev	SE Mean
R	123	0.1001	0.0627	0.0057
A	202	0.0934	0.0581	0.0041

Estimate for difference: 0.00670

95% CI for difference: (-0.00678, 0.02017)

T-Test of difference = 0 (vs not =): T-Value = 0.98 P-Value = 0.329 DF = 323

Both use Pooled StDev = 0.0599

Two-Sample T-Test and Confidence Interval: Below, Above

	N	Mean	StDev	SE Mean
B	68	0.0987	0.0388	0.0047
A	202	0.0934	0.0581	0.0041

Estimate for difference: 0.00531

95% CI for difference: (-0.00957, 0.02018)

T-Test of difference = 0 (vs not =): T-Value = 0.70 P-Value = 0.483 DF = 268

Both use Pooled StDev = 0.0539

Two-sample T-test for Poisson's Ratio during elastic deformation in tests using strain gauges

Two-Sample T-Test and Confidence Interval: 1U-Reservoir, 1U-Below

	N	Mean	StDev	SE Mean
1U-R	108	0.1137	0.0519	0.0050
1U-B	21	0.1037	0.0396	0.0086

Estimate for difference: 0.0100

95% CONFIDENCE INTERVAL for difference: (-0.0137, 0.0337)

T-Test of difference = 0 (vs not =): T-Value = 0.84 P-Value = 0.405 DF = 127

Both use Pooled StDev = 0.0502

Two-Sample T-Test and Confidence Interval: 1U- Reservoir, 1U-Above

	N	Mean	StDev	SE Mean
1U-R	108	0.1137	0.0519	0.0050
1U-A	78	0.1442	0.0466	0.0053

Estimate for difference: -0.03056

95% Confidence Interval for difference: (-0.04515, -0.01598)

T-Test of difference = 0 (vs not =): T-Value = -4.13 P-Value = 0.000 DF = 184

Both use Pooled StDev = 0.0498

Two-Sample T-Test and Confidence Interval: 1U- Below, 1U- Above

	N	Mean	StDev	SE Mean
1U-B	21	0.1037	0.0396	0.0086
1U-A	78	0.1442	0.0466	0.0053

Estimate for difference: -0.0406

95% Confidence Interval for difference: (-0.0626, -0.0185)

T-Test of difference = 0 (vs not =): T-Value = -3.65 P-Value = 0.000 DF = 97

Both use Pooled StDev = 0.0452

Two-Sample T-Test and Confidence Interval: 5U-Above, 5U-Below

	N	Mean	StDev	SE Mean
5U-A	167	0.0857	0.0503	0.0039
5U-B	24	0.0890	0.0422	0.0086

Estimate for difference: -0.0033

95% Confidence Interval for difference: (-0.0245, 0.0180)

T-Test of difference = 0 (vs not =): T-Value = -0.30 P-Value = 0.763 DF = 189

Both use Pooled StDev = 0.0494

Two-Sample T-Test and Confidence Interval: 5U-Reservoir, 5U-Below

	N	Mean	StDev	SE Mean
5U-R	21	0.0993	0.0373	0.0081
5U-B	24	0.0890	0.0422	0.0086

Estimate for difference: 0.0103

95% Confidence Interval for difference: (-0.0138, 0.0344)

T-Test of difference = 0 (vs not =): T-Value = 0.86 P-Value = 0.394 DF = 43

Both use Pooled StDev = 0.0400

Two-sample T-test for Poisson's Ratio during elastic deformation in tests using strain gauges

Two-Sample T-Test and Confidence Interval: 5U-Reservoir, 5U-Above

	N	Mean	StDev	SE Mean
5U-R	21	0.0993	0.0373	0.0081
5U-A	167	0.0857	0.0503	0.0039

Estimate for difference: 0.0135
 95% Confidence Interval for difference: (-0.0089, 0.0359)
 T-Test of difference = 0 (vs not =): T-Value = 1.19 P-Value = 0.235 DF = 186
 Both use Pooled StDev = 0.0490

Two-Sample T-Test and Confidence Interval: Lithology Types 6, 4

	N	Mean	StDev	SE Mean
6	48	0.1184	0.0469	0.0068
4	72	0.0802	0.0483	0.0057

Estimate for difference: 0.03824
 95% Confidence Interval for difference: (0.02061, 0.05586)
 T-Test of difference = 0 (vs not =): T-Value = 4.30 P-Value = 0.000 DF = 118
 Both use Pooled StDev = 0.0478

Two-Sample T-Test and Confidence Interval: Lithology Types 6, 3

	N	Mean	StDev	SE Mean
6	48	0.1184	0.0469	0.0068
3	197	0.1148	0.0578	0.0041

Estimate for difference: 0.00359
 95% Confidence Interval for difference: (-0.01411, 0.02130)
 T-Test of difference = 0 (vs not =): T-Value = 0.40 P-Value = 0.690 DF = 243
 Both use Pooled StDev = 0.0558

Two-Sample T-Test and Confidence Interval: Lithology Types 6, 2

	N	Mean	StDev	SE Mean
6	48	0.1184	0.0469	0.0068
2	102	0.0997	0.0414	0.0041

Estimate for difference: 0.01874
 95% Confidence Interval for difference: (0.00379, 0.03369)
 T-Test of difference = 0 (vs not =): T-Value = 2.48 P-Value = 0.014 DF = 148
 Both use Pooled StDev = 0.0432

Two-Sample T-Test and Confidence Interval: Lithology Types 4, 2

	N	Mean	StDev	SE Mean
4	72	0.0802	0.0483	0.0057
2	102	0.0997	0.0414	0.0041

Estimate for difference: -0.01950
 95% Confidence Interval for difference: (-0.03299, -0.00600)
 T-Test of difference = 0 (vs not =): T-Value = -2.85 P-Value = 0.005 DF = 172
 Both use Pooled StDev = 0.0444

Two-sample T-test for Poisson's Ratio during elastic deformation in tests using strain gauges

Two-Sample T-Test and Confidence Interval: Lithology Types 3, 2

	N	Mean	StDev	SE Mean
3	197	0.1148	0.0578	0.0041
2	102	0.0997	0.0414	0.0041

95% Confidence Interval for difference: (0.00247, 0.02782)
 T-Test of difference = 0 (vs not =): T-Value = 2.35 P-Value = 0.019 DF = 297
 Both use Pooled StDev = 0.0528

Two-Sample T-Test and Confidence Interval: Lithology Types 3, 4

	N	Mean	StDev	SE Mean
3	197	0.1148	0.0578	0.0041
4	72	0.0802	0.0483	0.0057

Estimate for difference: 0.03464
 95% Confidence Interval for difference: (0.01961, 0.04967)
 T-Test of difference = 0 (vs not =): T-Value = 4.54 P-Value = 0.000 DF = 267
 Both use Pooled StDev = 0.0554

Two-Sample T-Test and Confidence Interval: Reservoir, Below

	N	Mean	StDev	SE Mean
R	129	0.1113	0.0500	0.0044
B	45	0.0958	0.0412	0.0061

Estimate for difference: 0.01548
 95% Confidence Interval for difference: (-0.00089, 0.03185)
 T-Test of difference = 0 (vs not =): T-Value = 1.87 P-Value = 0.064 DF = 172
 Both use Pooled StDev = 0.0479

Two-Sample T-Test and Confidence Interval: Reservoir, Above

	N	Mean	StDev	SE Mean
R	129	0.1113	0.0500	0.0044
A	245	0.1044	0.0561	0.0036

Estimate for difference: 0.00696
 95% Confidence Interval for difference: (-0.00461, 0.01853)
 T-Test of difference = 0 (vs not =): T-Value = 1.18 P-Value = 0.238 DF = 372
 Both use Pooled StDev = 0.0541

Two-Sample T-Test and Confidence Interval: Below, Above

	N	Mean	StDev	SE Mean
B	45	0.0958	0.0412	0.0061
A	245	0.1044	0.0561	0.0036

Estimate for difference: -0.00852
 95% Confidence Interval for difference: (-0.02579, 0.00875)
 T-Test of difference = 0 (vs not =): T-Value = -0.97 P-Value = 0.332 DF = 288
 Both use Pooled StDev = 0.0541

Two-sample T-test for Poisson's Ratio during elastic deformation in tests using strain gauges

Two-Sample T-Test and Confidence Interval: 5U, 1U

	N	Mean	StDev	SE Mean
5U	212	0.0875	0.0483	0.0033
1U	419	0.1056	0.0529	0.0026

Estimate for difference: -0.01814
 95% Confidence Interval for difference: (-0.02665, -0.00963)
 T-Test of difference = 0 (vs not =): T-Value = -4.18 P-Value = 0.000 DF = 629
 Both use Pooled StDev = 0.0514
 Two-sample T for 5U-R vs 1U-R

Two-Sample T-Test and Confidence Interval: 5U-Reservoir, 1U-Reservoir

	N	Mean	StDev	SE Mean
5U-R	21	0.0993	0.0373	0.0081
1U-R	108	0.1137	0.0519	0.0050

Difference = mu 5U-R - mu 1U-R
 Estimate for difference: -0.0144
 95% Confidence Interval for difference: (-0.0379, 0.0092)
 T-Test of difference = 0 (vs not =): T-Value = -1.21 P-Value = 0.229 DF = 127
 Both use Pooled StDev = 0.0499

Two-Sample T-Test and Confidence Interval: 1U-Above, 5U-Above

	N	Mean	StDev	SE Mean
1U-A	78	0.1442	0.0466	0.0053
5U-A	167	0.0857	0.0503	0.0039

Estimate for difference: 0.05848
 95% Confidence Interval for difference: (0.04521, 0.07175)
 T-Test of difference = 0 (vs not =): T-Value = 8.68 P-Value = 0.000 DF = 243
 Both use Pooled StDev = 0.0491

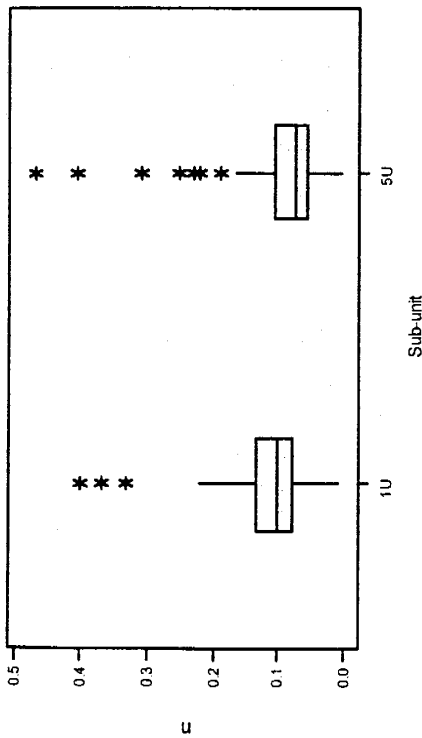
Two-Sample T-Test and Confidence Interval: 1U-Below, 5U-Below

	N	Mean	StDev	SE Mean
1U-B	21	0.1037	0.0396	0.0086
5U-B	24	0.0890	0.0422	0.0086

Estimate for difference: 0.0147
 95% Confidence Interval for difference: (-0.0100, 0.0394)
 T-Test of difference = 0 (vs not =): T-Value = 1.20 P-Value = 0.238 DF = 43
 Both use Pooled StDev = 0.0410

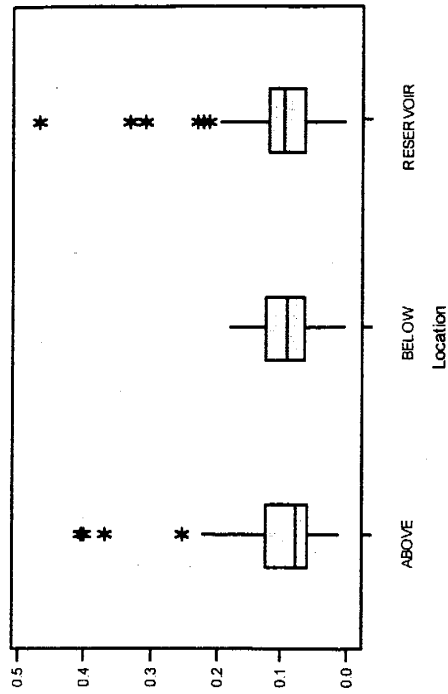
Boxplots of Poisson's Ratio by Sub-unit

(means are indicated by solid circles)



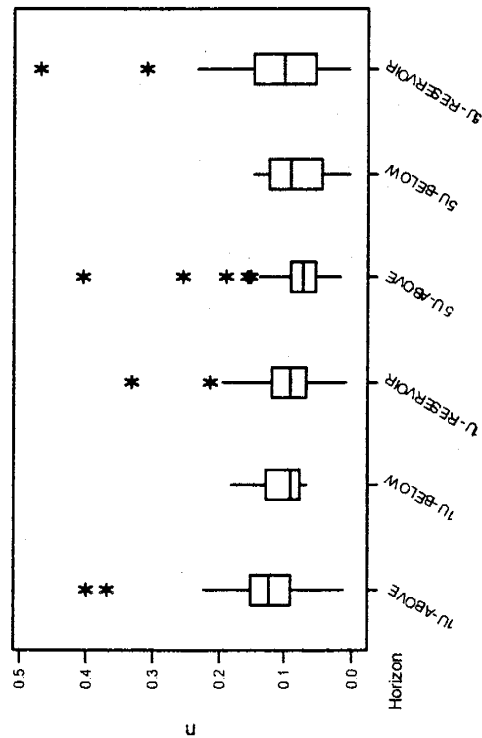
Boxplots of Poisson's Ratio by Location

(means are indicated by solid circles)



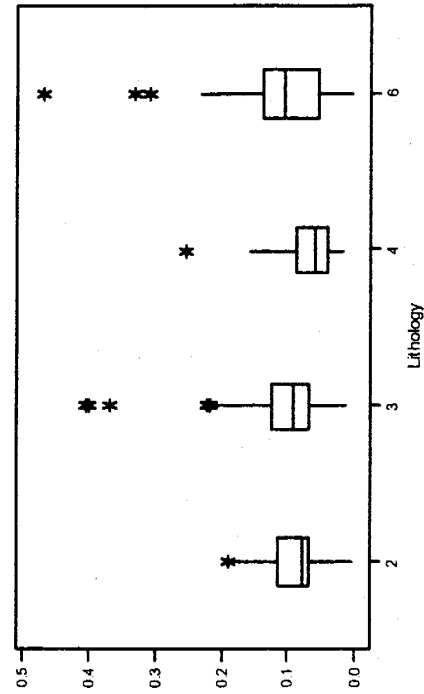
Boxplots of Poisson's Ratio by Horizon

(means are indicated by solid circles)



Boxplots of Poisson's Ratio by Lithology

(means are indicated by solid circles)

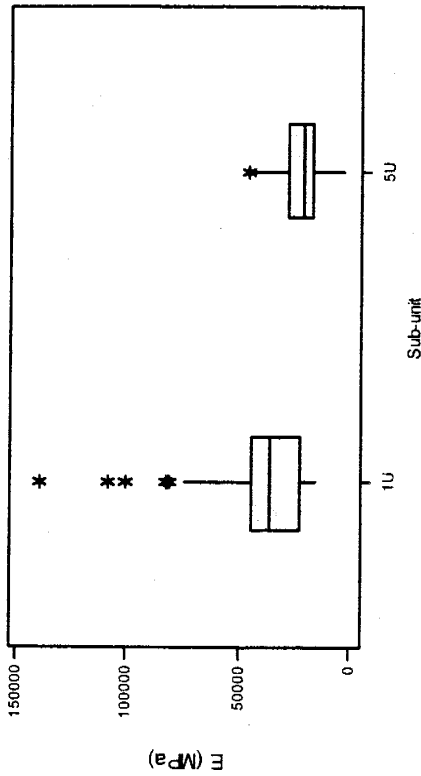


Boxplots of Poisson's Ratio for elastic deformation

Box connects first and third quartiles, horizontal line drawn through median, vertical line drawn through range of values, * represents outliers

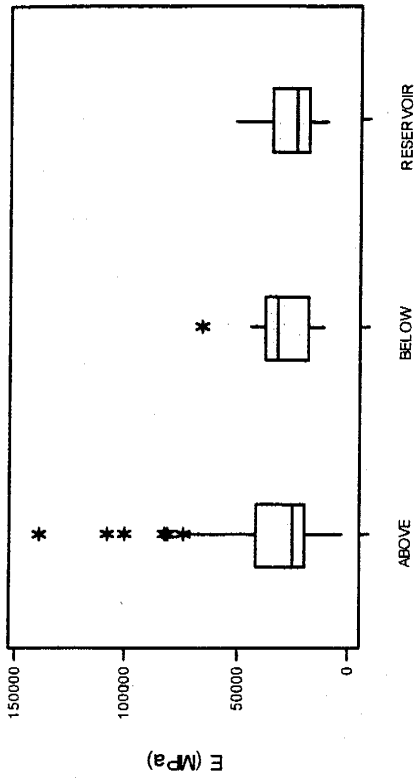
Boxplots of E (MPa) by Sub-unit

(means are indicated by solid circles)



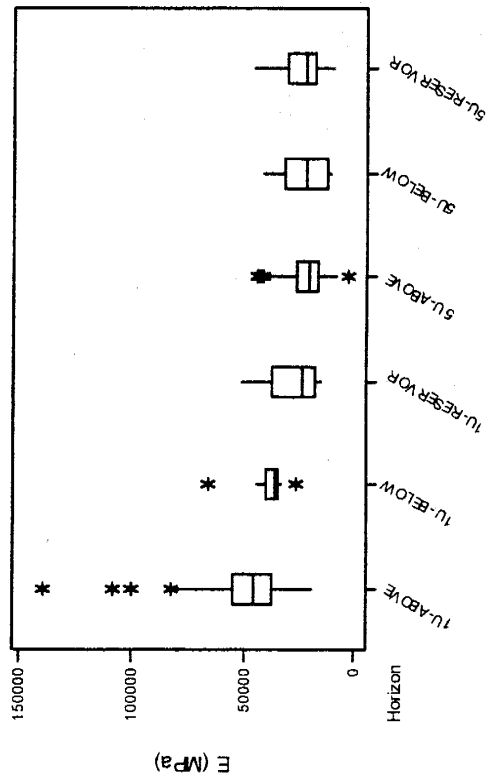
Boxplots of E (MPa) by Location

(means are indicated by solid circles)



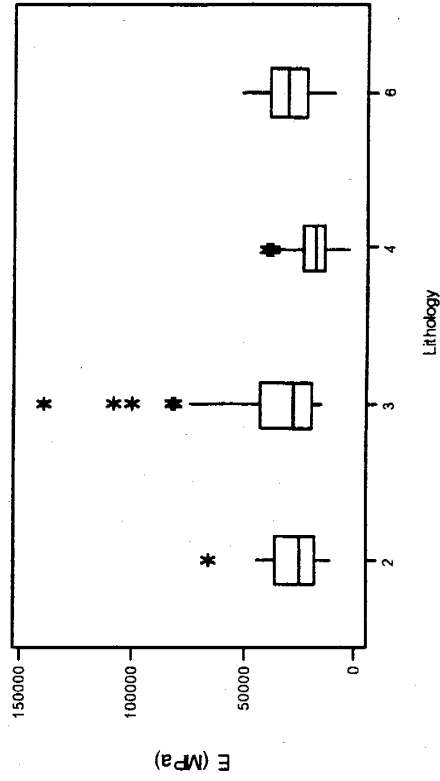
Boxplots of E (MPa) by Horizon

(means are indicated by solid circles)



Boxplots of E (MPa) by Lithology

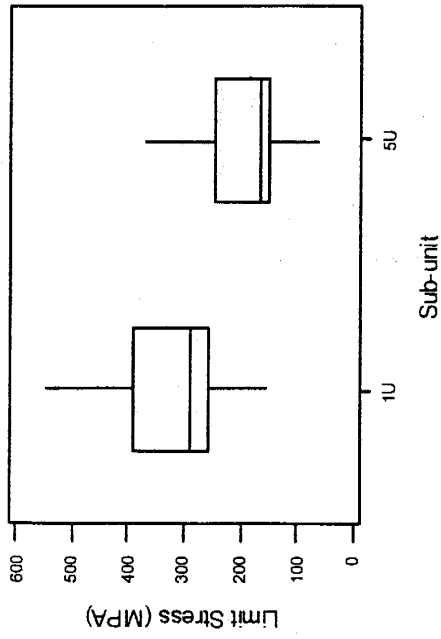
(means are indicated by solid circles)



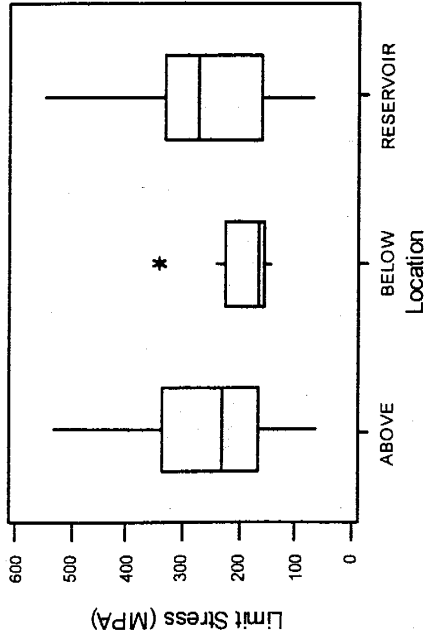
Boxplots of Young's Modulus (MPa) for elastic deformation

Box connects first and third quartiles, horizontal line drawn through median, vertical line drawn through range of values, * represents outliers

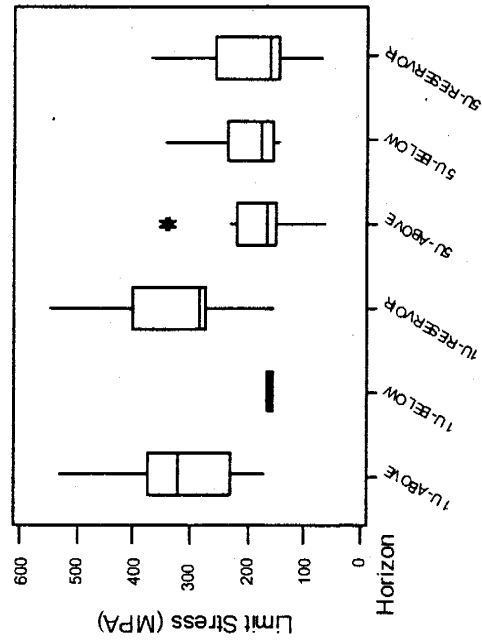
Boxplots of Limit Stress by Sub-unit



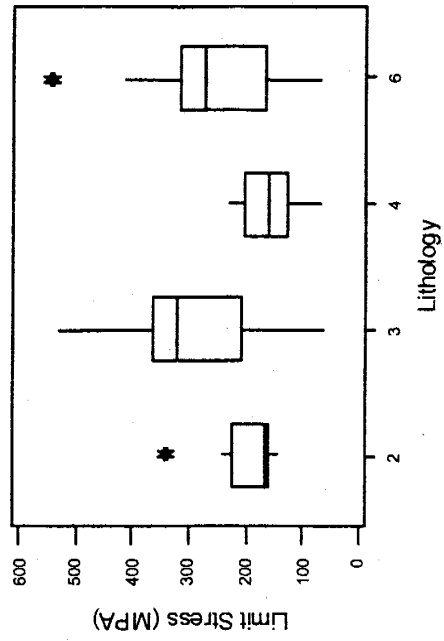
Boxplots of Limit Stress by Location



Boxplots of Limit Stress by Horizon



Boxplots of Limit Stress by Lithology

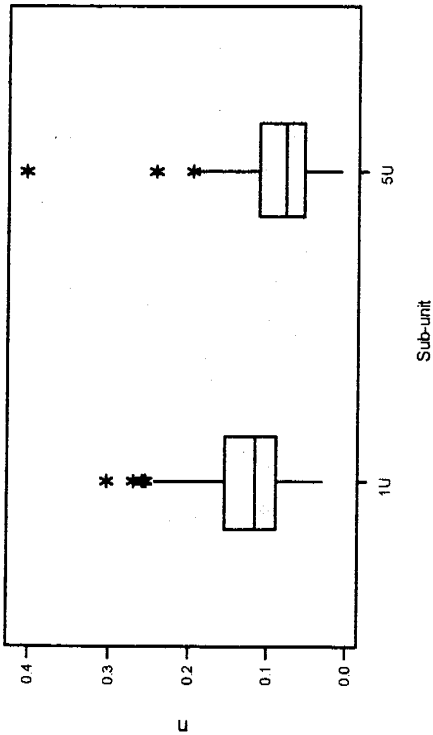


Boxplots of Limit Stress (MPa)

Box connects first and third quartiles, horizontal line drawn through median, vertical line drawn through range of values, * represents outliers

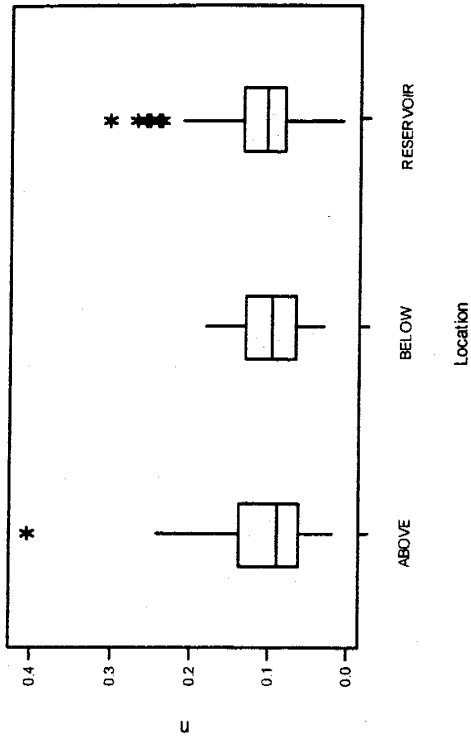
Boxplots of Poisson's Ratio by Sub-unit

(means are indicated by solid circles)



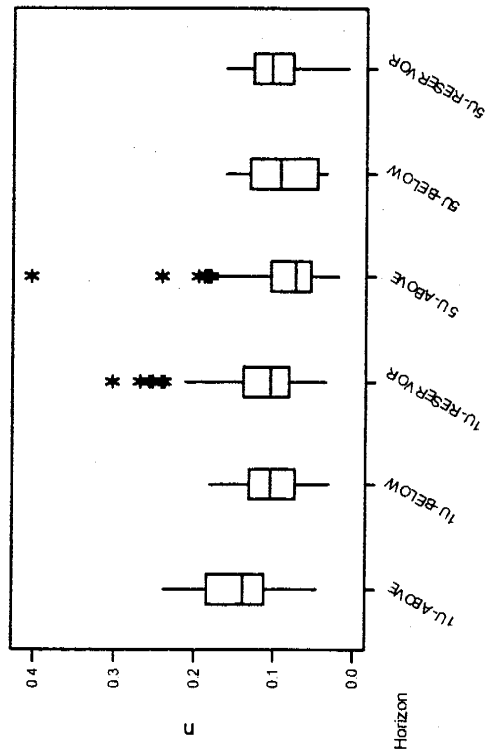
Boxplots of Poisson's Ratio by Location

(means are indicated by solid circles)



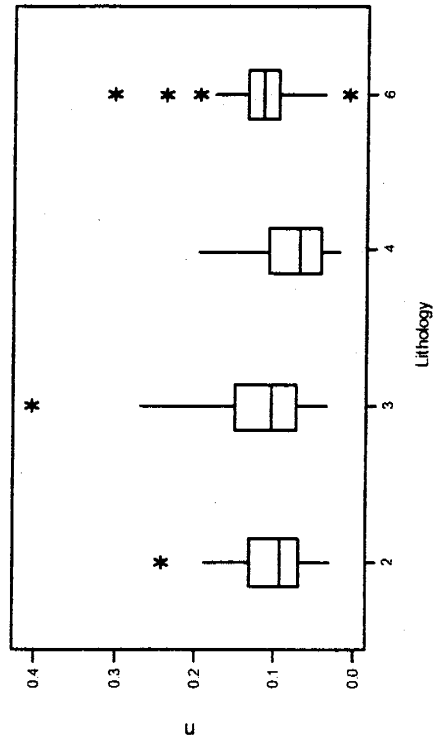
Boxplots of Poisson's Ratio by Horizon

(means are indicated by solid circles)



Boxplots of Poisson's Ratio by Lithology

(means are indicated by solid circles)

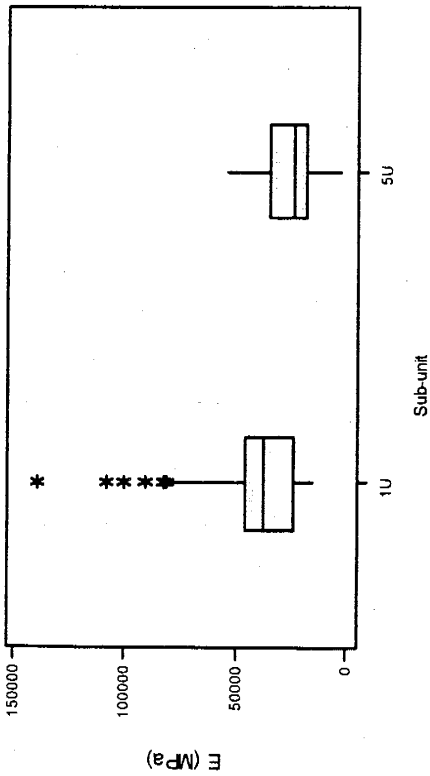


Boxplots of Young's Modulus (MPa) for elastic and plastic deformation

Box connects first and third quartiles, horizontal line drawn through median, vertical line drawn through range of values, * represents outliers

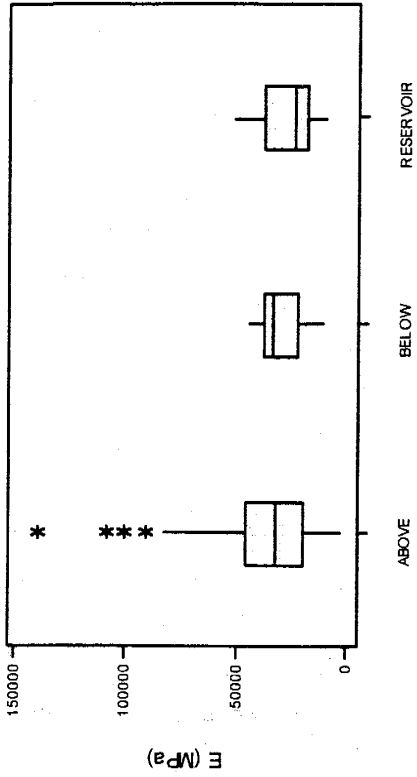
Boxplots of E (MPa) by Sub-unit

(means are indicated by solid circles)



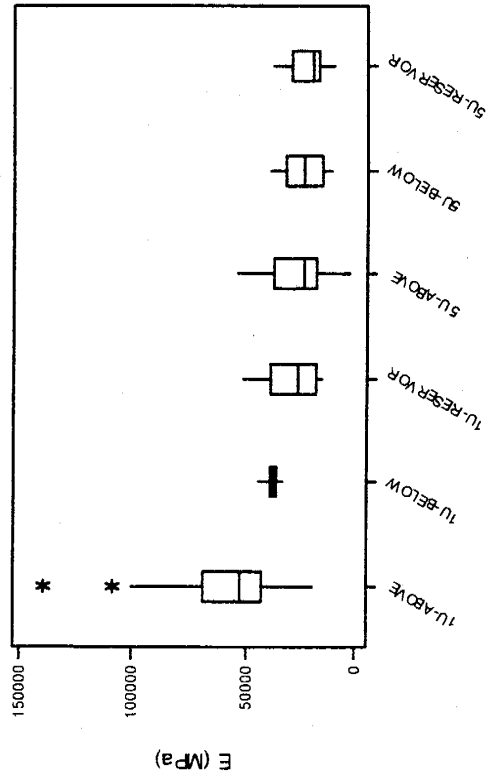
Boxplots of E (MPa) by Location

(means are indicated by solid circles)



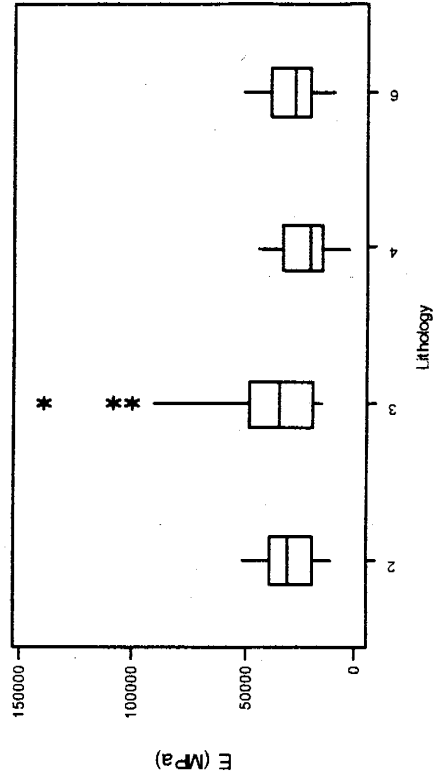
Boxplots of E (MPa) by Horizon

(means are indicated by solid circles)



Boxplots of E (MPa) by Lithology

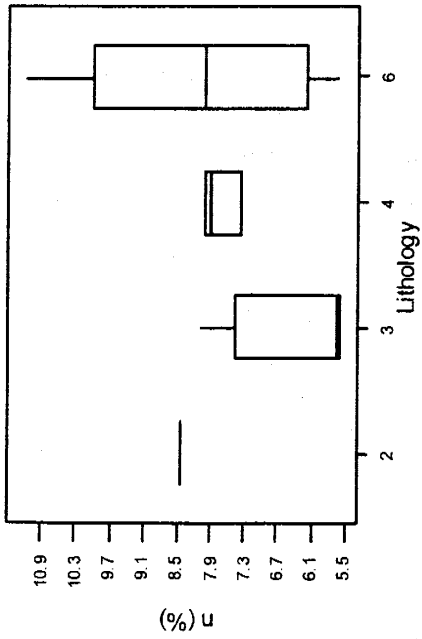
(means are indicated by solid circles)



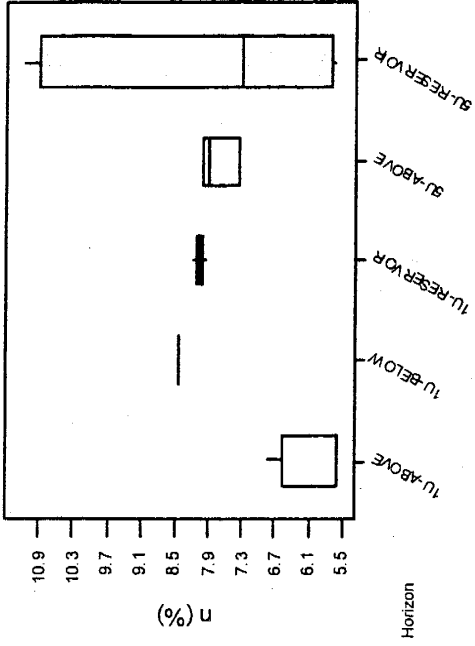
Boxplots of Young's Modulus (MPa) for elastic and plastic deformation

Box connects first and third quartiles, horizontal line drawn through median, vertical line drawn through range of values, * represents outliers

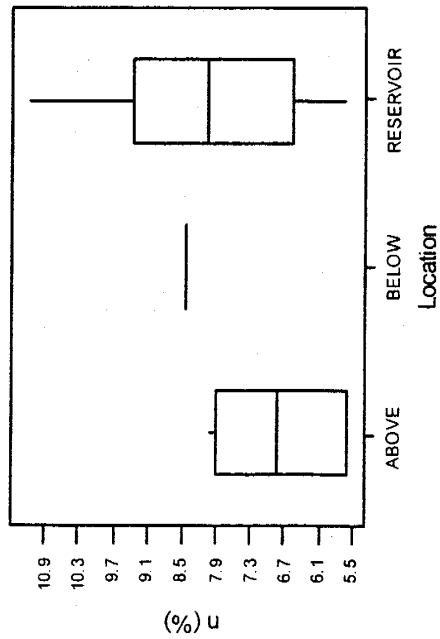
Boxplots of Porosity (%) by Lithology



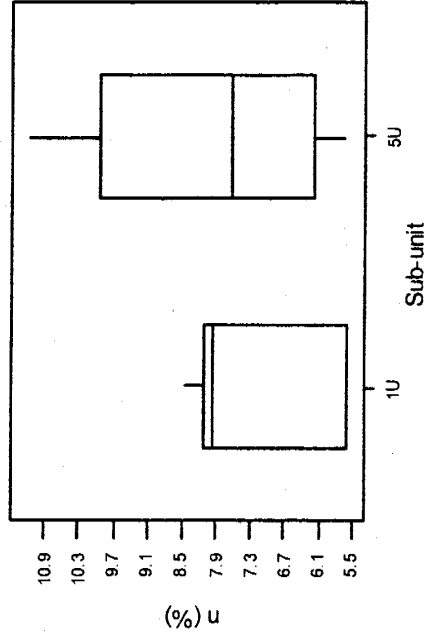
Boxplots of Porosity (%) by Horizon



Boxplots of Porosity (%) by Location



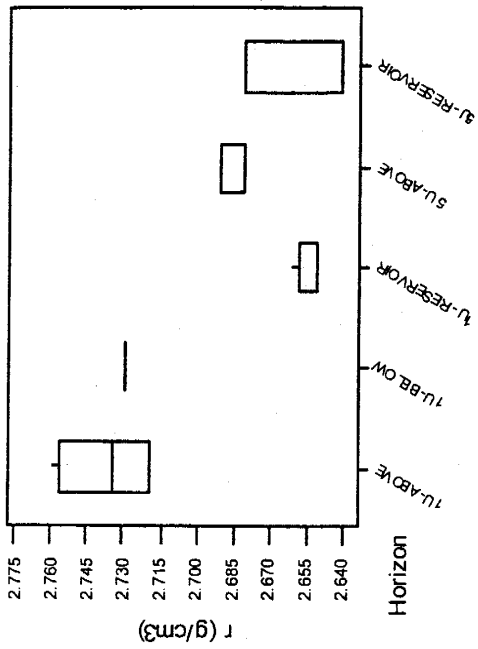
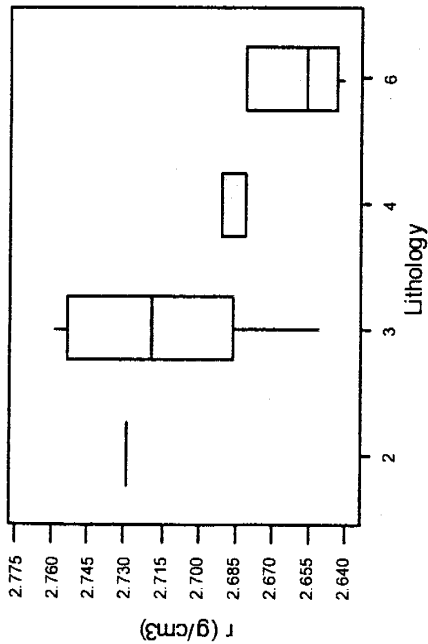
Boxplots of Porosity (%) by Sub-unit



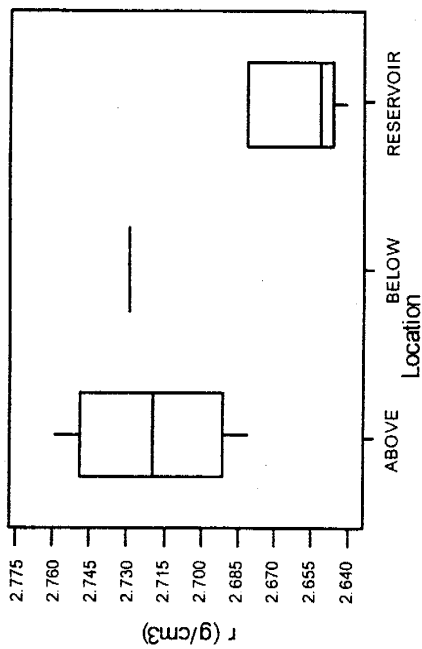
Boxplots of Porosity (%)

Box connects first and third quartiles, horizontal line drawn through median, vertical line drawn through range of values, * represents outliers

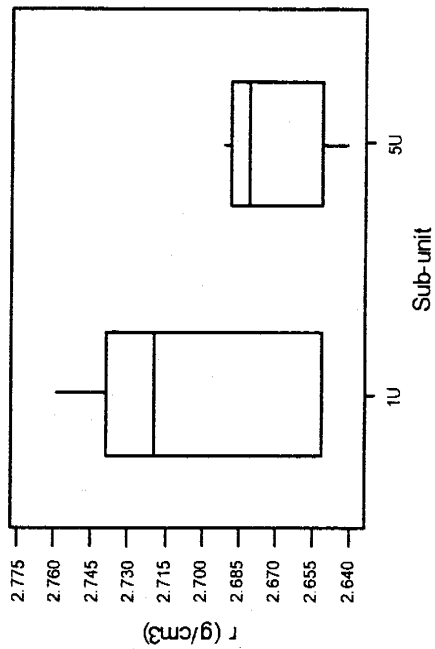
Boxplots of Bulk Density (g/cm³) by Lithology



Boxplots of Bulk Density (g/cm³) by Location



Boxplots of Bulk Density (g/cm³) by Sub-unit

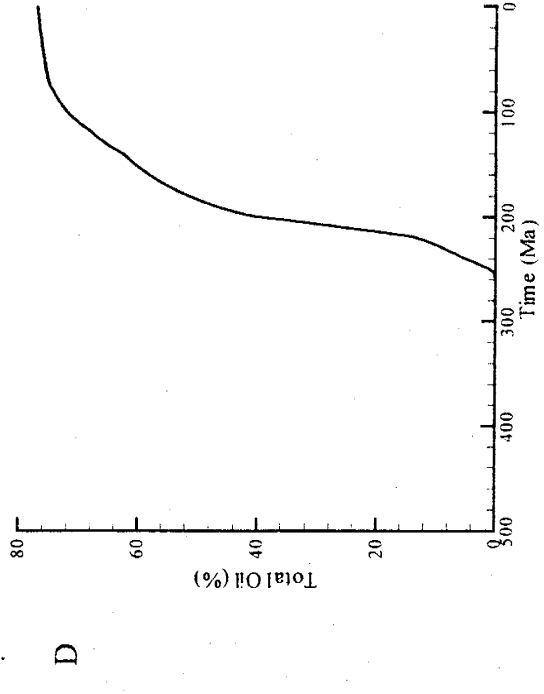
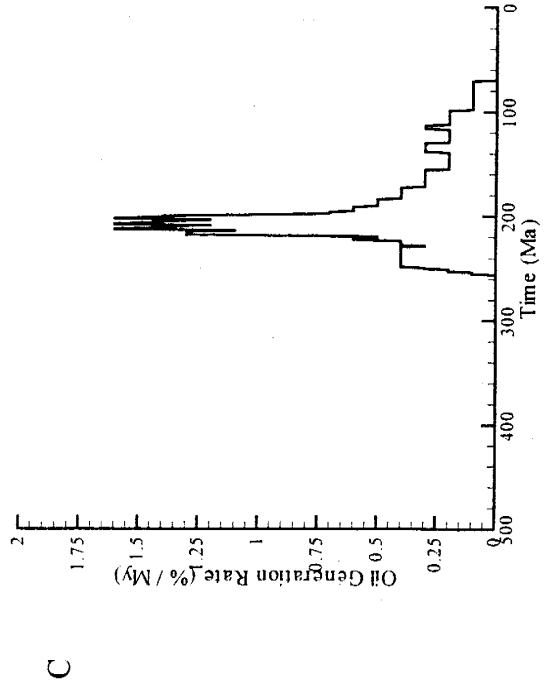
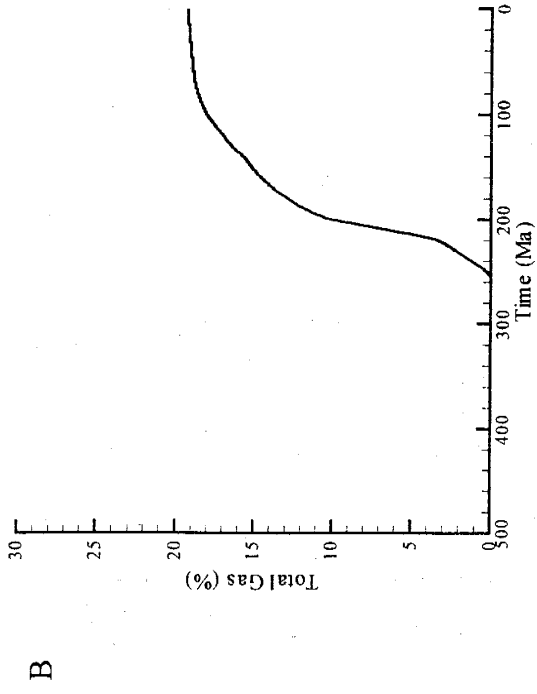
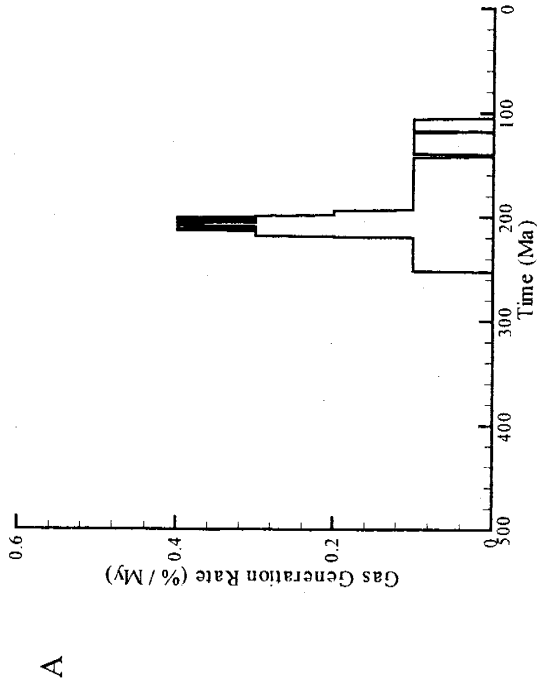


Boxplots of Bulk Density (g/cm³)

Box connects first and third quartiles, horizontal line drawn through median, vertical line drawn through range of values, * represents outliers

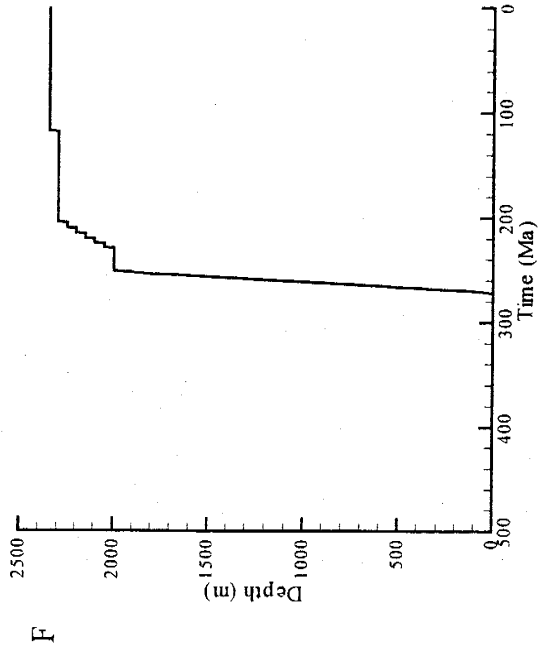
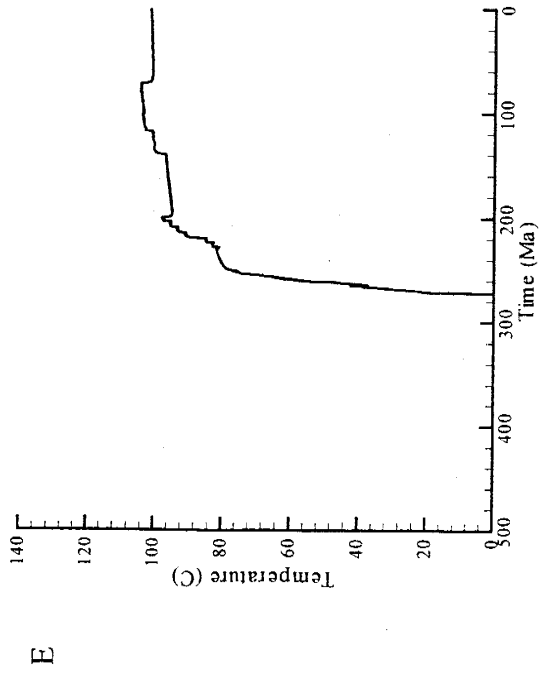
APPENDIX B

Results of modeling study



B1

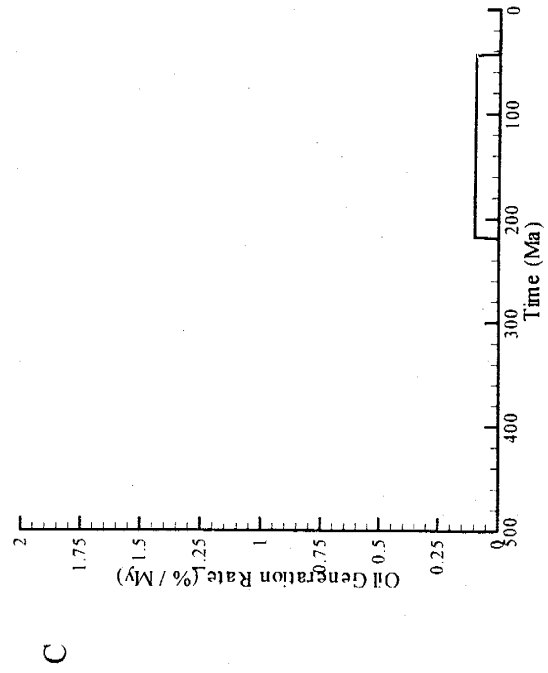
Results of modeling study



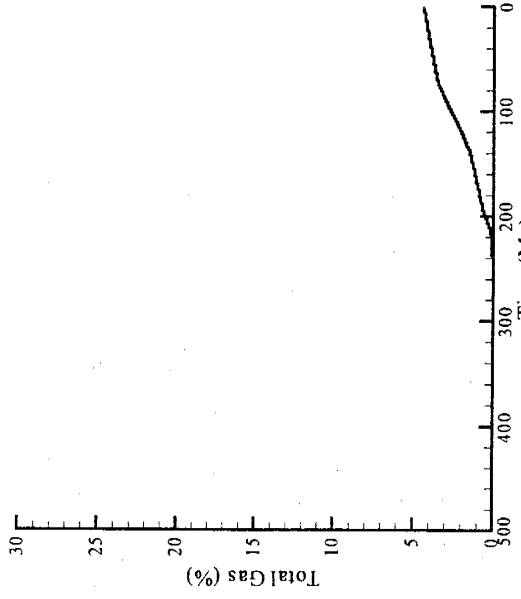
Results of sensitivity analysis with high thermal conductivity values

A

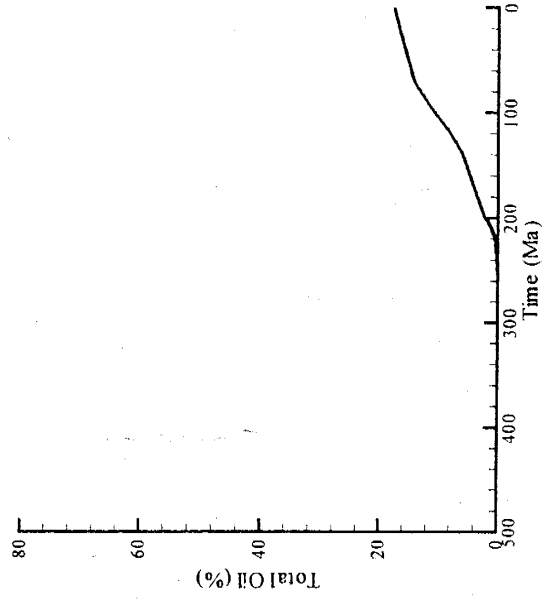
Gas production rates too low - all plot on x axis



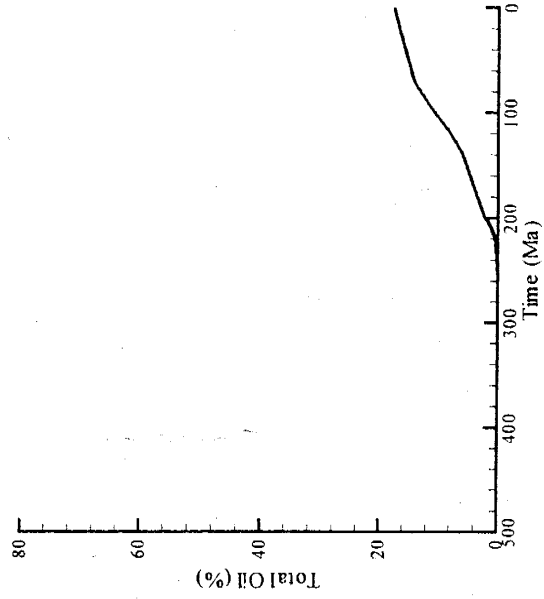
B



C

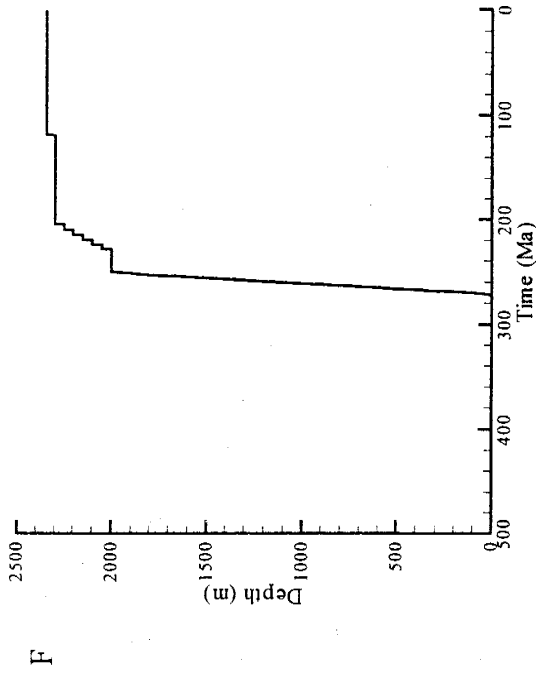
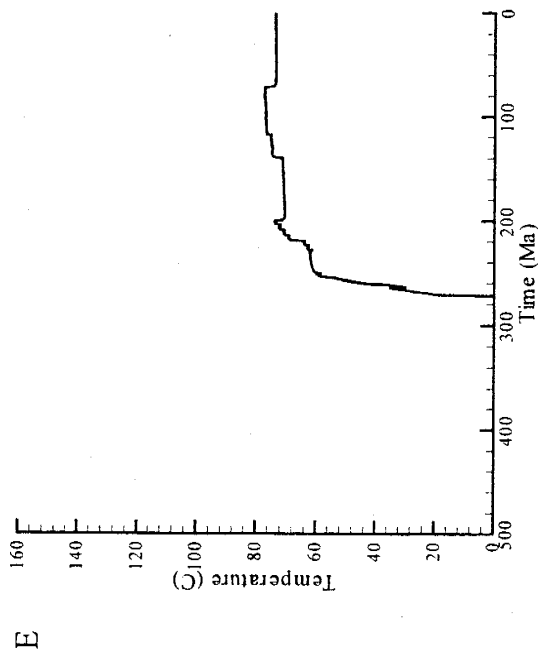


D

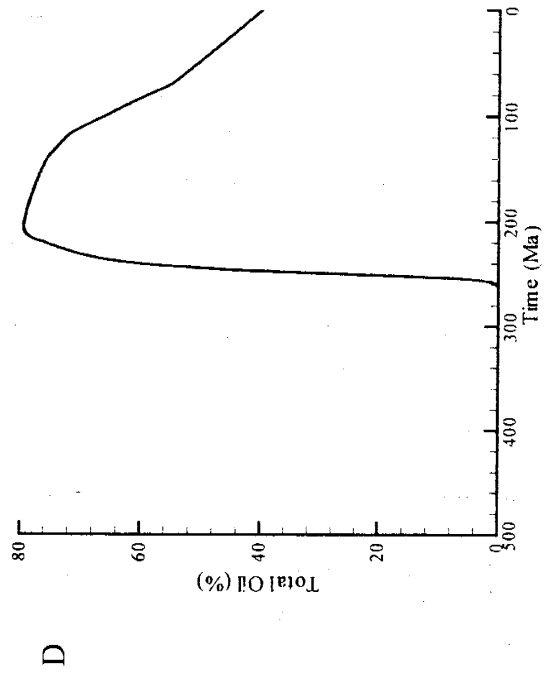
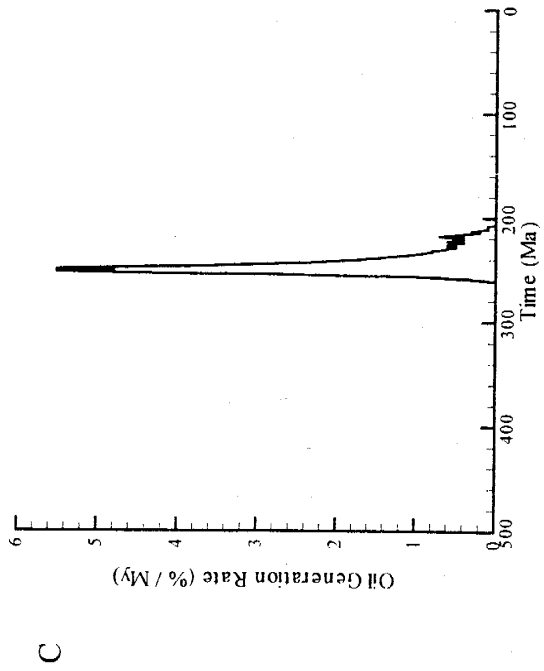
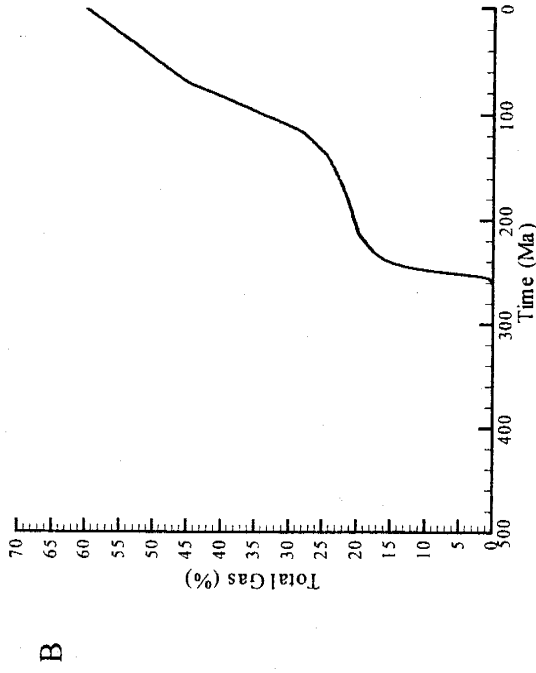
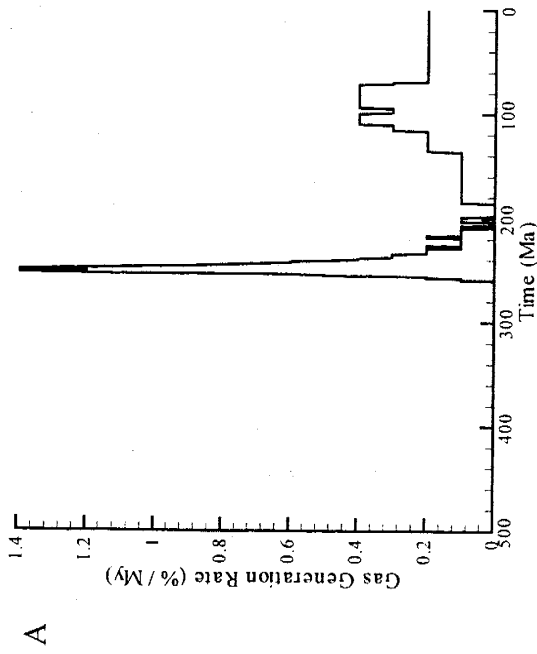


B3

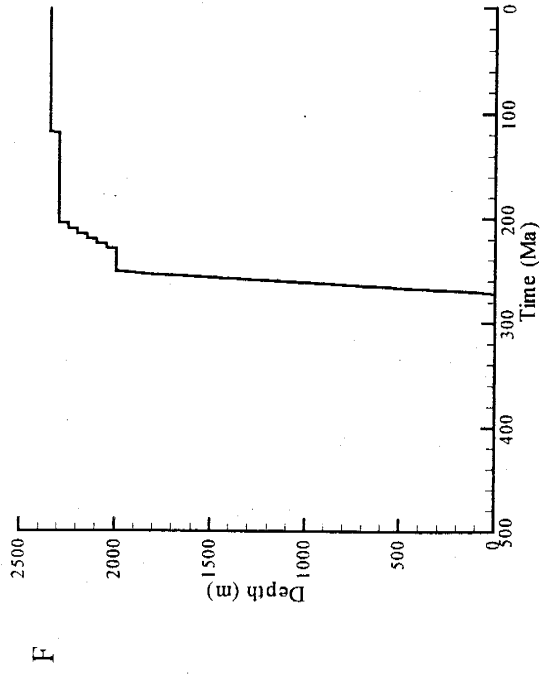
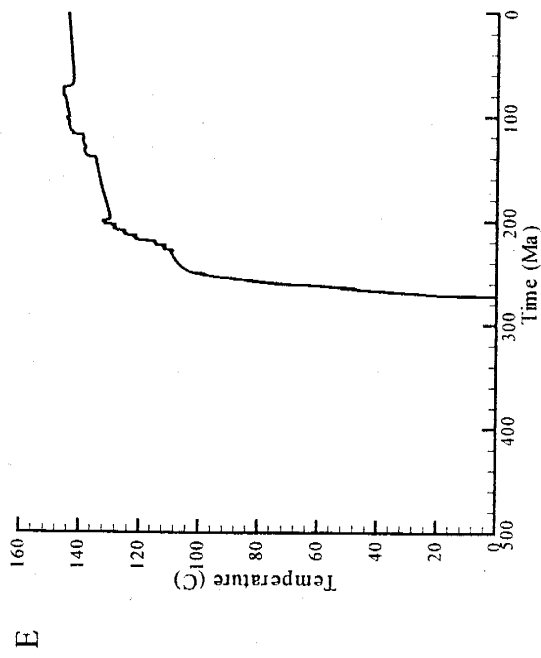
Results of sensitivity analysis with high thermal conductivity values



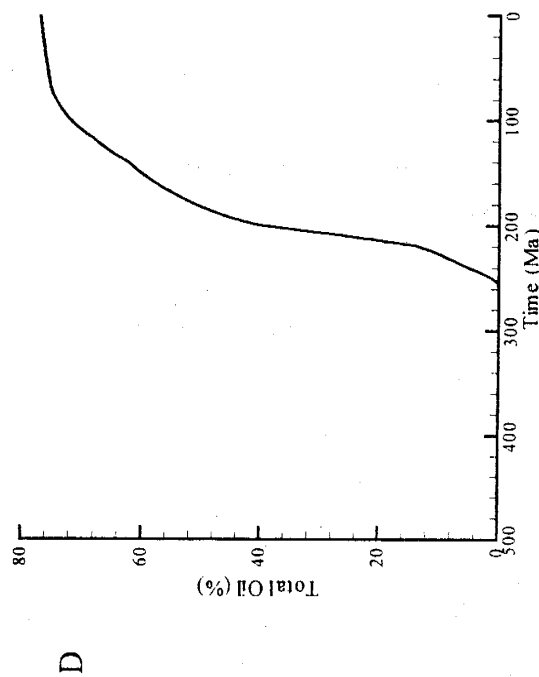
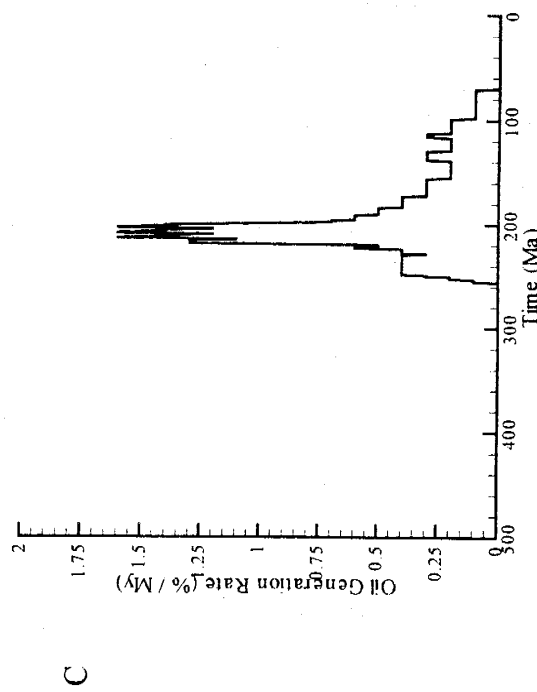
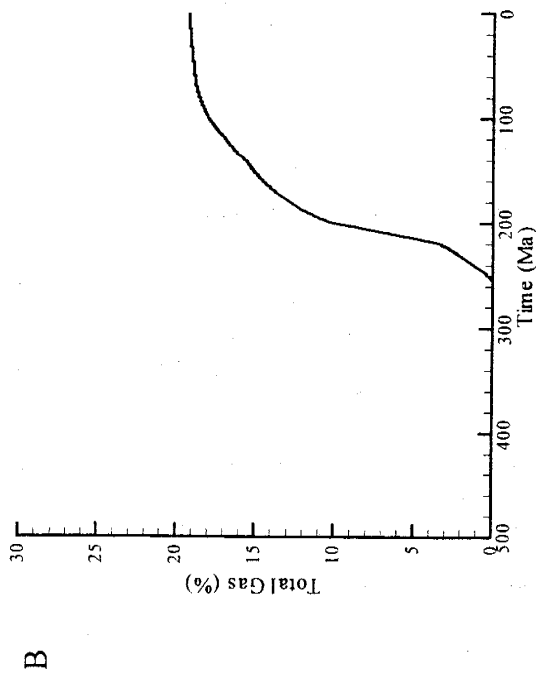
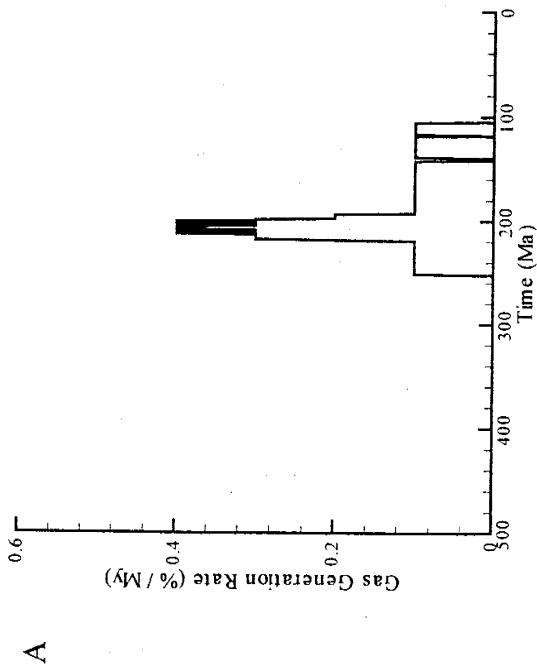
Results of sensitivity study with low thermal conductivity values



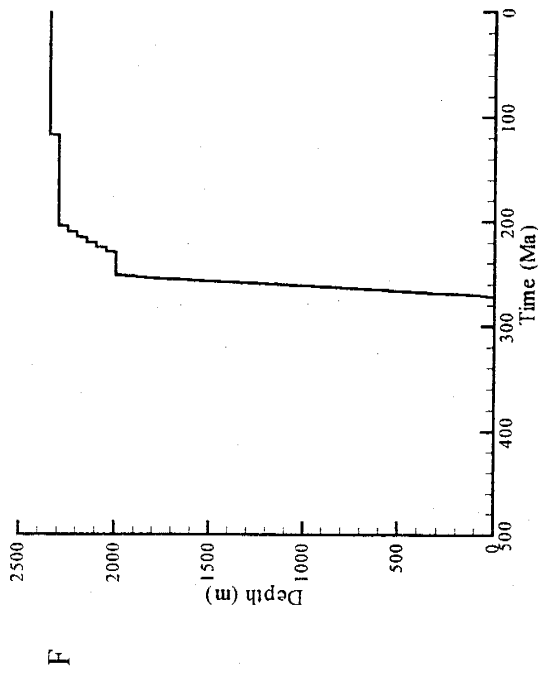
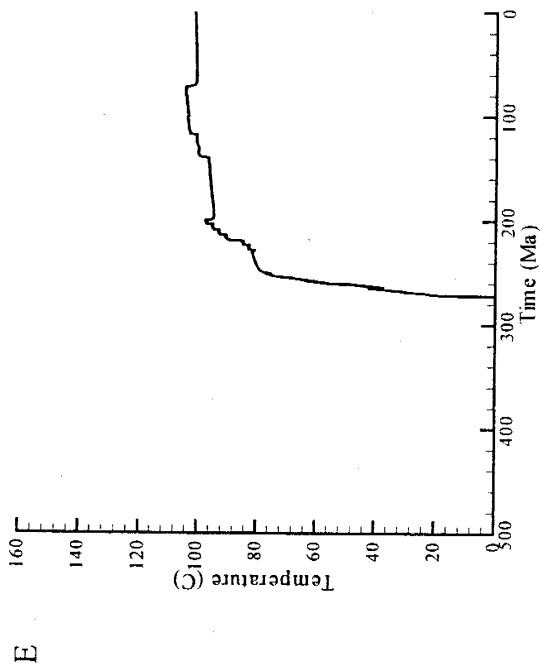
Results of sensitivity study with low thermal conductivity values



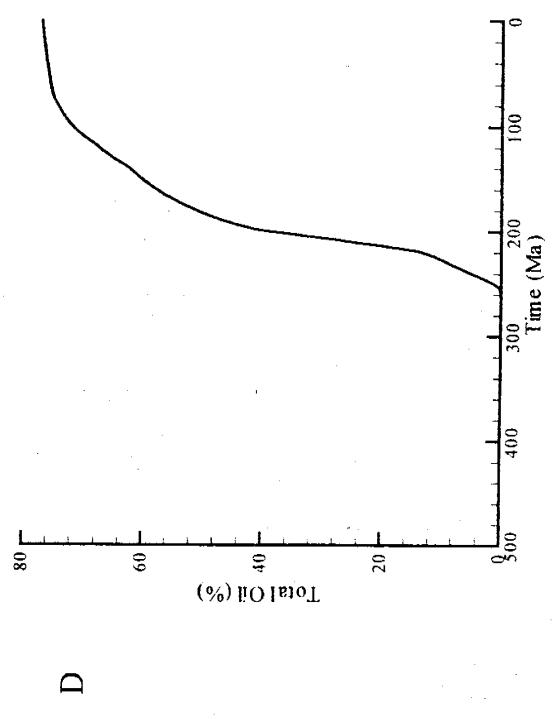
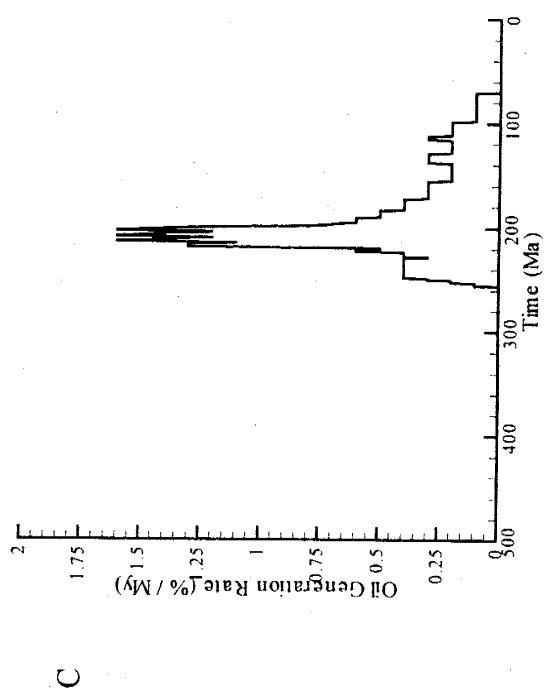
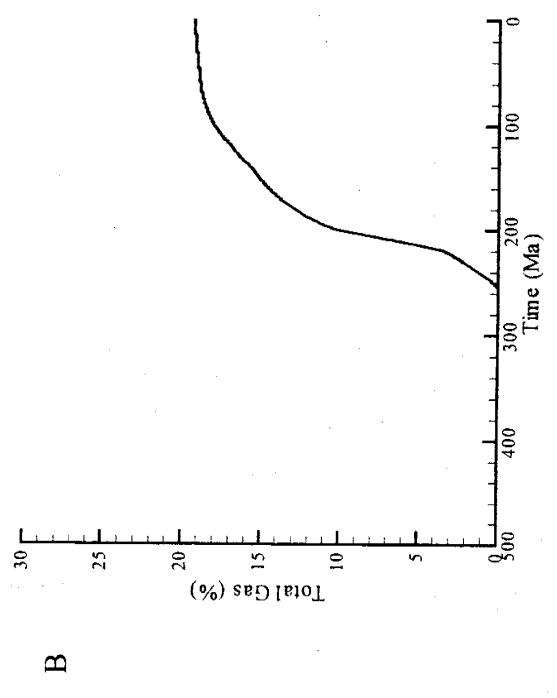
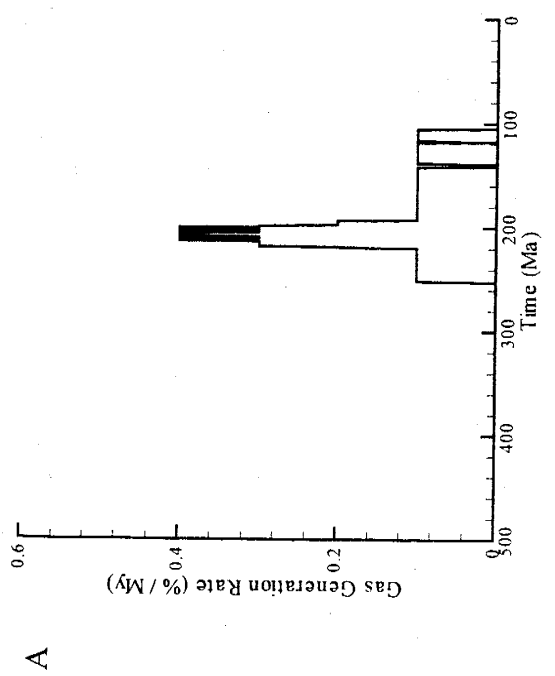
Results of sensitivity study with high original porosity values



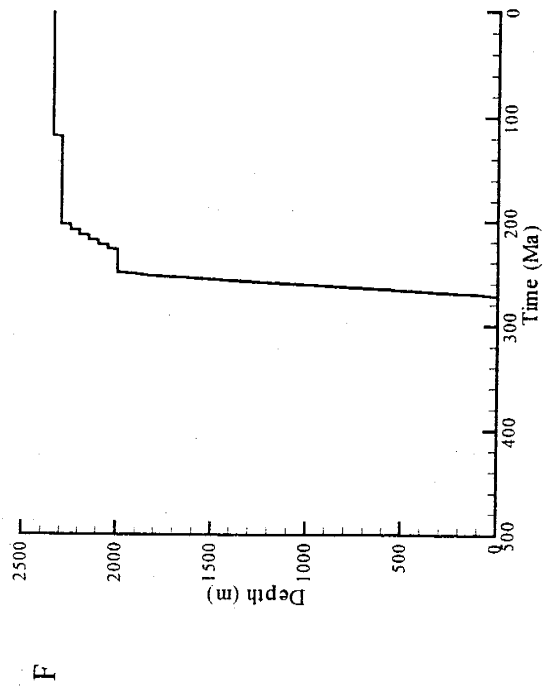
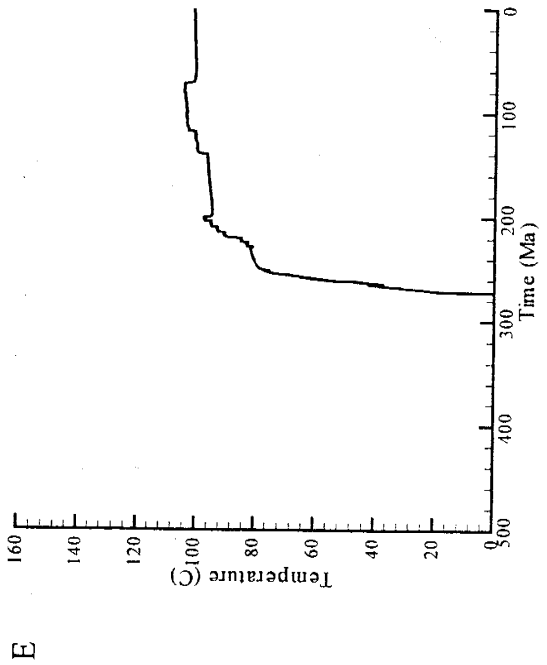
Results of sensitivity study with high original porosity values



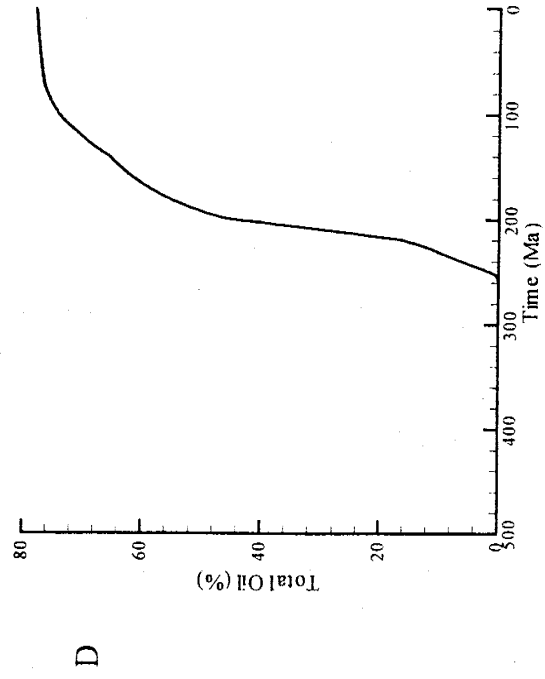
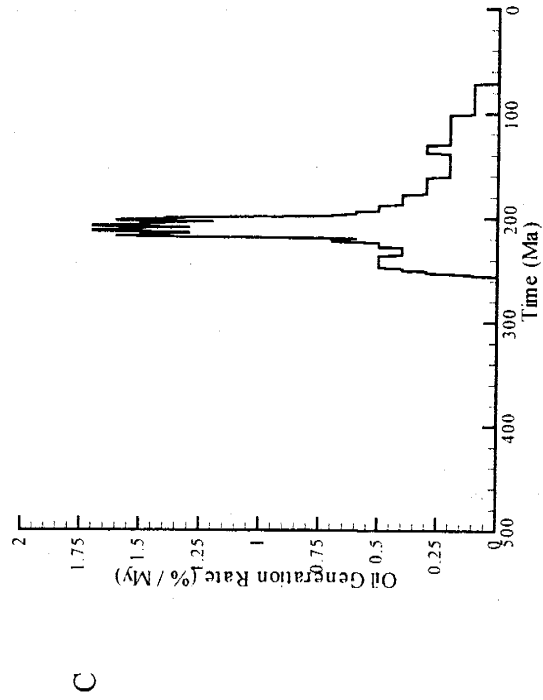
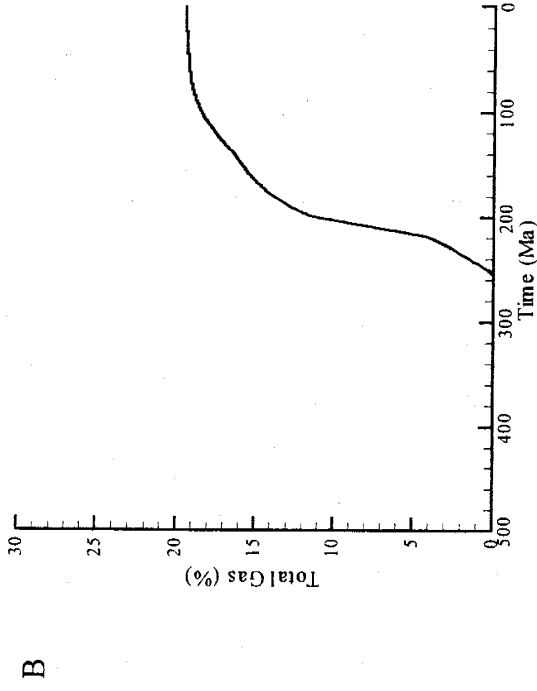
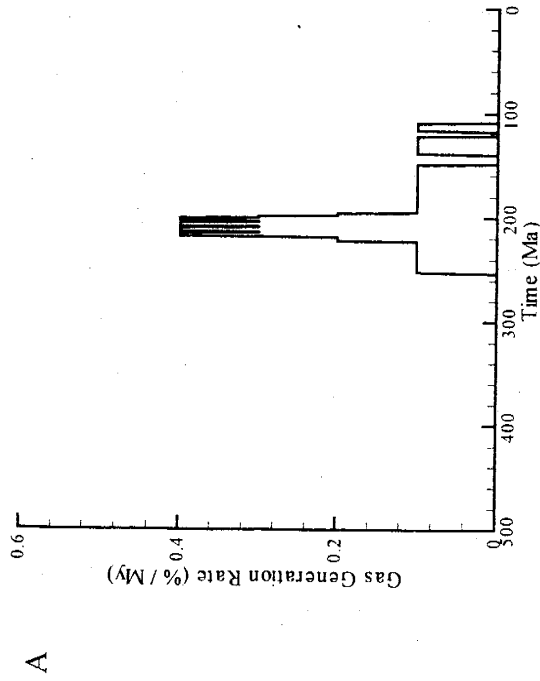
Results of sensitivity study with low original porosity values



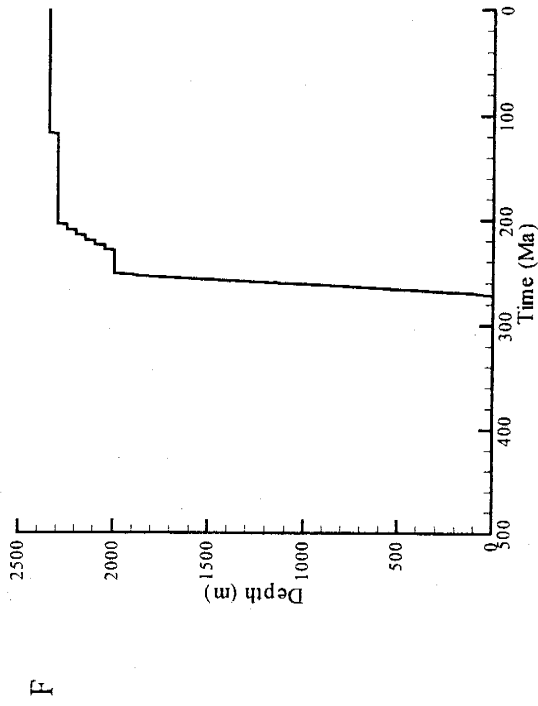
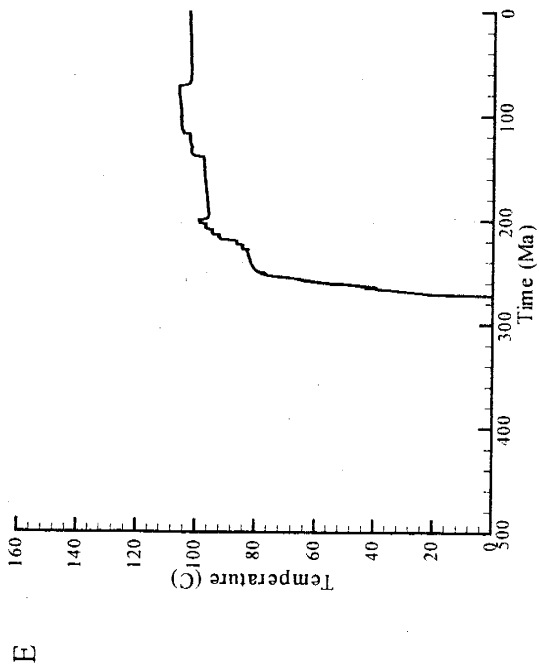
Results of sensitivity study with low original porosity values



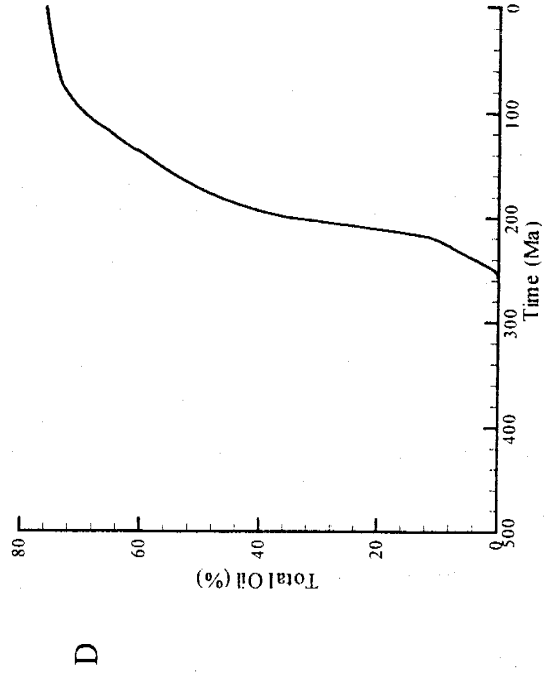
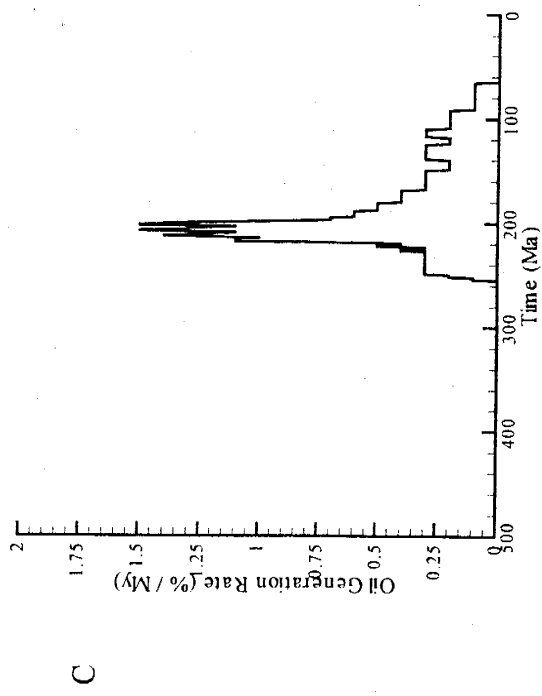
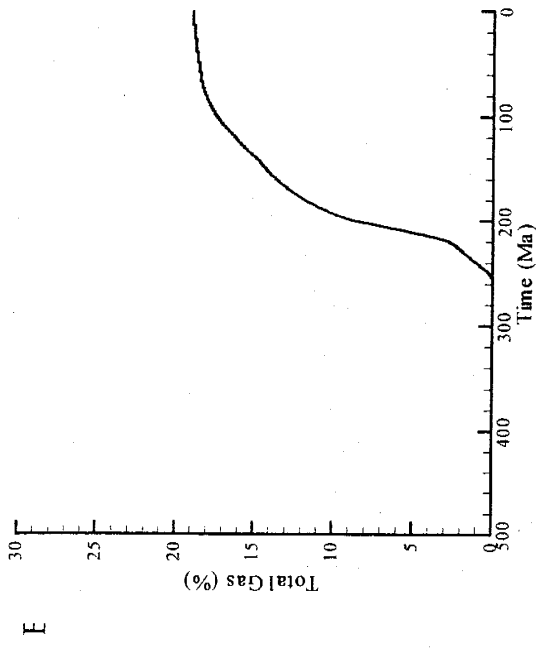
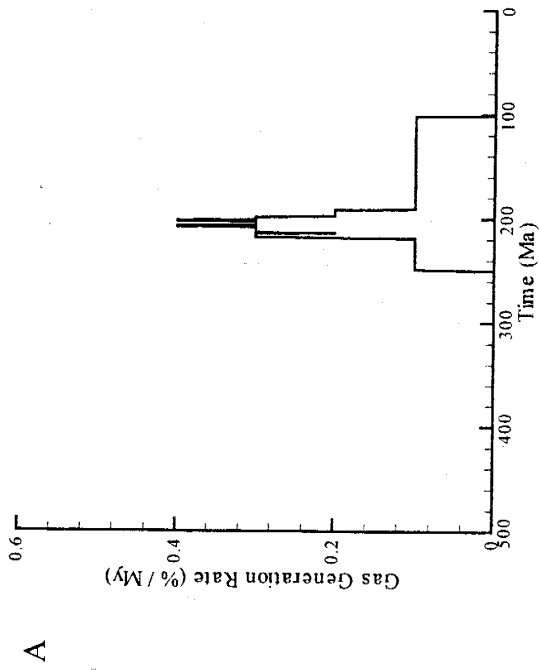
Results of sensitivity study with high original temperature values



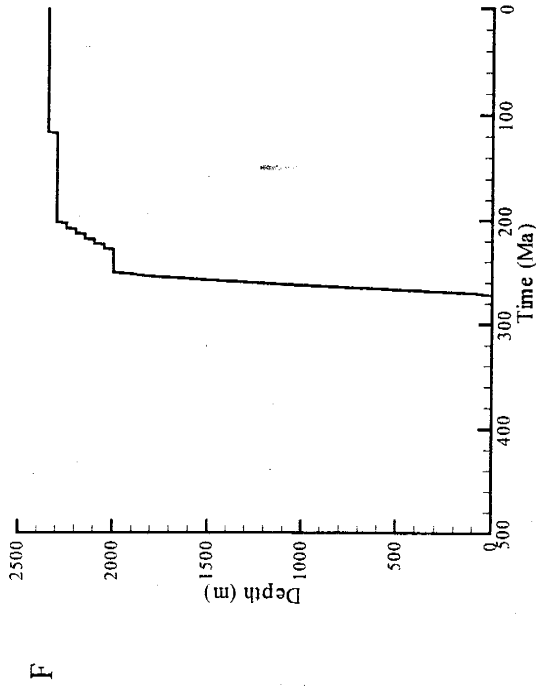
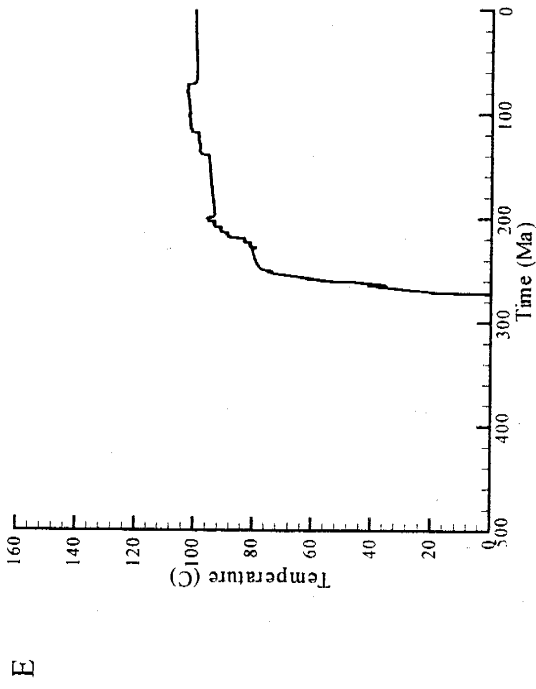
Results of sensitivity study with high original temperature values



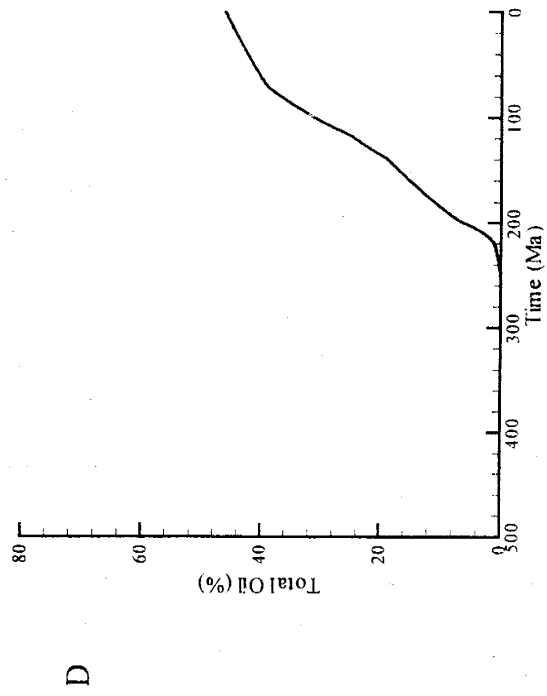
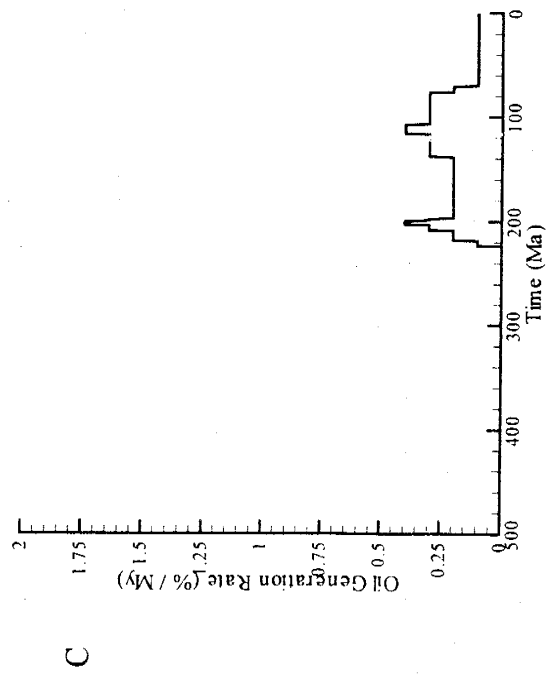
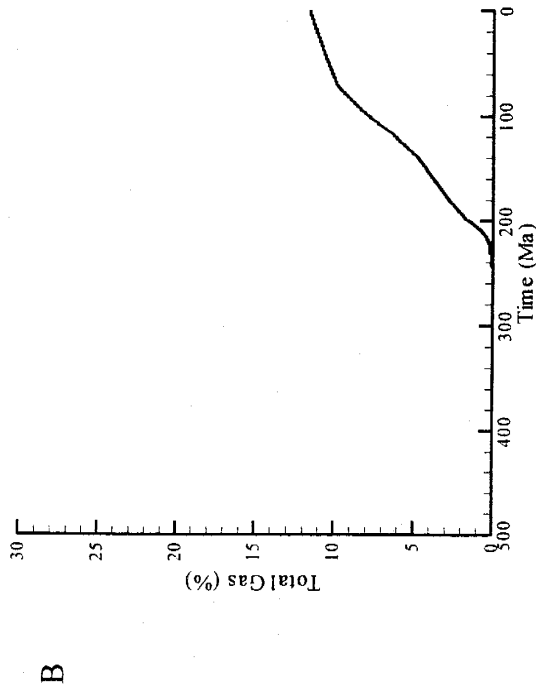
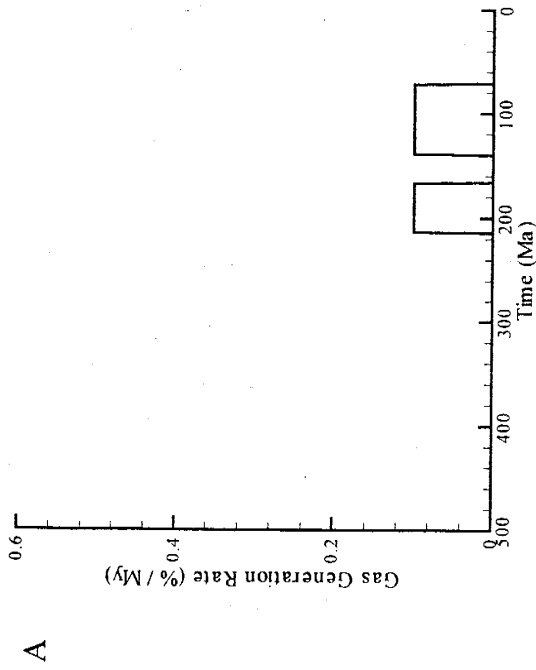
Results of sensitivity study with low original temperature values



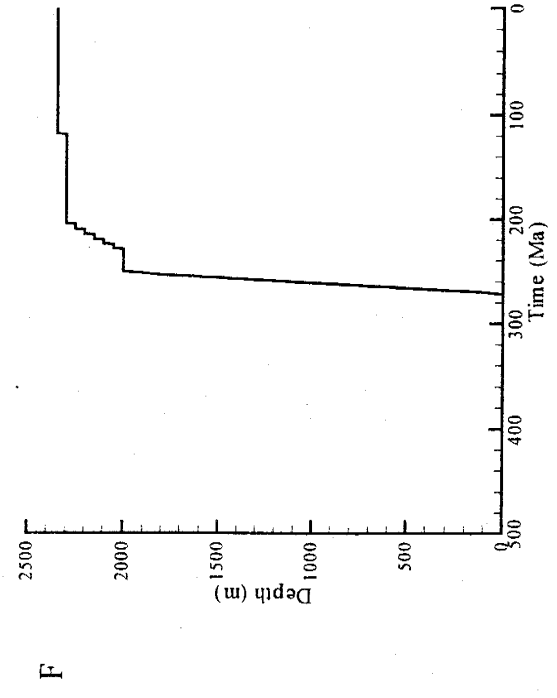
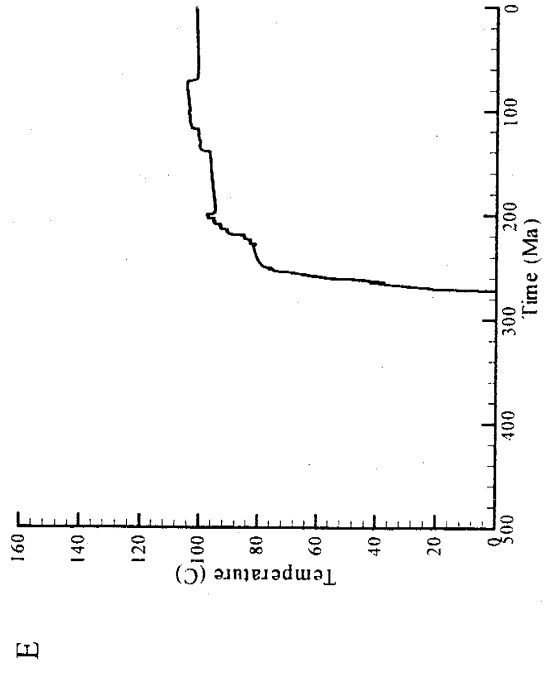
Results of sensitivity study with low original temperature values



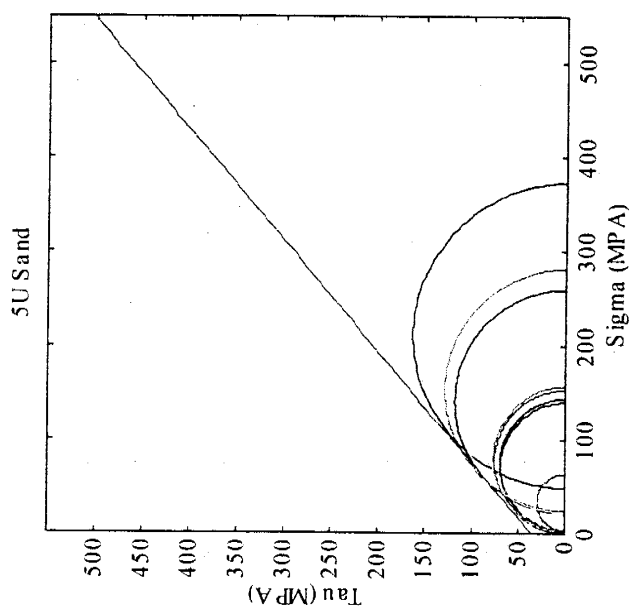
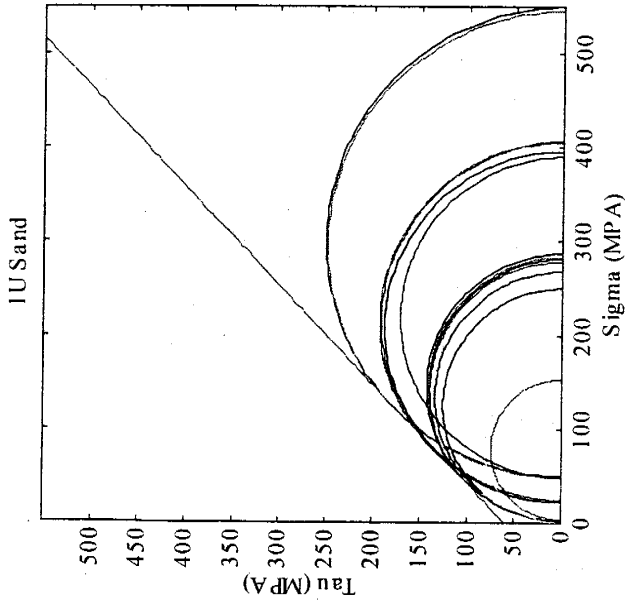
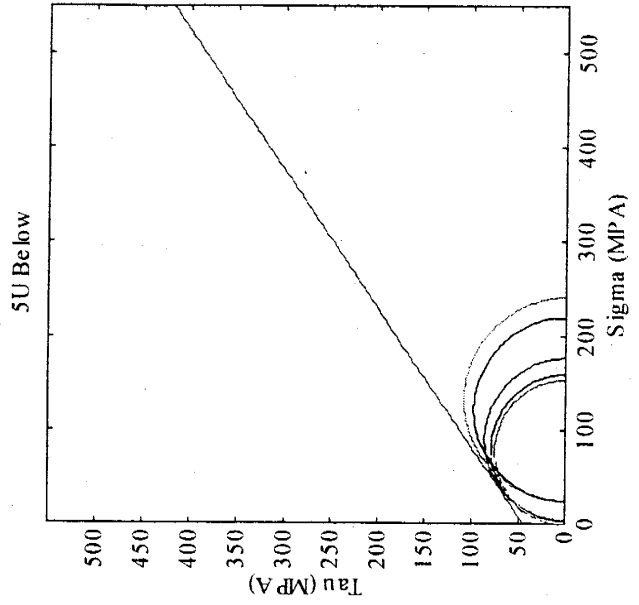
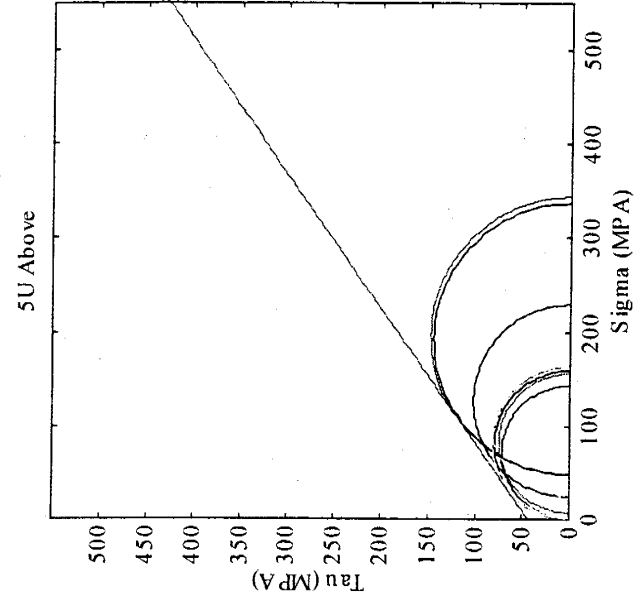
Results of sensitivity study with terrigenous sediment parameters

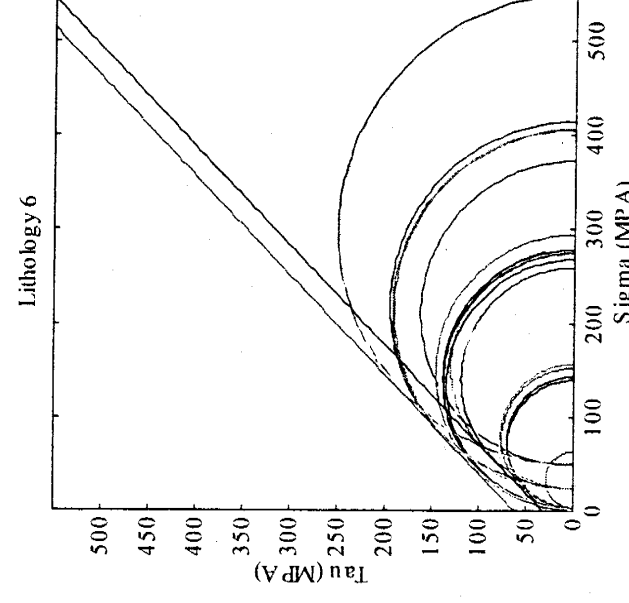
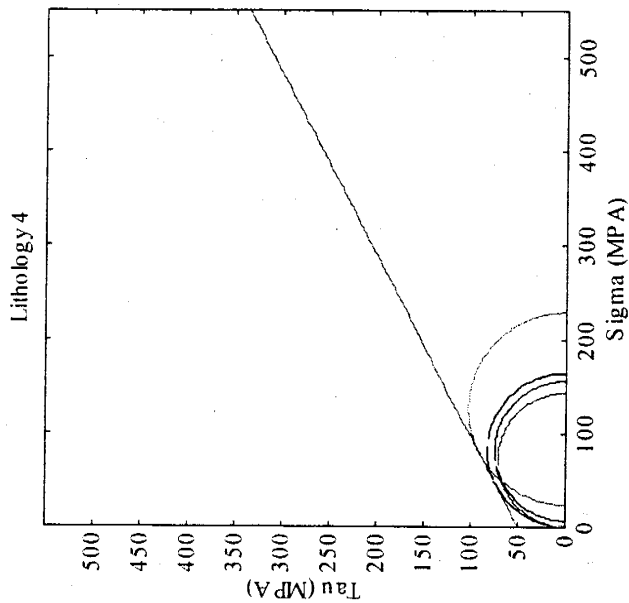
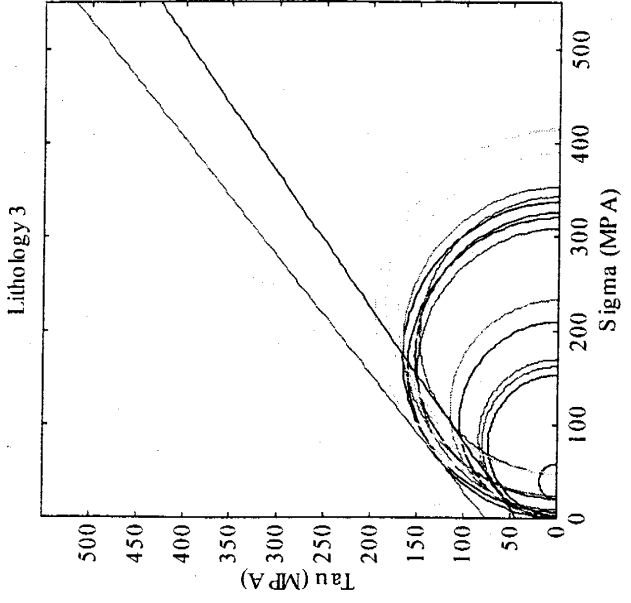
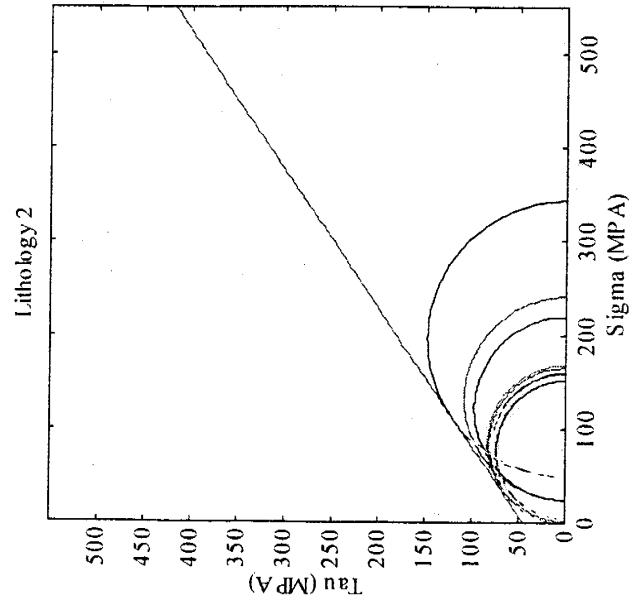


Results of sensitivity study with terrigenous sediment parameters

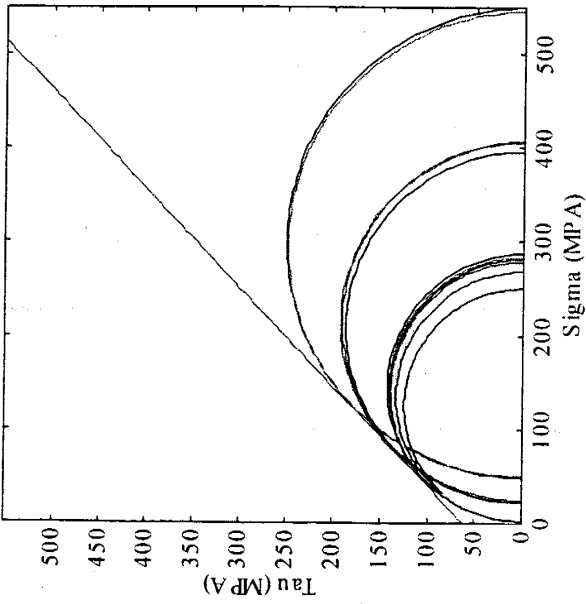


APPENDIX C

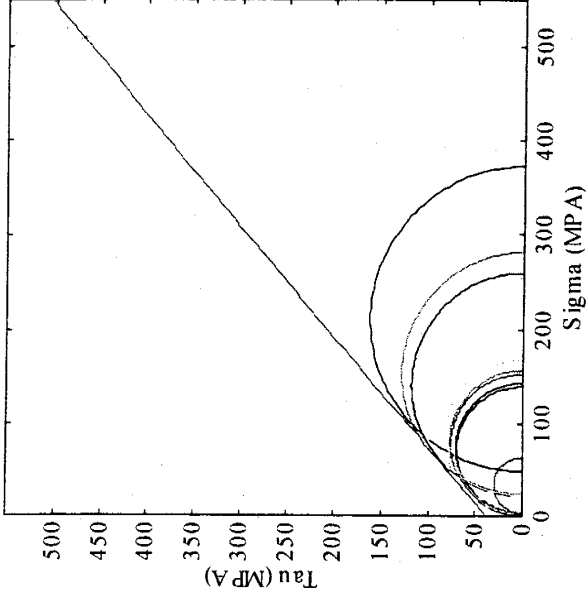




1U Lithology 6



5U Lithology 6



Failure envelope slopes and intercepts used in this study

CATEGORY	SLOPE	INTERCEPT	ALTERNATE SLOPE	ALTERNATE INTERCEPT
ABOVE	0.7	44	0.8	75
RESERVOIR	0.9	38	1	56
BELOW	0.7	40		
1U ABOVE	0.8	75		
1U RESERVOIR	0.97	62		
1U BELOW	0.9	50	0.8	78
5U ABOVE	0.75	38		
5U RESERVOIR	0.85	35		
5U BELOW	0.75	42		
LITHOLOGY 2	0.75	40		
LITHOLOGY 3	0.75	40	0.85	72
LITHOLOGY 4	0.7	38		
1U, LITHOLOGY 6	0.95	62		
5U, LITHOLOGY 6	0.9	34		

